

Ionic liquids : are they worth their salts?

Citation for published version (APA):

Bäuerlein, P. S. (2009). *Ionic liquids : are they worth their salts?* [Phd Thesis 1 (Research TU/e / Graduation TU/e), Chemical Engineering and Chemistry]. Technische Universiteit Eindhoven.
<https://doi.org/10.6100/IR652932>

DOI:

[10.6100/IR652932](https://doi.org/10.6100/IR652932)

Document status and date:

Published: 01/01/2009

Document Version:

Publisher's PDF, also known as Version of Record (includes final page, issue and volume numbers)

Please check the document version of this publication:

- A submitted manuscript is the version of the article upon submission and before peer-review. There can be important differences between the submitted version and the official published version of record. People interested in the research are advised to contact the author for the final version of the publication, or visit the DOI to the publisher's website.
- The final author version and the galley proof are versions of the publication after peer review.
- The final published version features the final layout of the paper including the volume, issue and page numbers.

[Link to publication](#)

General rights

Copyright and moral rights for the publications made accessible in the public portal are retained by the authors and/or other copyright owners and it is a condition of accessing publications that users recognise and abide by the legal requirements associated with these rights.

- Users may download and print one copy of any publication from the public portal for the purpose of private study or research.
- You may not further distribute the material or use it for any profit-making activity or commercial gain
- You may freely distribute the URL identifying the publication in the public portal.

If the publication is distributed under the terms of Article 25fa of the Dutch Copyright Act, indicated by the "Taverne" license above, please follow below link for the End User Agreement:

www.tue.nl/taverne

Take down policy

If you believe that this document breaches copyright please contact us at:

openaccess@tue.nl

providing details and we will investigate your claim.

Ionic Liquids - Are they worth their salts?

PROEFSCHRIFT

ter verkrijging van de graad van doctor aan de
Technische Universiteit Eindhoven, op gezag van de
rector magnificus, prof.dr.ir. C.J. van Duijn, voor een
commissie aangewezen door het College voor
Promoties in het openbaar te verdedigen
op vrijdag 30 oktober 2009 om 16.00 uur

door

Patrick Steven Bäuerlein

geboren te Lippstadt, Duitsland

Dit proefschrift is goedgekeurd door de promotor:

prof.dr. D. Vogt

Copromoter:

dr. C. Müller

Omslag: Boekenbent en Patrick S. Bäuerlein

Achtergrond: public domain picture from www.photos8.com

Druk: Wöhrmann Print Service, Zutphen

Copyright © 2009 by Patrick Steven Bäuerlein

A catalogue record is available from the Eindhoven University of Technology Library

ISBN: 978-90-8570-406-5

Dit proefschrift is goedgekeurd door de manuscriptcommissie:

Prof. Dr. Dieter Vogt (Technische Universiteit Eindhoven)

Dr. Christian Müller (Technische Universiteit Eindhoven)

Prof. Dr. Peter Wasserscheid (Friedrich-Alexander-Universität Erlangen-Nürnberg)

Dr. Ian J.S. Fairlamb (The University of York)

Prof. Dr. André B. de Haan (Technische Universiteit Eindhoven)

Contents

1	About Ionic Liquids	1
1.1	History of Ionic Liquids	2
1.2	Synthesis of Ionic Liquids	6
1.3	Characteristics of Ionic Liquids	9
1.4	Selected Applications of Ionic Liquids	19
1.5	How environmentally friendly are ionic liquids?	24
2	Ionic π -acidic alkene ligands in Pd(0)-catalysed Hiyama cross-coupling reactions	33
2.1	Introduction	34
2.2	Synthesis of ionic π -acidic alkene ligands	39
2.3	Catalysis	52
2.4	Experimental	73
2.5	Selected crystallographic data	85
3	First ionic tagging of heterocyclic ligands derived from pyrylium salts	89
3.1	Introduction	90
3.2	Synthesis of ionic phosphinines and pyridines	94
3.3	Conclusion	103
3.4	Experimental	104
4	Ionic liquids under scrutiny - Their impact on the hydroaminomethylation reaction	115
4.1	Introduction	116
4.2	Results and Discussion	119
4.3	Conclusion	136
4.4	Experimental	137

Contents

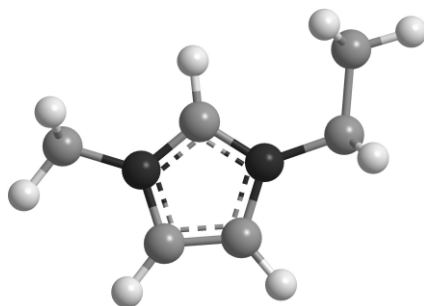
5	Biocatalysis in a biphasic ionic liquid/water system	145
5.1	Introduction	146
5.2	Investigation of a biphasic system	151
5.3	Conclusions	164
5.4	Experimental	165
6	Tandem reactions - An atom-efficient simple route to heterocyclic compounds	171
6.1	Introduction	172
6.2	Synthesis of the substrates	175
6.3	Imidazole substrate	175
6.4	Benzimidazole substrate	185
6.5	Conclusions	191
6.6	Experimental	192
	Summary	202
	Samenvatting	204
	Curriculum Vitae	206
	List of publications	207
	Dankwoord	208

1

Chapter 1

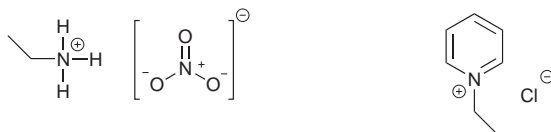
About Ionic Liquids

Ionic Liquids receive more and more attention as alternative reaction media due to their properties which clearly discriminate them from water or classical organic solvents. They are tuneable like no other solvent and therefore unique. A short introduction to these unique solvents and their properties is given in this chapter to outline their characteristics and application.



1.1 History of Ionic Liquids

On the first glance ionic liquids (ILs)^[1-4] seem to be merely a special type of salt, a salt with a melting point below 100°C by convention and at least one organic ion.^[1] But in fact they are more. They are exceptional in many ways. Their ability to be liquid even at room temperature sparked a lot of interest in the chemical society. Where classical solvents as toluene, diethyl ether or methanol are bound in their application by e.g. their boiling point, ionic liquids do not encounter this problem. Their vapour pressure is negligible under most reaction conditions used.^[5,6] Their constraints are more to be seen in their thermal stability, physical properties and chemical inertness. Furthermore, their potential as green solvents thanks to their lack of volatility attracted a lot of interest as they have been successfully employed in various technical processes.^[7] But arguably the most outstanding quality after all is their modularity to which they owe their name 'designer solvents'.



First publication 1914

First patent 1934

Figure 1.1: First ionic liquids reported

First ionic liquids date back to 1914,^[8] when ethylammonium nitrate was firstly synthesised. This organic salt already was a room temperature ionic liquid, but didn't prompt any significant interest at this time. This was surprising as this discovery brought out a new class of solvents. It took about two decades (1934) before the next ionic liquid was presented to the public in a patent. In this patent it was claimed that certain organic salts have the ability to dissolve cellulose and alter its reactivity.^[9] However, also this publication did not trigger any noteworthy interest in the scientific community. Later on, in 1948 this ionic liquid was followed by chloroaluminate based ionic liquids.^[10] At this point ionic liquids were still more interesting to electrochemists rather than to organic or catalytic chemists. Just one paper about a homogeneous

reaction, the hydroformylation, in an ionic liquid was published by Parshall in 1972.^[11] But other scientists had chosen to focus more on their electrochemical properties like e.g. Swain *et al.*^[12] He used an tetraalkylammonium ionic liquid to describe kinetic and electrochemical effects. In 1975 the Osteryoung group and Gilbert *et al.* studied the physical properties of a pyridinium-based chloroaluminate ionic liquid, an ionic liquid that raised hope to be applicable in batteries, especially by the United States Air Force.^[13,14] This hope had to be abandoned due to the easy reducibility of the pyridinium moiety, a real constraint for application in batteries. Thus, seven years later in 1982 Wilkes and Hussey^[15] tried to look for a less reducible cation by MNDO¹ calculations comparing several known heterocyclic cations with the outcome that imidazolium² presented itself as the most stable cation. At this point the prominence of the imidazolium based ionic liquids commenced. A status they have kept up to now, also because of their often low viscosity and price compared to other cations. At a later date Seddon and Hussey were investigating metal complexes in ionic liquids trying to understand spectroscopic and complex chemical aspects of these metal compounds.^[16,17] But it required about a decade (1985/86) before the chemical properties of ionic liquids were rediscovered and successfully established in reactions like the Friedels-Craft acetylation^[18] or nucleophilic aromatic substitution.^[19] In these reactions the ionic liquid itself played a catalytic role in reaction. Inspired by these results in 1990 Chauvin *et al.* and Wilkes *et al.* employed transition metal catalysts in acidic ionic liquids to catalyse the dimerisation of propene and the polymerisation of ethene.^[20,21] Based on these successful reactions Wilkes and Zaworotko^[22] refined homogeneous reactions in ionic liquids by applying more stable species in 1992. The tetrafluoroborate-based ionic liquids proved to be tolerant to multiple functional groups and more resistant in the presence of water compared to the chloroaluminate ones. These attributes made them excellent candidates for hydroformylation reactions of olefins. This successful application of a tetrafluoroborate ionic liquid paved the way for more combinations of cations and anions.^[22,23] Therefore one could say that the use of this ionic liquid was a pioneering step in the further development of ionic liquids in catalysis. More ionic liquids were synthesised by combining various cations and

¹Modified Neglect of Differential Overlap

²already known since 1884

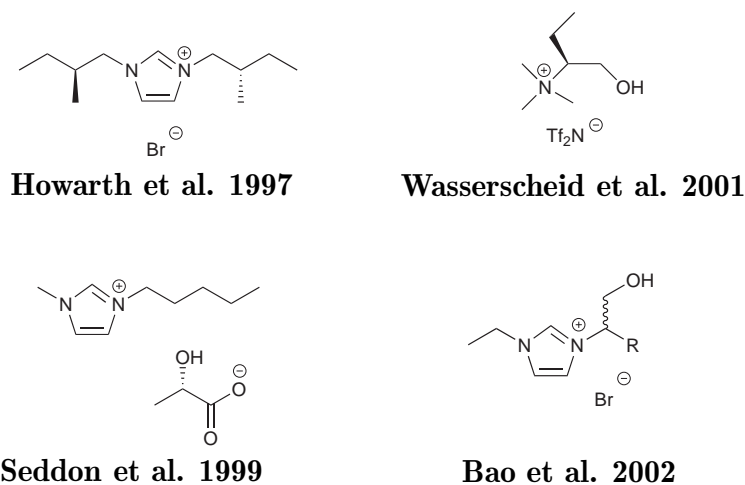
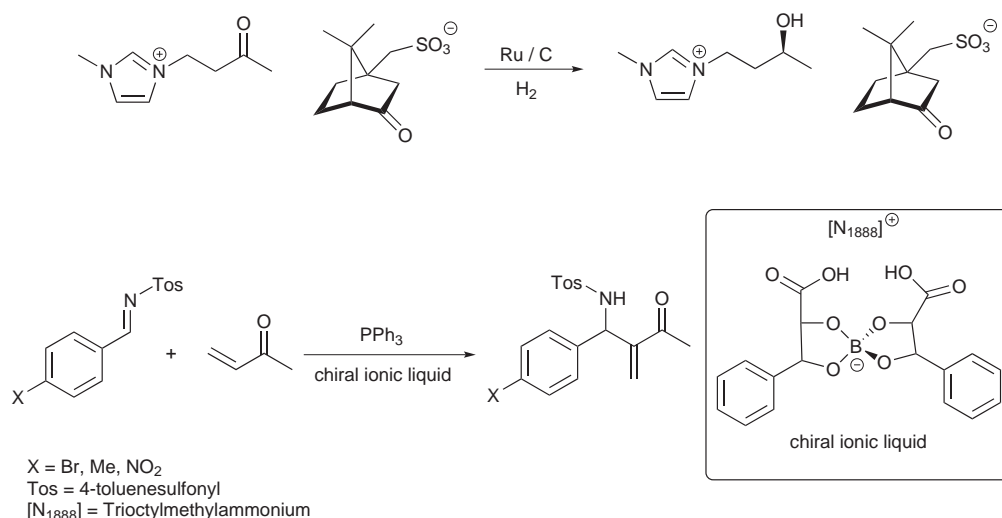


Figure 1.2: First chiral ionic liquids reported

anions.^[24,25] New anions e.g. the weakly coordinating anions like hexafluorophosphate and bis(trifluoromethanesulfate)imine (Tf_2N) were introduced. This helped in the process of understanding the physical properties of the organic salts^[26,27] and enabled more organic reactions to be conducted in ionic liquids as these ionic liquids proved to be more stable.^[28,29] Meanwhile most of the common and most applicable organic reactions have been successfully established in an ionic liquid system. In some cases the ionic liquid was used to increase solubility of substrates. In other cases the role of the ionic liquid was more crucial as it acted as a promoter. Another advantage of ionic liquids was that they are in some cases able to separate the reactive phase and the substrate phase, allowing a straightforward separation of product and catalyst.^[30] The often laborious workup of reaction mixtures was simplified. Along with the development of new ionic liquids by anion exchange, also the tuning of the cation was given priority to. Introduction of functional groups and even implementing a chiral centre were the main goals.

For that reason Howarth *et al.* synthesised a chiral imidazolium-based ionic liquid and described its use in a Diels-Alder reaction in 1997.^[31] In this case the chiral information was stored in the cation unlike in the ionic liquid reported by Seddon *et al.* in 1999.^[28] That ionic liquid carried the chiral information in the anion, a lactate. The advantage

of this ionic liquid over the imidazolium-based one can mainly be seen in the costs. Seddon used a readily available substance from the chiral pool for the synthesis. Simply by anion exchange this ionic liquid was prepared. No laborious synthesis was necessary. Later on, in 2001, Wasserscheid *et al.* seized on the suggestion to use the chiral pool as a source for chiral ionic liquids by synthesising them from amino acids.^[32] The chirality was determined by use of Mosher's acid and ^{19}F NMR spectroscopy. The drawback of these ionic liquids was primarily found in their lack of stability, viscosity and inconveniences to synthesise them, despite the synthesis was elaborated. After this, in 2003, Bao *et al.* reported on the first synthesis of imidazolium-based ionic liquid, containing only one stereogenic carbon atom, descended from amino acids. In a four step synthesis, starting from an amino acid, they made these chiral ionic liquids, which satisfactorily meet specifications that a convenient ionic liquid ought to fulfil. The melting point is below room temperature, the thermal stability is given up to temperatures of around 180°C and they are resistant to water.^[33] Other important aspects in the history of ionic liquids are the discoveries of Wasserscheid and Leitner. They demonstrated that the chiral information stored in the ionic liquid can be successfully transferred to the reactants. Wasserscheid *et al.* showed this transfer of chiral information from the anion to the cation in a camphorsulfonic acid- based ionic liquid in a hydrogenation reaction of a ketone^[34] suggesting a close cation-anion interaction. The chirality was transferred through ion-pairing from the camphor sulfonic acid to the alcohol. Leitner *et al.* successfully employed an ionic liquid, based on a chiral borate, in a Baylis-Hillman reaction (Scheme 1.1 on the following page).^[35] To this reaction great importance is attached as the ionic liquid served both as the solvent and the carrier of the chiral information. The catalyst applied in this reaction was achiral. The ionic liquid interfered with the catalytic cycle by forming an intermediate. Thus, the chiral information was solely transferred from the solvent to the product by interaction with the reaction intermediates. Examples of chirality transfer from a solvent are rare, therefore this discovery stresses the advantage of ionic liquids over conventional solvents for certain applications. Later on, the group of Leitner showed in a hydrogenation reaction again that the chiral information does not necessarily has to come from the ligands.^[36,37] A protic ionic liquid was the carrier of the chiral information, whilst the ligands used were racemic. They successfully yielded *ee*'s of about 70%.



Scheme 1.1: Applied chiral ILs. Above: Hydrogenation^[34]; below: Baylis-Hillman reactions.^[35]

Recently, Wasserscheid *et al.* extended the scope of applicability of ionic liquids by immobilisation of ionic liquids on silica gel closing the gap between homogeneous and heterogeneous catalysis.^[38–41] These supported ionic liquid phases (SILP) were used in a continuous flow gas-phase hydroformylation of propene. This reaction took place in the supported ionic liquid phase, where the catalyst was situated.^[38] Due to this, catalyst retention and reuse was significantly improved. Table 1.1 on the next page shows briefly the sequence of the most important discoveries.

1.2 Synthesis of Ionic Liquids

Most of the ionic liquids are made by quaternisation of nitrogen^[42,43] or phosphorus^[44] in an organic molecule and, if desired, a subsequent anion exchange.^[45] Quaternisation is most of the times the first step to yield an organic salt. However, the quaternisation is often preceded by several reactions to synthesise a particular ionic liquid 'precursor'. The first step already paves the way to virtually an unlimited amount of 'precursors'. Further shaping of these salts can be achieved by the choice of the quaternisation reagent, generally organic halides^[45], alkyl sulfates^[46] and recently alkyl phosphates^[47]. Especially the

Table 1.1: Major steps in ionic liquids history

Year	Discovery	Literature
1914	First mention of an ionic liquid	[8]
1934	First ionic liquid patent	[9]
1948	Chloroaluminate ionic liquids were discovered	[10]
1972	Hydroformylation of ethene in an ionic liquid	[11]
1982	Imidazolium is recognised as a ionic liquid cation	[15]
1990/92	First homogeneous reaction in a room temperature ionic liquid	[28,29]
1997/99	Functionlised and chiral ionic liquids are introduced	[28,31]
2007/08	Chirality induced by chiral ionic liquids	[35–37]

last two classes of alkylating reagents are of interest as they constitute a halide free and low cost route to ionic liquids. In case of the haloalkanes the advantages are the price and the availability of these compounds. There is a wide range commercially available. The reactivity of the halides depends on their electrophilicity. Chlorides are less reactive than iodides. The organic salts of these haloalkanes are comparably formidable for an anion exchange by which the halide can be removed from the ionic liquid.

To quaternise the heteroatom there are two major ways to achieve this. Firstly, it can be performed in apolar organic solvents such as toluene or 1,1,1-trichloroethane.^[45] The product will not be soluble in these kinds of solvents and therefore it can be easily separated from the organic layer. An even more elegant route is the solvent-free synthesis of ionic liquids. Many ionic liquids are liquid at standard reaction temperatures around 60°C and therefore no solvent is necessary.^[48] In all cases remaining solvent or substrates can be removed by distillation under reduced pressure and elevated temperatures due to the negligible vapour pressure and thermal stability of ionic liquids.

If desired, the anion can be exchanged in the next step giving the ionic liquid completely new physical properties, such as melting point or solubility. In many cases halide containing ionic liquids are used for the anion exchanged but also other anions such as sulfates are suitable candidates for this. Easily they can be exchange in a metathesis reaction by reacting the ionic liquid with another salt.

Figure 1.3 depicts some of the most prominent and widely used cations and anions for ionic liquids. Immediately the amount of possible combinations stands out. These 6 cations and 6 anions can already form 36 different organic salts.

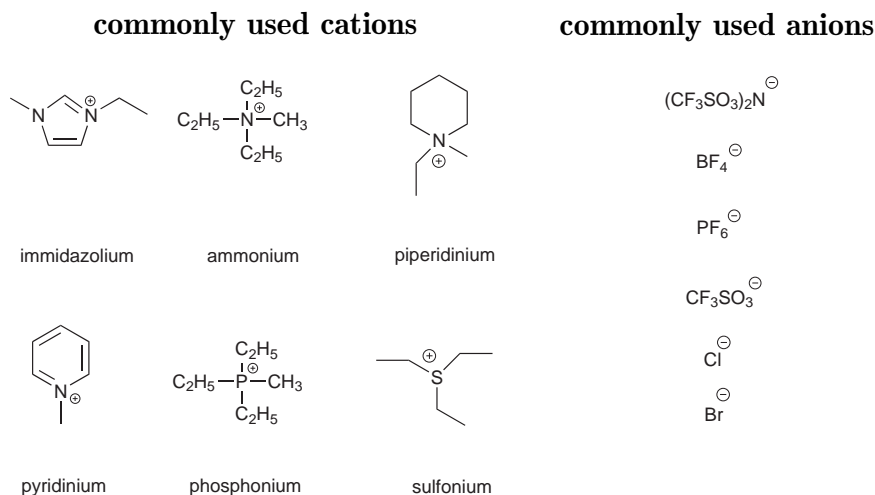
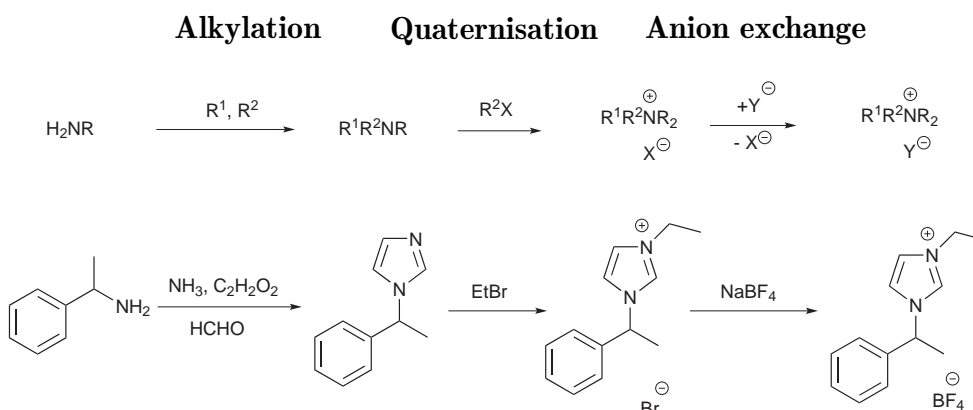


Figure 1.3: Examples of frequently used cations and anions

One can easily imagine that the number of possible ionic liquids built from these cations is formidable when changing the side chains, let alone when adopting more ions. To yield now organic salts it can generally be said that in a three/four step synthesis already a complex and functionalised ionic liquid can be made. Simple ones can be prepared in one step. Nonetheless, it is desirable to keep the reaction steps at a minimum to contain costs as ionic liquids ought to serve as solvents and therefore an economical synthesis is crucial. Basically it can be said that their advantages over classical solvents must outweigh their costs. To make use of natural compounds or large scale chemicals helps to keep costs at a minimum.

Scheme 1.2 on the next page shows the most common way to synthesise ionic liquids using the example of a chiral ionic liquid.^[33] In the first step the 'precursor' is synthesised from a primary amine by transforming it into a tertiary amine. By this, also an imidazole ring is formed. In the next step the imidazole is quarternised resulting in a bromide-containing ionic liquid. The last step is a metathesis reaction.



Scheme 1.2: Above: General synthesis of an ionic liquid; below: Example of an ionic liquid synthesis^[33]

Bromide is exchanged for tetrafluoroborate, a less coordinating anion. Alternatively, also carbonic, sulfonic or boric acid anions are often implemented in ionic liquids, especially when the anion is supposed to play a crucial role in the reaction, as Wasserscheid *et al.*^[34] showed in a hydrogenation and Leitner *et al.*^[35] demonstrated in a Baylis-Hillman reaction (Scheme 1.1 on page 6).

Apart from quaternisation also acid-base reactions can lead to ionic liquids. This method is a straightforward route to chiral ionic liquids in one step as the chiral pool offers a lot of chiral acids that can be reacted with an amine to an organic salt. In combination with chiral bases, even diastereomeric salts can be made.

1.3 Characteristics of Ionic Liquids

Ionic Liquids are discriminated mainly by five major attributes, the melting point, viscosity, density, stability and miscibility/solubility.^[49–51] A sixth important attribute, the conductivity, is more of interest to physical chemists and shall not be discussed here in detail. Information concerning that topic can be found in literature.^[45] In the last decade also a lot of publications concerning the prediction of physical properties of ionic liquids have been published. In these publications it has been demonstrated that physical properties like melting point can be calculated within certain limits.^[52–57] Very often

theoretical and practical values are almost coincident. Therefore these approaches offer a way to cut the often laborious lab work of synthesising ionic liquids to a minimum by giving in advance an idea which combinations of cations and anions will yield a suitable ionic liquid. Here, however, a detailed description of the theoretical approach will be left out, rather the observations and explanation of physical properties, which differ from classical solvents, take centre stage. Some of the most pronounced differences between organic solvents and ILs are listed in table 1.2.

Table 1.2: Comparison of organic solvents and ionic liquids

Property	Organic solvent	Ionic Liquid
Number of solvents	> 1000	> 1,000,000
Catalytic ability	little	common
Chirality	little	common
Vapour pressure	significant	negligible
Flammability	given	usually non-flammable
Solvation	weakly	strongly
Polarity	Conventional polarity concept	Polarity differs
Tuneability	limited	'designer solvents'
Cost	low priced	all price classes
Recyclability	Green imperative	Cost imperative
Viscosity / cP	0.2 - 100	22 - 40,000
Density / g cm ³	0.6 - 1.7	0.8 - 3.3

Melting point

Possibly, the most important criterium for judging an ionic liquid is the melting point, an attribute defining the applicability like no other. This property relies on the nature of the cation and the anion as has been shown by Weingärtner *et al.*^[57,58] The influence of the cation becomes clear when looking at several melting points of chloride salts (Table 1.3 on the following page).

Symmetry appears to be an important factor.^[59,60] The less symmetric the cation is the lower the melting point. The imbalance in a cation can frustrate crystallisation. This

Table 1.3: Melting points of chloride salts

Entry	Ionic Liquid	Melting Point	Reference
1	EMIM Cl	89	[53]
2	BMIM Cl	41	[53]
3	HMIM Cl	- 75	[53]

EMIM = 1-ethyl-3-methylimidazolium, BMIM = 1-butyl-3-methylimidazolium, HMIM = 1-hexyl-3-methylimidazolium

can be demonstrated when looking at $[\text{MMIM}]\text{Cl}$ ³ with C_{2v} symmetry and a melting point of 125°C , whereas $[\text{EMIM}]\text{Cl}$ and $[\text{BMIM}]\text{Cl}$ ⁴ possess just C_1 symmetry and the melting points are 87 and 65°C respectively. For $[\text{P}_{888}]\text{PF}_6$ ⁵ the symmetry element is T_d . By changing the chain length of one of the alkyl groups the melting points drop and along with this also the symmetry drops to C_{3v} . A look at figure 1.4 also stresses the importance of asymmetric chain lengths.

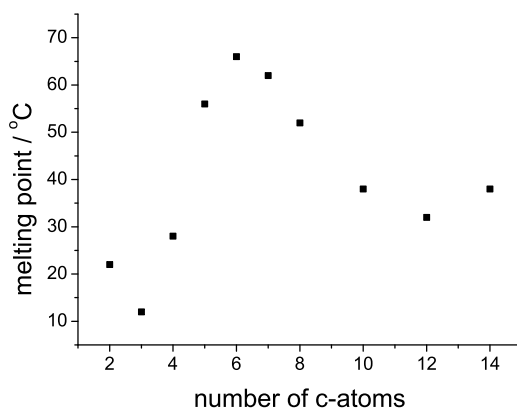


Figure 1.4: The melting point of $[\text{P}_{666n}][\text{PF}_6]$ as a function n .^[61]

³1,3-dimethylimidazolium

⁴EMIM = 1-ethyl-3-methylimidazolium, BMIM = 1-butyl-3-methylimidazolium

⁵Tetraoctylphosphonium

Roughly spoken, the less symmetrical a cation is, the lower the melting point. Further the length of the side chain reduces the symmetry for most anions, which explains the difference between EMIM and BMIM. However, when looking at melting points of Tf₂N salts of imidazolium cations it becomes obvious that these salts do not fit with this trend. In addition, also pyridinium salts act counterintuitively. When a butyl chain is exchanged for a pentyl one the melting point increases.^[57] Looking at two phosphonium ionic liquids the same tendency can be observed. Other important factors are intermolecular interaction (hydrogen bond, Van-der-Waals force)^[45,62] and the charge distribution^[63].

Apart from the cation, the anion exerts influence on the melting point as well. A rough rule of thumb is that the bigger and less coordinating an anion is the lower the melting point of an organic salt, provided the same cation is used.^[56] Table 1.4 shows the melting points of three different imidazolium based ionic liquids, where this tendency is stressed. From the highly coordinating cation Br⁻ to Tf₂N⁻ a melting point difference of about 60°C can be measured.

Table 1.4: Melting point of [EMIM]⁺ salts

Entry	Ionic Liquid	Melting Point	Reference
1	EMIM Cl	89.0	[53]
2	EMIM BF ₄	11.0	[53]
3	EMIM Tf ₂ N	-17	[64]

EMIM = 1-ethyl-3-methylimidazolium

Viscosity

Along with the melting point the viscosity predominantly dictates the applicability of an ionic liquid. In general, it can be said that the viscosity of ionic liquids exceeds the one of water by a factor of ten up to a thousand (Table 1.5 on the next page). It is defined by the nature of the cation as well as the anion. Chain length in the cation and ramification can increase the viscosity significantly. Increasing the chain

length from C2 to C4 in e.g. an imidazolium based ionic liquid raises the viscosity by a factor of four. It is governed for the most part by hydrogen bridging and Van-der-Waals interactions.^[51] Furthermore, fluorinated side chains increase Van-der-Waals interaction and hence the viscosity.^[50] When looking at two fluorinated anions this effect can be observed. Table 1.6 on the following page shows a significant increase of the viscosity on changing the anion from CF_3SO_3^- to $\text{C}_4\text{F}_9\text{SO}_3^-$.

Table 1.5: Viscosity of different imidazolium bromides^[4]

Entry	Ionic Liquid	Viscosity η
1	EMIM BF_4	32
2	BMIM BF_4	115
3	OMIM BF_4	439
4	water	$8.90 \cdot 10^{-4}$

EMIM = 1-ethyl-3-methylimidazolium, BMIM = 1-butyl-3-methylimidazolium, 1-octyl-3-methylimidazolium

The same effect can be observed for the two carbonate anions. Interestingly, for ionic liquids it can be noticed that their viscosity often does not obey the Arrhenius equation.^[50,65] In many cases the Vogel-Tammann-Fulcher equation, an equation often applied for supercooled liquids, has to be used to describe the behaviour properly. This mainly becomes true for ionic liquids with small and symmetrical cations. For asymmetrical cations the Arrhenius law is applicable as long as no functional groups, such as carbonyl or hydroxy, are incorporated in the side chains. For those cases it can happen that none of the two equations here can be used, especially when the cations are highly unsymmetrical. It has to be emphasised that viscosity can be altered by addition of cosolvents. Often small amounts already have a pronounced effect and lower the viscosity significantly. This effect can become important when considering the application of a highly viscous ionic liquid in a reaction. The moment the substrate is added the viscosity might drop dramatically and is no longer an issue. Thus, an ionic liquid that already has been chemically tailored can further be shaped, this time physically. The same can apply for the melting point.

Table 1.6: Viscosity depending on anion size

Entry	anion	η [cP]
1	CF_3SO_3^-	90
2	$\text{n-C}_4\text{F}_9\text{SO}_3^-$	373
3	CF_3COO^-	73
4	$\text{n-C}_3\text{F}_7\text{COO}^-$	182

Miscibility and density

Miscibility and density are two crucial attributes of ionic liquids and should be mentioned altogether as they need to act in concert for many applications.

Solubility of organic compounds depends mainly on the chain length in the cation of an ionic liquid. In figure 1.5 on the next page the solubility of 1-octene plotted against the chain length is depicted. It becomes clear that the capability to dissolve 1-octene increases enormously when going from ethyl to hexyl. The hydrophobic region of the cation is hereby increased. When taking a look at an imidazolium cation several regions in this ion can be seen (fig. 1.6 on page 16). The hydrophobic part is here of interest as it defines the solubility. The more pronounced the hydrophobic part becomes the better apolar chemicals can be dissolved in the ionic liquid. Therefore by changing the side chain the solubility can be controlled. This especially becomes interesting for biphasic systems and extraction processes.^[66,67]

Whereas designing the cation mainly leads to an increase or decrease of the solubility of apolar compounds, the anion can have a profound effect on the solubility in polar solvents. The right choice of the anion can create a hydrophobic ionic liquid. Anions being famous for this are PF_6^- and Tf_2N^- . Their ionic liquids form a biphasic system with water and often with methanol. Provided the right choice of cation and anion is made, a hydrophobic ionic liquid, that does not mix with an apolar substance, can be synthesised. The hydrophobic part of the cation must be as short as possible and one of the above mentioned anions must be used. By this even triphasic systems are possible.^[1] When

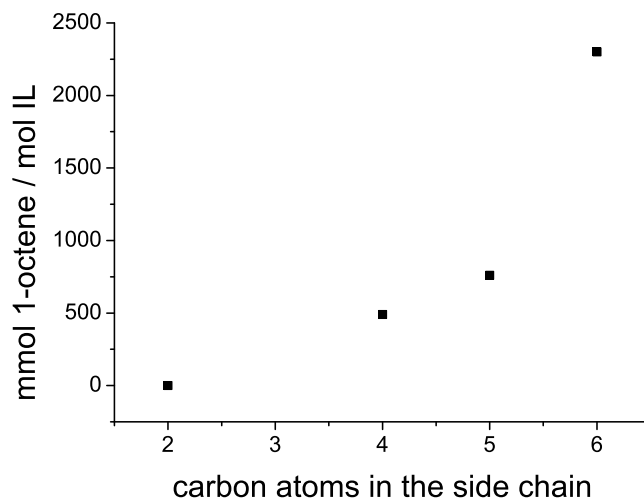


Figure 1.5: Solubility of 1-octene in different ionic liquids.^[1]

talking about multiphasic systems density bears a significant relevance. The density of the different layers should differ noticeable to guarantee quick and distinct phase separation. The density can be altered by the chain length in the cation and by the anion size. A longer side chain for imidazolium-based ionic liquids causes a decrease in the density, whereas for a certain cations a bigger anion results in an increased density.^[50,51] The temperature dependence of the density is linear. The density decreases linearly with increasing temperature.

The incapability of many ionic liquids to dissolve apolar compounds is taken advantage of in many cases as this allows the formation of biphasic reaction systems, that enable a quick and clean separation of a catalyst phase (ionic liquid) and the apolar substrates. This concept will be seized on in chapter four. Another possible application using limited solubility of apolar compounds in ionic liquid are extraction processes. De Haan *et al.* have demonstrated that it is possible to use a pyrrolidinium-based ionic liquid for the selective extraction of toluene from heptane.^[66]

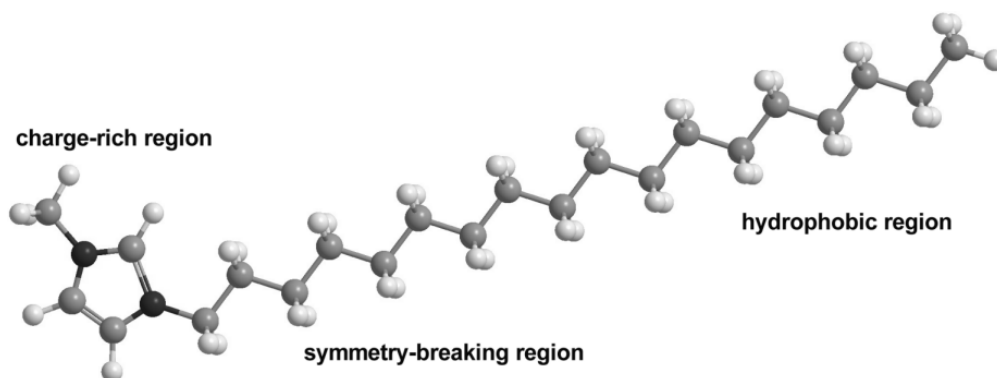
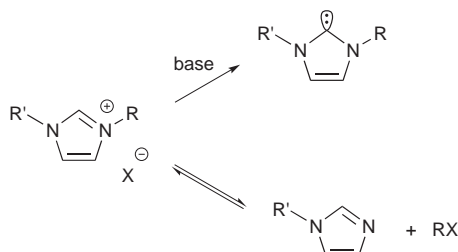


Figure 1.6: structural regions of a 1-methyl-3-octylimidazolium. From left: charge rich region; symmetry breaking region, which is responsible for the melting point; hydrophobic region being accountable for the melting point, the viscosity and the solubility^[53]

Stability and volatility

Ionic liquids do not have a measurable vapour pressure under most reaction conditions applied.^[5,6] It has been demonstrated, however, that some ionic liquids can be distilled in ultra-high vacuum at high temperatures. Nevertheless, to distil an ionic liquid at standard pressure, temperatures far beyond the thermal stability are needed. Most of the ionic liquids decompose between 100°C and 300°C. Mainly, the nature of the cation is responsible for the thermal stability. A protic ionic liquid normally decomposes when the boiling points of the base and acid, which it is made from, are reached. Ammonium, imidazolium and phosphonium cations are more stable, but here the counterion has a valuable effect. The same cation can bear higher temperatures when the anion is exchanged depending on its nucleophilicity, which can reverse the quarternisation (Scheme 1.3 on the next page).^[45,68] An effect almost all ionic liquids experience is discolouration upon heating, while being synthesised and also afterwards. This change of colour indicates that decomposition might take place. An educated guess would be the formation of oligomers or radicals, at least in the case of imidazolium-based ionic liquids. However, these coloured compounds seem not to be harmful to processes on big scale as BASF has been running a distillation process with an ionic liquid over a period of three months.^[69] Within the course of time the ionic liquid turned black, but this did

not have any effect on the performance of the process. The product did not adsorb any of the coloured impurities.



Scheme 1.3: Thermal and base-induced decomposition of an ionic liquid

Nevertheless, the thermal stability is higher than for most of the organic solvents. The weak point of ionic liquids is their lack of tolerance of bases. Often already small amounts of a base can decompose an ionic liquid easily, especially pyridinium-based ionic liquids show hardly any tolerance. In the case of imidazolium-based ionic liquids the formation of carbenes is possible due to the acidic proton in C2 position (scheme 1.3). The pKa value for this proton is between 21-24 in water and depends on the substituents as well as in the frame-work of the imidazolium cation.^[70] Also water can pose a threat to certain ionic liquids, especially to anions. It has been demonstrated that PF₆-containing ionic liquids have the tendency to hydrolyse.^[71] Rogers *et al.* were able to detect formation of HF and PO₃F₂ when using ionic liquids at elevated temperatures. For stability reasons the use of *e.g.* dialkylphosphate ionic liquids is reasonable as these are hydrolytically stable.^[47] These ILs, however, can undergo a transesterification reaction that can cause decomposition. Under acidic conditions the alkyl chains in phosphates and sulfates can be exchanged. One other criterium, which is important to judge the applicability of an IL, is the hygroscopic character. Hydration of many ammonium and imidazolium salts occurs instantly.^[72] This attribute of certain ILs might not be a problem for the stability of the IL itself, but can pose a threat to catalysts or substrates dissolved in it. Therefore, these ILs need to be handled under inert atmosphere.

These examples reveal that it is a delicate matter to choose a suitable ionic liquid. One must always have a close look at the reaction conditions applied to judge whether an ionic liquid is stable under these conditions.

Ionic Liquids at the molecular Level

To understand ILs in more detail it is of great importance to gain more insight in their molecular behaviour.^[58] Therefore, both in gaseous phase and liquid phase especially imidazolium-based ILs have been investigated. Quantum-chemical calculations in the gas phase have given an insight in the structure of the ion pairs (Figure 1.7). The calculations show that in case of the chloride anion, the preferred positions are close to the proton at the C2-position, whereas the anion can be found in plane and out of plane. The other positions close to C4 and C5 are less favourable. For the PF_6^- anion the situation is slightly different. This anion, as well as BF_4^- and Tf_2N^- , are in favour of the out-of-plane positions. These results allow the conclusion that the nature of the anion can have a remarkable and strong impact on the behaviour of the cations. Such effects have been reported for the activation of the C-H-bonds in imidazolium-based ILs by several groups.^[73-75]

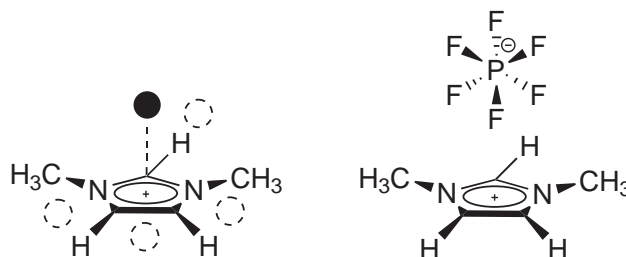


Figure 1.7: Stable positions of anions relative to the imidazolium cation. Left: Positions of the Cl^- . Dashed circles represent in-plane positions, the solid circle is the out-of-plane position; Right: Position of the PF_6^- .

Depending on the nature of the anion, the reactivity of the C-H-bonds change. These calculations, however, only describe the behaviour in the gas-phase. To receive more information on the liquid phase, neutron scattering experiments were conducted. These experiments shed light on the location of the chloride anion in an IL (Figure 1.8 on the following page). Also in the liquid the chloride gives preference to positions around the proton at the C2. In contrast to this anion, larger anions such as PF_6^- or Tf_2N^- , are located above the imidazolium moiety. Apart from the positions of the anion, it is of interest how the cations are arranged. It is postulated that π - π

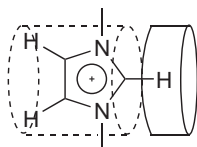


Figure 1.8: Schematic representation of the positions of chloride anions in an ionic liquid. The band around C2-H shows positions of high probability. The cylinder embracing the imidazolium shows the areas of low probability.

stacking is of great importance between adjacent rings, as well as van der Waals contacts between methyl groups. This brief overview barely scratches the surface of the actual molecular structure of ILs, especially as it is only concerned with the most prominent cations and anions. More information on this topic can be found in literature.^[58]

1.4 Selected Applications of Ionic Liquids

For many years now ionic liquids are being used in several reactions as a solvent. Their applicability has been demonstrated in transition metal catalysis,^[3] biocatalysis,^[76] organocatalysis^[77] and electrochemistry.^[4] But is their applicability restricted to the laboratory or are they also suitable for industrial processes? More than 1500 patents can be found when searching for the term 'ionic liquids' giving an indication that these advanced solvents bear a lot of potential for commercial applications. Several companies already employ ionic liquids successfully in industrial processes (Table 1.7).^[78]

Table 1.7: Examples of industrial processes with ionic liquids

Company	Process	Role of the ionic liquid
BASF	acid scavenging	auxiliary
BASF	chlorination	solvent
Degussa	compatibiliser	additive
Iolitec/Wandres	cleaning	additive

Here the beneficial contribution of ionic liquids to large scale processes will be de-

scribed for a few significant commercial processes. Apart from these reactions on commercial industrial scale there are several pilot plants involving ionic liquids. In the future the role of these organic salts is to become more important.

BASIL™ process

One of the most famous processes using ionic liquids is the BASIL™ process⁶. In 2002 this process to make alkoxyphenylphosphines was started by BASF as the first process using an ionic liquid on industrial scale. A side product of the reaction is HCl, which needs to be neutralised as decomposition of the main product would impend. Commonly applied methods, like adding tertiary amines, fail to work as the result of this neutralisation reaction is a suspension. These cause serious problems in industrial processes by increasing viscosity and thus insufficient mixing of the reactants is the consequence. In big reactors thorough stirring is crucial to avoid hot spots. Furthermore, work up of the products becomes laborious. To circumvent these problems several bases were tested and one base, imidazole, proved to be an efficient HCl scavenger as the salt formed by imidazole and HCl is an organic salt with a melting point around 75°C. This liquid can easily be separated from the reaction mixture as a biphasic system is formed. The upper layer is the product, while the lower layer is the ionic liquid. Another advantage is the catalytical contribution of 1-methylimidazole in accelerating the reaction.



Figure 1.9: BASIL process

Chlorination of 1,4-butanediol

Generally in industry SOCl_2 , PCl_3 or PCl_5 are used as chlorination agents. The major drawback of these compounds is their toxicity in combination with the enormous safety

⁶Biphasic Acid Scavenging utilising Ionic Liquids

efforts to handle them. Alternatively HCl can be employed. Here, however, an unwanted change in product formation can be observed. The unfavourable effect on the reaction outcome is owned to the low nucleophilicity of HCl. Instead of the 1,4-dichlorobutane as the main product, now the monosubstituted alcohol and THF predominate in the product mixture (Figure 1.10).

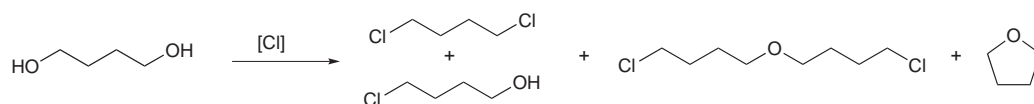


Figure 1.10: Chlorination of 1,4-butanediol

Interestingly the application of an ionic liquid is beneficial to the formation of mainly dichlorobutane. This can be attributed to an increased nucleophilicity of HCl. Seemingly the ether side products are cleaved again and react to the desired product. This conjecture is supported by results reported by Eli Lilly^[79] as it was found that in the presence of a protic pyridinium based salt the cleavage of 4-(4-methoxyphenyl)butanoic acid proceeds smoothly with high yields (Figure 1.11). The use of HBr and boiling acetic acids was disestablished. Solely, this organic salt was able to cleave the ether after two hours at 210°C. This was a remarkable finding as it also helps ionic liquids to be recognised as green solvents and additives, respectively. A predicate that does not necessarily come along with an ionic liquid (more on that topic in the following section).

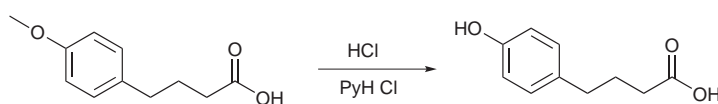


Figure 1.11: Cleavage of aromatic methoxy ethers

Ionic Liquids in tinting systems

Degussa developed a so far unusual application for ionic liquids. Generally, ionic liquids are seen as solvents, but here its part is different. It acts as a compatibiliser to support colour acceptance and compatibility in tinting systems (Fig-

ure 1.12 on the following page). The addition of an ionic liquid to a pigment paste prevents sedimentation and flocculation. Normally, water-based additives are preferred. These, however, cannot be used in combination with organic solvent-based systems. Here, the unique ability of some ionic liquids is advantageous. This compatibiliser now allows the addition of the pigments to water and organic solvent based paints.

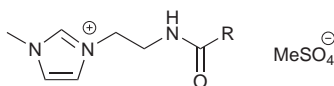


Figure 1.12: Example of an compatibiliser: TEGO[®] Dispers 662C

Ionic Liquids as cleaning fluids

Another unusual application for ionic liquids is as a cleaning agent. To properly clean high-value surfaces micrometer-sized droplets are used. These droplets can be electrostatically charged. To prevent this from happening normally inorganic salts, such as sodium chloride, are added. These salts bear the problem that they can block the nozzles, where the water droplets are formed. Therefore, employing a liquid additive seems to be logical. Wandres Micro-cleaning GmbH replaced NaCl by an ionic liquid and successfully avoids the problem of salt precipitation in the nozzles.

Catalyst immobilisation

One other important application of ILs is their role as reactive phase. As this concept will be amply discussed in the chapters to come, only a brief introduction will be given here. Owing to their polar character, ILs bear the potential to dissolve many ionic substances. Therefore, attaching an ionic tag to a ligand is a promising route to the immobilisation of catalysts. This would enable to close the gap between homogeneous and heterogenous reactions, as the high selectivity of the homogeneous catalyst would be combined with the excellent recyclability of its heterogeneous counterpart. Several groups have used the ionic tag concept successfully for a broad range of catalysts (Figure 1.13 on the next page).^[80] Van Leeuwen *et al.* highlighted the applicability of this

principle for the hydroformylation of 1-octene.^[81] They employed an entirely new ionic liquid, which gave excellent results regarding selectivity and recyclability. The groups of Vogt and Wang *e.g.* independently used ILs for the hydroaminomethylation.^[30,82] An ionic ligand (sulfoxantphos) was applied to 'trap' the ligand in the IL, which served as the reactive phase, while product and substrate formed a second layer on top of the ILs. Apart from enabling catalyst recycling, also the selectivity was improved noticeably. Also other important and well-known reactions became subject to the concept of ionic tagging. Dyson *et al.* successfully tagged Ru-complexes for biphasic hydrogenation reactions in water and ILs.^[83] They demonstrated that recycling was possible with both reactive phases. A very good example of catalyst immobilisation was presented by the groups of Guillemine and Yao.^[84,85] They reported independently on ionic-tagged Grubbs-Ru catalysts used for metathesis reactions. These catalysts were employed in biphasic systems using ILs and they showed high-activity combined with easily recyclability.

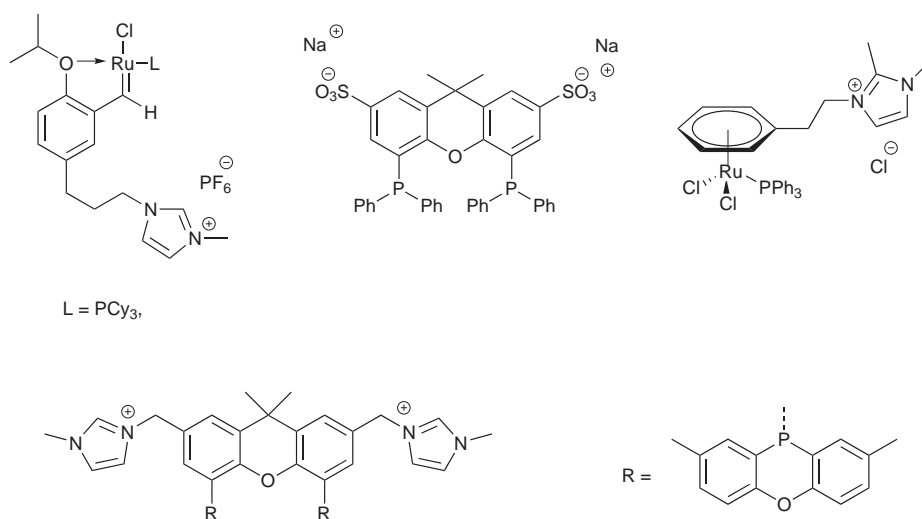


Figure 1.13: Examples of ionic-tagged ligands and catalysts. a) Grubbs-catalyst, b) sulfoxantphos applied by the groups of Vogt and Wang, c) Ru-complex reported by Dyson *et al.*, d) ligand reported by van Leeuwen *et al.*

1.5 How environmentally friendly are ionic liquids?

In the context of Green Chemistry^[86-90] Ionic Liquids are often generically classed as 'green' because of their low volatility.^[5,6] A criterium that, if stand-alone, does not suffice to tag this label to a solvent. This property only stresses that air-born toxicity is negligible but does not give away any conclusion concerning toxicity to the environment, when accidentally or even deliberately released from chemical processes into aquatic environments. Many ionic liquids show high solubility in water and therefore their release can cause potentially severe pollution. Also the process to synthesise ionic liquids must be taken into account. In the beginning of ionic liquid-conceived research hardly any publication centred on this unpopular matter. Only in the last decade, especially in its latest years, several groups focused on the effects of various ionic liquids on the environment, pointing out that these new solvents can have very well noxious and pronounced effects on life forms. Mainly interference with bacteria and marine life was under scrutiny. Especially the popular imidazolium-based ionic liquids^[91-94] along with non- aromatic ionic liquids^[95] were assessed. Rodríguez *et al.*^[96] showed in their Microtox⁷ study that the toxicity effect against *V. fischeri*⁸ of imidazolium-based ionic liquid correlates directly with the alkyl-chain length, an effect also observed by Pham *et al.*^[97] and Ranke *et al.*^[98] by analysing the photosynthetic response of *P. subcapitata*⁹. This effect can probably be attributed to the increasing lipophilic character of the ionic liquids as also other groups have shown.^[99] However, the anion evidently does not have a significant influence. Further, the group of Rodríguez highlighted that the biodegradation of ionic liquids is rather poor. Their persistence in the environment revealed that micro-organisms do not accept them as a carbon source, except for a few examples.^[100] Therefore, an accumulation of ionic liquids in the environment is an issue. However, a major limitation of all these studies so far is that extrapolation of them is not possible. From the effect on e.g. *V. fischeri* it can not be concluded how and if ionic liquids affect other bacteria, e.g. bacteria in waste-water plants, or in ecological systems in general. Along with the assessment of the effects of ionic liquids on lower life forms other studies

⁷standard test procedure (ISO 11348-3, 1998)

⁸*Vibrio fischeri*, a marine bacterium

⁹a photosynthetically active algae

are concerned with effects on phytotoxicity ¹⁰. For *S. quadricauda* and *C. reinhardtii*, two types of algae, it has been demonstrated that the amount of ionic liquid directly correlates to the decrease in growth.^[101] An effect, that as well becomes obvious, when having a closer look to the growth of radish and spring barley.^[102] But also higher life forms are affected by ionic liquids. In *Danio rerio* (zebra fish) evidence of toxicity and histological damage has been found due to exposure to ionic liquids.^[103] Therefore the median lethal concentration LC₅₀ was identified, a value giving away when 50% of the subjects died within a continuous period of exposure of 96 hours. This value was found to be around 100 mg per litre water indicating that already small amounts of ionic liquids in water can have a severe effect on life.

Although these studies do not cover all areas of the environment, it can be stated that the toxic effects of ionic liquids are not negligible and deserve a more thorough investigation, especially concerning the effect on the food chain and on complex ecological systems. In the past, examples have been found that the concentration of a substance in e.g. the sea is of no direct harm to humans, but can become deadly at a later stage. The most prominent case took place in Japan,^[104] where methylmercury toxins accumulated in fish and therefore posed a threat to humans, causing the Minamata¹¹ disease. Nevertheless this last section is not mentioned to denigrate ionic liquids, but to exemplify that categorising substances is not always straightforward. One has to evaluate and balance reasons for the application of ionic liquids. There are always advantages and disadvantages. When employing an ionic liquid in a process, this process does not necessarily become green, but it can be turned into a 'greener' process than its predecessor and even this can be an advance.

In September 2009, an open access database on ILs will be launched containing physical properties and bio-compatibility data: www.il-eco.uft.uni-bremen.de.

¹⁰The effect of toxins on plant growth

¹¹a city in the south-west of Japan

Bibliography

- [1] P. Wasserscheid, *Chem. Unserer Zeit* **2003**, *1*, 52–63.
- [2] T. Welton, *Coord. Chem. Rev.* **2004**, *248*, 2459–2477.
- [3] P. Wasserscheid, W. Keim, *Angew. Chem.* **2000**, *112*, 3926–3945.
- [4] P. Wasserscheid, T. Welton, *Ionic Liquids in Synthesis, Vol. 2*, Wiley-VCH, Weinheim, 2nd ed., **2008**.
- [5] M. J. Earle, J. M. S. S. Esperanca, M. A. Gilea, J. N. Canongia Lopes, L. P. N. Rebelo, J. W. Magee, K. R. Seddon, J. A. Widegren, *Nature* **2006**, *439*, 832–834.
- [6] P. Wasserscheid, *Nature* **2006**, *439*, 797.
- [7] C. Gordon, *Appl. Catal. A* **2001**, *222*, 101–117.
- [8] S. Sugden, H. Wilkins, *J. Chem. Soc.* **1929**, 1291–1298.
- [9] C. Gränacher, *Cellulose solution*, **1934**.
- [10] F. Hurley, T. Wier Jr., *Electrochem. Soc.* **1951**, *98*, 207–212.
- [11] G. W. Parshall, *J. Am. Chem. Soc.* **1972**, *94*, 9716–9719.
- [12] C. G. Swain, A. Ohno, D. K. Roe, R. Brown, T. Maugh II, *J. Am. Chem. Soc.* **1967**, *89*, 2648–2649.
- [13] H. L. Clum, V. R. Koch, L. L. Miller, R. A. Osteryoung, *J. Am. Chem. Soc.* **1975**, *97*, 3264–3265.
- [14] R. Gale, B. Gilbert, R. Osteryoung, *Inorg. Chem.* **1978**, *17*, 2728–2729.
- [15] J. S. Wilkes, C. L. Hussey, *Selection of Cations for Ambient Temperature Chloroaluminate Molten Salts Using MNDO Molecular Orbital Calculations*, Frank j. seiler resarch laboratory technical report, **1982**.
- [16] P. Hitchcock, T. Mohammed, K. Seddon, J. Zora, C. Hussey, E. Ward, *Inorg. Chim. Acta* **1986**, *113*, 125–126.
- [17] A. J. Dent, K. R. Seddon, T. Welton, *J. Chem. Soc. Chem. Commun.* **1990**, 315–316.

- [18] J. A. Boon, J. A. Levisky, J. L. Pflug, J. S. Wilkes, *J. Org. Chem.* **1986**, *51*, 480–483.
- [19] S. E. Fry, N. J. Pienta, *J. Am. Chem. Soc.* **1985**, *107*, 6399–6400.
- [20] Y. Chauvin, B. Gilbert, I. Guibard, *J. Chem. Soc. Chem. Commun.* **1990**, 1715–1716.
- [21] R. T. Carlin, R. A. Osteryoung, *J. Mol. Catal.* **1990**, *63*, 125–129.
- [22] J. S. Wilkes, M. J. Zaworotko, *J. Chem. Soc. Chem. Commun.* **1992**, 965–967.
- [23] Y. Chauvin, L. Mussmann, H. Olivier, *Angew. Chem. Int. Ed.* **1995**, *34*, 2698–2700.
- [24] J. H. Davis Jr., K. J. Forrester, *Tetrahedron Lett.* **1999**, *40*, 1621–1622.
- [25] M. Hasan, I. Kozhevnikov, M. Siddiqui, A. Steiner, N. Winterton, *Inorg. Chem.* **1999**, *38*, 5637–5641.
- [26] J. Holbrey, K. Seddon, *J. Chem. Soc. Dalton Trans.* **1999**, 2133–2140.
- [27] C. Gordon, J. Holbrey, A. Kennedy, K. Seddon, *J. Mater. Chem.* **1998**, *8*, 2627–2636.
- [28] M. J. Earle, P. McCormac, K. R. Seddon, *Green Chem.* **1999**, *1*, 23–25.
- [29] D. Crofts, P. J. Dyson, K. M. Sanderson, N. Srinivasan, T. Welton, *J. Organomet. Chem.* **1999**, *573*, 292–298.
- [30] B. Hamers, P. S. B auerlein, C. M uller, D. Vogt, *Adv. Synth. Catal.* **2008**, *350*, 332–342.
- [31] J. Howarth, K. Hanlon, D. Fayne, P. McCormac, *Tetrahedron Lett.* **1997**, *38*, 3097–3100.
- [32] P. Wasserscheid, A. B osmann, C. Bolm, *Chem. Commun.* **2002**, 200–201.
- [33] W. Bao, W. Z., Y. Li, *J. Org. Chem.* **2003**, *68*, 591–593.
- [34] P. S. Schulz, N. M uller, A. B osmann, P. Wasserscheid, *Angew. Chem. Int. Ed.* **2007**, *46*, 1293–1295.
- [35] R. Gausepohl, P. Buskens, J. Kleinen, A. Bruckmann, C. Lehmann, J. Klankermayer, W. Leitner, *Angew. Chem.* **2006**, *118*, 3772–3775.
- [36] D. Chen, M. Schmitkamp, G. Francio, J. Klankermayer, W. Leitner, *Angew. Chem. Int. Ed.* **2008**, *47*, 7339–7341.
- [37] M. Schmitkamp, D. Chen, W. Leitner, J. Klankermayer, G. Francio, *Chem. Commun.* **2007**, 4012–4014.
- [38] A. Riisager, P. Wasserscheid, R. van Hal, R. Fehrmann, *J. Catal.* **2003**, *219*, 452–455.

- [39] A. Riisager, R. Fehrmann, M. Haumann, P. Wasserscheid, *Eur. J. Org. Chem.* **2006**, 695–706.
- [40] A. Riisager, B. Jorgensen, P. Wasserscheid, R. Fehrmann, *Chem. Commun.* **2006**, 994–996.
- [41] S. Werner, T. Weiss, M. Haumann, N. Szesni, P. Wasserscheid, *Chem.-Ing.-Tech.* **2008**, *80*, 1260.
- [42] J. S. Wilkes, J. A. Levisky, R. A. Wilson, C. L. Hussey, *Inorg. Chem.* **1982**, *21*, 1263–1264.
- [43] R. H. Dubois, M. J. Zaworotko, P. S. White, *Inorg. Chem.* **1989**, *28*, 2019–2020.
- [44] J. Knifton, *J. Mol. Catal.* **1987**, *43*, 65–78.
- [45] P. Bonhote, A. Dias, N. Papageorgiou, K. Kalyanasundaram, M. Graetzel, *Inorg. Chem.* **1996**, *35*, 1168–1178.
- [46] J. D. Holbrey, W. M. Reichert, R. P. Swatloski, G. A. Broker, W. R. Pitner, K. R. Seddon, R. D. Rogers, *Green Chem.* **2002**, *4*, 407–413.
- [47] E. Kuhlmann, S. Himmler, H. Giebelhaus, P. Wasserscheid, *Green Chem.* **2007**, *9*, 233–242.
- [48] K. R. Seddon, S. A., M. J. Torres, *Pure Appl. Chem.* **2000**, *72*, 2275.
- [49] E. Hagiwara, Y. Ito, *J. Fluorine Chem.* **2000**, *105*, 221–227.
- [50] H. Tokuda, K. Hayamizu, K. Ishii, M. A. B. Hasan Susan, M. Watanabe, *J. Phys. Chem. B* **2004**, *108*, 16583–16600.
- [51] H. Tokuda, K. Hayamizu, K. Ishii, M. A. B. Hasan Susan, M. Watanabe, *J. Phys. Chem. B* **2005**, *109*, 6103–6110.
- [52] D. M. Eike, J. F. Brennecke, E. J. Maginn, *Green Chem.* **2003**, *5*, 323–328.
- [53] L. Lopez-Martin, E. Burello, P. Davey, K. Seddon, *ChemPhysChem.* **2008**, *8*, 1753–1754.
- [54] S. Zahn, G. Bruns, J. Thar, B. Kirchner, *Phys. Chem. Chem. Phys.* **2008**, *10*, 6921–6294.
- [55] J. S. Torrecilla, F. Rodriguez, J. L. Bravo, G. Rothenberg, K. R. Seddon, L. Lopez-Martin, *Phys. Chem. Chem. Phys.* **2008**, *10*, 5826–5831.
- [56] J. M. Slattery, C. Daguinet, P. Dyson, T. J. S. Schubert, K. I., *Angew. Chem. Int. Ed.* **2007**, *46*, 5384–5388.
- [57] I. Krossing, J. M. Slattery, C. Daguinet, P. J. Dyson, A. Oleinikova, H. Weingärtner, *J. Am. Chem. Soc.* **2006**, *128*, 13427–13434.

- [58] H. Weingärtner, *Angew. Chem. Int. Ed.* **2008**, *47*, 654–670.
- [59] K. R. Seddon, *Kinet. Katal.* **1996**, *37*, 743–748.
- [60] K. R. Seddon, *Kinet. Katal.* **1996**, *37*, 693–697.
- [61] M. J. Earle, A. Ramani, A. J. Robertson, K. R. Seddon, *Chem. Commun.* **2008**.
- [62] A. Elaiwi, P. B. Hitchcock, K. R. Seddon, N. Srinivasan, Y. M. Tan, T. Welton, J. A. Zora, *J. Am. Chem. Soc. Dalton Trans.* **1995**, 3467–3472.
- [63] H. Stegemann, A. Rhode, A. Reiche, A. Schnittke, H. Füllbier, *Electrochim. Acta* **1992**, *37*, 379–383.
- [64] Y. Shimizu, Y. Ohte, Y. Yamamura, K. Saito, *Chem. Phys. Lett.* **2009**, *470*, 295–299.
- [65] O. O. Okoturo, T. J. Vandernoot, *J. Electroanal. Chem.* **2004**, *568*, 167–181.
- [66] G. W. Meindersma, A. B. de Haan, *Chem. Eng. Res. Des.* **2008**, *86*, 745–752.
- [67] N. Hofmann, A. Bauer, A. Frey, M. Auer, V. Stanjek, P. S. Schulz, N. Taccardi, P. Wasserscheid, *Adv. Synth. Catal.* **2008**, *350*, 2599–2609.
- [68] M. Mutch, J. Wilkes, *Proc. Electrochem. Soc.* **1998**, *98*, 254–260.
- [69] M. Maase in *Ionic Liquids in Synthesis, Vol. 2* (Eds.: P. Wasserscheid, T. Welton), Wiley-VCH, Weinheim, **2008**, pp. 663–687.
- [70] T. L. Amyes, S. Diver, J. P. Richard, F. M. Rivas, K. Toth, *J. Am. Chem. Soc.* **2004**, *126*, 4366–4374.
- [71] R. P. Swatloski, J. D. Holbrey, R. D. Rogers, *Green Chem.* **2003**, *5*, 361–363.
- [72] T. Welton, *Chem. Rev.* **1999**, *99*, 2071–2083.
- [73] L. Starkey Ott, S. Campbell, K. R. Seddon, R. G. Finke, *Inorg. Chem.* **2007**, *46*, 10335–1–344.
- [74] R. R. Deshmukh, R. Rajagopal, K. V. Srinivasan, *Chem. Commun.* **2001**, 1544–1545.
- [75] A. Kovacevic, S. Grundemann, J. Miecznikowski, E. Clot, O. Eisenstein, R. Crabtree, *Chem. Commun.* **2002**, 2580–2581.
- [76] R. A. Sheldon, R. M. Lau, M. J. Sorgedragger, F. van Rantwijk, *Green Chem.* **2002**, *4*, 147–151.
- [77] N. S. Chowdari, D. B. Ramachary, C. F. Barbas III, *Synlett* **2003**, *12*, 1906–1909.

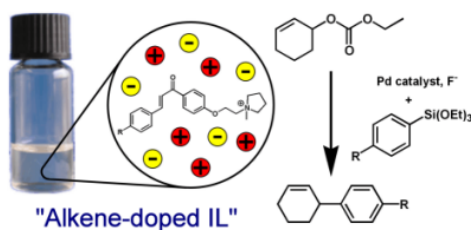
- [78] N. V. Plechkova, K. R. Seddon, *Chem. Soc. Rev.* **2008**, *37*, 123–150.
- [79] C. R. Schmid, C. A. Beck, J. S. Cronin, M. A. Straszak, *Org. Process Res. Dev.* **2004**, *8*, 670.
- [80] R. Sebesta, I. Kmentová, S. Toma, *Green Chem.* **2008**, *10*, 484–496.
- [81] R. P. J. Bronger, S. M. Silva, P. C. J. Kamer, P. W. N. M. van Leeuwen, *Dalton Trans.* **2004**, 1590–1596.
- [82] Y. Y. Wang, M. M. Luo, Q. Lin, H. Chen, X. J. Li, *Green Chem.* **2006**, *8*, 545–548.
- [83] T. J. Geldbach, G. Laurenczy, R. Scopelliti, P. J. Dyson, *Organometallics* **2006**, *25*, 733–742.
- [84] N. Audic, H. Clavier, M. Mauduit, J. C. Guillemin, *J. Am. Chem. Soc.* **2003**, *125*, 9248–9249.
- [85] Q. Yao, Y. Zhang, *Angew. Chem. Int. Ed.* **2003**, *42*, 3395–3398.
- [86] J. H. Clark, *Green Chem.* **2006**, *8*, 853–860.
- [87] J. H. Clark, *Green Chem.* **1999**, 1–8.
- [88] J. H. Clark, S. J. Tavener, *Org. Process Res. Dev.* **2007**.
- [89] J. C. Warner, A. S. Cannon, K. M. Dye, *Environmental Impact Assessment Review* **2004**, *24*, 775–799.
- [90] W. Nelson in *Ionic Liquids - Industrial Applications to Green Chemistry, Vol. 818*, American Chemical Society, Washington D.C., **2002**.
- [91] A. Latala, P. Stepnowski, M. Nedzi, W. Mrozik, *Aquat. Toxicol.* **2005**, *73*, 91–98.
- [92] S. Stolte, M. Matzke, J. Arning, A. Boschen, W. R. Pitner, U. Welz-Biermann, B. Jastorff, J. Ranke, *Green Chem.* **2007**, *9*, 1170–1179.
- [93] C. Samori, A. Pasteris, P. Galletti, E. Tagliavini, *Environ. Toxicol. Chem.* **2007**, *26*, 2379–2382.
- [94] S. Studzinska, B. Buszewski, *Anal. Bioanal. Chem.* **2008**.
- [95] J. Salminen, N. Papaiconomou, R. Kumar, J. M. Lee, J. Kerr, J. Newman, J. M. Prausnitz, *Fluid Phase Equilib.* **2007**, *261*, 421–426.
- [96] A. Romero, A. Santos, J. Tojo, A. Rodriguez, *J. Hazard. Mater.* **2008**, *151*, 268–273.
- [97] T. P. T. Pham, C. W. Cho, J. Min, Y. S. Yun, *J. Biosci. Bioeng.* **2008**, *105*, 425–428.

Bibliography

- [98] J. Ranke, A. Müller, U. Bottin-Weber, F. Stock, S. Stolte, J. Arning, R. Stormann, B. Jastorff, *Ecotox. Environ. Safe.* **2007**, *67*, 430–438.
- [99] R. P. Swatloski, J. D. Holbrey, S. B. Memon, G. A. Caldwell, K. A. Caldwell, R. D. Rogers **2004**, 668–669.
- [100] S. Morrissey, B. Pegot, D. Coleman, M. T. Garcia, D. Ferguson, B. Quily, N. Gathergood, *Green Chem.* **2009**, *11*, 475–483.
- [101] K. K.J., G. Lamberti, *Green Chem.* **2008**, *10*, 104–110.
- [102] P. Baczewski, B. Bachowska, T. Biaas, R. Biczak, W. M. Wieczorek, A. Baliska, *J. Agric. Food Chem.* **2007**, *55*, 1881–1892.
- [103] C. Pretti, C. Chiappe, D. Pieraccini, M. Gregori, F. Abramo, G. Monni, L. Intorre, *Green Chem.* **2006**, *8*, 238–240.
- [104] M. Harada, *Crit. Rev. Toxicol.* **1995**, *25*, 1–24.

Ionic π -acidic alkene ligands in Pd(0)-catalysed Hiyama cross-coupling reactions

Collectively, palladium-catalysed cross-coupling reactions constitute some of the most applied and versatile tools in organic synthesis, e.g. natural product, pharmaceutical target synthesis and drug discovery. They have been applied in many solvents including ionic liquids. Nevertheless, research on these C-C-coupling reactions in ionic liquids is still in the fledging states and the advantages of ionic liquids have not yet been fully recognised, especially in case of the Hiyama cross-coupling. Also the use of alkene ligands such as dibenzylidene acetone or chalcones is neglected. In this chapter the application of 'doped' ionic liquids in the Hiyama cross-coupling will be discussed. New π -acidic ionic alkene ligands were synthesised and immobilised in these organic salts.



P.S. Bäuerlein, I.J.S. Fairlamb, A.G. Jarvis, A.F. Lee, C. Müller, J.M. Slattery, R. Thatcher, D. Vogt, A. Whitwood, *ChemCommun.* **2009**, accepted.

2.1 Introduction

Alkene ligands in Pd-catalysed cross-coupling reactions

Collectively, palladium(0)-catalysed cross-coupling reactions, like Suzuki, Stille, Negishi, Sonogahira, Kumada and Hiyama (Figure 2.1) constitute some of the most applied and versatile tools in organic synthesis,^[1-7] e.g. natural product, pharmaceutical target synthesis and drug discovery.^[8]

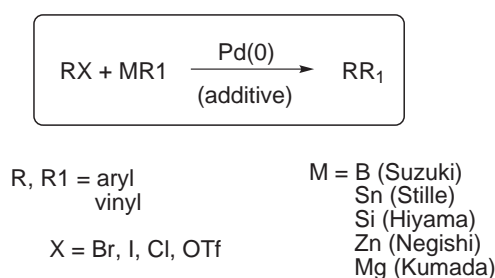


Figure 2.1: Pd-catalysed C-C Bond formation

Their popularity originates in their ability to be easily applicable and their tolerance to a widely spread number of functional groups. This qualifies them to be employed in the synthesis of highly complex molecules, e.g. dehydrotubifoline or phomactin A (Figure 2.2).^[9,10]

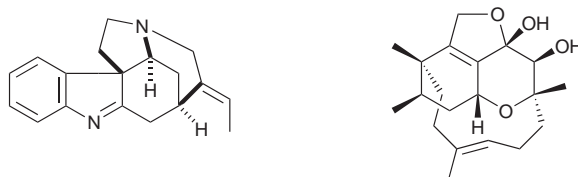
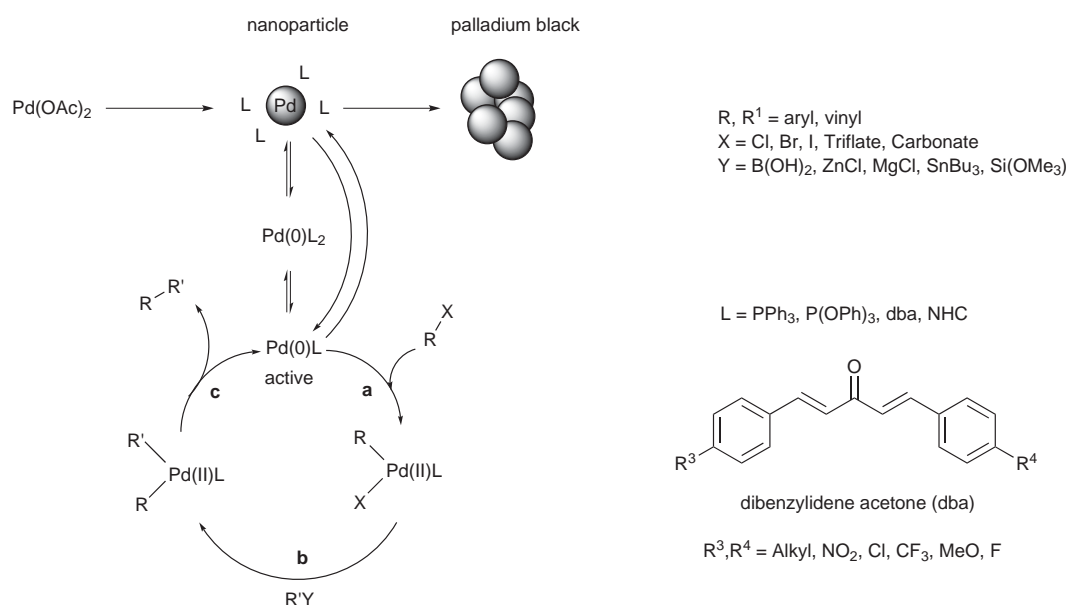


Figure 2.2: Natural products: From left to right: dehydrotubifoline and phomactin A^[10]

Figure 2.3 on the following page shows the generally accepted mechanism. Mainly aryl- and vinylhalides or triflates serve as substrates. These can react with organometallic compounds, generally based on zinc, tin, magnesium, boron or silicon. The former


 Figure 2.3: Generally accepted catalytic cycle for palladium cross-coupling reactions^[1]

two show good reactivity without further activation, whereas the three latter ones need an additive to be reactive in the transmetalation reaction (step b in Figure 2.3). The halides and the organometallic compounds are coupled by a palladium catalyst changing its oxidation states between 0 and II during the course of the reaction. In literature it is assumed that the catalytic cycle starts from a Pd(0) species, being formed *in situ* from a palladium precursor, usually Pd(II) acetate. Next the halide substrate is added oxidatively to the palladium (step a in Figure 2.3). Here the reactivity of the substrate is crucial. Generally by far the most reactive species are aryl- and vinylbromides or iodides. The strength of the C-Cl bond in chlorides often prevents a successful oxidative addition. But as these substrates are numerable and cheap they are attractive substrates. Therefore, activation of these substrates is a prime concern. Meanwhile a lot of progress was made on advancing the catalytic system. Several examples of successful cross-coupling reactions with a wide range of chlorides has been reported.^[1,11]

In the next step, the transmetalation, a nucleophile replaces the halide in the Pd(II) species by an organic group. Here often activation of the organometallic species is required. In the case of the Suzuki and Hiyama reactions the formation of a higher

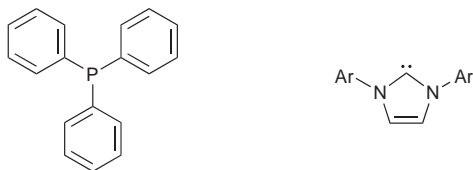


Figure 2.4: Examples of σ -donor ligands. From left to right: triphenylphosphine, NHC

valent complex is necessary to provide sufficient reactivity. The last step of the catalytic cycle involves the reductive elimination of the product closing the circle by regenerating the Pd(0) species. In this kind of reactions predominantly strong σ -donor ligands such as phosphines or carbenes (Figure 2.4) are employed and therefore in the beginning mainly their optimisation is made progress with, especially to enable the application of chloride compounds.

Meanwhile their effects on the catalytic activity are amply investigated. However, for long the research on other types of ligands has lagged behind. The importance of π -acceptor ligands, such as dba (dibenzylidene acetone, Figure 2.3 on the preceding page), has just recently been realised and these ligands have meanwhile emerged as exceedingly important in cross-coupling reactions.^[12] It became obvious that they can have pronounced effects on the outcome of coupling reactions, as they interact both with the Pd(0) and Pd(II) species, that are involved in the catalytic circle. Two ways of interaction can be discriminated. In case of the Pd(0) predominantly the alkene ligand acts as a π -acceptor, because of the π -basic properties of Pd(0). For the Pd(II) the alkene ligand becomes a π -donor. Due to this interactions the alkene ligands can have considerable effects on the elementary steps in the cross-coupling reactions. Firstly, the alkene ligands can stabilise nanoparticulate and mononuclear Pd(0) preventing the formation of palladium black. Secondly the rate of the elementary steps, oxidative addition and reductive elimination, can be altered significantly by the nature of the alkene ligands. This modification can be reached *e.g.* by changing substituents in the aryl moiety of the dba ligands. By this the electronic properties of the alkene part are controlled. The oxidative addition is slowed down when a π -acidic ligand is attached to the metal in comparison to a σ -donor ligated palladium species. Hence, the rate of the reductive elimination increases when employing alkene ligands. This effect seems to be counterpro-

ductive regarding the goal to ease the oxidative addition of halides to Pd(0). However, this effect adjusts the rate of the oxidative addition to the rate of the transmetalation. As a consequence the overall concentration of Pd(II) is kept to a minimum, which otherwise could lead to unwanted side reactions (e.g. homocoupling). The modification of the ligand by changing substituents or functional groups can further shape the influence of the ligand on the elementary steps.

Fairlamb *et al.* have highlighted, using the example of functionalised dba ligands, the influence of the substituents on the Suzuki-Miyaura coupling reaction. They decided to investigate the influence of the functionalised ligands on the Pd-catalysed reaction of 4-chlorotoluene with phenylboronic acids. They could show that electron withdrawing substituents slow down the reaction whereas electron donating ones have the opposite effect. From their investigation on dba ligands the following reactivity can be concluded: MeO > CF₃ > NO₂.^[13] Also calculations of the electron density of several dba ligands support that observation. The HOMO and LUMO orbitals of MeO-functionalised ligands have the highest electron density in contrast to CF₃.^[14] Figure 2.5 on the next page shows the HOMOs for 4,4'-MeO-dba and 4,4'-NO₂-dba.

It becomes obvious that the MeO-dba has a higher electron density than the NO₂-dba. Apart from an influence on the elementary steps it can be observed that electron rich alkenes do not bind that strongly to the palladium in comparison to electron poor alkenes, which have a more pronounced interaction. This effect can have a significant influence on the reaction rate. The stronger the ligand is bound to the palladium the higher the chance that the Pd(0) is fully ligated and not active in catalysis. However, the stronger a ligand can bind, the more effectively palladium is shielded and unwanted accumulation to catalytically inactive palladium black is prevented.

Hiyama-reaction

The Hiyama reaction^[6,15,16] is one of many cross-coupling reactions, but by far the less investigated one, especially concerning their application in ILs. Whereas reactions such as Suzuki and Heck reactions have been investigated amply,^[17,18] more research on Hiyama reaction still needs to be done. This is surprising, as this reaction is a powerful tool for C-C-coupling, using non-toxic and easily accessible siloxane substrates.^[15] In

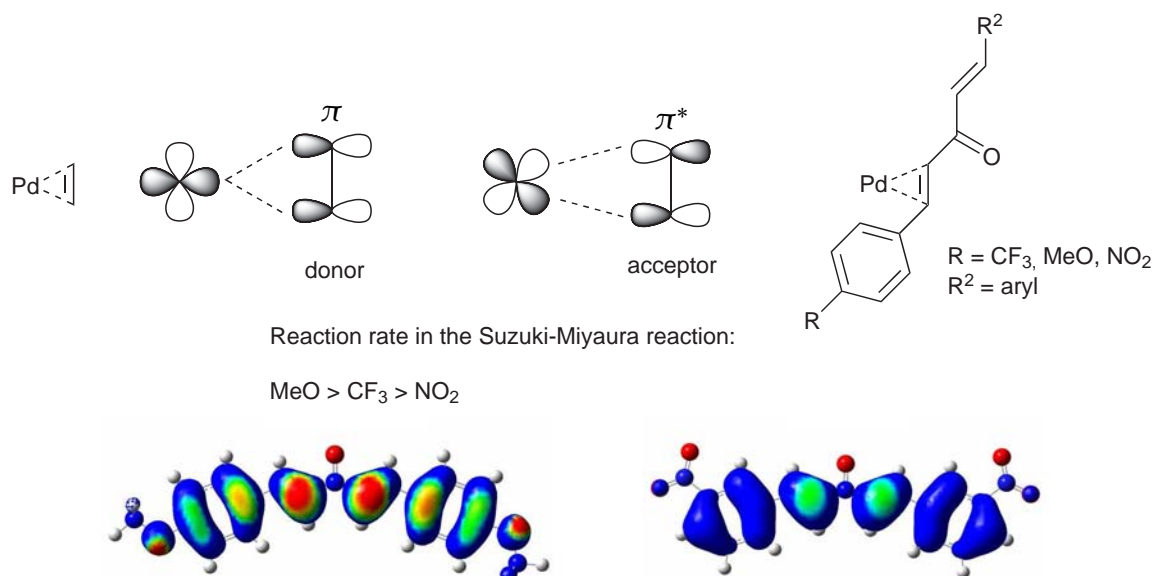


Figure 2.5: Above: π -bonding in Pd alkene complexes^[13]; Below: electron density of a MeO (left) and a NO₂ (right) dba-ligand. Red areas are electron-rich.^[14]

the Hiyama coupling the reaction between halides and siloxanes is mediated by Pd(0) (Figure 2.6). Latter need activation by a fluoride source to be transformed into the active hypervalent Si-compound. Usually TBAF or CsF are applied, but meanwhile also fluoride-free Hiyama reactions are known.^[19] In the Hiyama reaction, too, usually σ -donors are predominately employed. Only recently Denmark *et al.* left the commonly walked path and applied π -acceptor ligands, such as dba, in this kind of coupling reaction and achieved promising results. They also highlighted the problematic in removing these apolar ligands from the product due to their similar physical properties.

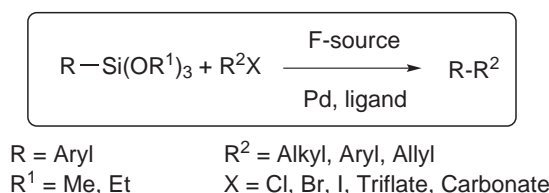


Figure 2.6: General reaction equation of the Hiyama reaction

Aim of this research

It can be said in general, that one of the main drawbacks of applying alkene ligands in cross-coupling reactions is the fact they often share similar polarities to the desired products. This complicates product purification enormously as the separation process is laborious. As mentioned before, Denmark *et al.* showed this problem using dba ligands in an elegant study.^[20] They investigated the palladium-promoted coupling reaction of aromatic bromides with allylic silanolates and realised that increasing the amount of ligand can complicate product purification. Therefore, in this chapter the synthesis of new π -acidic alkene ligands with an ionic tag will be described. This approach is expected to address the problem of product separation in an elegant way by altering the catalyst with respect to its physical properties. Ligands and products will no longer share similar properties, hence separation should become straightforward. As solvent for this new class of ligands ionic liquids (ILs) were chosen as they are expected to help separating ligands and products by keeping the ligand 'locked in'. This concept of doping an ionic liquid with catalysts has emerged as a fruitful and valuable concept of catalyst immobilisation in many reactions before already.^[21] Up to this moment, this technique is adapted to well-established reactions such as hydroformylation, hydroaminomethylation or olefine metathesis reactions. For example in case of the rhodium or rhenium-catalysed metathesis remarkable results were achieved. Guillemine and Yao reported independently on catalysts, that showed high activity and were conspicuously recyclable. Apart from this approach, another way is the immobilisation of catalyst on dendric structures by 'clicking' the ligand to these weight-enlarged molecules. This method allows easy catalyst recovery in combination with excellent conversion and selectivity for the Suzuki coupling reaction.^[22]

2.2 Synthesis of ionic π -acidic alkene ligands

The synthesis was achieved using standard and modified procedures to yield the desired ligands. Three different classes of alkene ligands were synthesised. The first class are functionalised chalcones. The next one includes an acetobenzylidene group as framework. Therefore two basic chemicals, cinnamic acid and styryl methyl ketone, were modified.

The third class is a functionalised asymmetric dba-ligand.

Chalcone-based ligands

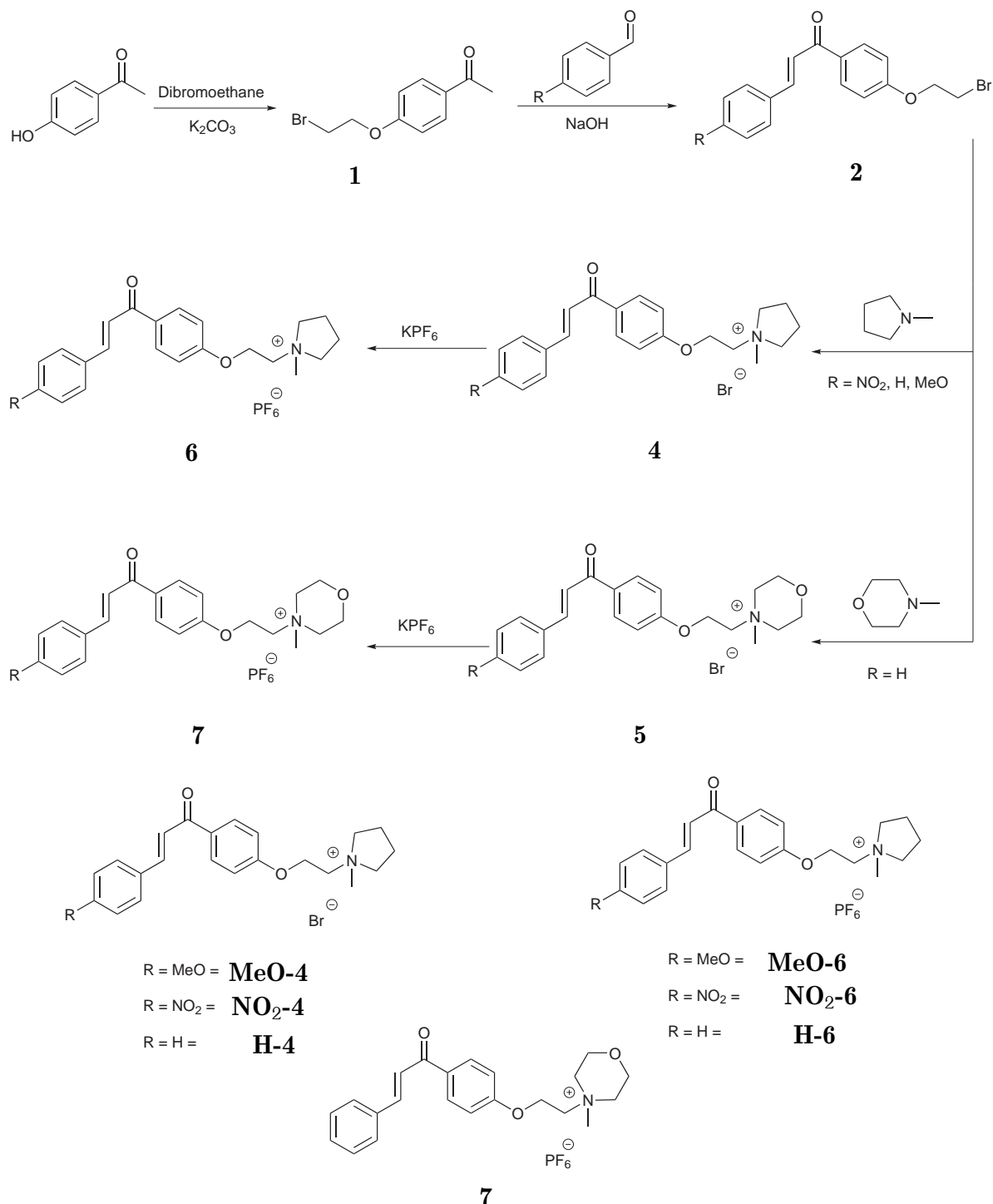
2.2.0.1 Approach using 4-hydroxyacetophenone

Chalcone-based π -acidic ligands can be synthesised in a four-step synthesis (Scheme 2.1 on the next page). The first step deals with the functionalisation of the acetophenone building block. This part of the molecule has been chosen as the carrier of the ionic group, as functional groups in the benzaldehyde part can be used to tune the electronic properties of the π -system.

In the first reaction the acetophenone part was synthesised from 4-hydroxyacetophenone and dibromoethane. As solvents ethyl acetate, acetone and 3-pentanone have been tested. Only the pentanone gave high yield (80%) after 16 h reaction time, as here a reaction temperature of 100°C could be reached. In the case of acetone and ethyl acetate the yield was considerably lower after 16 h reaction time. Further an excess of dibromoethane and vigorous stirring was crucial to avoid formation of the double substituted bromoethane. In addition the use of potassium carbonate instead of sodium carbonate was of the essence. Application of sodium carbonate caused a very low yield. Next the 4-bromoethoxyacetophenone **1** and the benzaldehyde derivative were transformed into a chalcone **2** by a Claisen-Schmidt condensation. Here the choice of solvent was of the essence. Whereas the condensation of **3** with the unfunctionalised benzaldehyde could be performed in an alkaline mixture of water and ethanol, the use of water in combination with the functionalised benzaldehydes turned out to be problematic regarding purification.

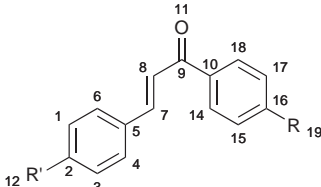
Removal of water from the products could only be achieved with great effort and loss of products. Therefore the reaction has to be conducted in a methanol/ethanol mixture. The functionalised product **2** could later be collected by filtration and purified by washing with methanol. In all cases the yield was higher than 85%. Further purification was possible, if necessary, by recrystallisation from hot ethanol. Subsequently these chalcones **2** were dissolved in warm toluene (80-90°C) and *N*-methylpyrrolidine or *N*-methylmorpholine respectively were added to introduce the ionic group by quaternisation of the nitrogen. The solution was stirred for 16 h and after completion white

2 Ionic π -acidic alkene ligands in Pd(0)-catalysed Hiyama cross-coupling reactions



Scheme 2.1: Synthesis of the chalcone-based ligands **4,6** and **7**, the six ligands depicted below are synthesised via this route

solids could be collected. Washing several times with ether removed the remaining amine. The yield of the salts **4** or **5** respectively was about 60 up to 70%. The products, however, were hygroscopic. A common condition of organic bromides. Therefore the bromide was exchanged for hexafluorophosphate, an anion, which is known to form water repelling organic salts.^[23] The bromides were dissolved in water and a solution of potassium hexafluorophosphate was added. Immediately a white precipitate was formed. This was collected and washed with water. In this step the yields of the pyrrolidinium ligands **6** and the morpholinium ligand **7** were excellent (90%). All compounds were fully characterised by ^1H , ^{13}C and ^{19}F NMR-spectroscopy. Single crystals, suitable for X-ray analysis, were obtained for compounds **6**, **MeO-4** and **H-4** by recrystallisation from a DCM/diethyl ether mixture at 4°C . Selected bond length and angles are listed in table 2.1 and the molecular structures in the crystal are shown in figures 2.9, 2.8, and 2.7.

Table 2.1: Selected bond length and angles for 4'-methoxychalcone, **MeO-4**, **H-4**, **H-6**


Bond / Å	4-methoxychalcone ^[24]	MeO-4	H-4	H-6
C7-C8	1.333	1.337(3)	1.342(4)	1.326(6)
C8-C9	1.490	1.477(3)	1.481(4)	1.484(6)
C9-O11	1.228	1.230(2)	1.235(3)	1.234(5)
C9-C10	1.468	1.489(3)	1.486(4)	1.479(6)
Angle / °				
C1-C2-C3	119.56	119.91(17)	120.2(3)	118.8(5)
C14-C10-C18	117.95	118.37(17)	120.6(2)	119.7(4)
C15-16-17	118.51	120.45(17)	118.4(2)	117.6(4)
C8-C9-10	119.15	119.44(16)	120.0(2)	118.6(4)
Torsion Ph-Ph	33.3	5.85	5.57	25.56

The ligands were compared for an influence of the functional groups and the counterion on bond lengths, angles and structure. All chalcone salts analysed adopt the *cisoid*

conformation. This is consistent with the majority of the chalcones reported in literature.^[25] The double bond lengths extracted from the crystallographic data do not significantly change, when the substituents are changed in the aryl moieties. The difference in bond length is within the dimension of the error and can therefore not be linked to a possible influence of the ligands on the catalysis. All bond lengths and angles of the enone moiety are similar for all investigated ionic chalcones. In addition, comparison of the neutral 4'-methoxychalcone to ligand **MeO-4** does reveal that introducing the ionic group does not affect the structure in a considerable magnitude. Both angles and bond lengths in the enone part are almost coincident. The only deviation is the angle where the side chain containing the ionic group is introduced. Here the angle is about 2° larger for the ionic chalcone **MeO-4**. However, this might only be a crystal packing effect and does not say anything about the torsion angles in solution. Furthermore, the substituent in the aryl moiety does not have a strong effect on the torsion angle between the two phenyl rings in contrast to the anion. Apparently here the anion does induce - at least in the crystal - a distortion of the molecular structure by twisting the chalcone. In case of the bromide chalcones **MeO-4**, **H-4** and the neutral 4'-methoxychalcone the differences in the aromatic part are not significant. The bond lengths are comparable, as well as the angles. Latter do not deviate significantly from 120° . The only exception are the angles at the substituted parts.

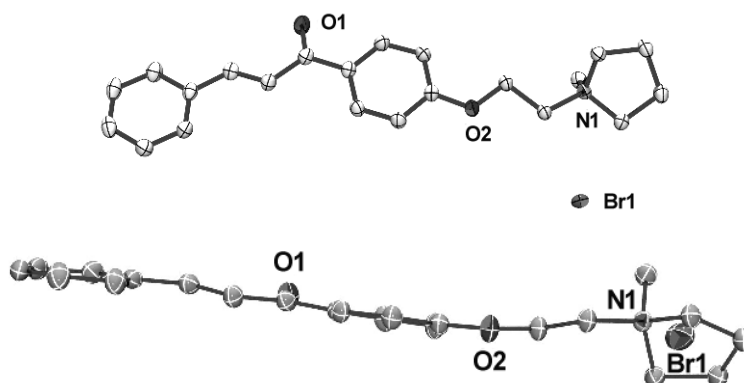


Figure 2.7: ORTEP representation of compound **H-4**. Displacement ellipsoids are drawn at 50% probability level. All hydrogen atoms are omitted for clarity. Above: top view, Below: front view.

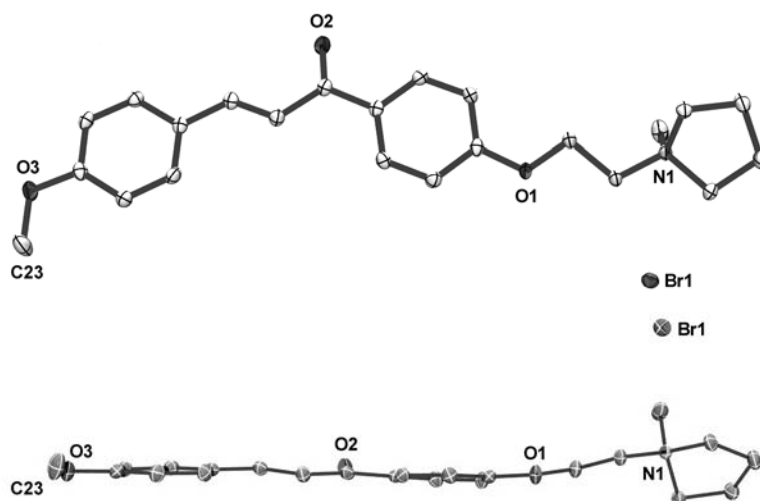


Figure 2.8: ORTEP representation of compound **MeO-4**. Displacement ellipsoids are drawn at 50% probability level. All hydrogen atoms are omitted for clarity. Above: top view, Below: front view.

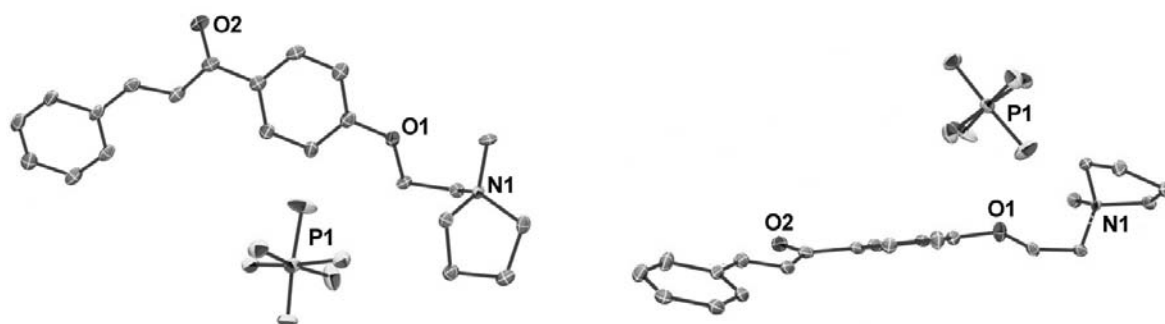
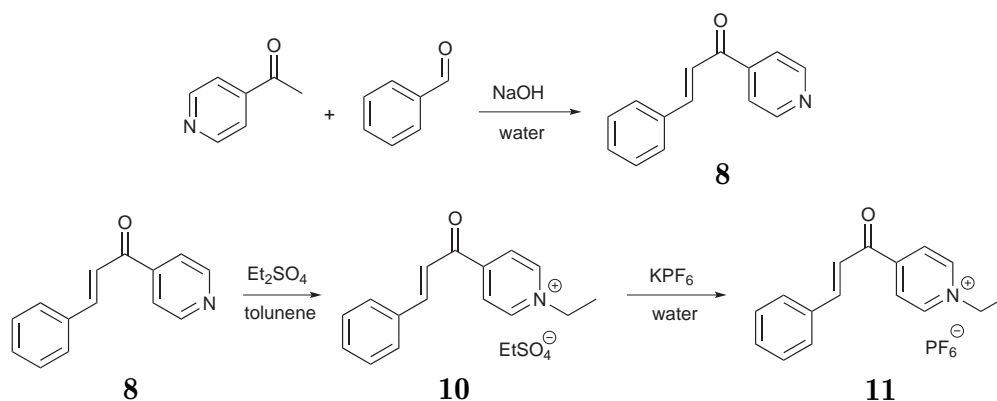


Figure 2.9: ORTEP representation of compound **H-6**. Displacement ellipsoids are drawn at 15% probability level. All hydrogen atoms are omitted for clarity. Left: top view, Right: front view.

2.2.0.2 Approach using 4-acetylpyridine

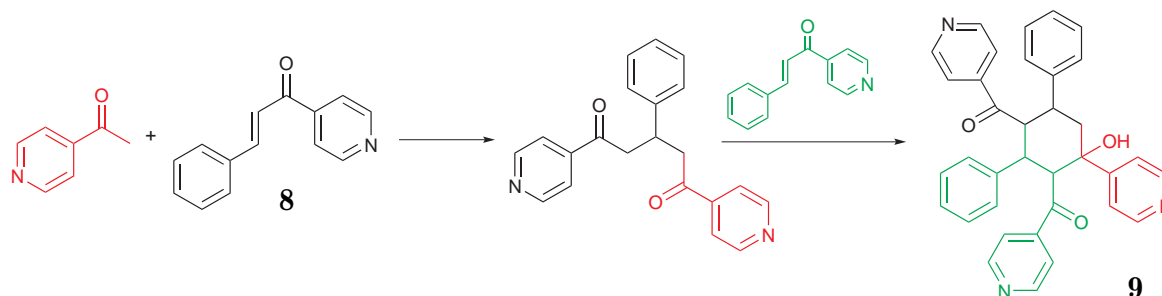
Another approach to introduce an ionic group was tested to reduce the amount of steps in the ligand synthesis (Scheme 2.2).



Scheme 2.2: Synthesis of the pyridinium-based ligand **11**

Starting from 4-acetylpyridine and benzaldehyde a chalcone containing a pyridine moiety was intended to be made. However, applying the same conditions as for the synthesis of the bromoethoxychalcones **2** proved to be a wrong decision as the chalcone **8** became subject to a Michael-type reaction. Immediately reaction with a second acetylpyridine and chalcone **8** in a cascade reaction led to a species that was identified by NMR and MS as the six-membered ring **9** with a mass of 539.62 g/mol. This type of structure was first reported in 1896 by Kostanecki and is a product formed by highly reactive ketones such as 4-acetylpyridine (Scheme 2.3 on the following page).^[26]

To prevent further reaction of the chalcone formed, reaction conditions were varied. However, neither slow addition of the pyridine nor changing the temperature had effect. In all cases the major product was the ring structure. This is interesting, considering that the employment of 2-acetylpyridine results predominantly in the formation of the corresponding diketone.^[27] Obviously, the nitrogen being in *para*-position to the alkene-moiety dramatically increases the reactivity of the chalcone. Two entirely different synthetic routes were tested to tackle this problem. Firstly the pyridine was quarternised. In this case, however, the second step, the Claisen-Schmidt condensation, could not be



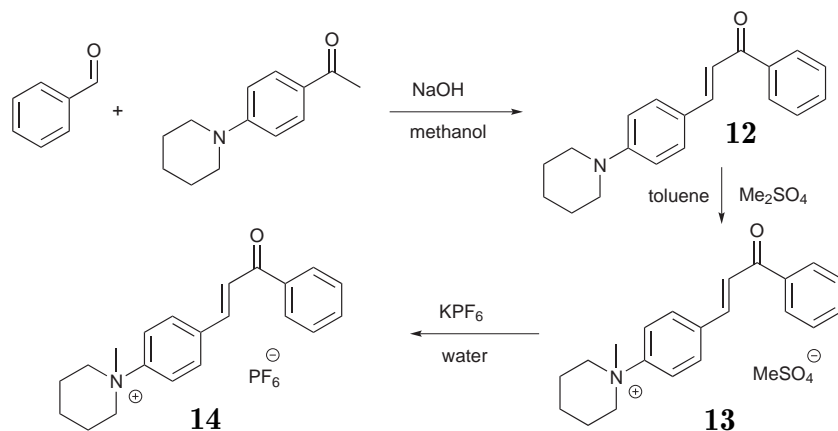
Scheme 2.3: Formation of the cyclic trimer first reported by Konstanecki in 1896

conducted successfully. The alkaline conditions caused a decomposition of the pyridinium salt, as expected. Pyridinium cations show little tolerance towards bases. In another approach both benzaldehyde and 4-acetylpyridine were added in a ratio of 3:1 to a 10 mol% aqueous solution of NaOH to reduce the possibility of the Michael-type reaction. This solution was shaken every 30 min over a period of 2 hours and then left standing at 4°C for 16 hours. A yellow solid was collected. The desired chalcone **8** could be extracted with chloroform. In the last two steps the pyridinium-based chalcone **8** was quaternised and in the resulting ethylsulfate salt **10** the anion was exchanged for PF_6^- to yield the ligand **11**. The ligand was fully characterised by ^1H , ^{13}C , ^{19}F NMR spectroscopy and mass spectrometry.

2.2.0.3 Approach using 4'-piperidinoacetophenone

Another interesting precursor is the piperidin-based chalcone **12** as it could be synthesised easily from basic chemicals by simple condensation of benzaldehyde and 4'-piperidinoacetophenone and carries already a functional group that can be quaternised (Scheme 2.4 on the next page).

However, this step proved to be more complicated. Several alkylating agents were tried to yield the desired ionic chalcone but only dimethylsulfate at refluxing temperature gave the ionic ligand as a red product **12** that was insoluble in toluene (Table 2.2 on the following page). The reason might be the fact that the nitrogen atom is sp^2 -hybridised and therefore, the free electron pair shows a significantly decreased nucleophilicity. Only the highly reactive Me_2SO_4 quaternised the nitrogen. Immediate



Scheme 2.4: Synthesis of the piperidinium-based ligand **14**

dissolving **13** in water and addition of KPF₆ caused the formation of the dark green water insoluble solid **14**. This ligand was washed with water and pentane. The ligand was fully characterised by ¹H, ¹³C, ¹⁹F NMR spectroscopy and mass spectrometry.

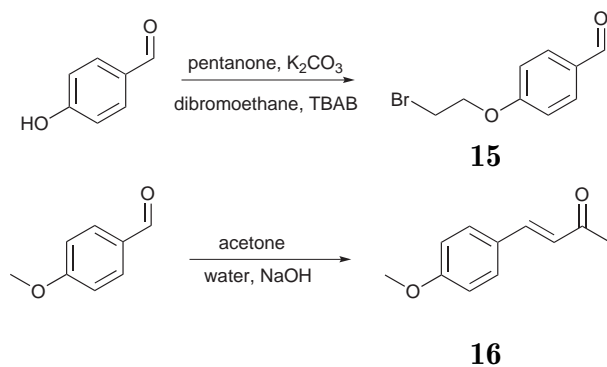
Table 2.2: Tested alkylating reagents for the synthesis of **14**

entry	reagent	time /h	outcome
1	bromoethane	12	no reaction
2	bromopentane	12	no reaction
3	diethyl sulfate	12	no reaction
4	bromoethane	24	no reaction
5	bromopentane	24	no reaction
6	dimethyl sulfate	10	full conver
7	bromooctane	24	no reaction

Conditions: All reactions were performed in toluene at reflux temperature

Ionic asymmetric dba-ligand

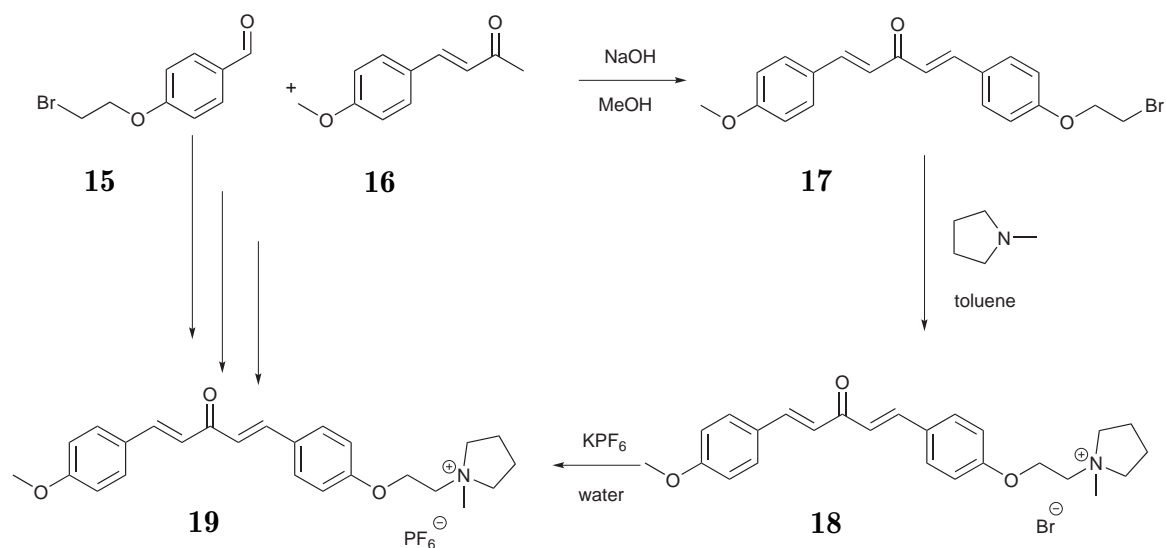
The asymmetric dba-ligand was successfully synthesised via a five-step synthesis (Scheme 2.5).



Scheme 2.5: Synthesis of 4-methoxybenzylidene acetone **16**

In the first two steps the two building blocks, the 4'-bromoethoxybenzaldehyde **15** and the 4'-methoxybenzylideneacetone **16** were made. The benzaldehyde **15** was synthesised by alkylation of 4'-hydroxybenzaldehyde with dibromoethane. Three equivalents of the dibromoethane had to be used to avoid formation of the double substituted ethane. Further the application of TBAB (tetrabutylammonium bromide) was crucial as it catalyses this reaction giving excellent yields (90%) of **15**. Failure to use TBAB resulted in no conversion of the benzaldehyde. The benzylideneacetone **16** was synthesised using the same reaction conditions applied for the pyridinium chalcone **8**. Three equivalents acetone and one equivalent 4'-methoxybenzaldehyde were added to an aqueous 10 mol% NaOH-solution. After completion a yellow solid could be collected. This salt was washed with water to give the benzylideneacetone **16** in reasonable yield (90%).

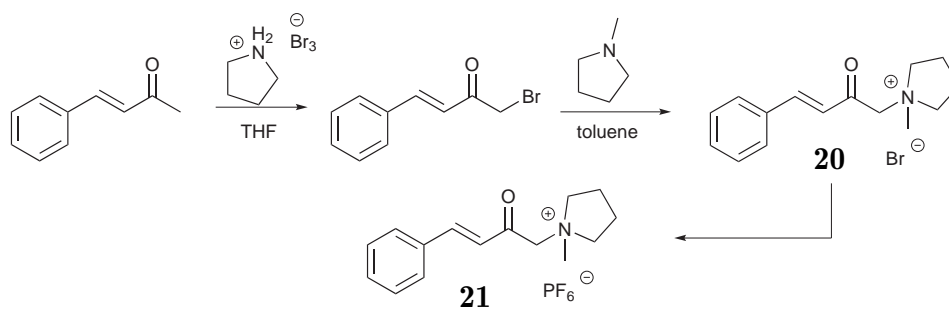
These two building blocks were now combined in a condensation reaction to yield the neutral asymmetric dba **17** (Scheme 2.6 on the following page). This ligand was further reacted with *N*-methylpyrrolidine and the resulting organic salt **18** was subject to a metathesis reaction to exchange the bromide for the less coordinating PF_6^- anion. The desired asymmetric ionic dba ligand **19** was a yellow powder. The ligand was fully characterised by 1H , ^{13}C , ^{19}F NMR spectroscopy and mass spectrometry.



Scheme 2.6: Synthesis of the asymmetric dba ligand **19**

Mono aromatic ligands

Two different precursors have been chosen to serve as framework for the ionic ligands, cinnamic acid and methyl styryl ketone. The latter one was reacted with pyrrolidine hydrotribromide in THF (Scheme 2.7).



Scheme 2.7: Synthesis of benzylidene acetone-based ligand **21**

After one hour the THF was removed and the reaction mixture was subject to a quick column filtration over silica with ether/pentane (1:6) as eluent. The product was immediately concentrated, dissolved in toluene and *N*-methylpyrrolidine was added quickly as

the brominated product changed colour rapidly, indicating decomposition. On addition of the pyrrolidine a white solid was formed instantly and isolated. Subsequently, this bromide salt **20** was dissolved in water and the bromide was exchanged for PF_6^- to yield the desired mono aromatic ligand **21** in an overall yield of about 80%. The ligand was fully characterised by ^1H , ^{13}C , ^{19}F NMR-spectroscopy and mass spectrometry. Furthermore, a single crystal, suitable for X-ray analysis, was obtained for compound **20** by recrystallisation from a DCM/diethyl ether mixture at 4°C . The molecular structure as well as selected bond lengths of this compound are depicted in figure 2.10.

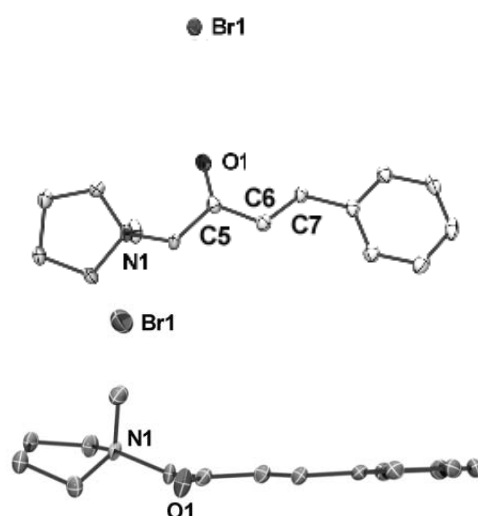
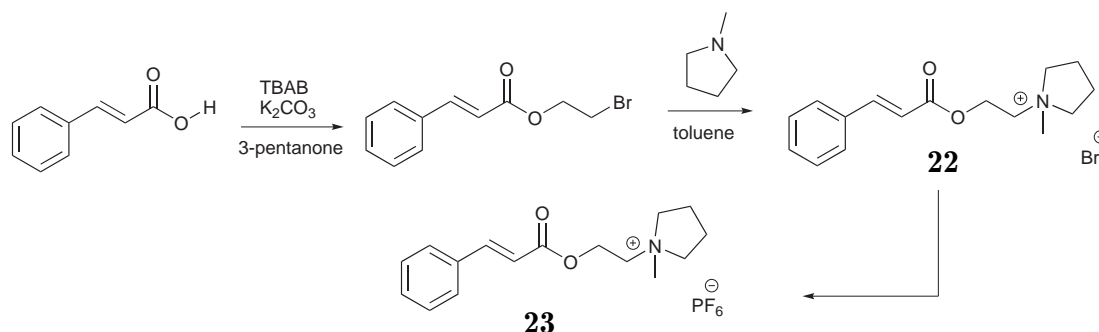


Figure 2.10: ORTEP representation of compound **20**. Displacement ellipsoids are drawn at 50% probability level. All hydrogen atoms are omitted for clarity. Above: top view, Below: front view. Selected bond lengths in Å: C6-C7 = 1.331(3), C5-O1 = 1.213(3).

Comparing the enone part of this ligand to the chalcones (Table 2.1 on page 42) shows that the carbonyl bond is shorter. Also the lengths of the C9-C10 bond do not match. In case of the chalcones it is significantly longer. These effects are probably due to the different nature of the ligand **20**. As the enone part is only linked to one aromatic system its properties are obviously changed. This can indicate that the nature of the ionic tagging can have an influence on the coordinational behaviour in this case. To support this theory the enone double bond of ligand **20** was compared to the one of 4-phenylbut-

3-en-2-one(benzalacetone). It becomes obvious that the close proximity of the double bond to the ammonium moiety in the ligand influences the bond length significantly. The double bond length in the ligand is 1.331(3) Å, whereas it is 1.4990(15) Å in the non-charged enone.^[28] Therefore, the nature of the ammonium part can influence the electronic properties of the double bond in contrast to the chalcone ligands, in which the charge is too remote from the double bond. Cinnamic acid was used as another building block for an alkene ligand. In the presence of four equivalents of dibromoethane the cinnamic acid was reacted (Scheme 2.8).



Scheme 2.8: Synthesis of cinnamic acid-based ligand **23**

In the end the mixture contained two new compounds that were identified as the disubstituted dibromoethane and the monosubstituted dibromoethane. GC revealed that only 20% of the mixture contained the desired compound. As only the monosubstituted one could further react no purification was necessary. The product mixture was dissolved in toluene and *N*-methylpyrrolidine was added. At elevated temperature (90°C) a white solid was formed, that was collected and washed with H₂O and Et₂O. ¹H NMR showed that it was the desired bromide salt **22**. Further exchange of the anion gave the ionic cinnamic acid-based ligand **23**. The ligand was fully characterised by ¹H, ¹³C, ¹⁹F NMR spectroscopy and mass spectrometry.

2.3 Catalysis

As a benchmark reaction for the Pd-catalysed Hiyama coupling the reaction between an alkene carbonate and a triethoxyphenylsilane has been chosen (Figure 2.11).

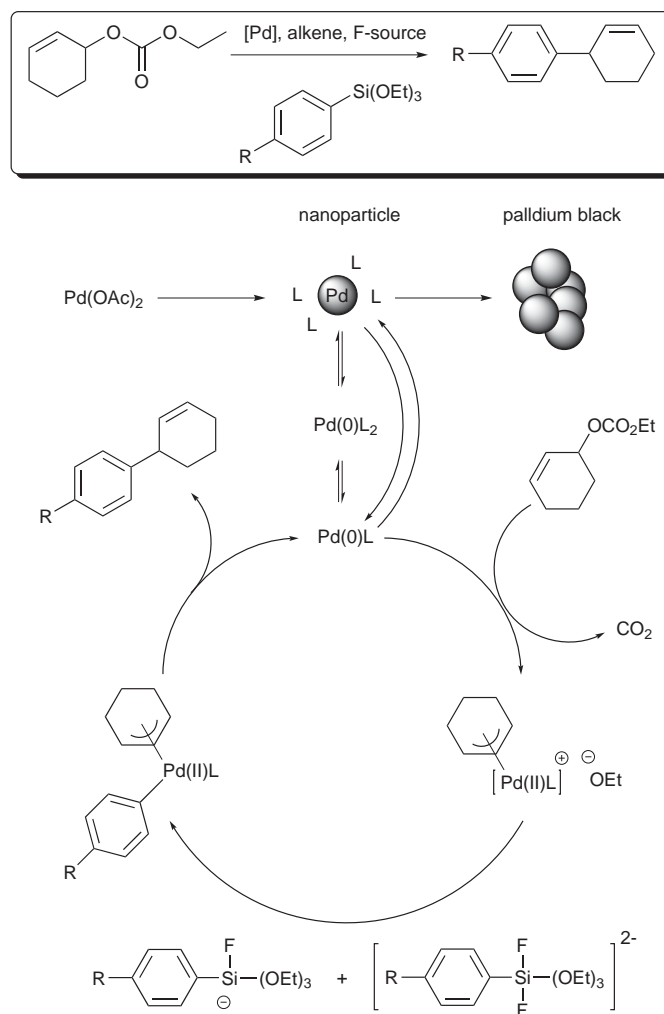


Figure 2.11: Generally accepted mechanism of the Hiyama-coupling^[1,29]

The carbonate was preferred to a bromide to avoid formation of bromide salts during the reaction that could contaminate the catalyst. Furthermore, as nothing is known about Hiyama-couplings in ILs and little is published about C-C-coupling reactions with

alkene ligands in ILs, the Hiyama reaction was investigated using different ILs, fluoride sources, substrates, ligands and catalyst loadings.

Role of the ionic liquid

A rational approach to understand the influence of ILs on the Pd-catalysed Hiyama reaction, is to apply various ILs. Firstly, the reaction with Pd/**H-6** was tested in the commonly used imidazolium-based ILs. However, the reaction failed to work in 1-pentyl-3-methyl imidazolium bis(trifluoromethylsulfonyl) amide ([PMIM][Tf₂N]) completely (Table 2.3).

Table 2.3: Role of the solvent

Entry	Solvent	Outcome
1	[PMIM][Tf ₂ N]	no reaction
2	[PM ₂ IM][Tf ₂ N]	no reaction
3	[MPPyr][Tf ₂ N]	full conversion
4 ^a	water	no reaction
5 ^a	water/THF (2:1)	no reaction

Conditions: 4 mL solvent, 50°C, 0.712 mmol cyclohex-2-enyl ethyl carbonate, 0.142 mmol SiPh(OEt)₃, 2.84 mmol TBAF trihydrate, 8 mol% Pd(OAc)₂, 20 mol% **H-6**, 17h. [a] in this case the bromide ligand **H-6** was used due its better solubility in water

GC analysis did not show any trace of product formation or side products. An explanation could be that the formation of palladium nanoparticles could not be observed. It is well-known that imidazolium cations can oxidatively be added to transition metals and form complexes rather than serving as a stabiliser for nanoparticles (Figure 2.12 on the next page).^[30-32]

In the case of iridium it has been demonstrated that the presence of 1,3-dialkylimidazolium IL significantly suppresses the iridium(0)-catalysed acetone hydrogenation by formation of an inactive Ir(III) species.^[30] In this reaction evidence was found that *N*-heterocyclic carbenes are formed and coordinated to the metal. Evidence also exists that the reaction of imidazolium-based ionic liquids with the metal takes place in case of palladium.^[31,33] These formed carbene complexes can further react and form

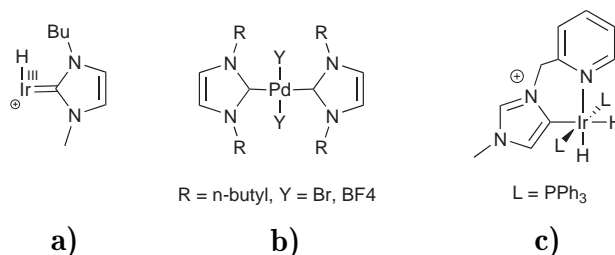


Figure 2.12: Imidazolium complexes

- a) C2-iridium complex by Seddon *et al.*^[30], b) C2-Palladium complex by Srinivasan *et al.*^[31],
c) C5-iridium complex by Kovacevic *et al.*^[32]

palladium nanoparticles. This, however, can only be triggered at elevated temperature (100°C) or by ultrasound. Under the conditions applied (50°C) the palladium is therefore simply deactivated. To circumvent the problem of carbene formation 1,2-dimethyl-3-pentylimidazolium bis(trifluoromethylsulfonyl) amide ([PM₂IM][Tf₂N]) as ionic liquid was used. Intriguingly also in this IL no conversion was observed, despite the fact that the C2-atom did not carry any acidic proton. An explanation for this can be found when looking at the work of Kovacevic *et al.* They demonstrated with iridium complexes that also protons on the C5-atom in the imidazolium are acidic.^[32] Even if this proton is not as reactive as the C2-proton, the vast excess of imidazolium compared to palladium is a reasonable explanation for the effective deactivation of the catalytic system. For the Suzuki reaction Yang *et al.* have demonstrated the nature of the cation is crucial.^[34] They showed that palladium salts can react with the imidazolium cation and form stable salts, suitable for X-ray analysis. They also come to the conclusion that the application of acidic-proton free ILs is beneficial to the reaction. These results underline that the predominance of imidazolium-based ILs in catalysis may be limited under certain conditions. The application of ILs without acidic proton, such as ammonium-based ILs, might in some cases be a necessary step. Therefore 1-methyl-1-pentylpyrrolidinium bis(trifluoromethylsulfonyl) amide ([PMPyr][Tf₂N]) was chosen. As counter ion Tf₂N⁻ was used as pyrrolidinium cations in combination with anions, such as BF₄⁻ and PF₆⁻ do not form liquids at lower temperatures. Their melting points normally exceed room temperature by far and thus they are not applicable. Halide containing ILs were not used to avoid contamination of the catalyst. All reactions described proceed well in the

ligand-doped [PMPyr][Tf₂N]. Obviously the absence of acidic protons is crucial. Another interesting point that needed investigation was the applicability of water in this reaction as a cheap and 'green' replacement of the ILs. Therefore the reaction was conducted solely in water. However, in this case no reaction could be observed. This could probably be assigned to the lack of miscibility of the reactants with the solvent. The reaction mixture was not homogeneous. Also addition of THF as a co-solvent did not have a positive effect on the reaction. In this case the solubility of the ionic ligands is decreased dramatically.

Role of the fluoride source

A crucial step in the Hiyama cross-coupling reaction is the activation of the siloxane substrates. In order to guarantee a successful activation fluoride sources are of the essence. Therefore several sources were investigated in the Hiyama reaction with Pd/**H-6** (Table 2.4).

Table 2.4: Fluoride sources

Entry	Fluoride source	Eq.	Outcome
1	NaF	2	no reaction
2	KF	2	no reaction
3	CsF	2	no reaction
4	CsF	3	no reaction
5	TBAT	2	no reaction
6	TBAF hydrate	2	full conver.
7	TBAF in THF	2	full conver.

Conditions: 4 mL IL, 50°C, 17 h, 0.712 mmol cyclohex-2-enyl ethyl carbonate, 1.42 mmol SiPh(OEt)₃, 2-3 eq. fluoride substrate, 10 mol% Pd(OAc)₂, 20 mol% **H-6**, 17h

Typically TBAF¹ serves as the fluoride source. Especially in the case of the Hiyama reaction in ILs it should be a good activator due to its nature. It is an organic salt and therefore shows excellent solubility in the reaction system. The reaction proceeded smoothly when it was employed. By GC it could be seen that the siloxanes disappear

¹tetrabutylammonium fluoride

within minutes when TBAF was added to the reaction mixture forming the activated hypervalent complexes, as already seen in figure 2.11 on page 52. These two activated complexes were detected by means of mass spectrometry. Two different TBAF sources were tested, a TBAF solution in THF and the TBAF trihydrate. In both cases following the addition of the activator to the IL, the THF and water respectively were removed under reduced pressure at elevated temperature (60°C). Under these conditions a complete removal of water was not possible and also not advisable. In a thorough investigation by Sharma *et al.* it has been demonstrated that the complete removal of water causes decomposition of the TBAF as it becomes subject to Hoffmann elimination.^[35] Tetrabutylammonium, like many ammonium cations, is susceptible to E2 eliminations. Even at room temperature and under water-free conditions TBAF is not stable and copious amounts of HF_2^- and tributylamine contaminate it quickly.^[36]

Both TBAF sources proved to be suitable for the cross-coupling reaction. Comparison of the outcome of the reactions did not show any difference in selectivity or reaction rate. The way TBAF is added does evidently not influence the reaction. The TBAF, however, has some major drawbacks. It is an expensive and highly hygroscopic chemical. Especially the first disadvantage carries a lot of weight. Therefore inexpensive alkali fluorides were tested. Several of these inorganic salts were employed (CsF, NaF, KF). In all cases the solubility in the IL was insufficient. No reaction could be observed, also increasing the number of equivalents from two to three in case of the CsF did not promote the reaction. An activation of the siloxane was not observed. GC analysis showed that the siloxane substrate was still present. There is a strong possibility that this result was owed to the poor solubility of the salts, that could clearly be seen, even though the salts were finely ground. Furthermore, a hypervalent fluoride source was tested. TBAT^2 , a non-hygroscopic organic salt, was employed, but also here the formation of the cross-couple product failed to appear. In this case this may be attributed to an insufficient solubility of the salt, too. Another possibility might be the failure of releasing the fluoride ion from the hypervalent Si-centre due to thermodynamical reasons.

²tetrabutylammonium triphenylsilyldifluorosilicate

Role of the catalyst and substrate loading

Standard conditions in literature describe the use of 10 mol% Pd(OAc)₂ and 20 mol% ligand.^[29,37] As these reaction conditions are apparently the best in classical solvents, this must not necessarily apply for ILs. Therefore the catalyst loading was varied and the outcome after 17 hours reaction time was analysed. It became obvious that the reaction still proceeds smoothly when lowering the catalyst loading from 10 mol% to 4 mol% when using the unsubstituted chalcone ligand **6**. The reason might be that the nanoparticles serve as a reservoir for Pd(0) in solution and that the maximum capacity of dissolved Pd(0) is already reached with the lower palladium amount. Another reason might be that in case of the higher palladium loading, more nanoparticulate Pd is present. However, the particles might be bigger in size due to the higher concentration and a subsequent agglomeration. In order to proof that the formation of nanoparticulate Pd(0) is crucial to this reaction two standard reactions were performed. The reaction conditions in both vials were the same until after 15 min to one of the reaction mixtures a few drops of the catalyst poison CS₂ were added.^[38] After 1 h already a difference in colour was obvious when comparing both mixtures. In the flask with the poison nanoparticulate Pd could not be seen. The mixture was translucent and yellow. The other mixture, however, was dark green, a clear sign for the formation of nanoparticles. GC analysis after 17 h revealed that the CS₂-free system proceeded smoothly with full-conversion. In the other reaction mixture only small amounts of products could be found after 48 h. The marginal conversion might be attributed to the presence of a very small amount of palladium nanoparticles not visible to the naked eye. This outcome suggests that the particles are of the essence and allows the conclusion that the particles take a crucial part in the catalysis. Either the reaction takes place on the surface of the particles rather than by mononuclear palladium or the catalytic cycle commences with the nanoparticulated palladium. The substrate is oxidatively added to a palladium particle and subsequently, a Pd(II) species is released from the particle, coupling the allyl moiety to the aryl part. After reductive elimination, the palladium is reincorporated into a nanoparticle.

To minimise siloxane and TBAF loading the amount of siloxane along with the TBAF was lowered from 2 eq. to 1.5 eq. and 4 eq. to 3 eq. respectively without any loss in yield (Table 2.5 on the following page). Furthermore, GC-analysis gave evidence that

the siloxane is still converted completely into the hypervalent Si-species within minutes after addition of TBAF.

Table 2.5: Siloxane amount

Entry	Silane / Fluoride source	Eq.	Outcome
1	PhSi(EtO) ₃ /TBAF	2 / 4	full conver.
2	PhSi(EtO) ₃ /TBAF	1.8 / 3.6	full conver.
3	PhSi(EtO) ₃ /TBAF	1.5 / 3	full conver.

Conditions: 2 mL IL, 50°C, 0.44 mmol cyclohex-2-enyl ethyl carbonate, 0.66-0.88 mmol SiPh(OEt)₃, 1.24-1.76 mmol TBAF trihydrate, 4 mol% Pd(OAc)₂, 8 mol% **H-6**, 17h

Role of the ligand

2.3.0.4 Comparing different classes of ligands

The influence of the synthesised ionic ligands on the Pd-catalysed cross-coupling reaction was investigated. Thereby, the different ligand classes were compared. Substituent effects of chalcone-based ligands will be investigated and discussed later. Preliminary to the ligand variation the general value of the alkene ligand in the IL was to be proved by conducting the coupling reaction in the absence of these. As anticipated only traces of product were found under these conditions (entry 2 in Table 2.6 on page 60) in contrast to a reaction in which an alkene ligand was applied.

Nevertheless, it was conspicuous that palladium nanoparticles were formed and remained stable for at least several days. These nanoparticles were investigated by means of TEM. Figure 2.13 on the following page shows typical nanoparticles in the presence of a chalcone-based ligand in the IL. The nanoparticles have an average diameter of 2 nm and are spherical-shaped. No agglomeration could be observed for the nanoparticles despite the fact that ligand was absent. This is in accordance with the literature, because it is mentioned that ILs themselves can stabilise nanoparticles sufficiently.^[34,39]

To demonstrate the stabilising effect of alkene ligands on the nanoparticles, two experiments were conducted. Palladium nanoparticles were allowed to be formed by heating of Pd(OAc)₂ in THF, one time in the presence of an alkene ligand and one time in the

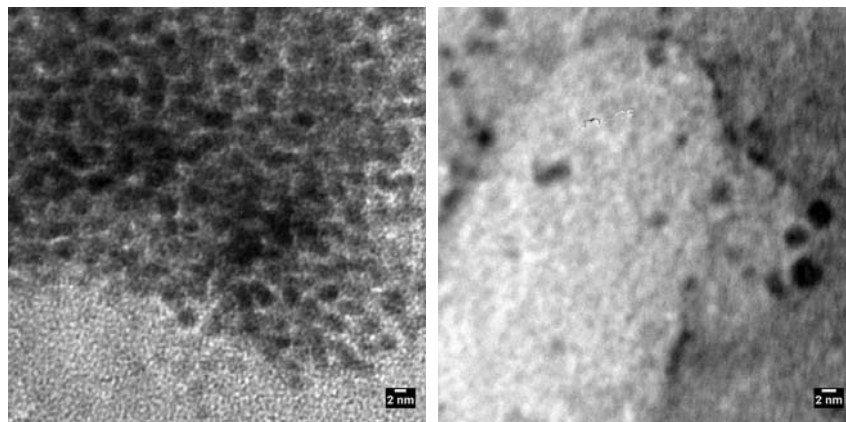


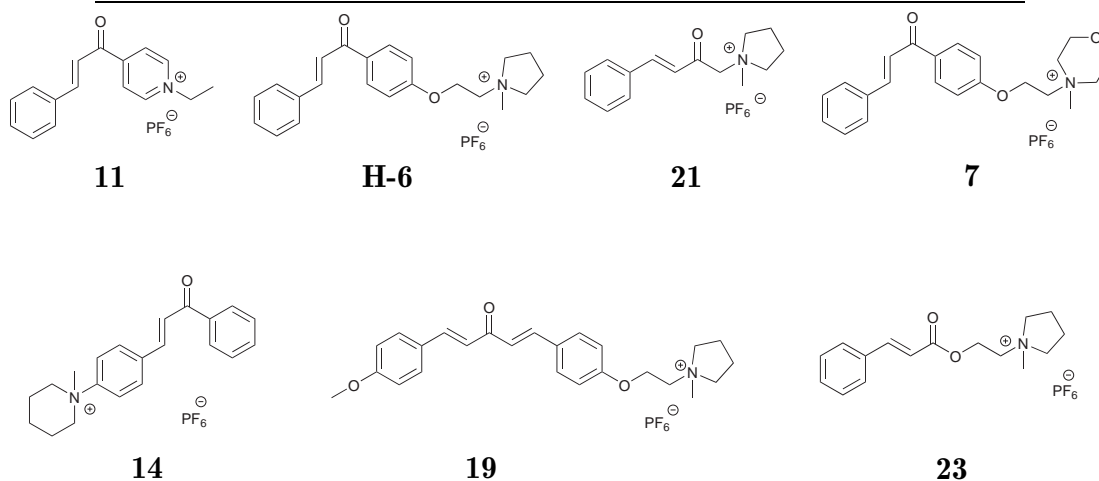
Figure 2.13: 1-3 nm large nanoparticles found in the presence of ligand **MeO-6** after several days.

Conditions: 4 mL IL, 50°C, 17 h, 0.712 mmol cyclohex-2-enyl ethyl carbonate, (1.42 mmol) PhSi(OEt)₃, 2.84 mL TBAF in THF (1 M), 10 mol% Pd(OAc)₂, 20 mol% **MeO-6**

absence. The sample lacking the alkene ligand showed within minutes after formation of nanoparticles agglomeration of the same, whereas in the other one the particles remained stable for weeks without any sign of palladium black. Pd/**21** and Pd/**H-6** showed good activity in the Hiyama cross-coupling (entries 1,3,4). After three hours in all three cases a significant amount of the substrate has reacted and within 17 hours the reaction was almost complete. The reaction with only one equivalent of ligand showed in the beginning a lower reaction rate, indicating that either the oxidative addition is slower or the size of the nanoparticles is bigger. The overall reaction time of 17 hours is in accordance with data obtained from reactions in classical solvents. Strikingly, all the other systems failed to work. Especially, in the case of Pd/**19** this was unexpected as catalysts based on these kinds of ligands are known to show good activity in Pd catalysed reactions. An explanation could be the solubility of the ligand. Nanoparticles were formed but the reaction mixture was not homogeneous. Therefore, the solubility of the ligand in the ionic liquid was tested and it became obvious that the ligand did not dissolve, even at elevated temperatures (70°C). Obviously, the apolar part prevents it from dissolving. This problem, however, could probably be tackled by increasing the side chain in the ionic liquid and hence increase its capability to dissolve less polar compounds.

Table 2.6: Catalytic results using different ligands

Entry	Ligand	Convers. after 3h /%	Convers. after 17h /%
1	21	9	95
2	none	0	traces
3	H-6	14	94
4 ^a	H-6 1 eq.	8	93
5	11	0	0
6	14	0	0
7	23	0	0
8	19	0	0
9	7	0	traces



Conditions: 2 mL IL, 50°C, 0.44 mmol cyclohex-2-enyl ethyl carbonate, 0.71 mmol SiPh(OEt)₃, 1.42 mmol TBAF trihydrate, 10 mol% Pd(OAc)₂, 20 mol% ligand.
a) ligand 10 mol%

Also in the case of the morpholinium based system Pd/**7** reduced solubility could be identified as the possible reason for the failure of the reaction. The pyridinium based system Pd/**11** failed to work due to instability under the conditions applied. It decomposes quickly in the presence of TBAF, thereby turning black. Also the ester ligand **23** did decompose. The ester moiety seems to be fragile under the applied conditions. The turbid reaction mixture indicated a possible instability of the ligand. After a few minutes a white precipitate was formed in the reaction mixture. The outcome of the reaction with the piperidinium based system Pd/**14** could be caused by the positive charge incorporated into the conjugated systems reducing the electron density at the alkene part and hence the ligand is bound too strongly to the palladium. By fully ligating Pd(0) the concentration of the catalytically active species would be diminished.

2.3.0.5 Substituents effects of the chalcone ligands

Several studies have demonstrated that the substituent of neutral dba ligands can have pronounced effects on rates in Pd-catalysed cross-coupling reactions.^[13] Therefore also an effect of substituents in the ionic chalcone-based ligands can be expected (Figure 2.14).

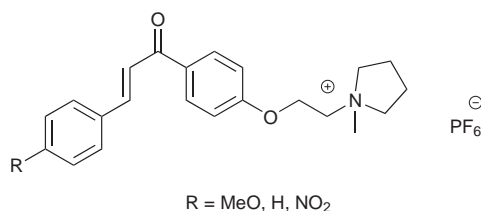


Figure 2.14: Substituted chalcone ligands **6**

The MeO-substituent should increase the electron density on the Pd particles. The opposite effect for is expected NO₂. As rational approach to verify this, three synthesised chalcones NO₂, H, MeO were compared. These ligands should differ in electron density in the alkene moiety and therefore have different effects on the reaction rate. Analytical studies of these three chalcones point out that there is indeed a distinct influence on the electronic properties. Table 2.7 on the following page shows the chemical shifts for protons next to the substituents and the two protons in the alkene part.

Table 2.7: ^1H NMR-shifts of selected protons from chalcone-ligands^a

Entry	Ligand	Aromatic proton / ppm	Alkene proton / ppm	Alkene proton / ppm
1	MeO-2	6.93	7.71	7.37
2	H-2	7.58	7.75	7.49
3	NO₂-2	8.21	7.78	7.61
4	MeO-4	7.13	7.73	7.58
5	H-4	-	-	-
6	NO₂-4	8.23	8.19	7.94
7	MeO-6	7.15	7.73	7.73
8	H-6	7.85	7.93	7.81
9	NO₂-6	8.32	8.13	7.86

a) proton shifts of neutral ligands measured in chloroform, proton shifts of bromide ligands measured in methanol, proton shifts of PF_6^- ligands measured in acetone.

As anticipated, from the electron donating substituent to the electron withdrawing one the protons are shifted downfield. This effect is most pronounced for the proton located closely to the substituent. On the more remote protons at the alkene double bond this effect is weaker, but still obvious. When taking a look at the UV-VIS spectra (Figure 2.15 on the next page) of the ligands **2**, **4** and **6** an impact of the substituents on the absorption can be seen as well. These chromophor groups show a hypsochrome effect. Interestingly, when comparing the spectra of the substituted ligands **2** and **4** seemingly the introduction of the ionic group does not effect the electronic properties of the chalcone (right graph in Figure 2.16 on the following page). The fact that this group is remote from the aromatic system could be an explanation for this observation. This is, however, different for the styryl-based ligand (left graph in Figure 2.16 on the next page). There the introduction of the ionic group changes the absorption frequencies.

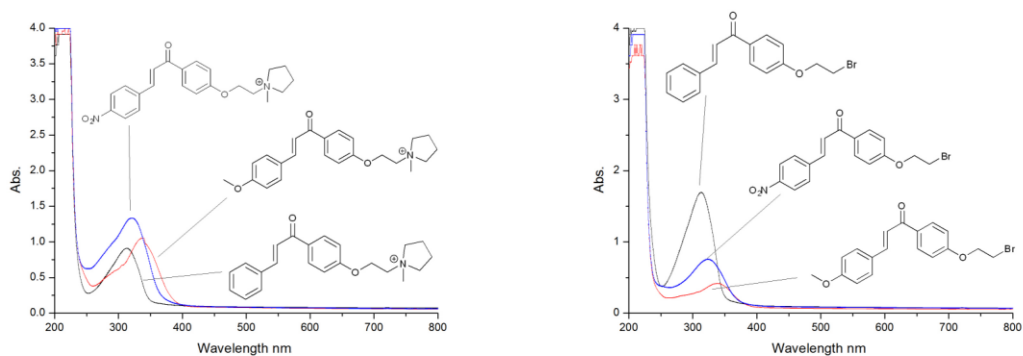


Figure 2.15: Substituent effect on the absorption in the ionic ligand (left) and the neutral ligand (right)

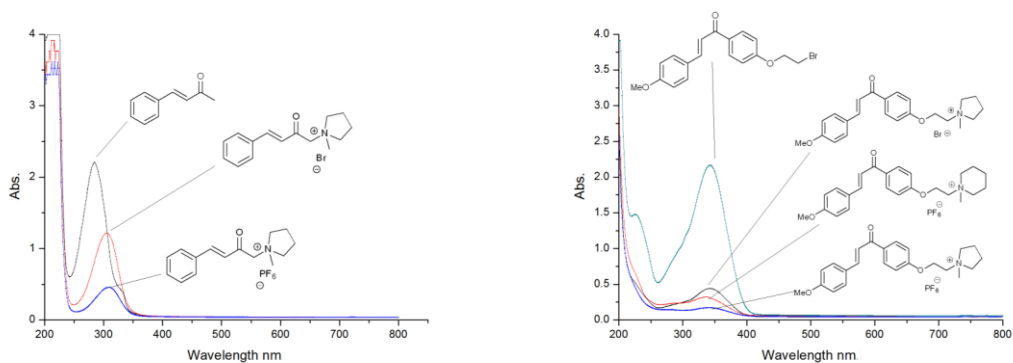


Figure 2.16: Substituent and anion effect on the styryl based ligand (left) and the MeO-based chalcones (right)

The data shown in table 2.8 immediately point out that all three chalcones are suitable for the Pd-catalysed Hiyama reaction. However, there is also evidence that the substituent has a distinct influence on the outcome of the reaction.

Table 2.8: Substituent effects in chalcone-based ligands

Entry	IL	Ligand	t/h	Convers.	Isomers	colour
1	[PMPyr][Tf ₂ N]	NO₂-6	3	9%	n.d.	red
2	[PMPyr][Tf ₂ N]	H-6	3	14%	n.d.	green
3	[PMPyr][Tf ₂ N]	MeO-6	3	17%	traces	green
4	[PMPyr][Tf ₂ N]	NO₂-6	17	27%	n.d.	red
5	[PMPyr][Tf ₂ N]	H-6	17	85%	1%	green
6	[PMPyr][Tf ₂ N]	MeO-6	17	99%	12 %	green

Conditions: 2 mL IL, 50°C, 0.44 mmol cyclohex-2-enyl ethyl carbonate, 0.71 mmol SiPh(OEt)₃, 1.42 mmol TBAF trihydrate, 4 mol% Pd(OAc)₂, 8 mol% ligand.

When looking at the conversion after 3 hours, the system Pd/**NO₂-6** shows a significant difference compared to the system Pd/**H-6** and the MeO chalcone-based system Pd/**MeO-6** under the same conditions, whereas Pd/**MeO-6** has the highest conversion. These results suggest that the electron density at the double bond in the ligand is apparently altered by the substituent and consequently the catalytic activity of the metal centre is changed (Figure 2.17 on the next page).

The electron deficient ligand is bound more strongly to the palladium, thus less catalytically active palladium is most likely available and conversely. A closer look at the conversion after 17 hours reveals that the electron withdrawing group causes a considerable lower yield compared to the other two chalcones. This outcome cannot only be assigned to a lower reaction rate. One possible collateral effect might be the decomposition of the hypervalent silane after a while when it cannot react. Evidence for that was found by GC/MS analysis as a signal, that was assigned to benzene, could be found in the reaction mixture. By contrast, the carbonate substrate is stable in solution. GC/MS analysis also gave evidence for that as no change in the substrate intensity could be observed for several hours. Another explanation can be seen in the stability of the NO₂ ligand **NO₂-6**. Due to electron deficiency in this ligand the double bond is predisposed to Mannich type reaction. This side reaction was observed by

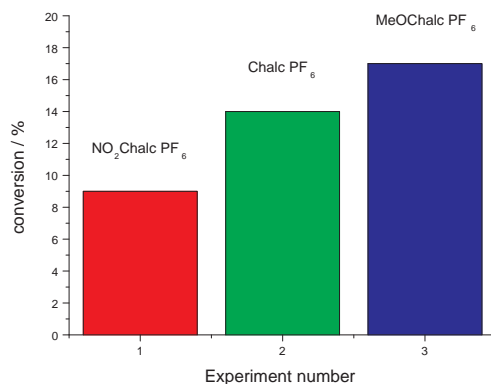


Figure 2.17: Substituent effect on the conversion after 3h reaction time. This figure reflects the data from the table 2.8 on the previous page at 3h reaction time

Conditions: 2 mL IL, 50°C, 0.44 mmol cyclohex-2-enyl ethyl carbonate, 0.71 mmol SiPh(OEt)₃, 1.42 mmol TBAF trihydrate, 4 mol% Pd(OAc)₂, 8 mol% ligand.

¹H NMR spectroscopy in acetone. The ligand decomposed within an hour at room temperature by reacting with acetone.

The fact that the MeO ligand based system Pd/**MeO-6** and Pd/**H-6** differ only 10% in conversion could be owed to the long reaction time as the reaction with Pd/**MeO-6** could have been finished earlier. The fact that in this case the reaction with the electron withdrawing group afforded a higher yield is most likely owed to the higher catalyst loading that has been chosen for these experiments to avoid decomposition of the activated siloxane. Further TEM analysis was performed on colloidal Pd formed *in situ* in these reactions to shed more light on the substituent effect. The size of the nano particles differs significantly. Particles from the reaction mixture with the chalcone **MeO-6** have an average size of 2 nm, whereas those from the **NO₂-6** doped IL have an average size of 15 nm (Figure 2.18 on the following page).

This suggests that the chalcone is directly involved in the particle formation or dissolution. This highlights the importance of substituents in this reaction. The more electron

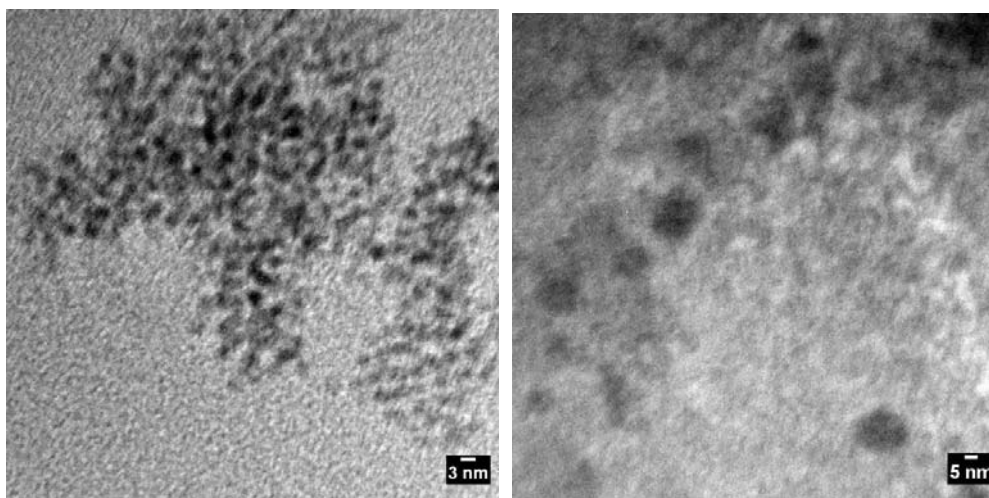


Figure 2.18: Nanoparticles found in the presence of different chalcone-based ligands. The left picture shows the 1-3 nm small particles when **MeO-6** is used. The right picture shows particles with a diameter of 15 nm when **NO₂-6** is applied. Conditions: 4 mL IL, 50°C, 17 h, 0.712 mmol cyclohex-2-enyl ethyl carbonate, (1.42 mmol) PhSi(OEt)₃, 2.84 mL TBAF in THF (1 M), 10 mol% Pd(OAc)₂, 20 mol% ligand.

donating the substituent is, the higher the electron density at the double bond and hence the particles are smaller. The reason for that might be that the stronger π -back donation from the Pd centre to the double bond caused by electron withdrawing substituents may destabilise smaller nanoparticles. More insight into the Hiyama reaction can be revealed by looking at the course of the reaction. Figure 2.19 on the next page displays the product/substrate ratio vs. time for Pd/**MeO-6** and Pd/**NO₂-6**. Both reactions show the same conversion within the first two hours.

Afterwards, however, the reaction catalysed by Pd/**MeO-6** accelerates, whereas the Pd/**NO₂-6** catalysed reaction is noticeably slower. The unusual start for Pd/**MeO-6** can be assigned to the formation of nanoparticles. These are formed *in situ*. Therefore in the first 2 h of the reaction the particles are still formed and the reaction cannot yet reach the maximum rate. Intriguingly the change of the functional group does not only effect the reaction rate, but also the formation of two side products. GC-analysis of the reaction mixture from ligand Pd/**MeO-6** showed two more peaks, that were identified

by GC/MS-analysis as isomers of the cross-coupling product (Figure 2.20).

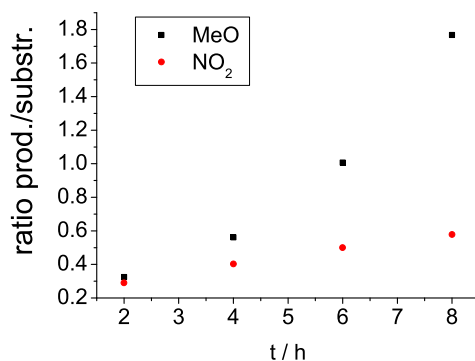


Figure 2.19: Rate comparison of ligand **MeO-6** and **NO₂-6**

Conditions: 2 mL IL, 50°C, 0.44 mmol cyclohex-2-enyl ethyl carbonate, 0.71 mmol PhSi(OEt)₃, 1.42 mmol TBAF trihydrate, 4 mol% Pd(OAc)₂, 8 mol% ligand.

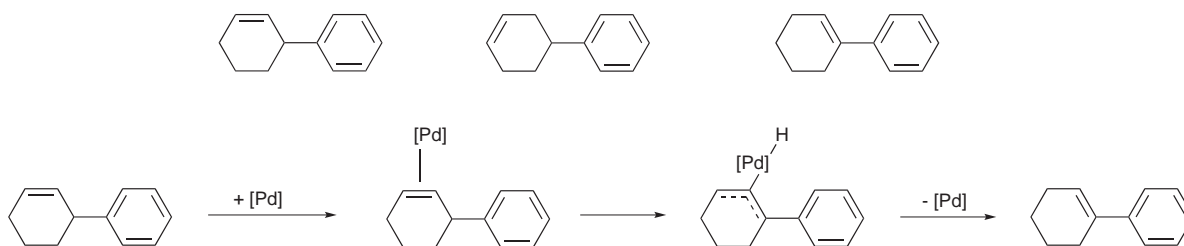


Figure 2.20: Product isomers: The upper picture displays the possible isomers, the lower picture shows the possible mechanism of the isomerisation step

In total 12% of the product mixture are isomers after 17 h reaction time with Pd/**MeO-6**. After 3 h reaction time only traces of the isomers can be found. In contrast to Pd/**MeO-6** the other two ligands Pd/**H-6** and Pd/**NO₂-6**, that have a more electron deficient alkene double bond, show no formation of these isomers. Apparently for this side reaction to occur it is crucial, that the back bond between metal and alkene is of a weak nature. Oxidative addition to an electron-richer metal facilitates the isomerisation.

One other vital question that needed to be answered was the effectiveness of the ionic tag of the ligand. The substrates were extracted from the reaction mixture with Et₂O and were subject to a quick silica column. When analysing the isolated yields by ¹H NMR and ¹⁹F NMR spectroscopy the attention was focused on evidence of ligand contamination. Both spectra did not show that the products were contaminated by ligand. The successful ligand immobilisation in the IL now suggested that these systems bear significant potential for catalyst reuse. Therefore, after the successful extraction of the product with ether, the problem remains that the byproducts formed during the Hiyama reaction remain in the IL increasing the viscosity significantly. To solve this problem, the IL was extracted several times with water as neither the IL nor the catalyst are soluble in water. Afterwards the IL doped with the Pd/**MeO-6** was dried, degassed, new substrate and TBAF were added and the reaction was started again. However, after 17 hours only small amounts of product could be detected by GC-analysis. As neither the GC-analysis nor the fact that no palladium black was formed offered any reasonable explanation, the catalytic system was scrutinised by TEM. Analysing the particle size instantly provided the scale issue as an explanation, as the nanoparticles differed considerably in size (Figure 2.21 on the next page).

The particles after the recycling experiment were considerably bigger (up to 20 times) in size. Before the extraction the average particle size was around 1-2 nm, after extraction with ether particles with a dimension of 20 nm were present. The experiment with the NO₂ ligand **NO₂-6** already showed that the particle size has a major effect on the catalytic activity of the system. Therefore, this result is conform to the other outcome. Apparently the extraction with water causes agglomeration of the particles.

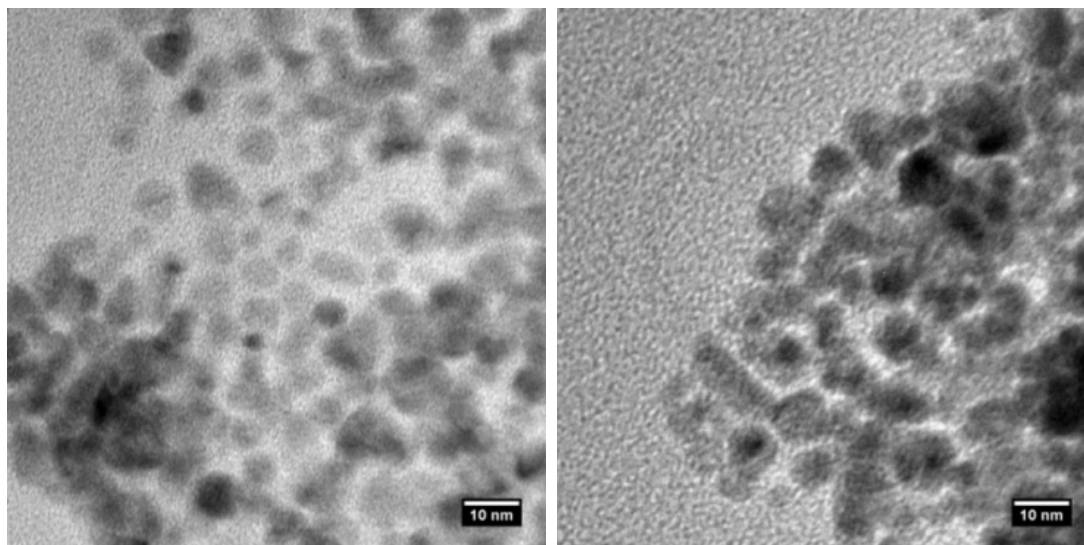


Figure 2.21: Pd-nanoparticles after extraction of the reaction mixture doped with Pd/MeO-6

Role of the substrate

It is known from literature that siloxane substrates with electron withdrawing groups in the aryl moiety enhance the reaction rate while electron donating groups slow the reaction down.^[29] In classical solvents the transmetalation step is rate-determining. Thus, substituents can manifest their influence. In order to investigate these substituents effects in an IL system three different substrates such as triethoxy phenylsilane, triethoxy *p*-tolylsilane and (4-chlorophenyl)triethoxysilane with different electronic properties were tested with Pd/H-6 and the reaction rates were compared (Figure 2.22 on the following page).

A considerable difference in reaction rates was observed, especially between the electron donating group (Me) and the electron withdrawing group (Cl). After 2 hours of reaction time four times as much of the chloro substrate was reacted. After 6 hours the difference between these two substrates rose up to the factor eleven. Comparing relative reaction rates highlights this difference. The reaction rate of the chloro substrate is about seven times bigger than the rate of the methyl substrate. Values measured are comparable to the ones published by DeShong *et al.* in THF.^[29]

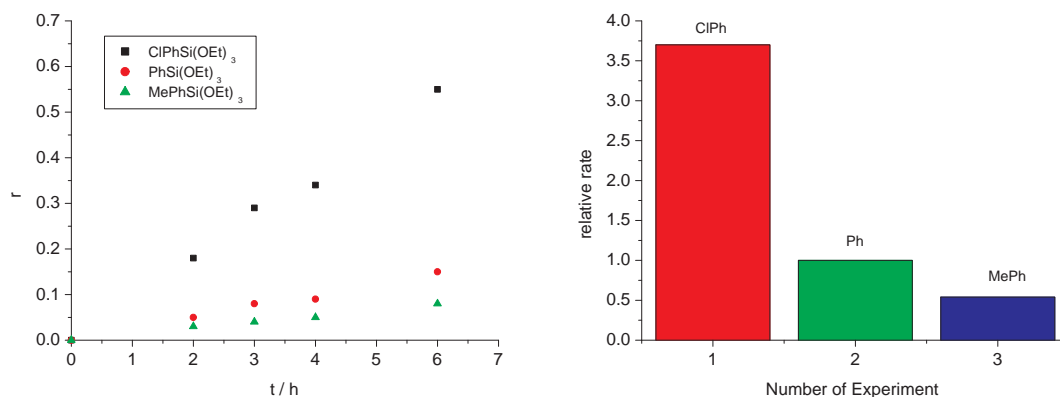


Figure 2.22: Rate comparison of different silane substrates in a one-pot reaction (Competition experiment). The left figure shows the progress of the product formation. $r = \text{product}/(\text{carbonate substrate})$. The right figure gives relative rates received from the gradient of the product formation. They are comparable to results reported by DeShong *et al.*

Conditions: 2 mL IL, 50°C, 0.44 mmol cyclohex-2-enyl ethyl carbonate, 0.71 mmol ArSi(OEt)₃, 1.42 mmol TBAF trihydrate, 4 mol% Pd(OAc)₂, 8 mol% **H-6**.

For the chlorosubstrate they found a value of 3.4 whereas in this study a value of 3.6 was measured. Evidently the IL does not have a significant effect on the transmetalation step. Such an effect would not be surprising as one could expect a more pronounced interaction between the ions of the IL and the hypervalent siloxane than between THF and the activated complex. Examples of ion pair interaction with ILs are numerous in literature. Also a closer look at the conversion at three hours reveals that the chlorosubstrate shows a significantly higher rate than the methylsubstrate (Table 2.9 on the next page). After 3 h 26% of the chloro substrate is converted into the cross-coupling product, whereas only 9% of the methyl substrate have reacted. Even after 23 h reaction time the yield was only 33%.

Table 2.9: Rate comparison of two different silane substrates

Entry	Substrate	Time / h	Conv. / %
1	MePhSi(EtO) ₃	3	9
2	MePhSi(EtO) ₃	23	33
3	ClPhSi(EtO) ₃	3	26
4	ClPhSi(EtO) ₃	23	full conver.

Conditions: 2 mL IL, 50°C, 0.44 mmol cyclohex-2-enyl ethyl carbonate, 1.5 eq. MePhSi(OEt)₃ or ClPhSi(OEt)₃, 3 eq. mmol TBAF trihydrate, 4 mol% Pd(OAc)₂, 8 mol% **H-6**

Substrate variation

Two more substrates were tested to see if these substrates are applicable in the Hiyama cross-coupling with the system Pd/**MeO-6**, *p*-bromo toluene and 3-bromocyclohex-1-ene (Table 2.10).

Table 2.10: Substrate variation

Entry	Ligand	Substrate	Time	Conv. / %
1	MeO Chalc PF ₆	3-bromocyclohex-1-ene	10 min	99
2	MeO Chalc PF ₆	cyclohex-2-enyl ethyl carbonate	17 h	99
3	MeO Chalc PF ₆	<i>p</i> -bromo toluene	17 h	0
4	TPPTS	<i>p</i> -bromo toluene	17 h	40 %

Conditions: 2 mL [PMPyr][Tf₂N], 50°C, 0.44 mmol substrate, 1.5 eq. PhSi(OEt)₃, 3 eq. mmol TBAF trihydrate, 4 mol% Pd(OAc)₂, 8 mol% ligand.

Contrary to expectations the toluene substrate did not show any reactivity. By contrast 3-bromocyclohex-1-ene was highly reactive compared to the carbonate. Within 10 min the substrate was completely cross-coupled. However, this reaction seems to be highly delicate as this substrate easily reacts with nucleophiles in the reaction mixture such as ethoxides released from the silane compound. GC/MS-analysis showed evidence for this. To verify this reaction methanol was added to the reaction mixture and GC/MS provided evidence for the reaction of the bromohexene with methanol. Reproducibility of this reaction was at this stage of the research difficult. As the alkene ligand

MeO-6 could not catalyse the cross-coupling between *p*-bromo toluene and the silane, TPPTS was employed here as well. Amazingly this ligand proved to be the right choice. Although the reaction is rather slow (conv. 40%), the reaction proceeds smoothly. However, the formation of nanoparticles was not observed. Seemingly, like CS₂, TPPTS did prevent the formation of the latter. These results allow the conclusion that the coupling reaction involving alkene substrates needs nanoparticulate Pd to catalyse the reaction, whereas in case of the bromotoluene, mononuclear Pd is the catalyst.

Conclusions

In this chapter the feasibility of ILs in the Hiyama cross coupling reaction was described and evaluated. The results obtained not only support the value of ILs in various organic reactions, but also shed light on the mechanism and the role of substances in the reaction. The data is in accordance with the generally accepted mechanism of the reaction. The experiments with the CS₂ support the fact that palladium(0) is indispensable for the coupling to take place. Furthermore, the rate determining step in the IL is the transmetallation, as has been proved before for classical solvents. In addition, sound proof for the influence of the cation on the reaction outcome has been obtained. The nature of the IL is crucial for the outcome of the reaction. The presence of an acidic ionic liquid is unfavourable for the reaction and application of non-acidic ILs had to be considered.

Another vital question, that has been answered, is the effectiveness of the catalyst immobilisation in the IL. We have demonstrated that the products can easily be separated from the catalysts, 'trapped' in the IL. The research on this reaction in ILs is still in its fledging states and therefore more research needs to be done to get a complete and comprehend picture of the reaction in these unique organic salts. The influence of the alkene ligands has now been demonstrated, but the role of σ -donating ligands still needs to be investigated, as well as ILs of different nature. Most certainly it is beneficial to applicability of this reaction systems, when the rather expensive Tf₂N⁻ anion could be exchanged for a more cost-efficient anion, such as PF₆⁻. This, however, has to come along with the application of a different cation.

2.4 Experimental

All chemicals were purchased from Aldrich, Acros or Merck and used as received. The liquids bought were degassed and the catalytical experiments were carried out under an atmosphere of dry argon or nitrogen using standard Schlenk techniques. NMR spectra were recorded on a Jeol ECX400 or Jeol ECX270 spectrometre, ^1H NMR, ^{13}C NMR were referenced using residual solvent peaks. ^{19}F NMR were referenced externally. Electro-spray ionisation (ESI) and chemical ionisation (CI) MS-measurements were performed on a Bruker microTOF instrument. The ILs were synthesised according to standard literature procedures and characterisation agrees with the literature. The ILs were degassed before being employed. The ligands characterisation data agrees with similar compounds reported in literature. Elementary analysis was performed on a Perkin Elmer 2400 series II CHNS/O Analyzer.

GC Analysis

GC: Shimadzu GC 17A
Column: Ultra 2 (crosslinked 5% Ph Me Siloxane), 25m, inner diameter 0.20 mm
film thickness 0.33 μm
Carrier gas: Helium 102 kPa (total flow 53 mL/min)

TEM details

A JEOL 2011 TEM, operating with a tungsten filament at 120 kV and 125 mA emission was used for all TEM measurement. Samples were prepared by diluting a drop of the reaction mixture in acetone, redispersing via ultra-sonication and mounting this solution on a holey carbon grid (Agar Scientific), which was air dried before being placed in the vacuum chamber. Micrographs were recorded using a Gatan digital camera and Digital Microscope software.

General procedure for the Hiyama coupling

To 4 mL of the IL, 2.84 mL (2.84 mmol, 4 eq.) 1 M TBAF solution in THF was added. The THF was removed in vacuo. To this mixture 121 mg (0.712 mmol, 1 eq.) of cyclohex-2-enyl ethyl carbonate and 342 mg (1.42 mmol, 2 eq.) of the aryl siloxane were added. This was followed by the addition of the ligand (0.1422 mmol, 0.2 eq.) and palladium acetate (0.0712 mmol, 0.1 eq.). The reaction was stirred at 50°C for 20 h. The product was extracted with 50 mL Et₂O and the organic layer was concentrated. The product (cyclohex-2-enylbenzene) was dissolved again in 3 mL ether and was subject to a silica filtration. The ether was removed again to give the product.

¹H NMR (CDCl₃) δ (ppm): 7.22 - 7.20 (m, 2H), 7.15 - 7.13 (m, 3H), 5.80 (m, 1H), 5.65 (m, 1H), 3.32 - 3.31 (b, 1H), 2.08 - 1.84 (b, 3H), 1.70 - 1.55 (b, 3H). **¹³C NMR**: 146.62, 130.43, 128.62, 128.51, 127.95, 126.21, 41.62, 32.33, 24.73, 20.91. **MS**: (m/z) 157.11 [M]⁺.

Cyclohex-2-en-1-ol

To 25 mL (0.241 mol) of 1-cyclohexenone in 100 mL dry THF 4.57 g (0.121 mol) LiAlH₄ was added. The suspension was stirred for 2h. The THF was removed under reduced pressure and the remaining slurry was quenched with MgSO₄ and water. The water layer was extracted with ethyl acetate three times and the organic layer was dried and concentrated.

¹H NMR (CDCl₃) δ (ppm): 5.81 (m, 1H), 5.73 (m, 1H), 4.31 (m, 4.17), 2.81 (s, 1H), 2.02 - 1.88 (m, 2H), 1.74 (m, 1H), 1.62 - 1.57 (m, 2H). **¹³C NMR**: 130.4, 130.0, 65.3, 32.1, 25.2, 19.3. Yield 80% (18.84 g).

Cyclohex-2-enyl ethyl carbonate

To 5 g (50.9 mmol, 1 eq.) of 2-cyclohexen-1-ol in 45 mL DCM and 6.15 mL (76.3 mmol, 1.5 eq.) of pyridine was added 7.58 mL (76.3 mmol, 1.5 eq.) of ethyl chloroformate slowly *via* a syringe under argon. The reaction was allowed to stir at room temperature for 5 days. The mixture was quenched with water and extracted with DCM (3 x 50 mL), dried over MgSO₄ and concentrated in vacuo.

^1H NMR (CDCl_3) δ (ppm): 5.92 - 5.89 (m, 1H), 5.72 - 5.71 (m, 1H), 5.04 (m, 1H), 4.13 - 4.09 (q, 2H, $J=7.14$ Hz), 2.00 - 1.58 (b, 6H), 1.24 - 1.22 (t, 3H, $J=7.15$ Hz). **^{13}C NMR**: 155.3, 133.6, 125.8, 71.6, 63.8, 28.0, 24.6, 18.3, 14.0. Yield 90% (7.80 g).

1-Methyl-1-pentyl pyridinium bis(trifluoromethylsulfonyl)amide

The ionic liquid was synthesised according to a modified literature procedure.^[40] To *N*-methylpyrrolidine (30 mL, 0.282 mol) in 30 mL toluene was added 1-bromopentane (34.95 mL, 0.282 mol). The reaction mixture was stirred at 50°C for 24 h. The toluene was decanted from the ionic liquid layer and the rest of toluene was removed under reduced pressure. The ionic liquid was dissolved in 50 mL of water and bis(trifluoromethylsulfonyl)imine lithium salt (86.08 g, 0.3 mol) was added to the solution. The mixture was stirred for 2h at 50°C and subsequently the water was decanted. The ionic liquid was washed seven times with water and afterwards dried under reduced pressure at 80°C.

^1H NMR ($\text{C}_2\text{D}_6\text{O}$) δ (ppm): 3.68 (b, 4H), 3.52 - 3.49 (m, 2H), 3.22 (s, 3H), 2.30 (b, 4H), 1.91 (b, 2H), 1.38 - 1.37 (m, 4H), 0.91 - 0.89 (t, 3H, $J=5.79$ Hz). **^{13}C NMR**: 127.34, 124.13, 120.92, 117.70, 66.46, 66.40, 50.11, 30.17, 25.03, 23.76, 23.34, 14.97. **^{19}F NMR**: -79.70. Yield: 90% (110 g)

1-(4-(2-Bromoethoxy)phenyl)ethanone (1)

To a solution of 5 g (36.72 mmol) 4-hydroxy acetophenone in 100 mL 3-pentanone was added 15.2 g (110.16 mmol) K_2CO_3 . The mixture was stirred for 30 min and 9.5 mL (110.16 mmol) 1,2-dibromoethane was added. The reaction mixture was stirred at 100°C for 16 hours. The pentanone and the dibromoethane were removed under reduced pressure. The remaining slurry was diluted in EtOAc and washed 3 times with water. The organic layer was dried and concentrated to give a pale brownish product. If the product is not yet pure, it can be recrystallised from ethanol.

^1H NMR (CDCl_3) δ (ppm): 7.93 (d, 2H, $J=8.85$ Hz), 6.96 (d, 2H, $J=8.85$ Hz), 4.37 - 4.34 (t, 2H, $J=6.25$ Hz), 3.68 - 3.65 (t, 2H, $J=6.25$ Hz), 2.56 (s, 3H). **^{13}C NMR**: 197.3, 162.3, 131.1, 130.9, 114.4, 67.7, 28.3, 26.1. **MS**: (m/z) 264.9835 $[\text{M}+\text{Na}]^+$ (Br^{79}), calc. 264.98. Yield: 80% (7.14 g).

(E)-1-(4-(2-Bromoethoxy)phenyl)-3-phenylprop-2-en-1-one (H-2)

To an aqueous alcoholic solution (12 mL - ratio EtOH:H₂O of 1:2) of 0.3 g NaOH (1.25 eq.) was added 1.44 g (5.92 mmol) bromoethoxy acetophenone. The reaction mixture was cooled in ice and 0.6 mL (5.92 mmol) benzaldehyde was added dropwise. The reaction mixture was stirred at 25°C for 16 hours. The solid formed was removed by filtration, washed with water and recrystallised from hot EtOH.

¹H NMR (CDCl₃) δ (ppm): 8.03 (d, 2H, $J=8.85$ Hz), 7.79 (d, 1H, $J=15.56$ Hz), 7.64 (m, 2H), 7.52 (d, 1H, $J=15.56$ Hz), 7.41 - 7.39 (m, 3H), 6.98 (d, 2H, $J=8.85$ Hz), 4.35 (t, 2H, $J=6.20$ Hz), 3.65 (t, 2H, $J=6.20$ Hz). **¹³C NMR**: 189.5, 162.6, 144.8, 135.6, 132.6, 131.5, 131.0, 129.5, 129.0, 122.3, 114.9, 68.1, 28.7. **MS**: (m/z) 353.0148 [M+Na]⁺ (Br⁷⁹), calc. 353.02. Yield: 92 % (1.80 g).

(E)-1-(2-(4-Cinnamoylphenoxy)ethyl)-1-methylpyrrolidinium bromide (H-4)

To 1 g (3.01 mmol) of (E)-1-(4-(2-bromoethoxy)phenyl)-3-phenylprop-2-en-1-one in 15 mL toluene was added 3 mL (excess) of N-methylpyrrolidine. The mixture was stirred at 60°C over night. The solid formed was collected and washed with ether several times.

¹H NMR (CDCl₃) δ (ppm): 8.02 (d, 2H, $J=8.92$ Hz), 7.77 (d, 1 H, $J=15.65$ Hz), 7.64 - 7.62 (m, 2H), 7.51 (d, 2H, $J=15.65$ Hz), 7.41 - 7.40 (m, 3H), 7.04 - 7.02 (d, 2H, $J=8.93$ Hz), 4.62 - 4.60 (m, 2H), 4.44 - 4.41 (m, 2H), 4.06 - 4.04 (m, 2H), 3.93 - 3.90 (m, 2H), 3.43 (s, 3H) 2.38 - 2.15 (br, 4H). **¹³C NMR**: 189.1, 161.1, 144.9, 135.1, 132.6, 131.2, 130.8, 129.2, 128.7, 121.7, 114.6, 65.7, 62.9, 62.5, 48.7, 21.3. MP: 160°C. **MS**: (m/z) 336.20 [M]⁺, calc. 336.20. Yield: 70% (0.88 g).

(E)-1-(2-(4-Cinnamoylphenoxy)ethyl)-1-methylpyrrolidinium PF₆ (H-6)

To 0.5 g (1.20 mmol) of (E)-1-(2-(4-cinnamoylphenoxy)ethyl)-1-methylpyrrolidinium bromide dissolved in water was added 0.24 g (1.1 eq.) KPF₆ dissolved in water. A white solid is formed instantly. The solid was collected and washed with water.

¹H NMR (C₂D₆O) δ (ppm): 8.19 (d, 2H, $J=8.98$ Hz), 7.87 (d, 1H, $J=15.60$ Hz), 7.83 - 7.81 (m, 2H), 7.77 (d, 1H, $J=15.61$), 7.47 - 7.45 (m, 3H), 7.18 (d, 2H, 8.96 Hz), 4.79 (m, 2H), 4.16 - 4.13 (s, 2H), 3.95 - 3.94 (m, 4H), 3.45 (s, 3H), 2.43 - 2.35 (m, 4H). **¹³C NMR**:

190.4, 164.3, 146.3, 134.8, 133.90, 133.60, 133.2, 131.7, 131.0, 124.5, 117.3, 82.40, 67.9, 65.1, 48.8, 23.55. ^{19}F NMR: -72.53 ($^1J_{\text{PF}} = 707.8$ Hz). MP: 184°C. MS: (m/z) 336.20 [M]⁺, calc. 336.20. Elemental Analysis: calculated for C₂₂H₂₆F₆NO₂P: %C 54.89, %H 5.44, %N 2.91, found: %C 54.25, %H 5.19, %N 2.73. Yield: 90% (0.52 g).

(E)-1-(4-(2-Bromoethoxy)phenyl)-3-(4-methoxyphenyl)prop-2-en-1-one (MeO-2)

To a suspension of 3 g (12.5 mmol) 4-bromoethoxy acetophenone in 25 mL MeOH was added 0.64 g (1.25 eq.) NaOH. The mixture was cooled in ice and 1.7 g (12.5 mmol) 4-methoxy benzaldehyde was added slowly. The reaction mixture was stirred at 25°C for 16 hours. The solid formed was removed by filtration and washed 3 times with MeOH. ^1H NMR (CDCl₃) δ (ppm): 7.96 (d, 2H, $J=8.94$ Hz), 7.70 (d, 1H, $J=15.58$ Hz), 7.54 (d, 2H, $J=8.73$ Hz), 7.35 (d, 1H, $J=15.58$ Hz), 6.93 (d, 2H, $J=8.93$ Hz), 6.88 (d, 2H, $J=8.79$), 4.30 (t, 2H, $J=6.24$ Hz), 3.79 (s, 3H), 3.61 (t, 2H, $J=6.23$ Hz). ^{13}C NMR: 188.7, 161.6, 161.5, 144.0, 131.9, 130.7, 130.1, 127.7, 119.4, 114.4, 114.2, 67.8, 55.4, 28.6. MS: (m/z) 383.0253 [M+Na]⁺ (Br⁷⁹), calc. 383.03. Yield 73 % (3.3 g).

(4-Methoxyphenyl)acryloyl)phenoxy)ethyl)-1-methylpyrrolidinium bromide (MeO-4)

To 1 g (2.77 mmol) of (E)-1-(4-(2-bromoethoxy)phenyl)-3-phenylprop-2-en-1-one in 15 mL toluene was added 2 mL of N-methylpyrrolidine. The mixture was stirred at 60°C over night. The solvent and the N-methylpyrrolidine were removed by filtration and the solid was washed several times with ether.

^1H NMR (CD₃OD) δ (ppm): 8.09 (d, 2H, $J=8.90$ Hz), 7.71 (d, 1H, $J=15.59$ Hz), 7.68 - 7.67 (m, 2H, $J=8.84$ Hz), 7.63 (d, 1H, $J=15.52$ Hz), 7.60 (d, 2H, $J=8.91$ Hz), 7.12 (d, 2H, $J=8.89$ Hz), 6.96 (d, 2H, $J=8.82$ Hz), 4.57 (m, 2H), 3.92 - 3.89 (m, 2H), 3.80 (s, 3H), 3.70 - 3.66 (m, 4H), 3.19 (s, 3H), 2.26 - 2.23 (m, 4H). ^{13}C NMR: 191.5, 164.1, 160.4, 146.4, 133.8, 132.6, 132.1, 129.3, 120.6, 116.1, 116.0, 66.7, 64.0, 63.9, 56.0, 49.3, 22.3. MS: (m/z) 336.20 [M]⁺, calc. 336.20. Yield 55.8 % (0.69 g).

(4-Methoxyphenyl)acryloyl)phenoxy)ethyl)-1-methylpyrrolidinium PF₆
(MeO6)

To 0.5 g (1.12 mmol) (E)-1-(2-(4-(3-(4-methoxyphenyl)acryloyl)phenoxy)ethyl)-1-methylpyrrolidinium bromide in 10 mL water 0.25 g (1.2 eq.) potassium hexafluorophosphate was added. The solution was stirred at room temperature for one hour. The solid formed was collected and washed with ether and water.

¹H NMR (C₂D₆O) δ (ppm): 8.17 (d, 2H, $J=8.90$ Hz), 7.79 - 7.75 (m, 4H), 7.16 (d, 2H, $J=8.82$ Hz), 7.02 (d, 2H, $J=8.82$ Hz), 4.82 - 4.76 (m, 2H), 4.16 - 4.14 (m, 4H), 3.94 - 3.92 (m, 2H), 3.87 (s, 3H), 3.45 (s, 3H), 2.47 - 2.32 (m, 4H). ¹³C NMR: 189.4, 163.8, 163.2, 145.3, 132.5, 132.2, 130.6, 129.6, 121.0, 116.3, 116.1, 69.0, 66.9, 64.2, 56.4, 40.1, 22.6. ¹⁹F NMR: -72.51 ($^1J_{PF} = 707.8$ Hz). MS: (m/z) 336.20 [M]⁺, calc. 336.20. Elemental Analysis: calculated for C₂₃H₂₈F₆NO₃P: %C 54.01, %H 5.52, %N 2.74, found: %C 53.83, %H 5.40, %N 2.48. Yield 68.4 % (0.39 g).

(E)-1-(4-(2-Bromoethoxy)phenyl)-3-(4-nitrophenyl)prop-2-en-1-one (NO₂-2)

To a ice-cooled suspension of 3 g (12.34 mmol) 4-bromoethoxy acetophenone in 30 mL Methanol/Ethanol (25:5) were added 0.62 g (1.25 eq.) NaOH and 1.87 g (12.34 mmol) nitrobenzaldehyde. The suspension was stirred at 25°C for 16 hours. The yellow solid formed was removed by filtration and washed 3 times with MeOH.

¹H NMR (CDCl₃) δ (ppm): 8.27 (d, 2H, $J=8.86$ Hz), 8.05 (d, 2H, $J=8.91$ Hz), 7.83 - 7.77 (m, 3H), 7.64 (d, 1H, $J=15.71$), 7.02 (d, 2H, $J=8.92$ Hz), 4.38 (t, 2H, $J=6.18$ Hz), 3.68 (t, 2H, $J=6.18$ Hz). ¹³C NMR: One carbon not observed, 188.6, 163.0, 148.4, 141.8, 141.6, 131.6, 129.4, 126.0, 124.8, 115.0, 68.2, 28.6. MS: (m/z) 376.20 [M]⁺, calc. 376.20. Yield 75 % (3.5 g)

1-Methyl-1-(2-(4-(3-(4-nitrophenyl)acryloyl)phenoxy)ethyl)pyrrolidinium
bromide (NO₂-4)

To 1 g (2.66 mmol) (E)-1-(4-(2-bromoethoxy)phenyl)-3-(4-nitrophenyl)prop-2-en-1-one in 10 mL toluene N-methylpyrrolidine (4 eq.) was added. The solution was stirred at 70°C for 24 h. The solid formed was collected and washed with ether.

^1H NMR (CDCl_3) δ (ppm): 8.14 (d, 2H, $J=8.43$ Hz), 7.96 (d, 1H, $J=8.81$ Hz), 7.70 (d, 2H, $J=8.86$ Hz), 7.67 (d, 1H, $J=16.40$ Hz), 7.57 (d, 1H, $J=15.60$ Hz), 6.97 (d, 1H, $J=8.81$ Hz), 4.48 - 4.46 (m, 2H), 3.95 (m, 2H), 3.69 - 3.57 (m, 4H), 3.12 (s, 3H), 2.44 - 2.09 (m, 4H). **^{13}C NMR**: couldn't be measured. Yield 58% (0.72 g).

(1-Methyl-1-(2-(4-(3-(4-nitrophenyl)acryloyl)phenoxy)ethyl)pyrrolidinium PF₆ (NO₂-6)

To 1 g (1.96 mmol) (E)-1-(2-(4-(3-(4-nitrophenyl)-acryloyl)phenoxy)ethyl)-1-methylpyrrolidinium bromide in 10 mL potassium hexafluorophosphate (1.1 eq.) was added. The solution was stirred at room temperature for one hour. The solid formed was collected and washed with ether and water.

^1H NMR ($\text{C}_2\text{D}_6\text{O}$) δ (ppm): 8.30 (d, 2H, $J=8.79$ Hz), 8.23 (d, 2H, $J=9.01$ Hz), 8.13 - 8.09 (m, 3H), 7.84 (d, 1H, $J=15.67$ Hz), 7.20 (d, 2H, $J=8.99$ Hz), 4.82 - 4.79 (m, 2H), 4.18 - 4.16 (m, 2H), 3.97 - 3.93 (m, 4H), 3.46 (s, 3H), 2.43 - 2.36 (m, 4H). **^{13}C NMR**: 190.0, 164.6, 151.4, 144.4, 143.3, 133.8, 132.2, 128.5, 126.7, 117.4, 67.9, 65.3, 65.1, 50.9, 23.5. **^{19}F NMR**: -72.55 ($^1J_{\text{PF}} = 707.68$ Hz). Elemental Analysis: calculated for $\text{C}_{22}\text{H}_{25}\text{F}_6\text{N}_2\text{O}_4$: %C 50.20, %H 4.79, %N 5.32, found: %C 50.25, %H 4.64, %N 4.78. Yield 80% (0.83 g)

(E)-1-Methyl-1-(2-oxo-4-phenylbut-3-enyl)pyrrolidinium bromide (20)

Styryl methyl ketone 2 g (13.68 mmol) was dissolved in 30 mL dry THF. Further pyrrolidone hydrotribromide 8 g (16.36 mmol) was dissolved in 50 mL THF. Both solutions were combined and stirred at rt for 1h. The THF was removed under reduced pressure. The substrate was subject to a silica column (1:6, Et₂:PE). The organic solvents were removed under reduced pressure. The product was then dissolved in toluene and n-methyl-pyrrolidine as added until no solid is formed anymore.

^1H NMR (CDCl_3) δ (ppm): 8.05 (d, 1H, $J=16.36$ Hz), 7.61 (m, 2H), 7.40 - 7.33 (m, 3H), 6.78 - 6.74 (d, 1H, $J=16.35$ Hz), 5.66 (s, 2H), 4.15 - 4.03 (m, 4H), 3.42 (s, 3H), 2.35 - 2.30 (m, 2H), 2.17 - 2.12 (m, 2H). **^{13}C NMR**: 191.2, 147.3, 133.5, 131.5, 129.0, 128.7, 122.8, 68.0, 65.2, 48.7, 20.7. **MS**: (m/z) 230.1539 [M]⁺, 230.15 calc. Yield 89% (3.78 g).

(E)-1-Methyl-1-(2-oxo-4-phenylbut-3-enyl)pyrrolidinium PF₆ (21)

2 g (6.45 mmol) (E)-1-methyl-1-(2-oxo-4-phenylbut-3-enyl)pyrrolidinium bromide was dissolved in 10 mL water. To this 1.3 g (1.1 eq.) potassium hexafluorophosphate was added. Immediately a white precipitate is formed and collected by filtration.

¹H NMR (C₂D₆O) δ (ppm): 7.73 (d, 1H, $J=16.0$ Hz), 7.65 - 7.63 (m, 2H), 7.41 - 7.36 (m, 3H), 6.90 (d, 1H, $J=16.4$ Hz), 4.97 (s, 2H), 3.93 - 3.91 (m, 2H), 3.80 - 3.77 (m, 2H), 3.37 (s, 3H), 2.26 - 2.24 (m, 4H). ¹³C NMR: 193.5, 147.9, 136.8, 134.2, 132.0, 131.6, 125.9, 82.4, 68.2, 51.9, 23.8. ¹⁹F NMR: -72.6 ($^1J_{PF} = 684.5$ Hz). MS: (m/z) 230.1539 [M]⁺, 230.15 calc. Elemental Analysis: calculated for C₁₅H₂₀F₆NOP: %C 48.01, %H 5.37, %N 3.73, found: %C 47.16, %H 4.98, %N 3.46. Yield 83% (2.00 g).

4-(2-Bromoethoxy)benzaldehyde (15)

To a solution of 5 g (40.90 mmol) 4-hydroxybenzaldehyde in 100 mL 3-pentanone was added 16.95 g (121.70 mmol) K₂CO₃ and 0.14 g (0.41 mmol) tetrabutylammonium bromide. The mixture was stirred for 30 min and 10.50 mL (121.70 mmol) 1,2-dibromoethane was added. The reaction mixture was stirred at 100°C for 16 hours. The pentanone and the dibromoethane were removed under reduced pressure. The remaining slurry was diluted in EtOAc and washed 3 times with water. The organic layer was dried and concentrated to give a pale brownish product.

¹H NMR (CDCl₃) δ (ppm): 9.90 (s, 1H), 7.85-7.82 (m, 2H), 7.03-6.99 (m, 2H), 4.37-4.36 (t, 2H, $J=11.08$ Hz), 3.67-3.65 (t, 2H, $J=11.35$ Hz). ¹³C NMR: 190.75, 165.00, 132.01, 128.00, 114.87, 67.94, 28.56. MS: (m/z) 226.98 [M]⁺. Yield 91% (8.5 g).

(E)-4-(4-Methoxyphenyl)but-3-en-2-one (16)

To a suspension of 5 g (36.72 mmol) 4-methoxybenzaldehyde in 100 mL water was added 7 mL of acetone. The mixture was shaken every 10 min and left standing at 4°C for the period of 90 min. Then it was allowed to react for 24 h at 4°C without stirring or shaking. After 24 h it was shaken again and left at 4°C for an additional period of 8 h. A yellow solid could then be collected by means of filtration. The solid was washed with water several times.

^1H NMR (CDCl_3) δ (ppm): 7.50-7.48 (d, 2H, $J=8.84$ Hz), 7.49-7.45 (d, 1H, $J=16.20$ Hz), 6.92-6.90 (d, 2H, $J=8.85$ Hz), 6.62-6.58 (d, 1H, $J=16.23$ Hz), 3.84 (s, 3H), 2.36 (s, 3H). **^{13}C NMR**: 198.37, 161.60, 143.22, 129.94, 127.05, 125.03, 55.38, 27.39. **MS**: (m/z) [M] $^+$. Yield 89% (4.77 g)

(1E,4E)-1-(4-(2-Bromoethoxy)phenyl)-5-(4-methoxyphenyl)penta-1,4-dien-3-one

(17)

To 1 g (5.68 mmol, 1 eq.) (E)-4-(4-methoxyphenyl)but-3-en-2-one in 10 mL methanol 0.29 g (1.25 eq.) NaOH was added. The mixture was stirred at 0°C and 1.30 g (1 eq.) 4-(2-bromoethoxy)benzaldehyde was added. The mixture was allowed to stir at rt for 16 h and filtered afterwards. The yellow solid was washed two times with methanol.

^1H NMR (CDCl_3) δ (ppm): 7.71 - 7.70 (d, 1H, $J=4.67$ Hz), 7.68 - 7.66 (d, 1H, $J=4.69$ Hz), 7.58 - 7.56 (d, 4H, $J=8.60$ Hz), 6.98 - 6.92 (m, 6H), 4.35 - 4.31 (t, 2H, $J=6.25$ Hz), 3.86 (s, 3H), 3.67 - 3.64 (t, 2H, $J=6.25$ Hz). **^{13}C NMR**: 188.8, 161.6, 159.9, 142.8, 142.4, 130.1, 128.3, 127.6, 123.9, 123.5, 115.1, 114.4, 67.9, 55.4, 28.7. Elemental Analysis: calculated for $\text{C}_{20}\text{H}_{19}\text{BrNO}_3$: %C 62.03, %H 4.95, found: %C 63.10, %H 4.54. Yield: 1.6 g (73%)

1-(2-(4-((1E,4E)-5-(4-Methoxyphenyl)-3-oxopenta-1,4-dienyl)phenoxy)ethyl)-1-methylpyrrolidinium bromide

(18)

To 1 g (2.58 mmol) (1E,4E)-1-(4-(2-bromoethoxy)phenyl)-5-(4-methoxyphenyl)penta-1,4-dien-3-one dissolved in 10 mL toluene n-methylpyrrolidine (4 eq.) were added. The solution was stirred for 24 h at 60°C . The solid formed was collected and washed with ether.

^1H NMR (CDCl_3) δ (ppm): 7.71 - 7.68 (d, 2H), 7.60 - 7.56 (m, 4H), 4.58 - 4.56 (m, 2H), 4.45 - 4.43 (m, 2H), 4.11 - 4.04 (m, 2H), 3.91 - 3.86 (m, 2H), 3.85 (s, 3H), 3.42 (s, 3H), 2.41 - 2.35 (m, 2H), 2.29 - 2.25 (m, 2H). **^{13}C NMR**: 188.7, 162.7, 157.3, 142.8, 142.3, 130.1, 128.3, 127.6, 123.8, 123.4, 115.1, 114.4, 67.9, 61.7, 61.1, 59.1, 56.7, 45.6,

23.6. Yield 50% (0.60 g)

1-(2-(4-((1E,4E)-5-(4-Methoxyphenyl)-3-oxopenta-1,4-dienyl)phenoxy)ethyl)-1-methylpyrrolidinium PF₆
(19)

To 1 g (2.12 mmol) of bromide salt (**18**) in 5 mL of water was given a solution of KPF₆ in 3 mL of water. Immediately a white solid is formed. The solid was collected and washed several times with water and ether.

¹H NMR DMSO δ (ppm): 7.89 - 7.70 (m, 6H), 7.24 - 7.00 (m, 6H), 4.51 - 4.40 (m, 2H), 3.83 - 3.80 (b, 5H), 3.58 - 3.57 (b, 4H), 3.09 (s, 3H), 2.11 (b, 4H). ¹³C NMR: 188.61, 161.67, 159.64, 142.76, 142.35, 130.76, 128.67, 127.78, 124.45, 115.65, 114.94, 64.77, 62.71, 62.15, 55.81, 48.47, 21.37. ¹⁹F NMR: -70.16 (¹J_{PF} = 720.5 Hz). Elemental Analysis: calculated for C₂₅H₃₀F₆NO₃P: %C 55.87, %H 5.63, %N 2.61, found: %C 55.54, %H 5.31, %N 2.47. Yield 70% (0.80 g).

(E)-3-Phenyl-1-(pyridin-4-yl)prop-2-en-1-one (**8**)

To a suspension of 5 mL (45.19 mmol) *N*-acetylpyridine in 100 mL aqueous 10 molar NaOH-solution was added 4.78 g (45.19 mmol) benzaldehyde. The mixture was shaken every 10 min and left standing at 4°C for the period of 90 min. Then it was allowed to react for 24 h at 4°C without stirring or shaking. After 24 h it was shaken again and left at 4°C for an additional period of 8 h. A yellow solid can then be collected by means of filtration. The solid was washed with water several times, dissolved in chloroform and filtrated. The filtrate was dried with MgSO₄ and finally concentrated to give a yellow solid.

¹H NMR (CDCl₃) δ (ppm): 8.83 - 8.81 (d, 2H, *J*=6.00 Hz). 7.84 - 7.80 (d, 1H, *J*=16.00 Hz), 7.76 (m, 2H), 7.65 - 7.63 (m, 2H), 7.44 - 7.40 (m, 4H). ¹³C NMR: 189.87, 150.79, 146.85, 144.39, 134.28, 131.21, 129.09, 128.69, 121.51, 121.20. MS: (m/z) 208.08 [M]⁺. Yield 80% (7.56 g).

4-Cinnamoyl-1-ethylpyridinium hexafluorophosphate (11)

To a solution of 1 g (2.61 mmol) (E)-3-phenyl-1-(pyridin-4-yl)prop-2-en-1-one in 10 mL toluene was added 0.4 g (2.61 mmol) diethylsulfate. The mixture was stirred at 60°C for 16 h. Subsequently, the solvent was removed under reduced pressure and the remaining solid dissolved in 10 mL water. To this solution 0.5 g (2.70 mmol) potassium hexafluorophosphate was added. Immediately a solid precipitated. The solid was washed several times with water.

$^1\text{H NMR}$ DMSO δ (ppm): 9.34 - 9.33 (d, 2H, $J=6.41$ Hz), 8.68 - 8.66 (d, 2H, $J=5.83$ Hz), 7.95 - 7.89 (m, 4H), 7.53 - 7.51 (m, 3H), 4.73 - 4.71 (q, 2H, $J=7.22$ Hz), 1.61 - 1.57 (t, 3H, $J=7.25$ Hz). $^{13}\text{C NMR}$: 187.33, 154.76, 148.25, 146.32, 134.52, 129.89, 129.57, 129.53, 126.73, 121.87, 57.15, 16.77. $^{19}\text{F NMR}$: -70.18 ($^1J_{\text{PF}} = 721.5$ Hz). Yield 50% (0.50 g).

(E)-3-Phenyl-1-(4-(piperidin-1-yl)phenyl)prop-2-en-1-one (12)

To a suspension of 10 g (49.20 mmol) 1-(4-(piperidin-1-yl)phenyl)ethanone in 50 mL MeOH was added 2.40 g (1.25 eq.) NaOH. The mixture was cooled in ice and 5.22 g (49.20 mmol) benzaldehyde was added slowly. The reaction mixture was stirred at 25°C for 20 hours. The solid formed was collected and washed 3 times with cold MeOH.

$^1\text{H NMR}$ (CDCl_3) δ (ppm): 8.02 - 7.98 (d, 2H, $J=9.09$ Hz), 7.81 - 7.77 (1, d, $J=15.63$ Hz), 7.65 - 7.63 (m, 2H), 7.60 - 7.56 (d, 1H, $J=15.63$ Hz), 7.43 - 7.38 (m, 3H), 6.91 - 6.89 (d, 1H, $J=9.10$ Hz), 3.38 - 3.35 (t, 2H, $J=6.31$ Hz), 1.71 - 1.68 (t, 2H, $J=6.31$ Hz). **MS**: (m/z) 290.16 $[\text{M}]^+$. Yield 90% (13 g).

(E)-1-(4-Cinnamoylphenyl)-1-methylpiperidinium hexafluorophosphate (14)

To 1 g (3.43 mmol) of **12** dissolved in 5 mL toluene was added 0.44 g (3.43 mmol) dimethyl sulfate. The reaction mixture was refluxed for 16 h. The resulting solid was collected and washed three times with ether. Subsequently, it was dissolved in 5 mL of water and 0.65 g (3.45 mmol) potassium hexafluorophosphate was added. Immediately a solid was formed. It was collected and washed four times with water.

$^1\text{H NMR}$ DMSO δ (ppm): 8.39 - 8.36 (d, 2H, $J=8.76$ Hz), 8.12 - 8.10 (d, 2H, $J=8.90$

Hz), 7.99 - 7.95 (d, 1H, $J=15.63$ Hz), 7.92 - 7.90 (m, 2H), 7.82 - 7.78 (d, 2H, $J=15.69$ Hz), 4.43 - 4.40 (m, 2H), 3.88 - 3.83 (m, 2H), 3.46 (s, 3H), 1.58 (b, 6H). Yield: 85% (1.31 g).

(E)-1-(2-(cinnamoyloxy)ethyl)-1-methylpyrrolidinium hexafluorophosphate
(23)

To 20 g (134.17 mmol) cinnamic acid dissolved in 300 mL 3-pentanone was added 46.36 g (2.5 eq.) potassium carbonate. Subsequently, 75.62 g (3 eq.) dibromoethane was given to the suspension. The reaction mixture is refluxed for 16 hours. The solvent and dibromoethane were removed under reduced pressure and to the remaining solid was given 100 mL water. The aqueous layer was extracted three times with 100 mL ethyl acetate. The organic layer was dried and concentrated. The solid was dissolved in 100 mL toluene and 11.50 g (134.17 mmol) *N*-methylpyrrolidine was added. The mixture was stirred at 60°C for 16 h and subsequently, toluene was removed under reduced pressure to yield a colourless solid. The solid was dissolved in 50 mL water and 25 g (134.17 mmol) potassium hexafluorophosphate was added. A white precipitate was formed, collected and washed three times with water.

¹H NMR DMSO δ (ppm): 7.73 - 7.68 (m, 3H), 7.44 - 7.43 (m, 3H), 6.71 - 6.67 (d, 1H, $J=16.06$ Hz), 4.58 (b, 2H), 3.76 - 3.73 (m, 2H), 3.59 - 3.51 (m, 4H), 3.08 (s, 3H), 2.10 (b, 4H). **¹³C NMR**: 166.01, 145.78, 134.29, 131.21, 129.43, 128.91, 128.89, 119.90, 117.92, 64.75, 64.69, 61.94, 58.94, 48.26, 48.24, 21.34. **¹⁹F NMR**: -70.17 -72.6 ($^1J_{PF} = 720.5$ Hz). Yield: 20% (10.80 g)

2.5 Selected crystallographic data

Table 2.11: Crystal data

	20	H-6	H-4	MeO-4
formula	C ₁₅ H ₂₀ BrNO	C ₂₂ H ₂₆ NO ₂ F ₆ P	C ₂₂ H ₂₆ BrNO ₂	C ₂₃ H ₂₈ BrNO ₃
FW / M	310.23	310.23	416.15	446.37
Crystal system	monoclinic	monoclinic	triclinic	-
Space group	P2 ₁ /n	P2 ₁ /c	P-1	P2 ₁ /c
A (Å)	10.6662(18)	9.9133(4)	8.2923(5)	10.5509(6)
B (Å)	13.109(2)	21.1994(7)	10.5937(6)	25.7087(16)
C (Å)	11.3363(18)	10.4816(4)	13.0176(8)	8.2257(8)
α (⁰)	90	90	102.082(1)	90
β (⁰)	115.960(3)	94.125(1)	94.398	111.2720(10)
γ (⁰)	90	90	112.711(1)	90
V(Å ³)	1425.18	2196.99	1015.67	2079.2
Z	4	4	2	4
T (K)	110	293	110	110
F(000)	640	1000	432	928
Reflections collected	13289	17891	10520	21232
R indices (all data)	R1 = 0.0481 wR2 = 0.0923	R1 = 0.0971 wR2 = 0.2166	R1 = 0.0446 wR2 = 0.1203	R1 = 0.0454 wR2 = 0.0794

Bibliography

- [1] A. Littke, G. Fu, *Angew. Chem. Int. Ed.* **2002**, *41*, 4176–4211.
- [2] I. J. S. Fairlamb, *Chem. Soc. Rev.* **2007**, *36*, 1036–1045.
- [3] P. W. N. W. van Leeuwen in *Homogeneous Catalysis* (Ed.: P. van Leeuwen), Kluwer Academic Publisher, Dordrecht, Boston, London, **2004**, pp. 271–298.
- [4] I. J. S. Fairlamb, *Annu. Rep. Prog. Chem. Sect. B* **2006**, *102*, 50–80.
- [5] I. J. S. Fairlamb, *Annu. Rep. Prog. Chem. Sect. B* **2002**, *98*, 123–158.
- [6] Y. Hatanaka, T. Hiyama, *J. Org. Chem.* **1988**, *53*, 918–920.
- [7] I. J. S. Fairlamb, P. S. Bäuerlein, L. R. Marrison, J. M. Dickinson, *Chem. Commun.* **2003**, *5*, 632–633.
- [8] E. Negishi, *Handbook of Organopalladium Chemistry for Organic Synthesis*, John Wiley Sons, NJ, **2002**.
- [9] K. Nicolaou, E. Sorensen, *Classics in Total Synthesis*, VCH, New York, **1996**.
- [10] K. C. Nicolaou, P. G. Bulger, D. Sarlah, *Angew. Chem. Int. Ed.* **2005**, *44*, 4442–4489.
- [11] D. Old, J. Wolfe, S. Buchwald, *JAmChemSoc* **1998**, *120*, 9722–9723.
- [12] I. J. S. Fairlamb, *Org. Biomol. Chem.* **2008**, *6*, 3645–3656.
- [13] I. J. S. Fairlamb, A. R. Kapdi, A. F. Lee, *Org. Lett.* **2004**, *6*, 4435–4438.
- [14] I. J. S. Fairlamb, F. L. Adam, *Organometallics* **2007**, *26*, 4087–4089.
- [15] T. Hiyama, *Pure Appl. Chem.* **1994**, *66*, 1471–1478.
- [16] K. Gouda, E. Hagiwara, Y. Hatanaka, T. Hiyama, *J. Org. Chem.* **1996**, *61*, 7232.
- [17] F. McLachlan, C. J. Mathews, P. J. Smith, T. Welton, *Organometallics* **2003**, *22*, 5350–5357.
- [18] A. J. Carmichael, M. J. Earle, J. D. Hollbrey, P. McCormac, K. R. Seddon, *Org. Lett.* **1999**, *1*, 997–1000.

Bibliography

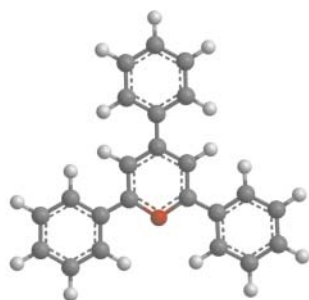
- [19] E. Alacid, C. Nájera, *Adv. Synth. Catal.* **2006**, *348*, 2085–2091.
- [20] S. E. Denmark, N. S. Werner, *J. Am. Chem. Soc.* **2008**, *130*, 16382–16393.
- [21] R. Sebesta, I. Kmentová, S. Toma, *Green Chem.* **2008**, *10*, 484–496.
- [22] M. Janssen, C. Müller, D. Vogt, *Adv. Synth. Catal.* **2009**, *351*, 313–318.
- [23] P. Wasserscheid, *Chem. Unserer Zeit* **2003**, *1*, 52–63.
- [24] L. Zhengdong, H. Liangren, S. Genbo, *Acta. Cryst.* **1992**, *C48*, 751–752.
- [25] D. Rabinovich, Z. Shakked, *Acta. Cryst.* **1974**, *B30*, 2829.
- [26] S. V. Konstaneki, G. Rossbach, *Chem. Ber.* **1896**, *29*, 1488–1494.
- [27] S. A. Moya, R. Pastene, H. Le Bozec, P. J. Baricelli, A. J. Pardey, J. Gimeno, *Inorg. Chim. Acta* **2001**, *312*, 7–14.
- [28] A. Degen, M. Bolte, *Acta. Cryst.* **1999**, *C55*, iv.
- [29] K. H. Shukla, P. DeShong, *J. Org. Chem.* **2008**, *73*, 6283–6291.
- [30] L. Starkey Ott, S. Campbell, K. R. Seddon, R. G. Finke, *Inorg. Chem.* **2007**, *46*, 10335–1–344.
- [31] R. R. Deshmukh, R. Rajagopal, K. V. Srinivasan, *Chem. Commun.* **2001**, 1544–1545.
- [32] A. Kovacevic, S. Grundemann, J. Miecznikowski, E. Clot, O. Eisenstein, R. Crabtree, *Chem. Commun.* **2002**, 2580–2581.
- [33] L. Xu, W. Chen, J. Xiao, *Organometallics* **2000**, *19*, 1123–1127.
- [34] H. Yang, Z. Fei, T. J. Geldbach, A. D. Philips, C. G. Hartinger, Y. Li, P. J. Dyson, *Organometallics* **2008**, *27*, 3971–3977.
- [35] R. K. Sharma, J. L. Fry, *J. Org. Chem.* **1983**, *48*, 2112–2114.
- [36] H. Sun, G. DiMagno, *J. Am. Chem. Soc.* **2004**, *127*, 2050–2051.
- [37] M. Mowery, P. DeShong, *Org. Lett.* **1999**, *1*, 2137.
- [38] J. A. Widegren, R. G. Finke, *J. MOL. CATAL. A-CHEM.* **2002**, *198*, 317–341.
- [39] G. S. Fonseca, A. P. Umpierre, P. F. P. Fichtner, S. R. Teixeira, J. Dupont, *Chem. Eur. J.* **2003**, *9*, 3263–3269.
- [40] P. Bonhote, A. Dias, N. Papageorgiou, K. Kalyanasundaram, M. Graetzel, *Inorg. Chem.* **1996**, *35*, 1168–1178.

3

Chapter 3

First ionic tagging of heterocyclic ligands derived from pyrylium salts

Phosphinines and pyridines are interesting ligands for transition metals and both can be prepared from pyrylium salts. Especially phosphinines are of particular interest as they are an alternative to commonly employed ligands, such as phosphines or phosphites. Ionic-tagged ligands of the latter kind are already applied successfully in homogeneously catalysed reactions, such as hydroformylations or hydroaminomethylations. Therefore, the synthesis of an ionic-tagged phosphinine is described in this chapter, as well as its nitrogen analogue.



3.1 Introduction

Characteristics of phosphinines and pyridines

In homogeneous catalytic reactions predominately phosphorus containing ligands play an important role. A range of ligands have been synthesised and the design of new classes of ligands is still in the focus of ongoing research. The most prominent ligands are the trivalent phosphines and phosphites, both in monodentate and bidentate versions. Hydrogenation, hydroformylation, and hydroaminomethylation are just a few of the homogeneously catalysed reactions where these ligands are successfully applied.^[1-5] Apart from these commonly used phosphorus containing ligands, phosphinines present themselves as suitable ligands (Figure 3.1).^[6-10] Müller *et al.* have demonstrated that these ligands are applicable in asymmetric hydrogenation reactions.^[11]

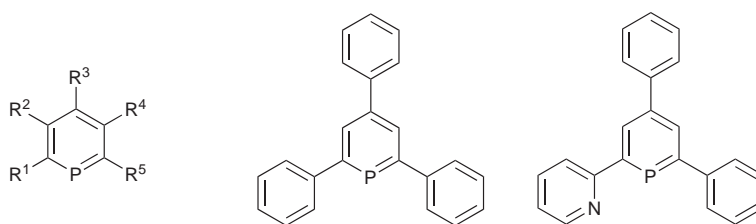


Figure 3.1: λ^3 -Phosphinines. From left to right: General structure, 2,4,6-triphenylphosphinine, donor-functionlised phosphinine^[10]

Phosphinines were first discovered by Märkl in 1966.^[7] That research was undoubtedly a substantial contribution to phosphorus chemistry and ligand design. The major difference of phosphinines compared to phosphines and phosphites is the incorporation of the phosphorus atom into an aromatic system, thus changing the hybridisation of the phosphorus from formally sp^3 to sp^2 . This class of ligands proved to be thermodynamically stable. By incorporating the phosphorus atom into an aromatic system, the carbon phosphorus double bond is stabilised significantly, a problem well-known for early phosphalkenes. This increases the applicability of $P=C$ double bond containing ligands considerably. The new class of ligands sparked a lot of interest in the chemical society and the groups of Ashe III, Dimorth, Bickelhaupt, Mathey and Le Floch

seized on investigating the properties and qualities of these compounds.^[6,12–20] The design of chiral and functionalised phosphinines for catalysis and materials is investigated by Müller *et al.*^[8–11] Phosphinines are aromatic systems with π -acceptor and weak σ -donor properties, which can be quantified by Tolman’s electronic parameter (χ). The value for phosphinines is comparable to the one of P(OPh)₃ (Table 3.1).^[8] A higher value usually indicates that a ligand is a better π -acceptor. A lower value is characteristic for ligands with σ -donor properties. The π -acceptor qualities and steric properties of phosphinines make them interesting ligands for the rhodium catalysed hydroformylation. Breit *et al.* have shown that turnover frequencies of up to 45000 h⁻¹ can be reached with phosphinine-based Rh-catalysts in the hydroformylation of 1-octene.^[21]

Table 3.1: Tolman’s electronic parameter for different ligands^[8]

Ligand	χ
P(OPh) ₃	29.1
2,4,6-Triphenylphosphinine	24
PPh ₃	12.9
PEt ₃	5.6

Phosphinines differ significantly from their nitrogen analogues, the pyridines. The latter ones are good σ -donors and poor π -acceptors in contrast. This has been shown by photoelectron and electron transmission spectroscopy as well as by theoretical calculations.^[22–26] The reason for this important distinction is the difference in the HOMOs and LUMOs of these two heterocyclic molecules (Figure 3.2 on the next page). In the parent phosphinine the lone-pair occupies the more diffuse HOMO⁻² orbital and it is less directional. Therefore, its σ -donor properties are limited. The π -acceptor properties depend on the energy level of the LUMOs. The phosphinines are better π -acceptors than pyridines as their LUMOs are lower in energy. In pyridines the lone-pair is represented by the HOMO, which is higher in energy compared to phosphinines and hence the pyridines are better σ -donors. Regarding their structural characteristics pyridines, benzenes and phosphinines differ significantly. Due to the larger size of the phosphorus atom these heterocycles are strongly distorted hexagons (Figure 3.3 on page 93).

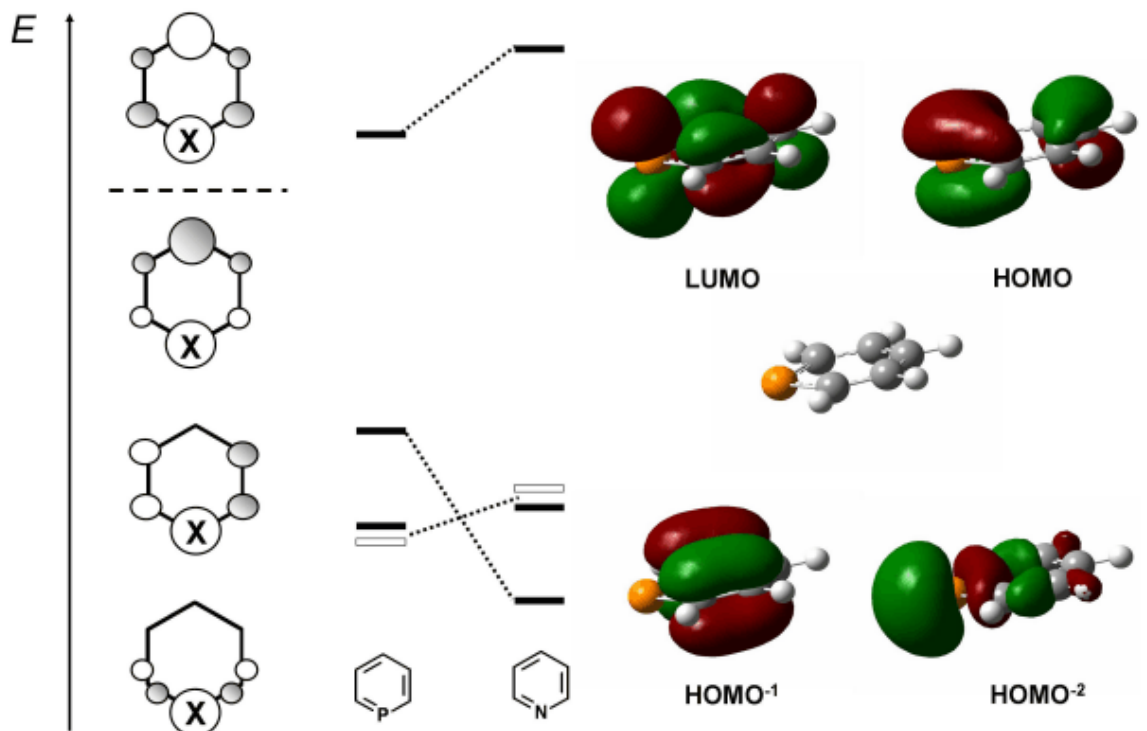


Figure 3.2: Frontier orbitals of phosphinine compared to pyridine (white rectangle: lone pair).^[8]

P-C bonds (1.741 Å) are longer than C-C bonds (1.391 Å) and their length lies in between P-C single bonds and P-C double bonds. As no real bond alternation can be seen, the existence of an aromatic systems can be assumed. The stretched P-C bonds cause the angle at the P atom (101.64°) to be considerably smaller than the rest of the angles in the ring (120.62°-123.49°).

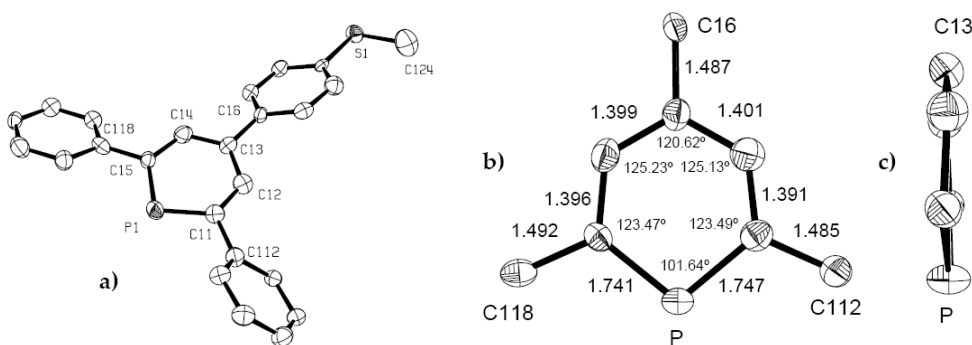
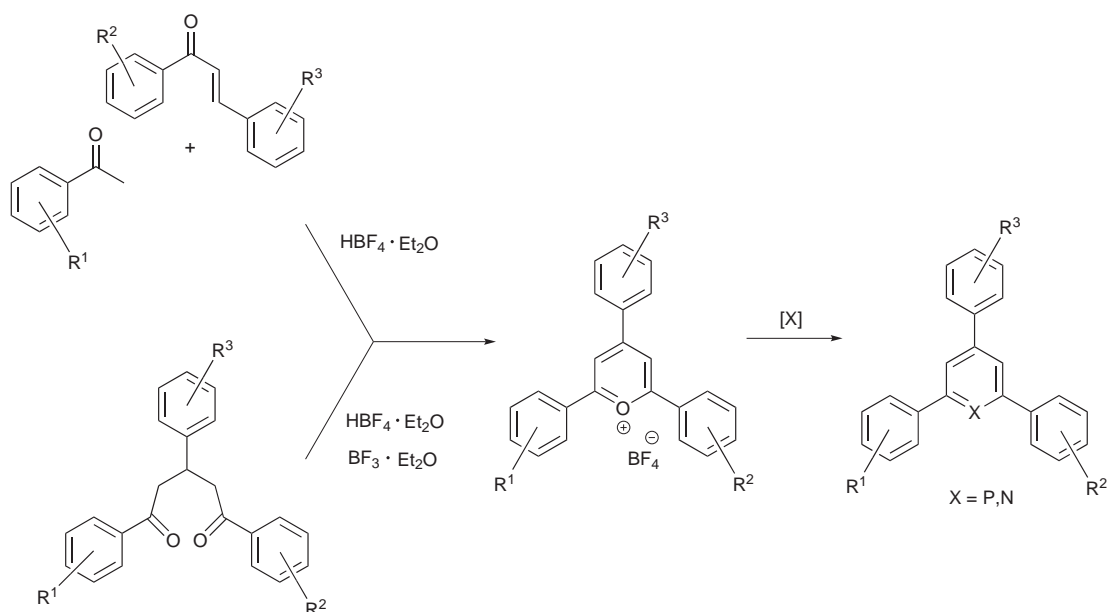


Figure 3.3: ORTEP representation of a 2,4,6-triarylphosphinine.^[27] Displacement ellipsoids are drawn at 50% probability level. All hydrogen atoms are omitted for clarity. a) full molecular structure in the crystal, b) front view, c) side view

General synthesis of triarylphosphinines and pyridines

Generally spoken the heterocyclic framework of triphenylphosphinines and pyridines consist of three modules, a benzaldehyde and two acetophenones, which are often readily available. The heterocycles can be prepared from their corresponding pyrylium salts, which themselves can be synthesised via two major routes (Scheme 3.1 on the next page). The first route starts from a chalcone and an acetophenone. In presence of an oxidant, usually another equivalent of the chalcone, and HBF_4 the pyrylium salt is formed. The second route begins with a diketone, which reacts with HBF_4 or $\text{BF}_3 \cdot \text{Et}_2\text{O}$ in the presence of benzylidene-2-acetophenone, as an oxidant, to the pyrylium salt. In the next step a strong N- or P-nucleophile is employed to replace the oxygen in the pyrylium salt and the pyridine and phosphinine respectively is formed. Usually $\text{P}(\text{CH}_2\text{OH})_3$ or $\text{P}(\text{SiMe}_3)_3$ are used as phosphorus sources. PH_3 is also suitable, but its employment is avoided due to its high toxicity, gaseous nature, and pyrophoric character. In case of the pyridine synthesis ammonium salts or ammonia act as nucleophiles.



Scheme 3.1: Modular synthesis of phosphinines and pyridines via pyrylium salts

3.2 Synthesis of ionic phosphinines and pyridines

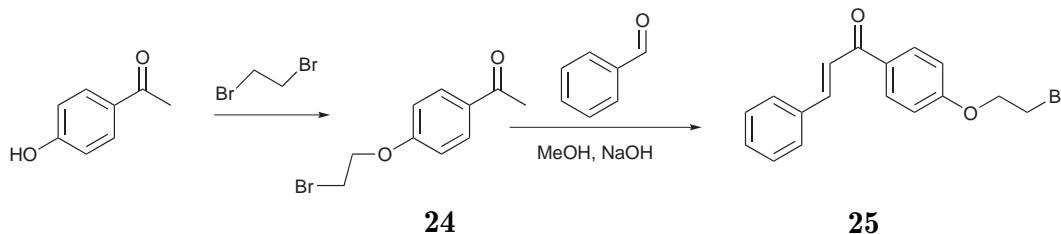
Ionic phosphinine ligands

Aim of this research is the synthesis of phosphinines ligand soluble in ionic liquids by means of ionic tagging. This concept has been proven to be beneficial to immobilisation purposes on many occasions.^[1,28]

3.2.0.6 Enone synthesis

The first step is the modification of the enone building block in a way that an ionic group can be tagged to it. Therefore, 4-hydroxyacetophenone was reacted with dibromoethane to yield 4-bromoethoxyacetophenone **24** (Scheme 3.2 on the following page). In a Claisen-Schmidt reaction the acetophenone **24** and the benzaldehyde formed the bromoethoxy functionalised chalcone **25** under basic conditions in methanol. The reaction mixture turned yellow/red after a while and within 12 hours a white solid was collected by filtration and obtained in high yields. This was washed several times with

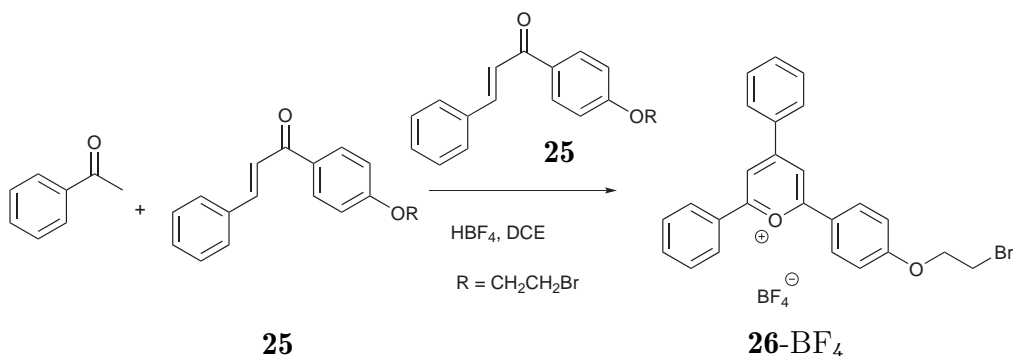
ice-cold methanol for purification purposes. Impurities were removed by recrystallisation from refluxing ethanol or methanol. **25** was fully characterised by means of ^1H NMR and ^{13}C NMR spectroscopy, as well as by mass spectrometry.



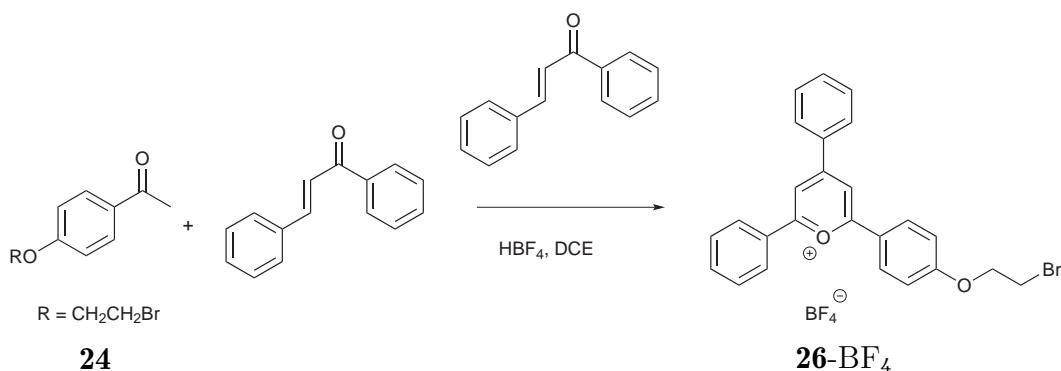
Scheme 3.2: Synthesis of bromoethoxy functionalised chalcone **25**

3.2.0.7 Synthesis of Bromoethoxy functionalised pyrylium salt

Two possible ways to synthesise the pyrylium salt were considered following a modified version described by Dimroth. The first route starts from chalcone **25** (Scheme 3.3 on the next page). Two equivalents of **25** were dissolved in 1,2-dichloroethane (DCE) and acetophenone was added to this solution. The mixture was heated up 70°C and afterwards two equivalents of HBF_4 were added slowly to the solution. The solution turned dark red immediately. Afterwards Et_2O was added to precipitate the pyrylium salt as a brown solid. This solid was dissolved in chloroform and precipitated with Et_2O two times. Unfortunately, a subsequent precipitation from methanol by addition of Et_2O gave the pyrylium salt **26** as an orange powder only in rather poor yield (less than 10 %). The other possible route starts from (E)-chalcone and the functionalised acetophenone **24** (Scheme 3.4 on the following page). This procedure has the advantage to use a commercially available chalcone as the hydrogen acceptor instead of using a chalcone that has to be prepared in a two step synthesis. After completion of the reaction the purification step was more laborious. Precipitation had to be conducted several times from DCM, chloroform and methanol before the pyrylium salt **26-BF₄** was obtained as an orange powder in reasonable yield (36 %). **26-BF₄** was fully characterised by ^1H and ^{13}C NMR spectroscopy as well as by elemental analysis. Crystals of the pyrylium salt **26-BF₄** suitable for X-ray analysis could not be obtained, as they were either too fragile or no single crystals.



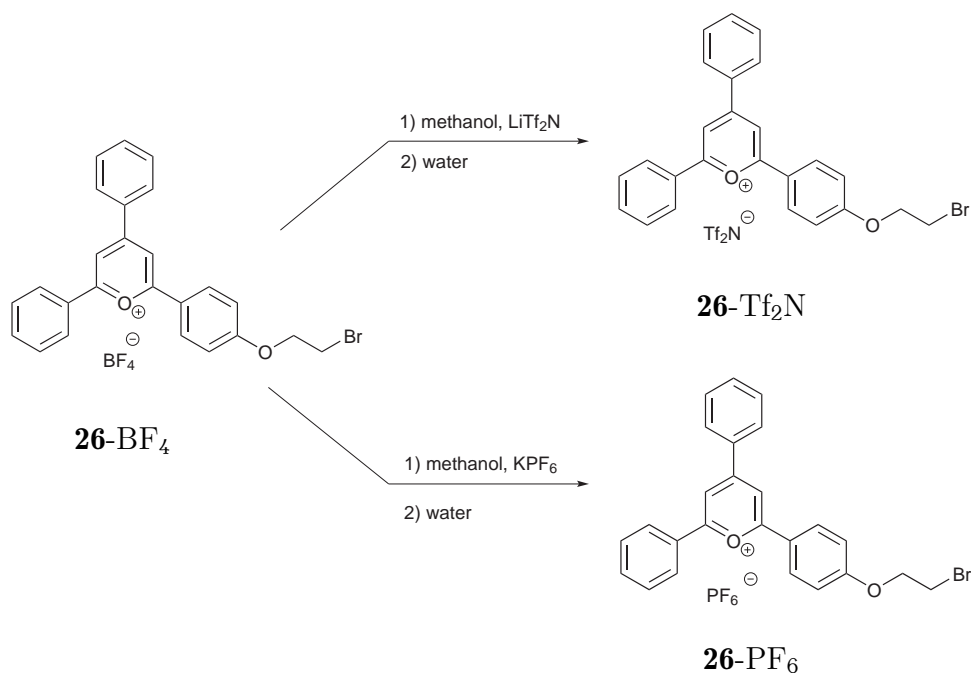
Scheme 3.3: Approach synthesing **26-BF₄** via the functionalised chalcone **25**



Scheme 3.4: Synthesis of bromoethoxy functionalised pyrylium salt **26-BF₄**

Therefore, the BF_4^- anion was exchanged for two different anions, PF_6^- and Tf_2N^- (bis(trifluoromethylsulfonyl)amide) (Scheme 3.5 on the next page) by dissolving **26-BF₄** in methanol and adding a solution of KPF_6 in methanol or LiTf_2N , respectively.

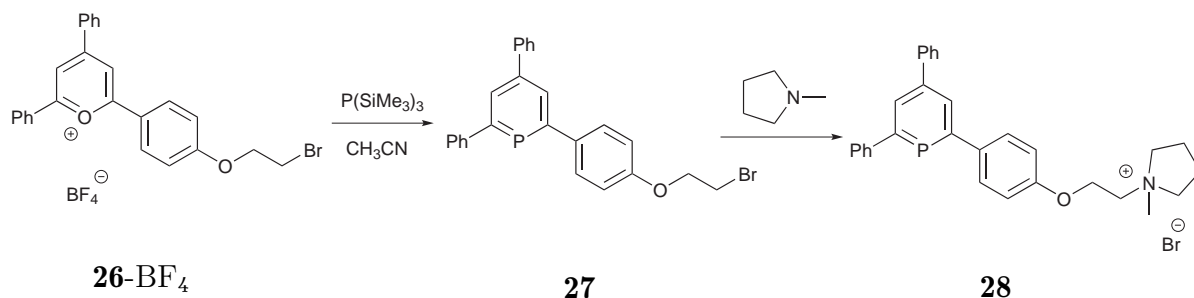
The solutions were allowed to stir at room temperature for 15 min and subsequently water was added to precipitate the two salts, **26-PF₆** and **26-Tf₂N** as an orange and a dark red powder. However, crystals suitable for X-ray diffraction could not be obtained. Various solvents and methods were tested, but the crystals were either grown together or too fragile. The two compounds were fully characterised by ^1H NMR and ^{13}C NMR spectroscopy. For compound **26-PF₆** also CHN analysis was obtained. In case of the pyrylium salt **26-Tf₂N** a satisfactory CHN analysis could not be obtained.



Scheme 3.5: Anion metathesis of pyrylium salt **26**

3.2.0.8 Synthesis and application of the mono-ionic phosphinine

The phosphorus is introduced into the ring structure of the pyrylium salt **26-BF₄** by nucleophilic attack of tris(trimethylsilyl)phosphine (P(Si(Me)₃)) (Scheme 3.6 on the following page). The pyrylium salt **26-BF₄** was dissolved in acetonitrile and an excess of P(Si(Me)₃) was added dropwise at room temperature. The reaction mixture was heated and refluxed for 6 h. After completion of the reaction, the remaining volatiles were removed under reduced pressure. The red residue was dissolved in DCM, added to an appropriate amount of silica and became subject to a flash-chromatography over neutral alumina with ethyl acetate as eluent. After evaporation of the solvent, the remaining solid was washed several times with Et₂O. ³¹P NMR spectroscopy in deuterated chloroform showed a signal at $\delta = 181.6$ ppm, which is characteristic for phosphinines. Purification was suspended and the crude product **27** was used in the next reaction step.

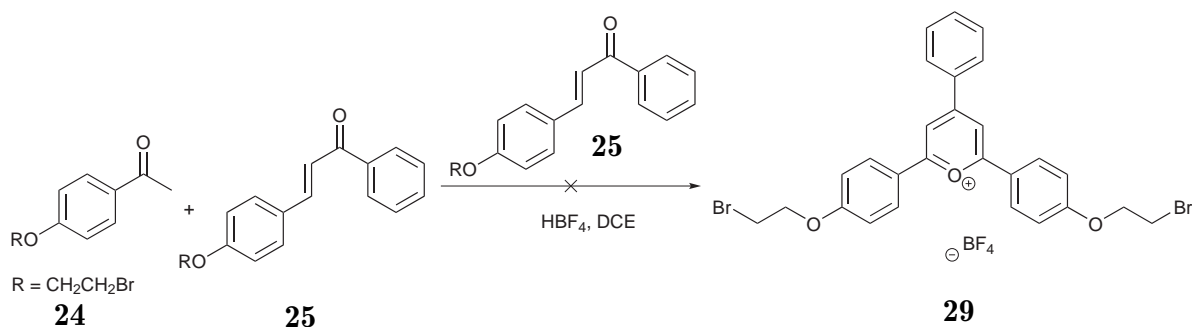
Scheme 3.6: Synthesis of tagged triphenyl phosphinine **28**

27 was dissolved in toluene, an excess of *N*-methyl pyrrolidine was added and the reaction mixture was stirred at 50°C for 12 hours (Scheme 3.6). The remaining volatiles were removed under reduced pressure and the remaining solid was washed several times with Et₂O until the Et₂O phase was colourless. The phosphinine **28** was obtained as a dark red powder soluble only in DMSO and poorly in chloroform. ³¹P NMR spectroscopy showed a resonance at $\delta = 180.5$ ppm in deuterated chloroform. A satisfactory ¹H NMR could not be obtained. However, all characteristic signals were detected indicating that **28** was indeed formed. However, resonances were rather broad and not distinct. Even at 100°C in DMSO no clear ¹H NMR spectrum was obtained. The reason for this is still unknown. To gain further evidence that the desired product was formed, elemental analysis was requested. This supports the assumption that the ionic ligand **28** was made.

Next, the catalytic activity of Rh/**28** in the Rh-catalysed hydroformylation of 1-octene was tested using Rh(acac)(CO)₂ as Rh precursor and eight equivalents of ligand **28**. Unfortunately at room temperature as well as at elevated temperature (40-70°C) the ligand failed completely to dissolve in the ionic liquid [PMIM][BF₄] (1-pentyl-3-methylimidazolium tetrafluoroborate). Also under reaction conditions at 100°C and 20 bar CO/H₂ (1:1) the ligand apparently did not dissolve as analysis of the reaction mixture gave no evidence for aldehyde formation after 4 hours reaction time. Only traces of isomerised 1-octene were found by GC-analysis. The insolubility of this ligand might be attributed to its ambivalent character, carrying an ionic group as well as a large apolar part. Logically an IL like [OMIM][BF₄] should be tried.

Synthesis of a centrosymmetric ionic phosphinine

To tackle the solubility problem a second ionic group was envisaged to introduce into the heterocyclic framework. Therefore, an attempt was started to react the bromoethoxy acetophenone **24** with the bromoethoxy chalcone **25** to yield the centrosymmetric pyrylium salt **29** (Scheme 3.7).



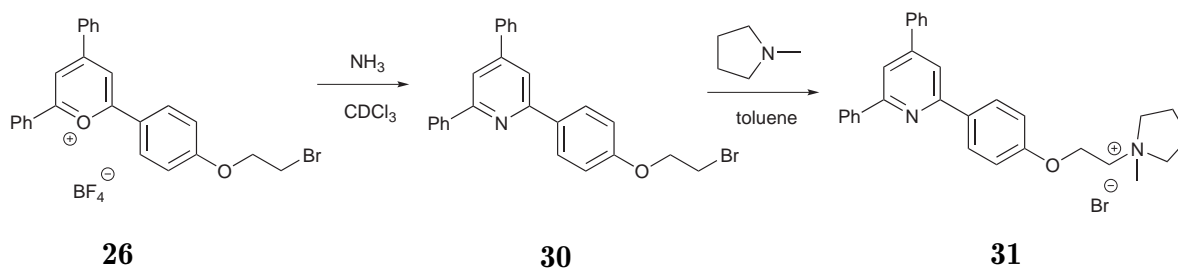
Scheme 3.7: Synthesis of centrosymmetric pyrylium salt **29**

Two equivalents of **25** were dissolved together with **24** in DCE. The solution was heated to 70°C and HBF₄ was added dropwise to the solution. The reaction mixture turned dark and after 6 hours reaction time it was allowed to cool down. At room temperature Et₂O was added and the solution was left stirring for 12 hours. After decanting the organic layer, the remaining solid was dissolved in methanol. Upon addition of Et₂O a dark red powder was received in very low yield. Analysis of this substance indicated that the desired product was not formed, as the characteristic signals for the ethoxy group could not be detected by ¹H NMR. Instead, one broad signal was found at δ = 3.5 ppm. Several attempts to synthesise this compound always led to the same result. Obviously the presence of the bromoethoxy group in the chalcone **25** frustrates formation of the pyrylium salt **28**.

Ionic pyridine ligands

The pyrylium salt **26** was dissolved in dry butanol following a procedure described by Dimroth.^[29] NH₃ was purged into the solution for about 30 min at 60°C. To this solution H₂O was added to cause precipitation of the pyridine ligand. The solid formed was

collected by filtration and washed with H₂O. However, the yield was rather low and the H₂O was difficult to remove from the ligand even under reduced pressure. Therefore a H₂O-free route was tested (Scheme 3.8). The pyrylium salt was dissolved in chloroform and ammonia was purged into this solution for one hour at 50°C. The solid formed was removed by filtration and the organic layer was concentrated. The product **30** was received as a beige-coloured solid in good yield and characterised by ¹H and ¹³C NMR spectroscopy. To introduce the ionic group, the ligand **30** was dissolved in toluene and *N*-methylpyridine was added to this solution. After 12 hours of stirring at 45°C the toluene was decanted and the ionic ligand **31** was collected as a white powder (Scheme 3.8). Purification was achieved by washing several times with Et₂O. The compounds were fully characterised by ¹H and ¹³C NMR spectroscopy, as well as by elementary analysis.

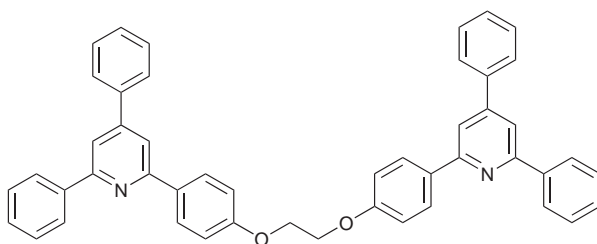


Scheme 3.8: Synthesis of tagged triphenyl pyridine

Dimeric pyridine

An interesting byproduct was obtained during the synthesis of **30**. It turned out that a minor side product was formed. This dimeric compound **32** crystallised and was identified as a side product of the pyrylium salt synthesis (Figure 3.4 on the next page).

This product can be formed by reaction of one equivalent of 1,2-dibromoethane with two equivalents of 4-hydroxyacetophenone (see Figure 3.2 on page 95). The corresponding bis-pyrylium salt was not detected before. Nevertheless, this structure was used to assess the influence of the side chain on the structure compared to an unfunctionalised pyridine ligand. Figure 3.5 on page 102 shows an ORTEP representation of the molecular structure of **32** in the crystal including selected bond lengths.

**32**Figure 3.4: Dimeric pyridine **32**

As observed for 2,4,6-triphenylpyridine, a disrotatory conformation of the phenyl substituents is preferred.^[30] However, the torsion angles are not coincident as can be seen in the symmetrical pyridine. One dihedral angle shows a significant deviation from those reported for 2,4,6-triphenylpyridine. Whereas in the reported structure the angles are all approximately 32° ,^[30] one angle in the bis-pyridine **32** differs from the others. The torsion angle between the pyridine ring and the functionalised moiety is approximately 17° in contrast to the 36° between the other rings. The substituted phenyl ring also influences the bond lengths in the pyridine core. Bonds facing the functionalised ring are shorter.

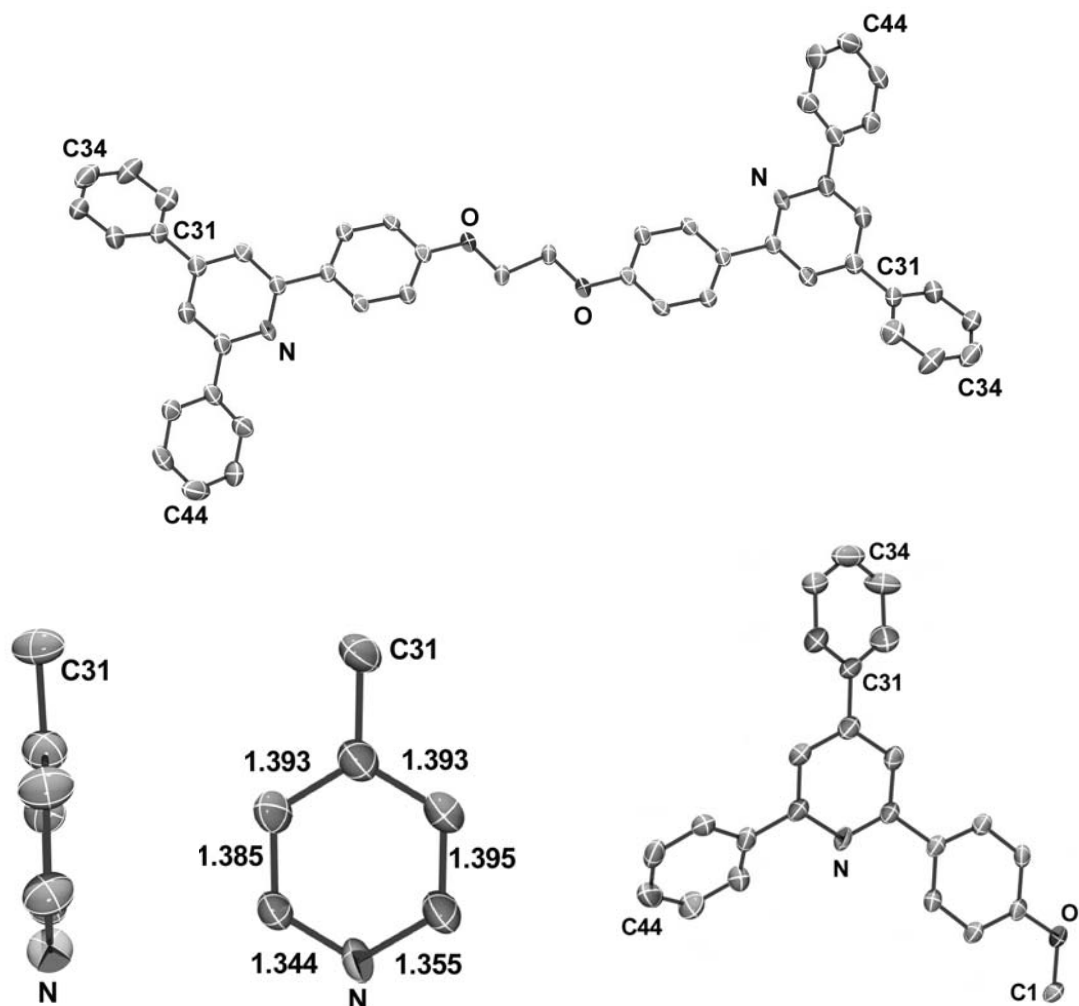


Figure 3.5: ORTEP representation of compound **32**. Above: full molecular structure of **32** in the crystal, Below from left to right: side view, core, front view (only parts of the structure are displayed). Displacement ellipsoids are drawn at 50% probability level. All hydrogen atoms are omitted for clarity. One ortho-phenyl ring was disordered and therefore omitted for clarity

3.3 Conclusion

In summary, the synthesis of an ionically tagged phosphinine ligand was successful. However, precise characterisation of the ligand was not possible, as the signals in the ^1H NMR spectrum were broad and not distinct. Nevertheless, all characteristic signals could be detected. The application of this ligand in the Rh-catalysed hydroformylation of 1-octene failed as the ligand was insufficiently soluble in the IL [PMIM][BF₄] even at reaction temperature (100°C) and 20 bar CO/H₂ (1:1). Another approach to increase the solubility by introducing two ionic groups into the heterocyclic framework failed. Obviously, the bromoethoxy group in the precursors disturbs the formation of the pyrylium salt. In another approach the mono substituted pyrylium salt was successfully converted into a pyridine, that could be tagged with an ionic group subsequently. A crystal of this compound suitable for X-ray diffraction was not obtained. However, a centro-symmetric pyridine ligand was crystallised as a minor byproduct and could be used to evaluate the influence of the side chain on the pyridine core. It became obvious that the side chain does have an impact on the bond length in the pyridine moiety.

3.4 Experimental

All chemicals were purchased from Aldrich, Acros or Merck and used as received. The liquids bought were degassed and the catalytical experiments were carried out under an atmosphere of dry argon or nitrogen using standard Schlenk techniques. NMR spectra were recorded on a Varian Unity Inova 500 (VT NMR) and Mercury 400-spectrometer. ^1H -NMR, ^{13}C -NMR were referenced using residual solvent peaks. ^{19}F NMR and ^{31}P NMR were referenced externally. The ionic liquid was degassed before being employed. Elementary analysis was performed on a Perkin Elmer 2400 series II CHNS/O Analyzer.

GC Analysis

GC: Shimadzu GC 17A
Column: Ultra 2 (crosslinked 5% Ph Me Siloxane), 25m, inner diameter 0.20 mm
film thickness 0.33 μm
Carrier gas: Helium 102 kPa (total flow 53 mL/min)

Procedure for the hydroformylation experiment

In a typical experiment, the autoclave was charged with a solution of 2.1 mg (8 μmol) $[\text{Rh}(\text{acac})(\text{CO})_2]$, 8 eq. ligand, 12 mmol 1-octene in 4 mL PMIM BF_4 . The autoclave was pressurised with 20 bar CO/H_2 (1:2), heated to 100°C and stirred for 4 h. After completion the reactor was cooled and the organic layer collected.

1-Methyl-3-pentyl-imidazolium tetrafluoroborate

1-Methylimidazole (60 mL, 0.752 mol) was mixed with 1-bromopentane (93.20 mL, 0.752 mol). The mixture was stirred at 50°C for 24 h. Subsequently, the liquid was diluted in acetone (100 mL) and then sodium tetrafluoroborate (85 g, 0.774 mol) was added. The mixture was stirred for 48 h at room temperature and then filtered. After evaporation of the acetone the liquid was filtered once more and washed with diethyl ether (30

mL). The remaining diethyl ether in the product was removed under vacuum afterwards.

¹H NMR (CD₃OD) δ (ppm): 8.83 (s, 1H), 7.60 (t, 1H, $J=1.80$ Hz), 7.54 (t, 1H, $J=1.77$ Hz), 4.20 (t, 2H, $J=7.39$ Hz), 3.91 (s, 3H), 1.91 - 1.87 (m, 2H), 1.40 - 1.32 (m, 4H), 0.92 (t, 3H, $J=7.13$ Hz). **¹³C NMR**: 136.40, 123.50, 122.19, 49.38, 35.02, 29.38, 27.92, 21.68, 12.75. **¹⁹F NMR**: -153.70.

1-(4-(2-Bromoethoxy)phenyl)ethanone (24)

To a solution of 5 g (36.72 mmol) 4-hydroxy acetophenone in 100 mL 3-pentanone was added 15.2 g (110.16 mmol) K₂CO₃. The mixture was stirred for 30 min and 9.5 mL (110.16 mmol) 1,2-dibromoethane was added. The reaction mixture was stirred at 100°C for 16 hours. The pentanone and the dibromoethane were removed under reduced pressure. The remaining slurry was diluted in EtOAc and washed 3 times with water. The organic layer was dried and concentrated to give a pale brownish product. If the product is not yet pure, it can be recrystallised from ethanol.

¹H NMR (CDCl₃) δ (ppm): 7.93 (d, 2H, $J=8.85$ Hz), 6.96 (d, 2H, $J=8.85$ Hz), 4.37 - 4.34 (t, 2H, $J=6.25$ Hz), 3.68 - 3.65 (t, 2H, $J=6.25$ Hz), 2.56 (s, 3H). **¹³C NMR**: 196.7, 161.9, 130.8, 114.2, 67.8, 28.6, 26.4. **MS**: (m/z) 264.98 [M+Na]⁺, calc. 264.98. Yield: 80% (7.14 g).

(E)-1-(4-(2-Bromoethoxy)phenyl)-3-phenylprop-2-en-1-one (25)

To an aqueous alcoholic solution (12 mL - ratio EtOH:H₂O of 1:2) of 0.3 g NaOH (1.25 eq.) was added 1.44 g (5.92 mmol) bromoethoxy acetophenone. The reaction mixture was cooled in ice and 0.6 mL (5.92 mmol) benzaldehyde was added dropwise. The reaction mixture was stirred at 25°C for 16 hours. The solid formed was removed by filtration, washed with water and recrystallised from hot EtOH.

¹H NMR (CDCl₃) δ (ppm): 7.98 - 7.96 (d, 2H, $J=8.85$ Hz), 7.75 - 7.72 (d, 1H, $J=15.56$ Hz), 7.58 - 7.47 (m, 2H), 7.49 - 7.45 (d, 1H, $J=15.56$ Hz), 7.35 - 7.33 (m, 3H), 6.93 - 6.91 (d, 2H, $J=8.85$ Hz), 4.31 - 4.28 (t, 2H, $J=6.10$ Hz), 3.61 - 3.58 (t, 2H, $J=6.10$ Hz).

^{13}C NMR: 188.69, 161.65, 144.21, 135.01, 131.70, 130.88, 130.42, 128.95, 128.39, 121.79, 114.46, 67.81, 28.64. **MS:** (m/z) 353.02 [M+Na]⁺, calc. 353.02. Yield: 92 % (1.80 g).

2-(4-(2-Bromoethoxy)phenyl)-4,6-diphenylpyrylium tetrafluoroborate (26-BF₄)

To a solution of (E)-chalcone and 4-bromoethoxyacetophenone in 30 mL dichloroethane at 70°C was added dropwise a ethereal solution of HBF₄ (52%). The blackish solution was allowed to stir at 70°C for 9 h. At room temperature 300 mL Et₂O were added to that solution. Immediately a black solid was formed. The ether was decanted and the remaining slurry was dissolved first in DCM and then in chloroform. Each time the solution was diluted with 200 mL of ether. The ether was decanted. Then the remaining solid was dissolved in warm methanol. A colour change to orange occurs. The methanol was also diluted with 200 mL of ether. The orange solid formed was collected and dried under vacuum.

2-(4-(2-bromoethoxy)phenyl)-4,6-diphenylpyrylium tetrafluoroborate (26-BF₄)

To an solution of (E)-1-(4-(2-bromoethoxy)phenyl)-3-phenylprop-2-en-1-one and 4-hydroxyacetophenone in 30 mL dichloroethane at 70°C was added dropwise a ethereal solution of HBF₄ (52%). The blackish solution was allowed to stir at 70°C for 9 h. At room temperature 300 mL ether were added to that solution. Immediately a black solid was formed. The ether is decanted and the remaining slurry was dissolved first in DCM and then in chloroform. Each time the solution was diluted with 200 mL of ether. The ether was decanted. Then the remaining solid was dissolved in warm methanol. A colour changed to orange occurs. The methanol was also diluted with 200 mL of ether. The orange solid formed was collected and dried under vacuum.

^1H NMR (CD₃CN) δ (ppm): 8.60 - 8.58 (m, 2H), 8.45 - 8.38 (m, 4H), 8.30 - 8.28 (m, 2H), 7.86 - 7.77 (m, 6H), 7.31 - 7.29 (m, 2H), 4.57 - 4.54 (t, 2H, $J=5.48$ Hz), 3.83 - 3.81 (t, 2H, $J=5.48$ Hz). **^{13}C NMR:** 170.82, 169.58, 165.34, 164.58, 134.99, 134.94,

133.07, 131.47, 130.00, 129.39, 129.13, 128.43, 121.60, 117.34, 116.25, 114.75, 114.50, 68.76, 29.69. ^{19}F NMR: -154.97. Elemental Analysis: calculated for $\text{C}_{25}\text{H}_{20}\text{BBrF}_4\text{O}_2$: %C 57.84, %H 3.88, found: %C 58.13, %H 3.77. Yield: 35 % (5.5 g).

2-(4-(2-Bromoethoxy)phenyl)-4,6-diphenylpyrylium bis(trifluoromethylsulfonyl)amide (26-Tf₂N)

To a solution of 100 mg (0.196 mmol) 2-(4-(2-bromoethoxy)phenyl)-4,6-diphenylpyrylium tetrafluoroborate in 1 mL warm methanol was given a solution of 169.04 mg (0.588 mmol) lithium bis(trifluoromethylsulfonyl)amide in 1 mL methanol. The mixture was left stirring for 10 min. Subsequently 6 mL water were added to precipitate the product as a bordeaux red solid. The solid was collected, washed several times with water and dried under vacuum.

^1H NMR (CD_3CN) δ (ppm): 8.61 - 8.59 (m, 2H), 8.46 - 8.43 (m, 2H), 8.41 - 8.39 (m, 2H), 8.30 - 8.28 (m, 2H), 4.58 - 4.55 (t, 2H, $J=5.50$ Hz), 3.84 - 3.81 (t, 2H, $J=5.49$ Hz). ^{13}C NMR: 170.83, 169.60, 165.35, 164.58, 135.06, 134.97, 134.91, 133.08, 131.56, 131.54, 131.45, 129.99, 129.44, 129.36, 129.13, 128.53, 128.42, 121.60, 116.23, 114.78, 114.53, 68.75, 29.69. ^{19}F NMR: -80.22. Yield: 86 % (120 mg).

2-(4-(2-bromoethoxy)phenyl)-4,6-diphenylpyrylium hexafluoroborate (26-PF₆)

To a solution of 100 mg (0.196 mmol) 2-(4-(2-bromoethoxy)phenyl)-4,6-diphenylpyrylium tetrafluoroborate in 1 mL warm methanol was given a solution of 108.23 mg (0.588 mmol) potassium hexafluorophosphate in 1 mL of warm methanol. The mixture was left stirring for 10 min. Subsequently 6 mL water were added to precipitate the product as a orange solid. The solid was collected, washed several times with water and dried under vacuum.

^1H NMR (CD_3CN) δ (ppm): 8.61 - 8.59 (m, 2H), 8.46 - 8.41 (m, 4H), 8.30 - 8.28 (m, 2H), 7.87 - 7.77 (m, 6H), 7.32 - 7.30 (m, 2H), 4.58 - 4.57 (t, 2H, $J=5.62$ Hz), 3.84 - 3.81 (t,

2H, $J=5.59$ Hz). ^{13}C NMR: 170.85, 169.13, 165.37, 164.58, 134.97, 34.90, 133.1, 131.46, 129.99, 129.36, 129.15, 128.51, 128.42, 117.32, 116.23, 114.80, 114.55, 68.75, 29.68. ^{19}F NMR: -72.04, -73.91. Elemental Analysis: calculated for $\text{C}_{25}\text{H}_{20}\text{BrF}_6\text{O}_2\text{P}$: %C 52.10, %H 3.49, found: %C 53.31, %H 3.27. Yield: 94 % (105 mg).

2-(4-(2-Bromoethoxy)phenyl)-4,6-diphenylphosphinine (27)

2.74 g (11.0 mmol, 3 equiv.) of $\text{P}(\text{SiMe}_3)_3$ was added dropwise at room temperature to a stirred solution of **26**- BF_4 (1.89 g, 3.65 mmol) in 15 mL of acetonitrile. The resulting dark reaction mixture was heated to 85°C and subsequently refluxed for 6 h. After cooling to room temperature, the volatiles were removed under vacuum. The residue was dissolved in CH_2Cl_2 and added to an appropriate amount of silica gel (ca. 3 g). Evaporation of the solvent was followed by flash-chromatography over neutral alumina with ethyl acetate. The crude product **27** was received as a red solid. Further purification was suspended and the crude product was used directly in the synthesis of **28**.

^{31}P NMR (CDCl_3) δ (ppm): 181.65

1-(2-(4-(4,6-Diphenylphosphinin-2-yl)phenoxy)ethyl)-1-methylpyrrolidinium bromide (28)

The crude product **27** (3.65 mmol) from the preceding synthesis was dissolved in 10 mL of toluene and 0.62 g (7.30 mmol, 2 eq.) *N*-methyl pyrrolidine was added. The reaction mixture was stirred at 50°C for 12 hours. A red precipitate was formed. The remaining volatiles were removed under reduced pressure and the solid was washed several times with Et_2O until the ether phase was colourless. The product **28** was received as a fine red powder.

^{31}P NMR (CDCl_3) δ (ppm): 180.01 $\text{C}_{30}\text{H}_3\text{BrNOP}$: %C 67.67, %H 5.87, %N 2.63, found: %C 69.43, %H 5.59, %N 2.45. Yield 25% (0.44 g).

2,6-Bis(4-(2-bromoethoxy)phenyl)-4-phenylpyrylium tetrafluoroborate (29)

To an solution of (E)-1-(4-(2-Bromoethoxy)phenyl)-3-phenylprop-2-en-1-one and 4-bromoethoxyacetophenone in 30 mL dichloroethane at 70°C was added dropwise a ethereal solution of HBF₄ (52%). The blackish solution was allowed to stir at 70°C for 9 h. At room temperature 300 mL ether were added to that solution. Immediately a black solid was formed. The ether was decanted and the remaining slurry is dissolved first in DCM and then in chloroform. Each time the solution was diluted with 200 mL of ether. The ether was decanted. Then the remaining solid was dissolved in warm methanol. A colour change to dark orange occurs. The methanol was diluted with 200 mL of ether. The orange solid formed was collected and dried under vacuum. However, no product was found.

2-(4-(2-Bromoethoxy)phenyl)-4,6-diphenylpyridine (30)

Into a solution of 0.5 g (0.96 mmol) 2-(4-(2-bromoethoxy)phenyl)-4,6-diphenylpyrylium tetrafluoroborate in chloroform ammonia was continuously added for one hour at 50°C. The solution changes colour from yellowish to colourless and a white precipitate was formed. This precipitate was separated from the solution. The solution was concentrated and the solid was dried under vacuum.

¹H NMR (CDCl₃) δ (ppm): 8.21 - 8.17 (m, 4H), 7.85 - 7.83 (d, 2H), 7.76 - 7.74 (d, 2H), 7.54 - 7.45 (m, 6), 7.06 - 7.04 (d, 2H), 4.40 - 4.37 (t, 2H), 3.70 - 3.67 (t, 2H). ¹³C NMR: 159.00, 157.40, 156.92, 150.16, 139.65, 139.16, 132.98, 129.01, 128.99, 128.93, 128.68, 128.51, 127.17, 127.10, 116.63, 116.41, 114.85, 67.91, 29.00. Yield: 85 % (0.35 g).

1-(2-(4-(4,6-Diphenylpyridin-2-yl)phenoxy)ethyl)-1-methylpyrrolidinium bromide (31)

0.5 g (1.16 mmol) 2-(4-(2-bromoethoxy)phenyl)-4,6-diphenylpyridine was dissolved in 10 mL of toluene/heptan (50:50) and 1 mL of *N*-methylpyrrolidine was added. The solution was left stirring for 16 h at 70°C. A white solid was formed and collected.

The organic layer was concentrated and the solid yielded was combined with the other solid. This cream-coloured powder was washed several times with diethylether and dried under reduced pressure.

¹H NMR (CD₃CN) δ (ppm): 8.32 - 8.28 (m, 4H), 8.06 - 8.05 (m, 2H), 7.95 - 7.92 (m, 2H), 7.62 - 7.51 (m, 6H), 7.16 - 7.15 (d, 2H, $J=8.99$ Hz), 4.53 (b, 2H), 3.79 - 3.77 (m, 2H), 3.62 - 3.61 (m, 4H), 3.13 (s, 3H), 2.24 (b, 4H). **¹³C NMR**: 158.49, 157.11, 156.60, 150.23, 139.40, 138.53, 133.04, 129.19, 129.18, 129.11, 128.71, 128.59, 127.33, 127.03, 117.69, 117.29, 114.74, 65.49, 62.76, 62.31, 48.73, 21.15. Elemental Analysis: calculated for C₃₀H₃₁BrN₂O: %C 69.90, %H 6.06, %N 5.43, found: %C 66.84, %H 6.04, %N 5.08. Yield: 75 % (0.45 g).

Selected crystallographic data

Table 3.2: Selected crystallographic data of pyridine compound **32**

32	
formula	C ₄₈ H ₃₆ N ₂ O ₂
Crystal system	monoclinic
Space group	P21/n
A (Å)	4.8979(3)
B (Å)	18.2410(14)
C (Å)	19.4452(13)
α (°)	90
β (°)	95.918(3)
γ (°)	90
V(Å ³)	1728.0(2)
Z	4
T (K)	150
F(000)	708.0
Reflections collected	2235
R indices (all data)	R1 = 0.070 wR2 = 0.212

X-ray structure of 32

$C_{48}H_{36}N_2O_2$, Fw = 672.79, colourless needle, 0.39 x 0.06 x 0.06 mm³, monoclinic, P21/n (no. 14), a = 4.8979(3), b = 18.2410(14), c = 19.4452(13) Å, β = 95.918(3)°, V = 1728.0(2) Å³, Z = 2, Dx = 1.293 g/cm³, μ = 0.08 mm⁻¹. 10092 Reflections were measured on a Nonius KappaCCD diffractometer with rotating anode (graphite monochromator, λ = 0.71073 Å) up to a resolution of $(\sin \theta / \lambda)_{\max} = 0.54$ Å⁻¹ at a temperature of 150(2) K. The crystal consisted of two fragments related by a 141° rotation approximately about the vector hkl=(5,0,-2). Intensity integration was performed with Eval15^[31] based on two orientation matrices. Only non-overlapping reflections were stored. The SADABS^[32] programme was used for absorption correction and scaling based on multiple measured reflections (0.61-1.00 correction range). 2235 Reflections were unique ($R_{int} = 0.084$), of which 1359 were observed [$I > 2\sigma(I)$]. The structure was solved with Charge Flipping using the programme PLATON.^[33] The structure was refined with SHELXL-97^[34] against F² of all reflections. Non hydrogen atoms were refined with anisotropic displacement parameters. All hydrogen atoms were introduced in calculated positions and refined with a riding model. The ortho-phenyl substituent at C16 was refined with two orientations in a 50:50 ratio. 271 Parameters were refined with 86 restraints (distance, angle and flatness restraints concerning the disorder and restraints to approximate isotropic behavior of the displacement parameters). R1/wR2 [$I > 2\sigma(I)$]: 0.0701 / 0.1742. R1/wR2 [all refl.]: 0.1260 / 0.2118. S = 1.024. Residual electron density between 0.31 and 0.27 e/Å³. Geometry calculations and checking for higher symmetry was performed with the PLATON programme.^[33]

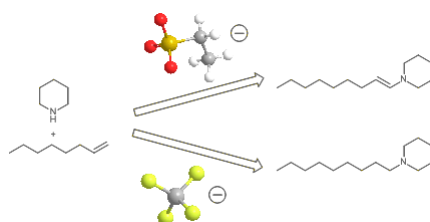
Bibliography

- [1] B. Hamers, P. S. Bäuerlein, C. Müller, D. Vogt, *Adv. Synth. Catal.* **2008**, *350*, 332–342.
- [2] B. Hamers, E. Kosciuski-Morizet, C. Müller, D. Vogt, *ChemCatChem* **2009**, *1*, published online.
- [3] K. Kunna, C. Müller, J. Loos, D. Vogt, *Angew. Chem. Int. Ed.* **2006**, *45*, 7289–7292.
- [4] P. W. N. M. van Leeuwen, *Homogeneous Catalysis*, Kluwer Academic Publishers, Dordrecht, Boston, London, **2004**.
- [5] P. W. N. M. van Leeuwen, C. Carmen, *Rhodium Catalyzed Hydroformylation, Vol. 22*, Kluwer Academic Publishers, Dordrecht, Boston, London, **2000**.
- [6] G. Märkl in *Multiple Bonds and Low Coordination in Phosphorus Chemistry* (Eds.: M. Reitz, O. J. Scherer), Thieme Verlag, Stuttgart, **1990**, p. 220.
- [7] G. Märkl, *Angew. Chem.* **1966**, *78*, 907–908.
- [8] C. Müller, D. Vogt, *Dalton Trans.* **2007**, 5505–5523.
- [9] C. Müller, E. A. Pidko, D. Totev, M. Lutz, A. L. Spek, R. A. van Santen, D. Vogt, *Dalton Trans.* **2007**, 5372–5375.
- [10] C. Müller, D. Wasserberg, J. J. M. Weemers, E. A. Pidko, S. Hoffmann, M. Lutz, A. L. Spek, S. C. J. Meskers, R. A. J. Janssen, R. A. van Santen, D. Vogt, *Chem. Eur. J.* **2007**, *13*, 4548–4559.
- [11] C. Müller, L. Guarrotxena Lopèz, H. Kooijman, A. L. Spek, D. Vogt, *Tetrahedron Lett.* **2006**, *47*, 2017–2020.
- [12] A. J. Ashe III, *J. Am. Chem. Soc.* **1971**, *93*, 3293.
- [13] K. Dimroth, W. Mach, *Angew. Chem. Int. Ed.* **1968**, 460–461.
- [14] P. de Koe, R. van Veen, F. Bickelhaupt, *Angew. Chem. Int. Ed.* **1968**, *6*, 567–568.
- [15] K. Dimroth, *Top. Curr. Chem.* **1973**, *38*, 1.
- [16] P. de Koe, R. van Veen, F. Bickelhaupt, *Angew. Chem. Int. Ed.* **1968**, *7*, 465–466.

- [17] F. Mathey, P. Le Floch, *Sci. Synth.* **2005**, *15*, 1097.
- [18] U. Bergsträßer, *Sci. Synth.* **2005**, *15*, 1181.
- [19] F. Mathey, *Angew. Chem. Int. Ed.* **2003**, *42*, 1578.
- [20] P. Le Floch in *Phosphorus-Carbon Heterocyclic Chemistry: The Rise of a New Domain* (Ed.: F. Mathey), Pergamon, Palaiseau, **2001**, pp. 485–533.
- [21] B. Breit, R. Winde, T. Mackewitz, R. Paciello, K. Harms, *Chem. Eur. J.* **2001**, *7*, 3106–3121.
- [22] D. E. F., M. C. Kozłowski, *J. Chem. Soc. Perkin Trans* **2001**, 439.
- [23] P. D. Burrow, A. J. Ashe III, D. J. Bellville, K. D. Jordan, *J. Am. Chem. Soc.* **1982**, *104*, 425.
- [24] A. Modelli, B. Hajgato, J. F. Nixon, L. Nyulaszi, *J. Phys. Chem. A* **2004**, *108*, 7440.
- [25] L. Nyulaszi, T. Veszpremi, *J. Phys. Chem.* **1996**, *100*, 6456.
- [26] L. Nyulaszi, *Chem. Rev.* **2001**, *101*, 1229.
- [27] C. Müller, M. Lutz, A. L. Spek, D. Vogt, *J. Chem. Crystallogr.* **2006**, *36*, 869–874.
- [28] R. Sebesta, I. Kmentová, S. Toma, *Green Chem.* **2008**, *10*, 484–496.
- [29] K. Dimroth, *Angew. Chem.* **1960**, *10*, 331–358.
- [30] J. Ondráček, J. Novotní, *Acta. Cryst.* **1994**, *C50*, 1809–1811.
- [31] X. Xian, A. M. M. Schreurs, L. M. J. Kroon-Batenburg, *Acta. Cryst.* **2006**, *A62*, 92.
- [32] G. M. Sheldrick, *SADABS: Area-Detector Absorption Correction*, **1999**.
- [33] A. L. Spek, *J. Appl. Cryst.* **2003**, *36*, 7–13.
- [34] G. M. Sheldrick, *Acta. Cryst.* **2008**, *A64*, 112–122.

Ionic liquids under scrutiny - Their impact on the hydroaminomethylation reaction

Ionic liquids received a great deal of attention lately as they can have a major impact on reactions regarding selectivity, feasibility and recyclability. For many reactions, such as hydrogenation, hydroformylation and cross-coupling reactions, the applicability has been successfully demonstrated. Especially regarding the biphasic catalysis, ionic liquids offer new opportunities. Therefore, this chapter deals with a biphasic reaction system. Attention is focused on the influence of ionic liquids on the outcome and course of the reaction. As reaction the hydroaminomethylation has been chosen due to its importance as source for tertiary amines; valuable chemicals for more complex molecules. This reaction is of special interest as it combines three reactions in one cascade and therefore the influence of the ionic liquid on more than one reaction can be investigated.



Part of this work has been published:

B. Hamers, P.S. Bäuerlein, C. Müller, D. Vogt, *Adv. Synth. Catal.* **2008**, 350(2), 332-342.

4.1 Introduction

Catalyst recovery

Homogeneous catalysts offer many advantages over heterogeneous ones. However, their advantages such as high selectivity are often accompanied by disadvantages such as high cost and insufficient recyclability. A crucial part of research in homogeneous catalysis is therefore catalyst recovery,^[1-5] especially when extremely expensive and rare metals like rhodium are employed. Several promising routes have been discovered. Homogeneous catalysts were successfully anchored to dendritic structures, allowing recovery by membrane separation.^[3] In general, weight and size enlargement are fruitful ways.^[2] They allow recovery by filtration or membrane reactors. Apart from this route to tackle the problem, ionic liquids (ILs)^[6-8] have proven themselves to be useful. Many reports have been published on this means of catalyst immobilisation.^[9] These unique solvents can dissolve ionic ligands and immobilise them as they form biphasic systems, like water, with many apolar substrates and allow straightforward product and catalyst separation. The catalyst remains in the ionic liquid. But in contrast to water, also long-chain substrates are applicable in the ILs. Solubility of the substrates usually limits the employment of water to short apolar substrates. Here, the ILs can contribute beneficially. They can dissolve a sufficient amount of substrate for the reaction to take place. In a comprehensive study by van Leeuwen *et al.* the applicability of this principle was highlighted for the hydroformylation of 1-octene.^[10] They synthesised an entirely new ionic ligand (Figure 4.1) soluble in 1-butyl-3-methyl-imidazolium hexafluorophosphate ([BMIM] [PF₆]).

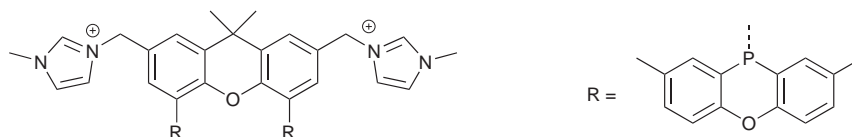


Figure 4.1: Novel dicationic ligand by van Leeuwen *et al.*

This ligand gave excellent results regarding selectivity and recyclability. In seven consecutive runs the catalyst always gave a l/b ratio of about 45 and did not show

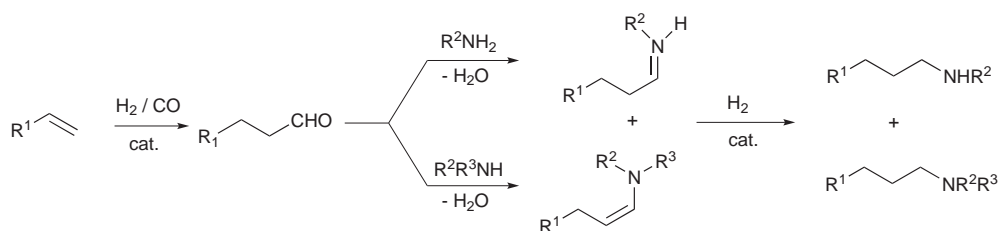
any loss of activity. Later on Wang *et al.* seized on this principle and reported on the application of a tosylate-based IL in the hydroaminomethylation (HAM).^[11] Applying a Rh/BISBIS¹ catalytic system they successfully demonstrated that the rhodium catalyst can be recycled several times. However, the effect of the nature of the cation and anion of the ionic liquids has never been investigated so far in detail for the rhodium-catalysed HAM or for the hydroformylation.

Hydroaminomethylation

The rhodium-catalysed hydroaminomethylation (HAM),^[11-14] is a reaction discovered at BASF by Reppe *et al.* In this reaction higher-substituted amines are formed from readily available and inexpensive alkenes and amines.^[15,16] The formation of amines in organic chemistry receives a great deal of attention as the products are of high value. They are needed for the production of *e.g.* polymers and pharmaceuticals.^[17] The HAM stands out from the numerous routes to form amines^[18] due to the fact that it circumvents several commonly known problems, such as stoichiometric salt formation in *e.g.* nucleophilic reactions and the use of expensive and often toxic chemicals, a problem commonly encountered when reducing nitro or nitrile compounds. These problems can be avoided in the HAM reaction. Therefore, this reaction is significantly 'greener'^[19,20] and more feasible than other routes. The HAM is an atom-efficient and one-pot reaction, with water as the only inevitable stoichiometric by-product. Starting from low-priced stock chemicals, such as alkenes and primary or secondary amines, tertiary amines are the products striven for. In total the hydroaminomethylation consists of three individual reactions, which form a sequence or cascade (Scheme 4.1 on the next page).

The first reaction is a Rh-catalysed hydroformylation of alkenes to aldehydes.^[21,22] In this step the selective formation of linear aldehydes is generally aimed for by the chemical industry as these are important bulk intermediates for large-scale syntheses. The (chiral) branched products, however, are indispensable intermediates for manufacturing small-scale organic compounds, *e.g.* asymmetric synthesis of pharmaceutically active molecules. The reaction can be steered by the ligands employed in this reaction. Bulky and bidentate ligands (Figure. 4.2 on the following page), such as Naphos or Xantphos,

¹sulfonated 2,29-bis(diphenylphosphinomethyl)-1,19 - biphenyl



Scheme 4.1: Hydromaminomethylation reaction

direct the reaction towards the formation of mainly linear products ($l/b > 50$). The application of sterically less hindered ligands allows the formation of more branched products. In contrast to an ordinary hydroformylation reaction, one has to bear in mind the basic conditions under which the HAM takes place. The presence of amines and significant amounts of water, exclude the application of water-sensitive ligands. In general, exclusively phosphine ligands are therefore employed as they are famous for their stability under these conditions. Alternatively phosphabarrelenes are proven to be suitable ligands, as they are inert to water and amines (Figure 4.2).^[23,24]

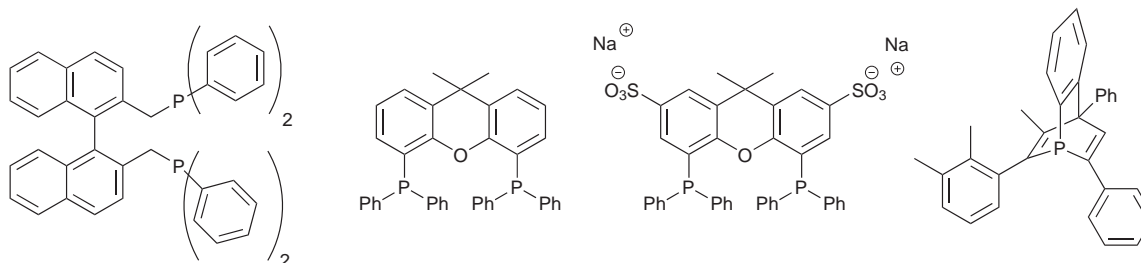


Figure 4.2: Ligands typically applied in the hydroformylation and hydroaminomethylation. From left to right: Naphos, Xantphos, Sulfoxantphos, phosphabarrelene

In the next step the aldehydes condensate with primary or secondary amines to imines or enamines, respectively. At this point it is crucial that this reaction proceeds quickly to impede side reactions, such as aldol reaction or hydrogenation of the aldehydes to alcohols. The enamines/imines are subsequently hydrogenated to the corresponding amines. Also here fast reduction of the double bond is crucial to shift the equilibrium

of the condensation continuously towards the condensation product, consequently suppressing side reactions of the aldehydes. There is, however, the possibility to prevent hydrogenation and almost selectively form imines or enamines without risking the formation of unwanted side products. This was achieved in the group of Beller by employing neutral rhodium precursors in combination with Naphos as ligand in toluene.^[25] Further investigations of Hamers *et al.* shed light on the reasons of this observation.^[26] They revealed that the protic character of a solvent is determining. Another key role is reserved for the catalyst precursor. The application of a neutral precursor is necessary as cationic rhodium species are well-known hydrogenation catalysts, whilst the neutral rhodium catalyst promote effectively the hydroformylation reaction.

As the HAM in organic solvents is well studied and the influence of organic solvents is amply understood, this chapter will deal with the application of various ionic liquids to steer and improve this important reaction. Interestingly, only little is known about the HAM in ionic liquids in contrary to the hydroformylation or hydrogenation reactions.

4.2 Results and Discussion

Application of a non-coordinating anion

Rh-catalysed HAM of long-chain alkenes is usually studied in toluene/methanol systems. However, this system bears the disadvantage that after each reaction, an energy-consuming work-up of the reaction mixture is necessary to separate catalyst, solvent, and product with the inescapable consequence to destroy the catalyst. To circumvent this problem ionic liquids were considered. Their ability to dissolve apolar compounds is defined and it is known that they can immobilise ionic catalysts and ligands. Therefore, ionic liquids are suitable candidates to solve this problem by forming biphasic systems (Figure 4.3 on the following page).

The Rh/Sulfoxantphos system was applied and 1-octene and piperidine were selected as bench mark substrates. The reactions were conducted in high pressure autoclaves. The ionic liquid 1-methyl-3-pentyl imidazolium tetrafluoroborate ([PMIM][BF₄]) was

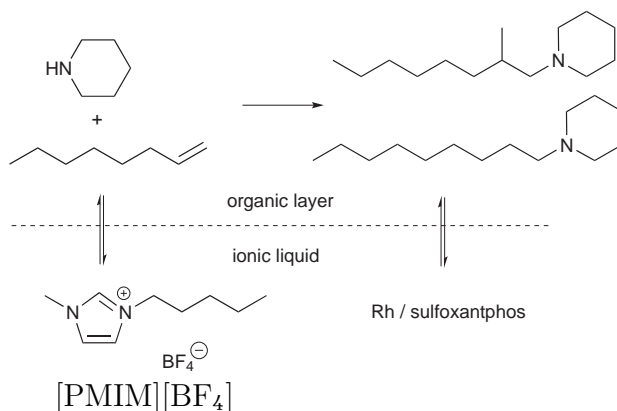


Figure 4.3: Hydroaminomethylation in a biphasic system using [PMIM][BF₄] as solvent and sulfoxantphos as ligand

chosen, due to its properties, such as low-melting point, low-viscosity, and excellent solubility of the catalyst and ligand. This IL formed a biphasic system at room temperature and at 120°C as well as before and after the reaction. The two layers separated swiftly and distinctly, when the stirrer was switched off. In a first attempt the reaction in toluene/methanol (1:1) and in [PMIM][BF₄] were compared under the same conditions (Table 4.1).

Table 4.1: Hydroaminomethylation in toluene/methanol and [PMIM][BF₄]

Entry	Cycle	S/Rh	Solvent	Conv. %	isom. octene %	Selectivity (amine) %	l/b
1	-	1150	Tol/MeOH	94.4	4.9	87.3	62
2	-	1150	[PMIM][BF ₄]	94.4	4.8	98.6	52.1
3	1	4000	[PMIM][BF ₄]	92.8	6.4	99.0	27.4
4 ^a	2	4000	[PMIM][BF ₄]	97.2	3.1	93.4	38.3
5	3	4000	[PMIM][BF ₄]	89.8	8.1	79.8	32.7
6 ^b	3	4000	[PMIM][BF ₄]	89.7	8.5	79.9	33.1

Conditions: 7 mL solvent, 19-24 mmol 1-octene, 22-88 mmol piperidine, [Rh(cod)₂BF₄] = 0.03 mol%, L/Rh = 4, T = 125°C, *p*(CO/H₂ (1:2)) = 36 bar (cold pressure), 400 rpm, 17 h
 a) substrate was 1-hexene, b) analysis of ether layer

Comparing the two solvents did not reveal any significant difference in the outcome (entries 1 and 2). Conversion and l/b ratio are almost identical. However, the selectivity to the amine in the ionic liquid is higher. The selectivity is lower in toluene/methanol due to the proton promoted aldol reaction. A higher methanol amount would ultimately cause even more aldol product to be formed, therefore solely employing methanol is not possible. The l/b ratio is only marginally better in the organic solvent. A l/b ratio of 62 defines that 98.4 % of amines are linear and 1.6 % are branched, whereas a value of 52 represents a mixture of 98.1 % linear and 1.9 % of branched product. Owing to formation of a biphasic system, recycling experiments were conducted. For this purpose, the product layer was removed from the autoclave under argon and new substrate was added. Three consecutive runs were carried out (entries 3 to 5). Notably, in all three cases almost no significant change in the reaction outcome could be observed. In the second run 1-hexene was used as substrate to rule out that traces of remained products from the first run falsified the analytic of the consecutive runs. Solely, the selectivity towards the amine is influenced in the third run. This might be attributed to the accumulation of water in the IL phase. Water was not removed, therefore its presence must have had an impact on the condensation equilibrium. Significant leaching of the ligand or catalyst could be excluded by ICP analysis and NMR spectroscopy. Several organic layers were analysed and the loss of rhodium was below detection limit ($Rh < 0.09\%$). ^{31}P NMR spectroscopy did not reveal any presence of phosphorus in the product layer. However, traces of IL were detected by 1H NMR and ^{19}F NMR spectroscopy. These could be removed completely by filtration over silica. To verify that the organic layer and the IL layer contained the same product composition, the IL and the organic layer both were analysed after the third run. The IL layer was removed from the autoclave and extracted several times with Et_2 . This solution was then analysed by GC. It can be seen that the organic layer reflects the product composition in the IL layer (entries 5 and 6). Other ionic liquids composed of non-coordinating anions were evaluated against BF_4^- (Table 4.2 on the following page), all of which form biphasic systems with the substrates. Firstly, it was proceeded from BF_4^- to the comparable anion PF_6^- (entries 1 and 2).

The reaction outcome in both cases is almost identical. No significant difference can be seen, although $[PMIM][PF_6]$ is, at least at room temperature, the more viscous IL, mak-

Table 4.2: Comparison of different weakly coordinating anions

Entry	IL	t h	Conv. %	l/b	am/en ^b	aldehyde %	aldol %
1	[PMIM][BF ₄]	17	99	27	> 100	n.d.	n.d.
2	[PMIM][PF ₆]	17	93	31	> 100	<1	n.d.
3	[PMIM][(CN) ₂ N]	17	n.r.	-	-	-	-
4	[PMIM][Tf ₂ N]	17	40	>0.5	>100	8	3.5
5	[PM ₂ IM][BF ₄]	17	37	>100	8	n.d.	1.8
6	[PMPyr][Tf ₂ N]	3	65	2	2	n.d.	2
7	[PMPyr][Tf ₂ N]	17	97	1.7	4	n.d.	3
8	[PMIM][BF ₄] ^a	17	97	11	6	n.d.	40

Conditions: 7 mL solvent, 19 mmol 1-octene, 22 mmol piperidine, [Rh(cod)₂BF₄] = 0.03 mol%, S/Rh = 1000, L/Rh = 4, T = 125°C, *p*(CO/H₂ (1:2)) = 36 bar (cold pressure), 400 rpm
a) Addition of 10 mg LiTf₂N, S/Li = 550 b) amine/enamine

ing its employment less attractive. Ligand and catalyst dissolve quickly. It can be rated as a negative aspect that this IL is known for its reactivity towards water.^[27] For this reason a negative impact on the reaction outcome could have been expected. Under these reaction conditions, however, this problem did not occur or at least did not influence the reaction in a noticeable way. Not surprisingly, the dicyanamide ((CN)₂N) containing IL is not suitable at all (entry 3). This effect can probably be assigned to the CN groups of the dicyanamide interfering with the catalyst. Solubility of the catalyst and ligand is excellent. Another weakly coordinating anion, the bis(trifluoromethylsulfonyl)amide (Tf₂N⁻) was employed. Here, the reaction outcome was surprising (entry 4), as the reaction was rather slow. The reason might be the poor solubility of the catalyst and ligand observed at room temperature. More striking, however, is the poor l/b ratio and amount of aldol product formed. The anion is known to be non-coordinating and cannot be the reason for this observation. A reasonable explanation would be the presence of traces of lithium ions in the IL, which could promote the aldol reaction as well as interfere with the catalyst. In fact, the IL is prepared from [PMIM] [Br] and LiTf₂N in a metathesis reaction. As lithium salts are known to be an effective catalyst for the aldol reaction, their presence in the IL could have been the reason for the increased amounts of aldol products. Although the IL was washed several times to remove impurities, complete re-

removal of lithium salt traces obviously could not be achieved. To prove this theory right, 10 mg LiTf_2N were added to a reaction in $[\text{PMIM}][\text{BF}_4]$. The outcome of this reaction confirms, that lithium ions can be responsible for the devastating effect on the HAM. The l/b ratio dropped from about 30 to 10 and vast amounts of aldol products were formed. Apart from promoting the aldol reaction, apparently Li(I) also interferes with the catalysts, as the l/b ratio is significantly decreased. It is therefore vital to remove lithium salts completely from the IL prior to use.

In order to probe the influence of the cation, $[\text{PMIM}]^+$ was exchanged for $[\text{PM}_2\text{IM}]^+$ to exclude any influence of the acidic proton at C2 position^[28] of the $[\text{PMIM}]^+$ cation under formation of carbenes (Figure 4.4).

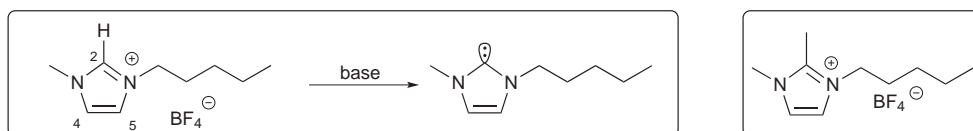


Figure 4.4: C2 position in $[\text{PMIM}][\text{BF}_4]$ (left) and $[\text{PM}_2\text{IM}][\text{BF}_4]$ (right)

As the effect of acidic protons on the hydrogenation in the HAM in organic solvents has been amply investigated by the groups of Vogt and Beller, no such research has been carried out so far for ILs. Therefore, the protic and non-protic ILs were compared (entries 1 and 5). It becomes obvious that the acidic proton plays a crucial role in the hydrogenation step. When employing $[\text{PM}_2\text{IM}][\text{BF}_4]$ the hydrogenation is considerably slowed down and as a consequence the whole cascade reaction. Nevertheless, the hydrogenation is not suppressed completely. The reason that the hydrogenation is still ongoing at a slower rate might be attributed to the presence of less reactive protons in C4 and C5 position of the imidazolium.^[29-31] This explanation is in accordance with observations made by Hamers *et al.* in classical solvents, comparing various alcohols as proton sources.^[26] With decreasing pK_a from methanol to *t*-butanol the hydrogenation activity diminished. Therefore, it is reasonable to assume that the same effect should be observed for other protic solvents.

To confirm that also in the case of the imidazolium cation the acidic proton is involved in the hydrogenation step and not a rhodium carbene species, the cationic rhodium pre-

cursor $\text{Rh}(\text{cod})_2\text{BF}_4$ and $[\text{PMIM}][\text{BF}_4]$ were dissolved in equimolar amounts of chloroform and stirred at 60°C for 6 hours to see if any carbene complexes can be detected by ^1H NMR spectroscopy. However, no reaction could be observed. The characteristic signal for the proton in C2 position (8.81 ppm) is still present in the ^1H NMR spectrum and the signal intensity of the characteristic proton remains the same. Furthermore, no changes in the spectrum could be seen that would indicate any reaction that could have taken place. This supports the theory that acidic protons are involved in the hydrogenation process and not carbene complexes. Another explanation might be the formation of alcohols by aldol condensation and therefore the appearance of acidic alcoholic protons. To proof the first theory right an ammonium based ionic liquid (Figure 4.5), *N*-pentyl-*N*-methyl pyrolidinium Tf_2N ($[\text{PMPyr}][\text{Tf}_2\text{N}]$) was used (entries 8 and 9). In this kind of IL no acidic proton is present. The reaction outcome confirmed the assumption that the acidic protons of $[\text{PM}_2\text{IM}]^+$ in C4 and C5 position were responsible for the hydrogenation to take place. In $[\text{PMPyr}][\text{Tf}_2\text{N}]$ more enamine is present and also aldol products were detectable. This indicates that the hydrogenation of the enamine is almost completely suppressed and therefore the equilibrium of the condensation reaction is in strong favour of the aldehydes. The accumulation of the aldehydes then results in an intensified reaction towards aldol products. Their formation can also here be ascribed to the presence of the Lewis acid lithium. The lithium ions amplify the already ongoing aldol reaction. The rather poor l/b ration, too, indicates the presence of lithium ions, as this IL also is made via an anion exchange using a lithium salt.

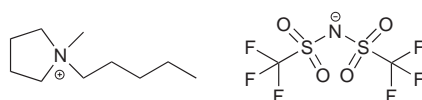


Figure 4.5: $[\text{PMPyr}][\text{Tf}_2\text{N}]$

Application of a coordinating anion

In the HAM, two catalytically active species are suspected (Figure 4.6). The cationic species **A** is supposed to be responsible for the hydrogenation step, whereas the neutral species **B** promotes the hydroformylation reaction. Both species are expected to be formed from the catalyst precursor $[\text{Rh}(\text{cod})_2]\text{BF}_4$ *in situ* under reaction conditions and are in dynamic equilibrium. Firstly the cationic complex **A** is formed from the precursor. Complex **B** can then be generated from complex **A** by reaction with a base. The fact that species **A** is charged raised the question if a coordinating counterion as part of an IL could have a considerable influence on the reactivity of this species.

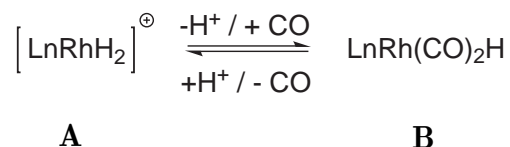
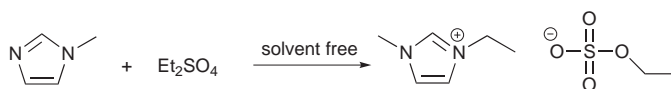


Figure 4.6: Equilibrium between cationic and anionic rhodium species

As the non-coordinating anions do not effect the catalyst itself, a more coordinating anion was employed and its impact on the reaction outcome observed and evaluated. As IL 1-ethyl-3-methyl imidazolium ethylsulfate ($[\text{EMIM}][\text{EtSO}_4]$) (Scheme 4.2) was chosen, due to its physical properties such as low viscosity, melting point and good solubility of the catalyst. In addition it forms a biphasic system with the substrates (Figure 4.7 on the next page).



Scheme 4.2: Synthesis of $[\text{EMIM}][\text{EtSO}_4]$

Furthermore, this IL can easily be synthesised in a solvent-free way at room temperature from readily available chemicals, such as 1-methylimidazole and diethylsulfate (Scheme 4.2). $[\text{PMIM}][\text{BF}_4]$ and $[\text{EMIM}][\text{EtSO}_4]$ were compared in the Rh-catalysed

HAM of 1-octene under the same conditions to see if there is a pronounced effect (Table 4.3). Interestingly, in case of the coordinating IL [EMIM][EtSO₄] the amount of enamine is significantly higher: whereas in the case of [PMIM][BF₄] almost solely amine was formed, more enamine than amine is present at the end of the reaction in case of [EtSO₄]⁻. As the hydrogenation species in the HAM is supposed to be the charged species, this result proves the theory that coordinating anions can interfere with the catalyst. As a consequence of the diminished hydrogenation rate, the amount of aldehyde increased noticeably. This is a consequence of the higher enamine concentration and hence the decelerated condensation reaction.

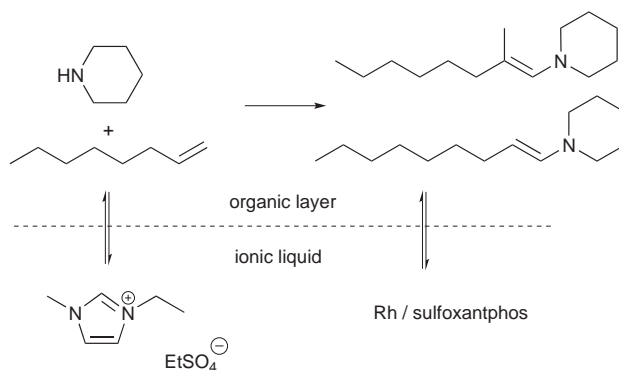


Figure 4.7: Hydroaminomethylation biphasic system of [EMIM][EtSO₄]

Table 4.3: Comparison of hydroaminomethylation in [EMIM][EtSO₄] and [PMIM][BF₄]

Entry	IL	S/Rh	Conv. / %	l/b	am/en ^a	aldehyde / %	aldol / %
1	A	1000	99	27	> 100	n.d.	< 1
2	A	4000	92	28	> 100	n.d.	< 3
3	B	1000	83	> 100	0.5	10	6.7
4	B	4000	57	> 100	0.3	11.8	12
5	B	4500	25	25	0.1	22	20

Conditions: 7 mL solvent, 19 mmol 1-octene, 22 mmol piperidine, [Rh(cod)₂BF₄] = 0.03 mol%, L/Rh = 4, T = 125°C, *p*(CO/H₂ (1:2)) = 36 bar (cold pressure), 400 rpm, 17 h, a) ratio amine/enamine, A = [PMIM][BF₄], B = [EMIM][EtSO₄]

Using a higher S/Rh ratio shows clearly the difference in reaction rate between

[EMIM][EtSO₄] and [PMIM][BF₄] (entries 2 and 4). In [PMIM][BF₄] the conversion reaches a formidable 92% after 17 h, whereas in [EMIM][EtSO₄] the conversion is about 57%. Apart from the lower conversion, a higher amount of enamine was detected. When increasing the S/Rh ratio in the [EMIM][EtSO₄] the conversion stops, but simultaneously the ratio amine/enamine changes from 0.5 to 0.1. It seems reasonable to assume that at a lower conversion the rhodium catalyst is still mainly hydroformylating, and as a consequence, the enamine accumulates. In case of [PMIM][BF₄] the difference is marginal (entries 1 and 2). A slightly lower conversion was observed. In both cases hardly any enamine was detected. Obviously at 125°C the catalyst is still able to almost fully convert the 1-octene and to hydrogenate the enamine. A reasonable explanation for the difference between these two ionic liquids might be a suppressed or decelerated hydrogenation activity caused by a strong interaction between the cationic rhodium species, responsible for the hydrogenation reaction, and the ethylsulfate anion.

DFT calculations were considered to gather evidence for this theory. In fact, the calculations indicate the possibility of this effect. For [Rh(cod)₂BF₄] in chloroform an enthalpy of -20 kJ/mol was calculated for the substitution of one 1-5-cyclohexadiene ligand by ethylsulfate. This result shows that an alkene can easily be replaced by one [EtSO₄]⁻ at the cationic rhodium centre (Figure 4.8). Coordination of a second ethylsulfate was found to be rather unlikely as this enthalpy for this reaction step would be 173 kJ/mol. According to the calculations the most reasonable coordination mode would be as a chelate. Therefore, it is possible for the anion to compete with the substrate for the vacant position at the catalytically active centre.

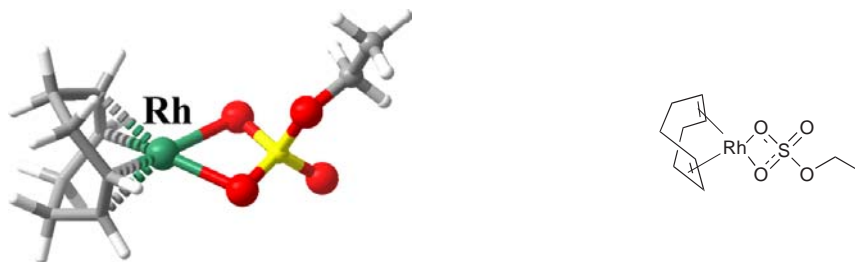


Figure 4.8: Structure of the neutral rhodium species in the presence of [EtSO₄]⁻ based on DFT calculations

To verify these calculations, two experiments were performed and analysed by ^1H NMR spectroscopy. $[\text{Rh}(\text{cod})_2]\text{BF}_4$ was dissolved in deuterated chloroform with equimolar amounts of $[\text{PMIM}][\text{BF}_4]$ and with equimolar amounts of $[\text{EMIM}][\text{EtSO}_4]$, respectively. The corresponding ^1H NMR spectra are depicted in figure 4.9. In case of the BF_4^- -IL the characteristic signals of coordinated 1,5-cyclooctadiene to the rhodium could still be seen at approximately 5.3 and 2.55 ppm (marked with an asterisk). The ^1H NMR spectrum with $[\text{EtSO}_4]^-$ present showed only signals of free 1,5-cyclooctadiene at 5.58 and 2.33 ppm (marked with an asterisk). Apparently, the alkene ligand was fully displaced from the Rh-centre. This is in contradiction to the DFT calculations. However, the calculations only hold true for a simplified system, without taking into account the other ions present (BF_4^- from the rhodium precursor and $[\text{EMIM}]^+$). Furthermore, upon addition of $[\text{EMIM}][\text{EtSO}_4]$ to the dissolved catalyst precursor a colour change from orange to yellow was observed. This observation was monitored by UV-VIS spectroscopy. The spectra of pure $[\text{Rh}(\text{cod})_2]\text{BF}_4$ in chloroform and $[\text{Rh}(\text{cod})_2]\text{BF}_4$ with $[\text{EMIM}][\text{EtSO}_4]$ are displayed in figure 4.10 on the following page. A considerable difference in the UV-VIS spectra can be noticed. In the spectrum of pure $[\text{Rh}(\text{cod})_2]\text{BF}_4$ a significant absorption at 480 nm is noticeable, whereas this signal is absent in the other spectrum, explaining the colour change. To rule out that the cation can be held responsible for the colour change, $[\text{PMIM}][\text{BF}_4]$ was added to the rhodium salt solution. Both spectra, the one with pure rhodium salt and the one with added $[\text{PMIM}][\text{BF}_4]$ are identical.

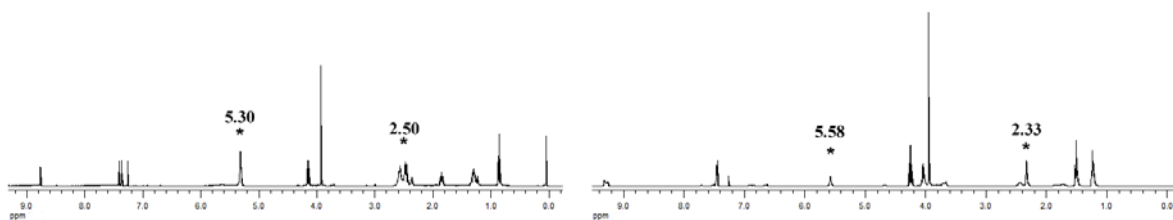


Figure 4.9: ^1H NMR of the $[\text{Rh}(\text{cod})_2]\text{BF}_4$ complex in CDCl_3 in the presence of $[\text{PMIM}][\text{BF}_4]$ (left) and $[\text{EMIM}][\text{EtSO}_4]$ (right)

Another interesting aspect that needed investigation is the influence of $[\text{EtSO}_4]^-$ on the ligand coordination. From the l/b ratio it could already be concluded that the coordinated ligand is not effected negatively in its selectivity by the presence of the

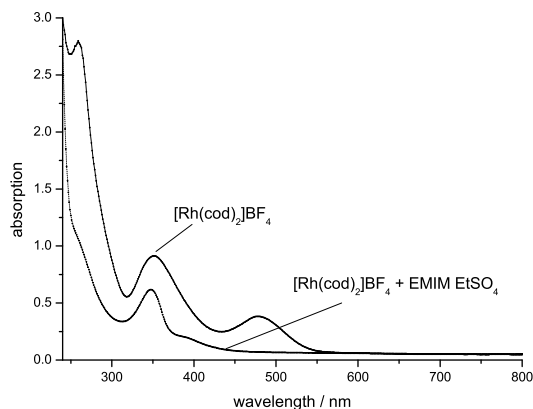


Figure 4.10: UV-VIS-spectra of $\text{Rh}(\text{cod})_2\text{BF}_4$ in the presence and absence of $[\text{EtSO}_4]^-$

anion. On the contrary, the l/b ratio were slightly better when applying $[\text{EMIM}][\text{EtSO}_4]$.

These results so far strongly support the impact of the anion in the hydrogenation reaction. Nevertheless, there is the chance of mass transfer limitation or solubility of the enamines in the ionic liquid being the reason for the slow reaction rate. To rule this out an iridium catalyst was added to the reaction mixture and its influence on the hydrogenation activity analysed. As Ir-catalysts are known to be formidable hydrogenation catalyst,^[32] the hydrogenation reaction should be faster in the presence of an Ir-complex and mass transfer limitation does not play a role. For this reason the reaction was started with $[\text{Rh}(\text{cod})_2]\text{BF}_4$ and stopped after 17.5 h at 25% conversion. The enamine/amine ratio at that moment was 9. Next, $[\text{Ir}(\text{cod})_2]\text{BF}_4$ dissolved in 2 mL $[\text{EMIM}][\text{EtSO}_4]$ was added to the reaction mixture. After 17.5 h the reaction was stopped again and the enamine was found to be almost completely hydrogenated. Furthermore, another 25% of 1-octene were converted to the corresponding aldehyde (Figure 4.11 on the next page).

Obviously, only the reaction rate of the hydrogenation step was increased. A significant change in the hydroformylation step could not be observed. This distinctive increase of the hydrogenation rate, however, indicates, that mass transfer or solubility limitation are not the reasons for the suppressed hydrogenation activity in this IL, as the addition of the Ir catalyst should not have effected the reaction rate in that case. The other conclusion that can be drawn from this reaction is the fact that the Ir system is not prone

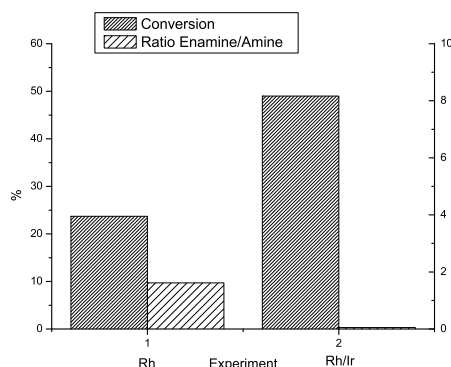


Figure 4.11: Addition of $[\text{Ir}(\text{cod})_2]\text{BF}_4$ to $[\text{EMIM}][\text{EtSO}_4]$

Conditions: Ionic liquid 5-7 mL, S/M = 4400, L/M = 4.4, T = 125°C, $p(\text{CO}/\text{H}_2 (1:2)) = 36$ bar (cold pressure), t = 17.5 h, rpm = 400.

to interaction with the coordinating anion. In order to probe whether the effect of the ethylsulfate is concentration dependent or not, reactions in PMIM BF_4 , EMIM EtSO_4 and a 1:1 mixture of both were compared. In case of the PMIM BF_4 system merely 2% enamine were still present at the end of the reaction, whereas the reaction in EMIM EtSO_4 gave about 35% (entries 2 and 3, Table 4.4 on the following page). As suspected, the amount of enamine at the end of reaction in the mixture (entry 1) is higher than in pure $[\text{PMIM}][\text{BF}_4]$ (entry 2), but considerably lower than in pure $[\text{EMIM}][\text{EtSO}_4]$ (entry 3). Due to the accumulation of enamine, also a higher concentration of aldol products could be detected compared to the reaction in $[\text{PMIM}][\text{BF}_4]$. Furthermore, the amount of isomerised octenes is increased by a factor of three in the $[\text{EMIM}][\text{EtSO}_4]$ compared to $[\text{PMIM}][\text{BF}_4]$, while the conversion is lower.

Prior investigations concentrated on the influence of the ILs on the whole reaction cascade of the HAM. For this reason the two rhodium-catalysed reactions were monitored apart from each other. Figure 4.12 on page 132 shows the hydroformylation of 1-octene and the hydrogenation of 1-(non-1-enyl)piperidine in these two ILs. The enamine was synthesised *in situ* from piperidine and nonanal. For the hydrogenation $[\text{Rh}(\text{cod})_2]\text{BF}_4$ was chosen and in the hydroformylation the neutral rhodium precursor $[\text{Rh}(\text{CO})_2(\text{acac})]$ was employed. Both substrates were added to the catalyst solution and after pressurising the autoclave the stirrer was activated. With respect to the activity of the catalysts

Table 4.4: Applied ionic liquids in the hydroaminomethylation reaction

Entry	Solvent	Conv.	Isom.	l/b	aldehyde	amine	enamine	aldol
		%	1-octene %		%	%	%	%
1	IL Mixture ^[a]	91.2	8.8	52.4	7.6	63.8	11.2	8.6
2	PMIM BF ₄	86.2	13.8	22.4	n.d.	84.4	1.6	n.d.
3	EMIM EtSO ₄	57.3	42.7	n.d.	11.8	9.9	34.4	1.2

Conditions: Ionic liquid 8 mL, S/Rh = 4000, L/Rh = 3.8, T = 125°C, $p(\text{CO}/\text{H}_2 (1:2)) = 36$ bar (cold pressure), t = 17.5 h.

a) [PMIM][BF₄]/[EMIM][EtSO₄] 1:1

it could be observed that for both reactions the reaction rate is higher in [PMIM][BF₄]. Conspicuously, in case of the hydroformylation the reaction rates differ by the factor of three (left graph in Figure 4.12 on the following page), whereas in case of the hydrogenation the factor is about 15 (right graph in Figure 4.12 on the next page). Hardly any hydrogenation reaction took place in [EMIM][EtSO₄], but as a consequence vast amounts of aldol products were formed. It can be concluded that in case of the hydrogenation reaction the presence of [EtSO₄]⁻ has a disastrous effect on the product formation. But also the hydroformylation reaction is effected by the anion, although this effect is not as pronounced. From previous experiments it becomes already clear that [EtSO₄]⁻ does not effect the coordination of the bidentate sulfoxantphos ligand. The l/b ratio in [EMIM][EtSO₄] is comparable to [PMIM][BF₄]. Therefore, the monodentate ligand TPPTS² was employed in combination with [Rh(cod)₂BF₄] in [EMIM][EtSO₄] and compared to sulfoxantphos (Table 4.5 on page 133).

As substrate the imine benzylidenephénylamine (BPA) was chosen. This imine shows an excellent solubility in [EMIM][EtSO₄]. Entries 1 and 3 show the conversion after 30 min reaction time. The catalyst based on the bidentate ligand reaches a 13 % conversion, whereas the catalyst based on TPPTS shows hardly any conversion. This catalyst needs about 14 h to reach the conversion of the catalyst based on sulfoxantphos at 30 min.

²3,3',3''-Phosphinidynetris(benzenesulfonic acid) trisodium salt

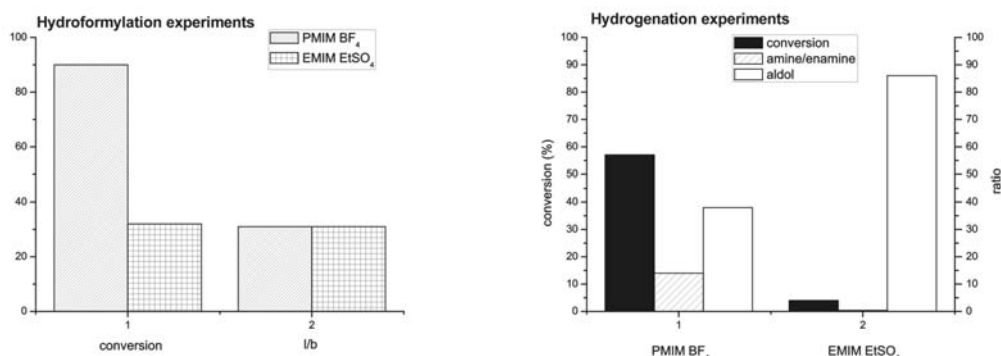


Figure 4.12: Comparison of [PMIM][BF₄] and [EMIM][EtSO₄] concerning hydrogenation of 1-(non-1-enyl)piperidine^a and hydroformylation of 1-octene^b

a) Conditions: 3 mL ionic liquid, 0.44 mL nonanal, 0.5 mL piperidine, 1 mg (0.25 μmol) [Rh(cod)₂]BF₄, 7.7 mg (0.98 mmol) Sulfoxantphos, S/Rh = 1000, L / Rh = 4, 125°C, 1 h, 400 rpm, $p(\text{CO}/\text{H}_2 (1:2)) = 36$ bar.

b) Conditions: 3 mL ionic liquid, 0.4 mL (2.55 mmol) 1-octene, 0.8 mg (0.20 μmol) [Rh(CO)₂ acac], 10 mg (1.27 μmol sulfoxantphos, S/Rh = 1300, L/Rh = 6.5, 80°C, 400 rpm, 2.5 h, (CO/H₂ (1:2)) = 36 bar

These results suggest that in case of the less bulky TPPTS the [EtSO₄]⁻ can bind more easily to the rhodium centre and hence shields it more effectively from the imine substrate. Probably it is easier for the anion to approach the catalytic centre, when the surrounding ligands are more flexible. To gain more insight into the course of the reaction, the product distribution in time (Figure 4.13 on the next page) was monitored. Each data point is an independent reaction as taking samples during the reaction was not possible. From figure 4.13 on the following page it becomes obvious that the reaction can be separated in two parts.

For the first seven hours a consumption of 1-octene is observed accompanied by the formation of enamine. When the concentration of the enamine reaches its maximum (about 40%) the reaction rate of the hydroformylation drops significantly. Whereas within the first seven hours about 60% of 1-octene were converted, it took more than 60 hours for another 5% to be converted. Strikingly, the hydrogenation reaction proceeds considerably faster. 5% of the enamine were hydrogenated in 12 hours reaction time. It is assumed that most of the rhodium is converted to a hydrogenation cata-

Table 4.5: Hydrogenation activity of Rh-sulfoxantphos and Rh-TPPTS in [EMIM][EtSO₄]

Entry	IL	ligand	t / h	conv. / %
1	[EMIM][EtSO ₄]	TPPTS 8 eq.	0.5	< 1
2	[EMIM][EtSO ₄]	TPPTS 8 eq.	14	15
3	[EMIM][EtSO ₄]	Sulfoxantphos 4 eq.	0.5	13

Conditions: 3 mL solvent, 2.58 mmol BPA, [Rh(cod)₂BF₄] = 0.025 μmol, S/Rh = 10000, T = 125°C, *p*(H₂) = 24 bar (cold pressure), 400 rpm.

lyst. Due to the enormous amount of enamine and ethylsulfate present, the equilibrium (Figure 4.14 on the next page) is shifted to the side of the cationic species and as a consequence the hydroformylation rate decreases.

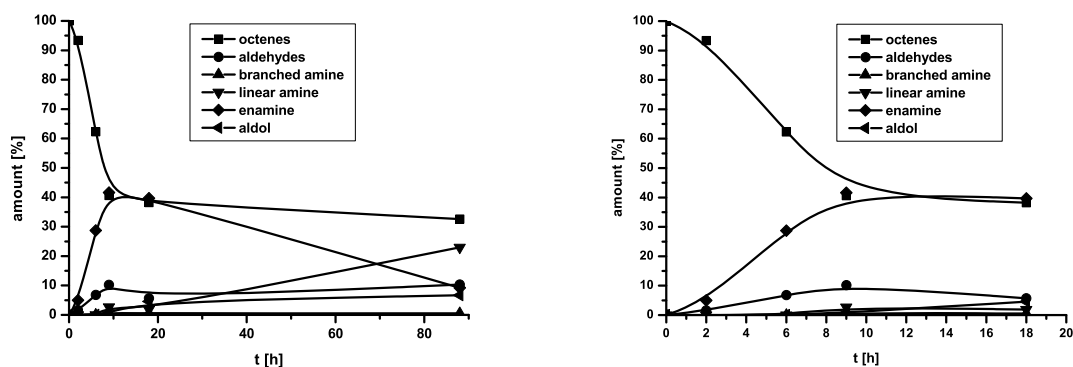


Figure 4.13: Product distribution during the hydroaminomethylation in [EMIM][EtSO₄]. The right figure shows the first 18 h. Conditions: [EMIM][EtSO₄] 7 mL, 16 mmol 1-octene, 19 mmol piperidine, S/Rh = 3000, L/Rh = 4, T = 125°C, *p*(CO/H₂ [1:2]) = 36 bar (cold pressure)

Apart from the anion, also the synthesis gas pressure should have an impact on the selectivity towards the enamine. For this purpose three different experiments were carried out (Figure 4.15 on the following page). Performing the reaction at 36 bar with a mixture of CO/H₂ = 1:2 gave 90% conversion with 20% enamine and 30% amine. Lowering the partial pressure of H₂ should be beneficial to the selectivity towards the enamine.

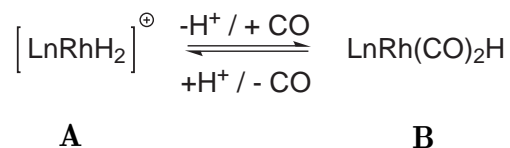
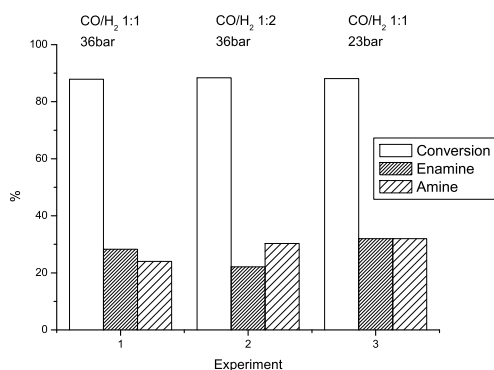


Figure 4.14: Equilibrium between the cationic and the anionic rhodium species

The reaction outcome verifies this assumption as less amine was formed and therefore more enamine is present, whereas the conversion is also 90%. However, performing the reaction at lower pressure with a 1:1 mixture (CO/H₂), results in an increase of amine and enamine. Probably the lower CO pressure causes a faster hydroformylation reaction, as it is known that a lower CO pressure can be beneficial for the hydroformylation reaction. As the hydroformylation is faster, consequently also the formation of enamine is accelerated.

Figure 4.15: Influence of pressure on the HAM in [EMIM][EtSO₄]

Conditions: [EMIM][EtSO₄] 5 mL, S/Rh = 3000, L/Rh = 4, T = 125°C, t = 18 h, rpm = 400.

As the [EMIM][EtSO₄] also forms a biphasic system, recyclability of this system was evaluated. With respect to the recyclability [EMIM][EtSO₄] and [PMIM][BF₄] show excellent behaviour (Table 4.6 on the next page). Five consecutive runs were conducted. In all cases the results are comparable with some fluctuation in the conversion and the selectivity towards the enamine. After each run, the organic layer was removed from the

autoclave under argon and new substrate was added. The increased conversion in the last runs might be due to the fact that amounts of product remained in the IL after each run. One other question, however, needed yet to be answered. Is the catalyst also in this IL successfully immobilised? Therefore, several organic layers were analysed for rhodium leaching by means of ICP-OES. In all cases essentially no rhodium leaching was detected, as the detection limit of the ICP-OES was reached ($\text{Rh} < 0.09\%$). Consequently, the catalyst is successfully immobilised in the IL.

Table 4.6: Recycling experiments in [EMIM][EtSO₄]

Cycle	Conv. / %	Amine / %	Enamine / %	Aldehyde / %	Aldol / %
1	57.3	3.3	34.4	11.8	1.2
1	69.3	2.7	46.7	8.6	3.8
2	69.0	2.6	43.2	8.7	5.7
3	61.8	1.9	39.7	5.7	4.6
4	63.5	2.4	36.8	6.3	6.8

Conditions: [EMIM][EtSO₄] 5 mL, S/Rh = 4000, L/Rh = 4, T = 125°C, $p(\text{CO}/\text{H}_2)$ (1:2) = 36 bar (cold pressure), t = 18 h.

4.3 Conclusion

By choice of the IL, the hydrogenation step in the HAM reaction can be controlled. Changing from a non-coordinating to a coordinating anion slows down the rate of the hydrogenation step by blocking the catalytically active site of the cationic rhodium catalyst. The substrate and the $[\text{EtSO}_4]^-$ compete for the vacant site at the catalyst. This has been shown by NMR and UV-VIS spectroscopy and is supported by DFT calculations. Comparison of the hydrogenation and hydroformylation reaction showed that the effect of the $[\text{EtSO}_4]^-$ on the hydrogenation step is prominent and outweighs the impact on the hydroformylation reaction. The hydrogenation reaction is clearly the slowest reaction in the cascade.

Furthermore, it has been shown that the nature of the cation is also of the essence. Acidic protons in the cationic part of the IL are crucial for a swift hydrogenation of the enamines. Replacing the C-H imidazolium cation by an ammonium cation suppresses the hydrogenation reaction. In addition to these insights into the reaction mechanism, the applicability of both, the non-coordinating and coordinating anions, in recycling experiments was proven. Several recycle runs were conducted, without any significant loss of activity, nor was any significant leaching of the catalyst detectable.

Apart from the influence of the ions on the reaction outcome, it became obvious that the application of ILs, made by a route involving lithium salts, is delicate. Traces of lithium ions remain in these ILs despite extensive purification. But the absence of these ions is imperative as they support aldol reactions. The yield of amines or enamines decreases significantly when traces of Li(I) salts are present.

4.4 Experimental

All chemicals were purchased from Aldrich, Acros or Merck and used as received. The liquids bought were degassed and the catalytical experiments were carried out under an atmosphere of dry argon or nitrogen using standard Schlenk techniques. All ionic liquids used were degassed prior to use. NMR spectra were recorded on a Varian Unity Inova 500 (VT NMR) and Mercury 400-spectrometer. ^1H -NMR, ^{13}C -NMR referenced using residual solvent peaks. ^{19}F NMR and ^{31}P NMR were referenced externally. GC-MS analysis was formed on a Pegasus MS HP. UV-VIS spectra were recorded on a Shimadzu UV-1650PC.

GC Analysis

GC: Shimadzu GC 17A
Column: Ultra 2 (crosslinked 5% Ph Me Siloxane), 25m, inner diameter 0.20 mm
film thickness 0.33 μm
Carrier gas: Helium 102 kPa (total flow 53 mL/min)

ICP-OES

Rhodium and phosphorus leaching were analysed by means of ICP-OES. Samples were prepared by removal of the volatiles from the organic layer under reduced pressure and subsequent calcination of the residue at 500°C over 72 h. Afterwards, the residue was dissolved in 2 mL HNO_3 (65%) and diluted with distilled water to 25 mL in a measuring flask. Before starting the measurements on the samples, a calibration curve for Rh and P was prepared. The measurements were performed with a SPECTRO CIROSCCD spectrometer equipped with a free running 27.12 MHz generator at a power of 1400 W. The sample introduction was performed by a cross-flow nebuliser with a double pass Scott-type spray chamber and a sample uptake rate of 2 mL min^{-1} . The outer gas flow was 12 L min^{-1} , the intermediate gas flow was 1 L min^{-1} and the nebuliser gas flow was 1.00 L min^{-1} .

Computational details

Density functional theory with the B3LYP^[33-35] hybrid exchange-correlation functional was used for the quantum chemical calculations. Full geometry optimizations were performed using the Gaussian 03 program. LanL2DZ^[36-38] basis set was used for the description of the Rh center. The full-electron 6-311+G(d) basis set was used for S, O, B, and F atoms, while P, C, and H atoms were treated by the 6-311G(d,p) basis set. No symmetry restrictions were used in the calculations.

The nature of the stationary points was evaluated from the analytically computed harmonic modes. No imaginary frequencies were found for the optimized structures corresponding to local minima on the potential energy surface. All of the energies obtained within DFT used for computing of the relative energies were corrected for the presence of solvent using the polarizable continuum model within the conductor reaction field (COSMO) approach developed by Klamt et al. as implemented in the Gaussian 03 program package using the standard parameters for chloroform as solvent.^[39,40]

General procedure for the hydroaminomethylation experiments

Reactions were performed in 75-mL home-made stainless steel autoclaves. In a typical experiment, the autoclave was charged with a solution of [Rh(cod)₂]BF₄ (7.2 mg, 17.8 μ mol; cod = 1,5-cyclooctadiene) or [Rh(CO)₂(acac)] (4.6 mg, 17.8 μ mol) (acac = acetylacetonate) or a combination of these Rh precursors and sulfoxantphos (55.8 mg, 71.3 μ mol) or xantphos (41.3 mg, 71.3 μ mol) in 4 mL of the ionic liquid or toluene/MeOH. 1-Octene (2.0 g, 18 mmol) and piperidine (1.7 g, 20 mmol) were added and the autoclave was purged three times using CO (p = 10-12 bar) to remove the remaining argon from the autoclave. Subsequently, the autoclave was pressurised with CO (p = 12 bar) and H₂ (p = 24 bar) and heated to reaction temperature. After 18 hours the autoclave was cooled to room temperature in an ice bath and the gases were vented. Phase separation was immediate and the product layer was removed from the autoclave by syringe under an argon atmosphere. The catalyst solution was ready to be used in a new catalytic run. The product layer was analysed by GC and GC/MS. In these analyses the l/b-ratio could be determined within an error range of 0.05%.

1-Methyl-3-pentyl-imidazolium tetrafluoroborate

1-Methylimidazole (60 mL, 0.752 mol) was mixed with 1-bromopentane (93.20 mL, 0.752 mol). The mixture was stirred at 50°C for 24 h. Subsequently, the liquid was diluted in acetone (100 mL) and then sodium tetrafluoroborate (85 g, 0.774 mol) was added. The mixture was stirred for 48 h at room temperature and then filtered. After evaporation of the acetone the liquid was filtered once more and washed with diethyl ether (30 mL). The remaining diethyl ether in the product was removed under vacuum afterwards.

$^1\text{H NMR}$ (CD_3OD) δ (ppm): 8.83 (s, 1H), 7.60 (t, 1H, $J=1.80$ Hz), 7.54 (t, 1H, $J=1.77$ Hz), 4.20 (t, 2H, $J=7.39$ Hz), 3.91 (s, 3H), 1.91 - 1.87 (m, 2H), 1.40 - 1.32 (m, 4H), 0.92 (t, 3H, $J=7.13$ Hz). $^{13}\text{C NMR}$: 136.40, 123.50, 122.19, 49.38, 35.02, 29.38, 27.92, 21.68, 12.75. $^{19}\text{F NMR}$: -153.70.

1-Methyl-3-pentyl-imidazolium hexafluorophosphate (PMIM PF_6)

1-Methylimidazole (60 mL, 0.752 mol) was mixed with 1-bromopentane (93.20 mL, 0.752 mol). The mixture was stirred at 50°C for 24 h. The liquid received was dissolved in 150 mL water and potassium hexafluorophosphate (147.25 g, 0.8 mol) was added to this solution. The mixture was stirred for 2 h and a biphasic system was formed. The water layer was decanted and the ionic liquid was washed five times with 100 mL water. The remaining water was removed under reduced pressure at 80°C.

$^1\text{H NMR}$ ($\text{C}_2\text{D}_6\text{O}$) δ (ppm): 8.92 (s, 1H), 7.72 (s, 1H), 7.66 (s, 1H), 4.35 (t, 2H, $J=7.34$ Hz), 4.03 (s, 3H), 1.94 (m, 2H), 1.35 (m, 4H), 0.88 (t, 3H, $J=7.02$ Hz). $^{13}\text{C NMR}$: 136.49, 123.85, 122.47, 49.54, 35.67, 29.51, 27.94, 21.77, 13.16. $^{19}\text{F NMR}$: -137.82, 139.70.

1-Methyl-3-pentyl-imidazolium bis(trifluoromethylsulfonyl)imine (PMIM Tf_2N)

1-Methylimidazole (30 mL, 0.376 mol) was mixed with 1-bromopentane (46.60 mL, 0.376 mol). The mixture was stirred at 50°C for 24 h. The resulting liquid was dissolved in 100 mL water and bis(trifluoromethylsulfonyl)imine lithium salt (114.77 g, 0.4 mol)

was added to this solution. The mixture was stirred for 2 h at 50°C and a biphasic system was subsequently formed. The water layer was decanted and the ionic liquid was washed seven times with 80 mL water. The remaining water was removed under reduced pressure at 80°C.

¹H NMR (C₂D₆O) δ (ppm): 9.02 (s, 1H), 7.77 (s, 1H), 7.70 (s, 1H), 4.36 (t, 2H, $J=7.33$ Hz), 4.06 (s, 3H, $J=5.79$ Hz), 1.96 (m, 2H), 1.36 (m, 4H), 0.90 (t, 3H, $J=7.01$ Hz). **¹³C NMR**: 136.52, 123.92, 122.52, 121.69, 119.45, 118.49, 49.60, 35.76, 29.55, 27.95, 21.76, 13.13. **¹⁹F NMR**: -79.95.

1,2-Dimethyl-pentyl-imidazolium tetrafluoroborate (PM₂IM BF₄)

1,2-Dimethylimidazole (7.0 g, 72.8 mmol) was mixed with 1-bromopentane (7.81 mL, 72.8 mmol) and 1,1,1-trichloroethane (25 mL) as a solvent. The mixture was stirred at 50 °C for 24 h. 1,1,1-Trichloroethane was decanted and the residue was diluted in acetone (30 mL) and sodium tetrafluoroborate (8.5 g, 77.4 mmol) was added. The mixture was stirred for 48 h at room temperature and then filtered. After evaporation of the acetone the liquid was filtered once more and washed with diethyl ether (30 mL). The remaining diethyl ether in the product was removed under vacuum afterwards.

¹H NMR (CD₃OD) δ (ppm): 7.48 (d, 1H, $J=2.13$ Hz), 7.44 (d, 1H, $J=2.13$ Hz), 4.15 (t, 2H, $J=7.40$ Hz), 3.81 (s, 3H), 2.61 (s, 3H), 1.84 (m, 2H), 1.37 (m, 4H), 0.93 (t, 3H, $J=7.04$ Hz). **¹³C NMR**: 145.55, 122.15, 120.74, 48.00, 33.96, 29.05, 28.00, 21.80, 12.79, 8.06. **¹⁹F NMR**: -154.06.

1-Ethyl-3-methyl ethylsulfate (EMIM EtSO₄)

To ice-cold 1-methylimidazole (30 mL, 0.376 mol) was added in drops diethylsulfate (47.15 mL, 0.360 mol). The mixture was allowed to warm up slowly to room temperature and was left stirring for 12 h. Residual 1-methylimidazole was removed at 90°C under reduced pressure.

¹H NMR (CDCl₃) δ (ppm): 9.24 (s, 1H), 7.43 (s, 1H), 7.41 (s, 1H), 4.13 (q, 2H, $J=7.17$

Hz), 3.89 - 3.82 (b, 5H), 1.37 (t, 3H, $J=7.27$ Hz), 1.07 (t, 3H, $J=7.77$ Hz). ^{13}C NMR: 136.65, 123.77, 122.10, 63.01, 44.92, 36.13, 15.38, 15.08.

1-Methyl-1-pentyl-pyrrolidinium bis(trifluoromethylsulfonyl)imine (PMPy Tf₂N)

To *N*-methylpyrrolidine (30 mL, 0.282 mol) in 30 mL toluene was added 1-bromopentane (34.95 mL, 0.282 mol). The reaction mixture was stirred at 50°C for 24 h. The toluene was decanted from the ionic liquid layer and the rest of toluene was removed under reduced pressure. The ionic liquid was dissolved in 50 mL of water and bis(trifluoromethylsulfonyl)imine lithium salt (86.08 g, 0.3 mol) was added to the solution. The mixture was stirred for 2h at 50°C and subsequently the water was decanted. The ionic liquid was washed seven times with water and afterwards dried under reduced pressure at 80°C.

^1H NMR (C₂D₆O) δ (ppm): 3.68 (b, 4H), 3.52 - 3.49 (m, 2H), 3.22 (s, 3H), 2.30 (b, 4H), 1.91 (b, 2H), 1.38 - 1.37 (m, 4H), 0.91 - 0.89 (t, 3H, $J=5.79$ Hz). ^{13}C NMR: 127.34, 124.13, 120.92, 117.70, 66.46, 66.40, 50.11, 30.17, 25.03, 23.76, 23.34, 14.97. ^{19}F NMR: -79.70. Yield: 90%

Bibliography

- [1] C. Müller, M. G. Nijkamp, D. Vogt, *Eur. J. Inorg. Chem.* **2005**, *20*, 4011–4021.
- [2] N. J. Ronde, D. Totev, C. Müller, M. Lutz, A. L. Spek, D. Vogt, *ChemSusChem* **2009**.
- [3] M. Janssen, C. Müller, D. Vogt, *Adv. Synth. Catal.* **2009**, *351*, 313–318.
- [4] K. Kunna, C. Müller, J. Loos, D. Vogt, *Angew. Chem. Int. Ed.* **2006**, *45*, 7289–7292.
- [5] D. J. Cole-Hamilton, *Science* **2003**, *299*, 1702–1706.
- [6] P. Wasserscheid, W. Keim, *Angew. Chem.* **2000**, *112*, 3926–3945.
- [7] N. V. Plechkova, K. R. Seddon, *Chem. Soc. Rev.* **2008**, *37*, 123–150.
- [8] M. Maase in *Ionic Liquids in Synthesis, Vol. 2* (Eds.: P. Wasserscheid, T. Welton), Wiley-VCH, Weinheim, **2008**, pp. 663–687.
- [9] R. Sebesta, I. Kmentová, S. Toma, *Green Chem.* **2008**, *10*, 484–496.
- [10] R. P. J. Bronger, S. M. Silva, P. C. J. Kamer, P. W. N. M. van Leeuwen, *Dalton Trans.* **2004**, 1590–1596.
- [11] Y. Y. Wang, M. M. Luo, Q. Lin, H. Chen, X. J. Li, *Green Chem.* **2006**, *8*, 545–548.
- [12] M. Ahmed, A. M. Seayad, R. Jackstell, M. Beller, *J. Am. Chem. Soc.* **2003**, *125*, 10311–10318.
- [13] M. Ahmed, H. Klein, R. Jackstell, M. Beller, *Science* **2002**, *297*, 1676–1678.
- [14] B. Hamers, P. S. Bäuerlein, C. Müller, D. Vogt, *Adv. Synth. Catal.* **2008**, *350*, 332–342.
- [15] W. Reppe, *Experientia* **1949**, *5*, 93.
- [16] W. Reppe, H. Vetter, *Liebigs Ann. Chem.* **1953**, *582*, 133–163.
- [17] *Comprehensive Organometallic Chemistry, Vol. 8*, (Eds.: J. P. Collman, B. M. Trost, T. R. Verhoeven), Pergamon Press, Oxford.
- [18] S. R. Sandler, W. Karo in *S. R. Sandler, W. Karo*, Academic Press, New York, **1981**.

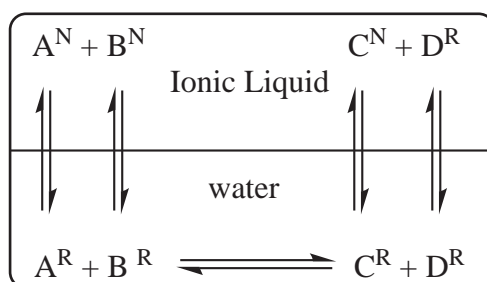
- [19] J. H. Clark, *Green Chem.* **2006**, *8*, 853–860.
- [20] J. H. Clark, *Green Chem.* **1999**, 1–8.
- [21] P. W. N. M. van Leeuwen, *Homogeneous Catalysis*, Kluwer Academic Publishers, Dordrecht, Boston, London, **2004**.
- [22] P. W. N. M. van Leeuwen, C. Carmen, *Rhodium Catalyzed Hydroformylation, Vol. 22*, Kluwer Academic Publishers, Dordrecht, Boston, London, **2000**.
- [23] C. Müller, D. Vogt, *Dalton Trans.* **2007**, 5505–5523.
- [24] C. Müller, *unpublished results*.
- [25] M. Ahmed, A. M. Seayad, R. Jackstell, M. Beller, *Angew. Chem. Int. Ed.* **2003**, *42*, 5615–5619.
- [26] B. Hamers, E. Kosciuski-Morizet, C. Müller, D. Vogt, *ChemCatChem* **2009**, *1*, published online.
- [27] R. P. Swatloski, J. D. Holbrey, R. D. Rogers, *Green Chem.* **2003**, *5*, 361–363.
- [28] T. L. Amyes, S. Diver, J. P. Richard, F. M. Rivas, K. Toth, *J. Am. Chem. Soc.* **2004**, *126*, 4366–4374.
- [29] A. Kovacevic, S. Grundemann, J. Miecznikowski, E. Clot, O. Eisenstein, R. Crabtree, *Chem. Commun.* **2002**, 2580–2581.
- [30] D. Bacciu, K. J. Cavell, I. A. Fallis, L. Ooi, *Angew. Chem. Int. Ed.* **2005**, *44*, 5282–5284.
- [31] H. Lebel, M. K. Janes, A. B. Charette, S. P. Nolan, *J. Am. Chem. Soc.* **2004**, *126*, 5046–5047.
- [32] Y. N. Cheong Chan, D. Meyer, J. A. Osborn, *Chem. Commun.* **1990**, 869–871.
- [33] A. D. Becke, *Phys. Rev.* **1988**, *A38*, 3098–3100.
- [34] A. D. Becke, *J. Chem. Phys.* **1993**, *98*, 1372–1377.
- [35] A. D. Becke, *J. Chem. Phys.* **1993**, *98*, 5648–5652.
- [36] P. J. Hay, W. R. Wadt, *J. Chem. Phys.* **1985**, *82*, 270.
- [37] P. J. Hay, W. R. Wadt, *J. Chem. Phys.* **1985**, *82*, 284.
- [38] P. J. Hay, W. R. Wadt, *J. Chem. Phys.* **1985**, *82*, 299.
- [39] V. Barone, M. Cossi, *J. Phys. Chem. A* **1998**, *112*, 1995.
- [40] F. Ecket, A. Klamt, *AIChE J.* **2002**, *48*, 369.

5

Chapter 5

Biocatalysis in a biphasic ionic liquid/water system

Ionic liquids are promising alternative reaction media. This accounts for both reactive and non reactive phases in a number of applications. In case of biocatalysis, however, the research is just at the beginning. This is mainly due to the fact, that so far organic solvents gave good results in biocatalysis in combination with water. However, many of these organic solvents are also known to be harmful to enzymes or whole cells. Therefore, it is highly desirable to replace them in many reactions. Ionic liquids can be a fruitful alternative as they are an entirely different class of solvents with unique properties. For that reason in this chapter the application of an ionic liquid / water system is compared to a MTBE / water system in the Lactobacillus brevis alcohol dehydrogenase catalysed transfer hydrogenation reaction.



5.1 Introduction

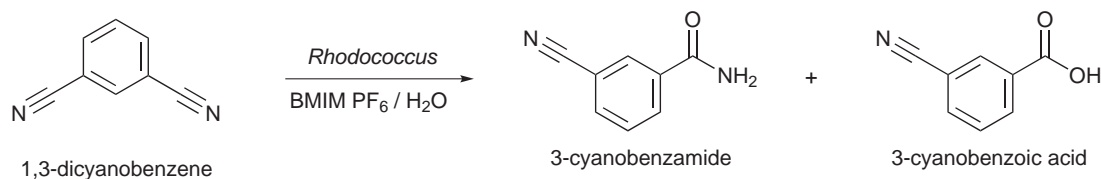
General Introduction to Biocatalysis in Ionic Liquids

The history of industrial biocatalysis reaches back as far as 1934 when the Reichstein process for the oxidation of D-sorbitol to L-sorbose by a microorganism was introduced.^[1] In the beginning it was generally accepted that enzyme applications are bound by its need for aqueous media. With increasing research activity in this field it became obvious that even in this media the application reaches its limits. New solvents such as toluene or MTBE were used to pave ways to new reaction systems. Meanwhile the use of organic solvents and water for biocatalysis is standard.^[2,3] For a few years now ionic liquids (ILs)^[4-6] receive a lot of attention in the field of biocatalysis as pure solvents, co-solvents and in biphasic systems, as they offer new possibilities. Various ILs have been used meanwhile, whereas the most prominent ones are based on imidazolium salts.^[7-10] Despite already being applied for decades in several metal- and organocatalysed reactions^[5,11-13] biocatalysis in ILs has emerged only recently. Their unique feature to close the gap between polar organic solvents and water makes them qualified solvents in biocatalysis. Whereas polar solvents, such as methanol, have the tendency to deactivate e.g. lipases, ILs do not show that tendency.^[8] A successful example was the acetylation of glucose by CaL-B¹ in ILs.^[14] The solubility of glucose was increased by the factor of 100 supporting the exclusive formation of the monoacetylated product in contrast to the reaction in toluene. Reports on improved reaction rates in ILs also do exist for the acetylation of monoprotected glycosides^[15] and the hydrolysis/alcoholysis of 3,4,6-tri-*O*-acetyl-glucal.^[16] Apart from lipase reactions, which beyond controversy form the biggest class, also the application of proteases and even whole cells has been reported. In 2000 the first report of the use of an IL in biocatalysis was published. Lye *et al.* reported on the application of a biphasic BMIM PF₆/water system for the conversion of 1,3-dicyanobenzene to 3-cyanobenzamide and 3-cyanobenzoic acid (Scheme 5.1 on the following page) by the bacterium *Rhodococcus* R312².^[17]

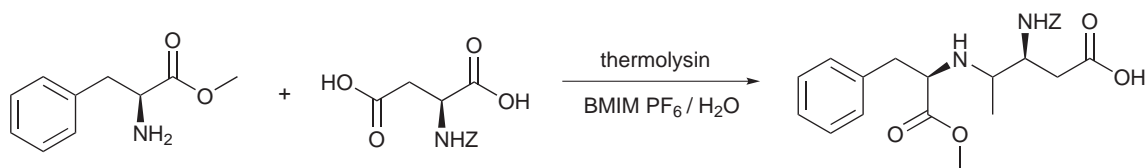
The idea behind this reaction system was the use of an IL as a reservoir or non-

¹ *Candida antarctica* Lipase B

² it belongs to the class of actinobacteria

Scheme 5.1: Rhodococcus in the biphasic system BMIM PF₆/H₂O

reactive phase for the substrates and products, whereas the biocatalyst is situated in the reactive water-phase.^[18] By this product and substrate inhibition was circumvented, a problem frequently observed in aqueous systems. Until then the use of toluene was common, which led to a cellular decomposition and therefore replacement was beneficial to this reaction. Alternatively also isolated enzymes can be employed in ILs. The first application of an enzyme has been reported by Erbedinger *et al.*^[19] They used the protease thermolysin to catalyse the synthesis of Z-aspartame in the biphasic BMIM PF₆⁻/water system (Scheme 5.2).

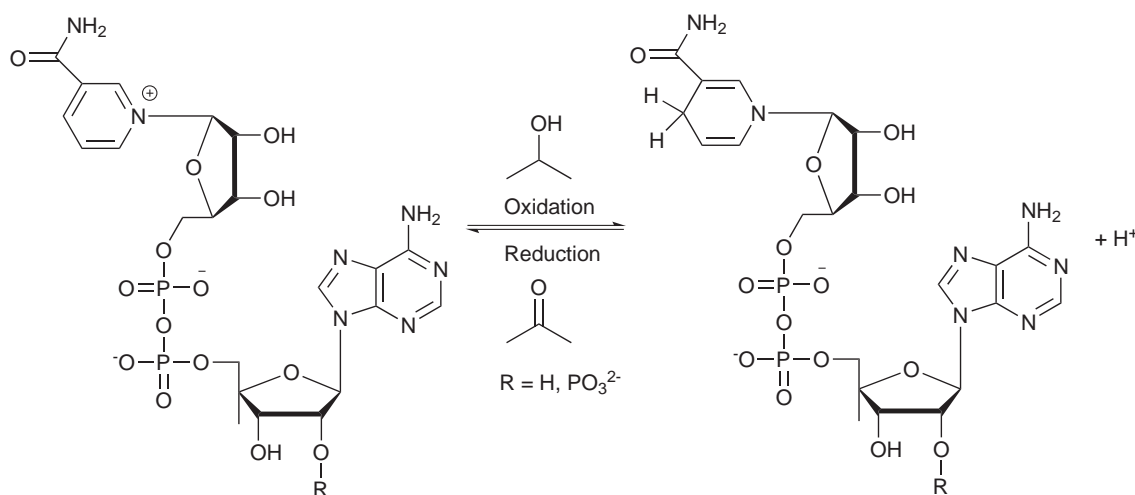


Scheme 5.2: Thermolysin-catalysed synthesis of Z-aspartame

The advantage of this reaction system over the classical ethyl acetate / water one becomes obvious when comparing the stability of the enzyme. While in both systems the conversion was nearly coincident, the stability of the enzyme in the ionic liquid system was significantly higher. In this system it was also demonstrated that the enzyme showed no catalytical activity, when suspended in the IL. The application of this enzyme was thus restricted to biphasic systems. Water is often structure-supporting, giving the enzyme the necessary shape to be catalytically active. Therefore many enzymes cannot work outside aqueous phases. Nevertheless, processes using exclusively ILs as the reaction media also do exist.^[10]

Another class of enzymes is the class of alcohol dehydrogenases, which can catalyse

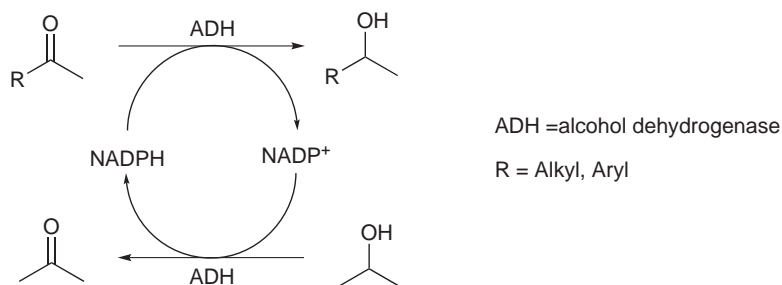
the enantioselective reduction of prochiral ketones to alcohols. These cofactor-dependent enzymes already have been successfully employed in biphasic systems using ILs. Kragl *et al.* demonstrated for 2-octanone that the use of an IL can be beneficial to the reaction (Scheme 5.4 on the following page).^[20,21] The cofactor needed by the enzyme is the expensive NADPH³ in order to hydrogenate the ketone. This cofactor NADPH is regenerated *in situ* by oxidation of excess 2-propanol. Thus, the overall reaction scheme is a transfer hydrogenation. Both the enzyme and the cofactor are dissolved in the water phase, whereas the substrates are mainly concentrated in the IL layer. The *in situ* regeneration of the cofactor is essential and only the successful regeneration makes its application feasible due to the high costs of NADPH. Furthermore, the successful shift of the chemical equilibrium towards acetone is of the essence for the reaction to proceed quickly, as the regeneration of the cofactor is often the rate determining step.

Scheme 5.3: NADPH and NADP⁺

Lactobacillus brevis alcohol dehydrogenase

The enzyme alcohol dehydrogenase of *Lactobacillus brevis* (LB-ADH) is a powerful tool for the synthesis of chiral alcohols. LB-ADH is a biocatalyst known for its good thermal stability and its inertness towards various solvents, such as organic solvents and ILs.^[20]

³nicotinamid adenin dinucleotide phosphate

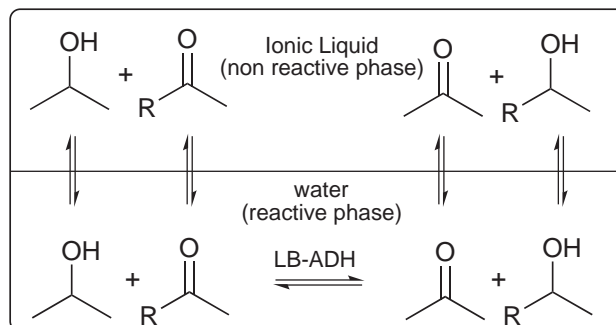


Scheme 5.4: General scheme for the alcohol dehydrogenase catalysed reaction

The activity of the enzyme highly depends on Mg^{2+} ions. Removing or ligating Mg^{2+} reduces the activity of the enzyme significantly.^[22] Like all ADHs its activity also depends highly on the presence of the cofactor NADPH and its successful regeneration in the catalytic cycle. The regeneration happens by oxidation of 2-propanol to acetone.

Partition coefficients

The rate of the regeneration in a biphasic system, however, is dependent on the partition coefficients (P) of the reactants. Figure 5.5 shows a general biphasic system IL/H₂O for the conversion of ketones to alcohols.



Scheme 5.5: water/ionic liquid biphasic reaction system

All the reactants are in equilibrium. Therefore, by choice of the correct non-reactive phase, the equilibrium can be shifted to the advantage of the rate of the transfer hydrogenation reaction. P is a value that defines where a certain substance is preferably situated in a biphasic system.

$$P = \frac{c(\text{substrate in the non-aqueous layer})}{c(\text{substrate in the aqueous layer})}$$

Beneficial for the reaction would be a high concentration of ketone substrate in the aqueous phase and a high concentration of the corresponding alcohol in non-aqueous phase. This would allow the non-reactive phase to act as a reservoir and at the same time remove the alcohol from the water phase. This means low P s for the ketones are highly desirable and high coefficients for the alcohols, respectively. Important is that always enough 2-propanol is present in the water phase to guaranty the new formation of NADPH+H⁺. Therefore the low miscibility of the non-reactive phase with 2-propanol is crucial for the reaction. Furthermore, acetone formed during the reaction must be soluble in the non-aqueous phase to shift the thermodynamical equilibrium to increase the rate of the regeneration of the cofactor. This step is crucial as it influences the overall reaction rate substantially. P are normally influenced by all compounds present

in the reaction system and their concentrations. In that case one speaks of non-ideal coefficients. In the ideal reaction system all P are not influenced by concentrations. When the impact of concentration and all compounds employed on P is significant, prediction of the behaviour of the system becomes difficult and it is not possible to say if at a certain stage of the reaction, the P is still advantageous for the reaction rate.

5.2 Investigation of a biphasic system

The aim of this study is to find a suitable IL for the transfer hydrogenation reaction catalysed by LB-ADH and to compare this IL/H₂O system to the classical MTBE/H₂O system. These are preliminary studies with the ultimate goal to apply the system in a continuous reactor. Furthermore, the P for various alcohols and ketones are measured to see how the P behaves at different concentrations and if ideal or non-ideal behaviour is observed. So far, this has never been done for these kinds of systems. 2-Butanone is used as substrate in the transfer hydrogenation reaction, as this substrate is the most delicate one due to its resemblance to acetone and also the similarity in nature of 2-propanol to 2-butanol makes 2-butanone a challenging substrate. An IL must be found that has a low P for 2-propanol and a high one for 2-butanol.

Role of the ionic liquid

As mentioned before, the IL has to meet several criteria for this reaction. The ideal IL in question has to be hydrophobic, hardly/non miscible with 2-propanol and applicable at room temperature. The insolubility of 2-propanol in the IL is essential to ensure a high concentration of the alcohol in the reactive phase, where the catalyst is situated. Concomitant with this insolubility of 2-propanol a good solubility of acetone must be given. These two requirements help to shift the thermodynamical equilibrium towards the products.^[18,20] The non-reactive phase serves as a reservoir for the substrates and removes the products from the reactive phase. The melting point of the IL must be below room temperature as elevated temperatures in biocatalysis are unfavourable. In addition a low viscosity is important. As the temperature of this reaction is room temperature the viscosity of the IL must be low.

One of the first ILs tested, was 1-octyl-3-methylimidazolium tetrafluoroborate (Figure 5.1).

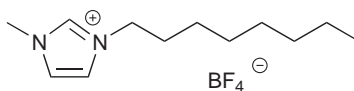
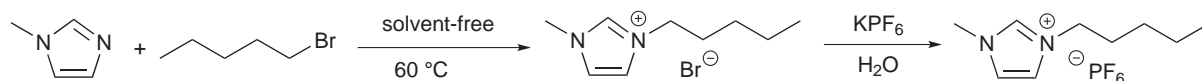


Figure 5.1: [OMIM][BF₄]

This relatively cheap IL can be synthesised from ground stock chemicals and it is water immiscible due to the long hydrophobic side chain. However, instead of forming a biphasic systems, the IL forms small droplets that hinder its applicability in a biphasic reaction system. Increasing the side chain to further strengthen the hydrophobic character failed because of the equally increasing viscosity rendering the IL inapplicable. Other water insoluble cations, containing long alkyl chains, such as Aliquat 336 (trioctylmethylammonium), have the disadvantage of high melting points and high viscosity.

Therefore it was anticipated to incorporate the hydrophobicity via the anion. Two anions are famous for forming water-repelling ILs, PF₆⁻ or Tf₂N⁻ (bis(trifluoromethylsulfonyl)amide). Both anions form with numerous cations ILs, that do not mix with H₂O. Latter ones also regularly form low-melting and less-viscous liquids. The major drawback here are the costs caused by this IL and the stoichiometric amount of toxic lithium salts being formed during their preparation. Therefore PF₆⁻ seems to be the more logical choice. ILs bearing this anion can be synthesised in a straightforward manner, are affordable and only potassium halides are formed as a side product. The major drawback of these ILs, however, is their stability. They are sensitive towards H₂O at higher temperatures. Therefore, the applicability in biocatalytic reactions can be considered. Several different types of cations, such as pyridinium- or imidazolium-based, were evaluated. The pyridine salts were ruled out due to their instability in the presence of nucleophiles. The most applicable class seems to be the class of imidazolium cations. Here, 1-methyl-3-pentyl-imidazolium was selected as the proper candidate. The length of the side chain (C5) allows it to be applicable even for long-chain ketones. Furthermore, it was selected as it is showed good physical properties,

such as low melting point and low-viscosity. Facile separation from water occurs leading to a clear phase boundary. Also, this IL is poorly miscible with 2-propanol but its ability to dissolve acetone is excellent. Higher alcohols, too, show good solubility in the IL. This is crucial as these products have to be removed from the reactive phase. This IL can be synthesised in a straightforward manner (Scheme 5.6). Firstly 1-methylimidazole is reacted with 1-bromopentane without the addition of a solvent. In the next step the bromide is exchanged for PF_6^- by combining a solution of the IL in H_2O with a solution of KPF_6 in H_2O . Immediately a biphasic system is formed. The new IL is washed several times with water and is dried under reduced pressure to remove the H_2O . A slightly yellow liquid is received.

Scheme 5.6: Solvent-free synthesis of [PMIM][PF_6]

5.2.0.9 Alcohols

Table 5.1: Partion coefficient of various alcohols

Alcohol	P IL	P MTBE	Highest P
2-butanol	non-ideal	ideal	MTBE
2-pentanol	non-ideal	ideal	MTBE
2-hexanol	non-ideal	non-ideal	MTBE
2-heptanol	non-deal	non-ideal	MTBE
2-octanol	non-ideal	non-ideal	MTBE
acetophenone	non-ideal	non-ideal	MTBE

The P s for six different alcohols (Table 5.1), were determined for their concentration dependence in both, the MTBE and the IL system (Figure 5.2 on page 155). The P in MTBE were higher in value for all alcohols tested compared to the IL system (Table 5.1). Sole exception is the P of 2-butanol in MTBE, when 2-propanol is added. This lowers the

coefficient considerably. The addition of 2-propanol to the phenylethanol system causes the MTBE system to become nearly ideal. Concentration dependence of the coefficient is almost negligible. Under these circumstances the IL system and the MTBE system are almost coincident. Apart from 2-pentanol, the MTBE systems showed non-ideal behaviour for all other alcohols measured, meaning they are dependent on the concentration of the substrate. The coefficients of the IL system did not reach a maximum value in the tested range. In case of 2-heptanol and 2-octanol this also held true for the MTBE systems. Furthermore, there is a considerable discrepancy in the coefficient for the alcohols. A clear tendency could not be recognized. It is, however, obvious that the highest values are reached for 2-heptanol, especially with increasing concentration. This substrate is in clear favour of the organic layer. Therefore, a sufficient extraction of the alcohol from the aqueous layer should be guaranteed. Interestingly in all cases the alcohols showed little or no ideal behaviour in the IL system. The optimum alcohol was in this system 2-pentanol. Its solubility in the IL was the highest of all alcohols screened. Probably the conformity of the chain length in the alcohol and the IL were the reason for the high solubility. A high coefficient is, however, only reached for more concentrated samples. At low concentration the maximum solubility in H₂O is not yet completely reached. These values measured showed, that long chain alcohols might not be extracted sufficiently from the reaction layer. The same holds true for 2-butanol. Its solubility in the IL is also limited. However, the *P* of this alcohol showed almost ideal behaviour, whereas in all the other cases non-ideal behaviour can be observed.

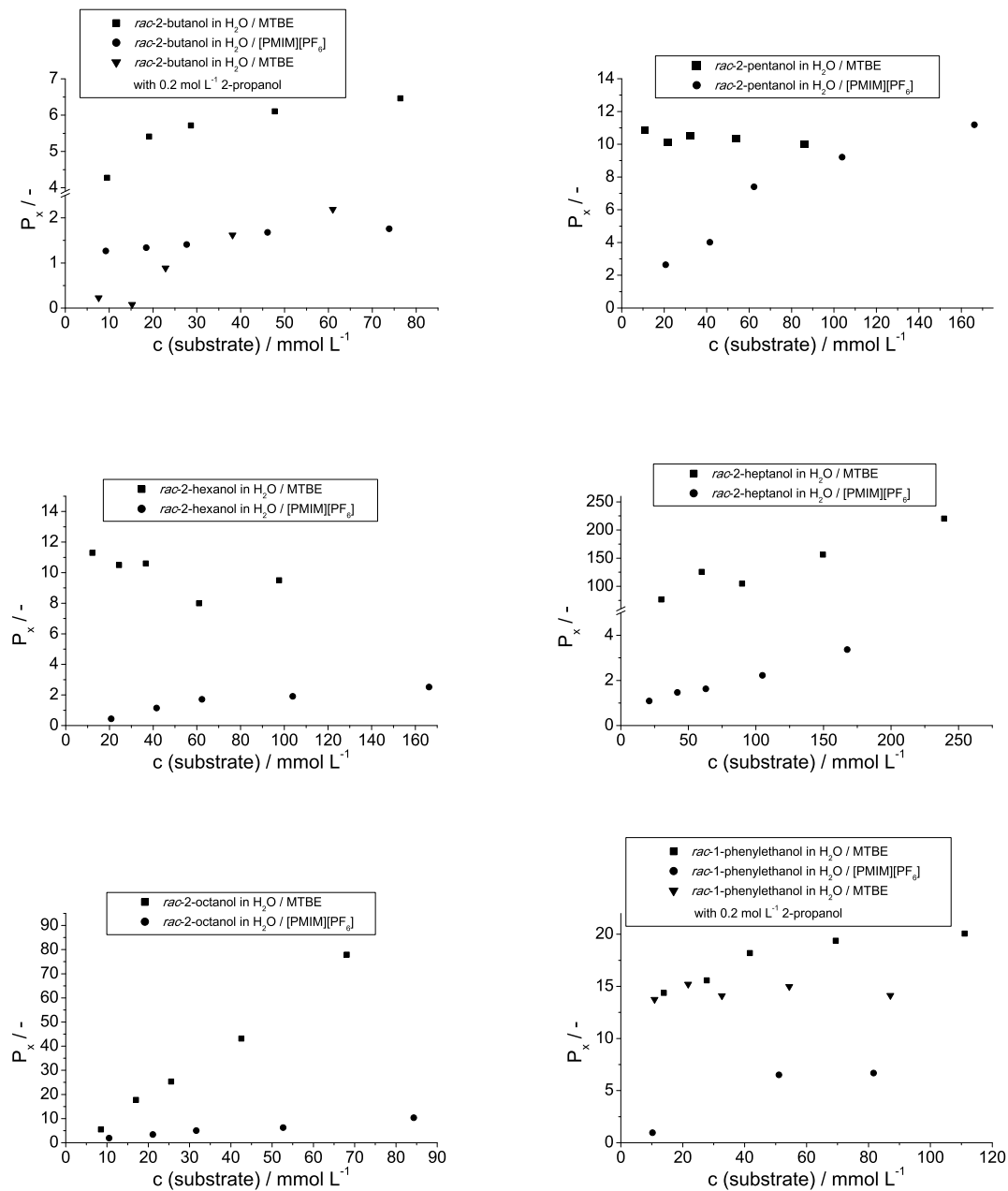


Figure 5.2: Partition coefficients of racemic alcohols at 20°C

5.2.0.10 Ketones

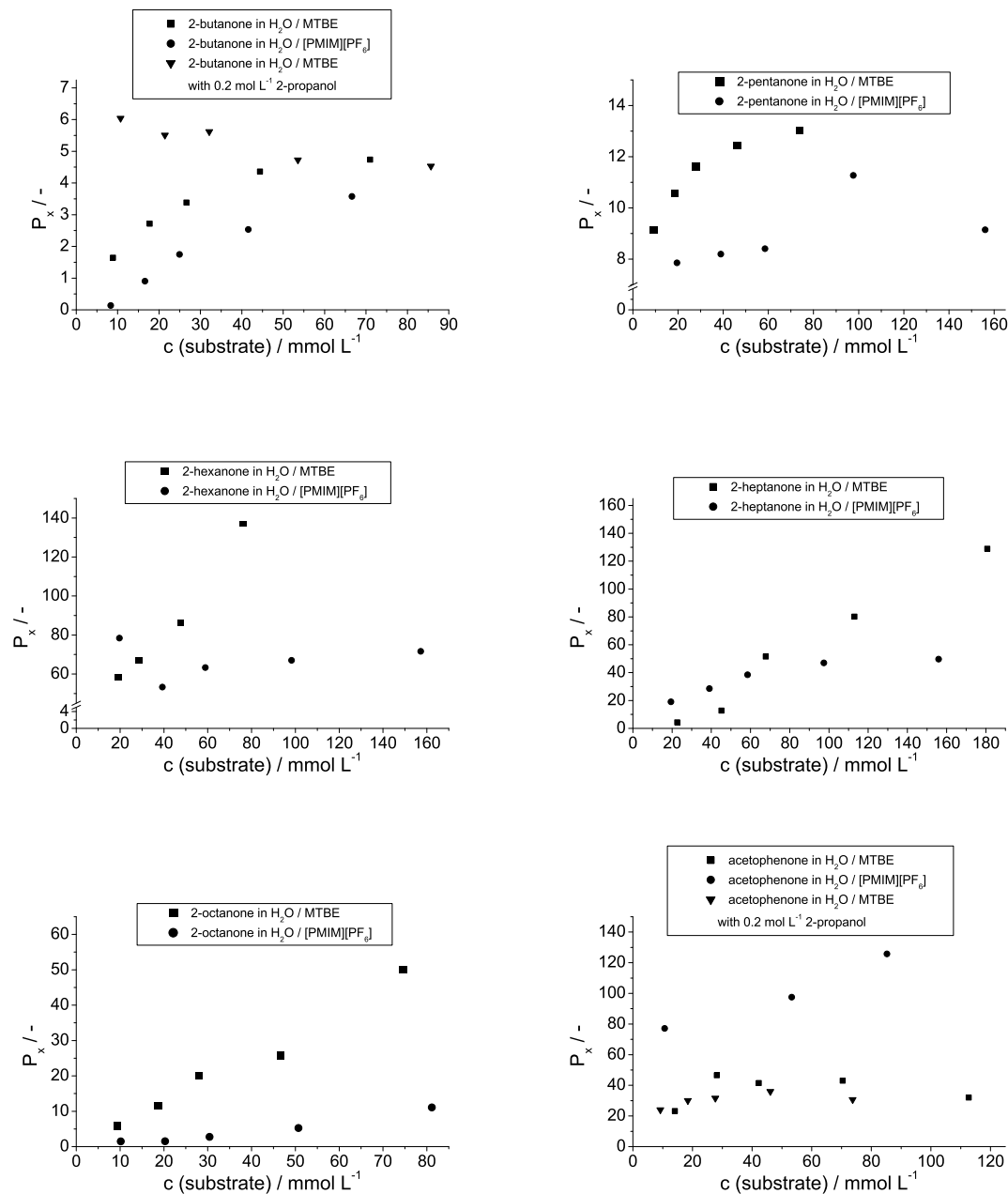
The P s for the ketones in both systems were measured and compared (Figure 5.7 on the next page). For every single system non-ideal behaviour was observed (Table 5.2).

Table 5.2: Partion coefficients of various ketones

Ketone	P_{IL}	P_{MTBE}	Highest P
2-butanone	non-ideal	non-ideal	MTBE
2-pentanone	non-ideal	non-ideal	MTBE
2-hexanone	non-ideal	non-ideal	MTBE
2-heptanone	non-ideal	non-ideal	MTBE
2-octanone	non-ideal	non-ideal	MTBE
acetophenone	non-ideal	non-ideal	IL

In case of the IL system the highest value of the aliphatic ketones was obtained for hexanone. This substrate shows the highest solubility. Only acetophenone had a higher P . For the IL system it was noticeable that no maximum for the coefficient could be found, for neither of the substrates. For all substrates the value of the coefficient increases, when the sample is more concentrated. Conspicuously there is a distinct difference in the P s between the two ketones 2-butanone and 2-pentanone compared to the other substrates. The short chained ketones have considerably lower coefficients, an attribute of advantage for the application in the biphasic reaction. This discrepancy can also be seen when looking at the P in the MTBE / water system. Long chain ketones were considerably better soluble in the non-aqueous phase than in the aqueous phase. Also acetophenone is in favour of the non-aqueous phase. Interestingly, for the MTBE system only in case of pentanone a maximum for the P could be found. In all other cases it depended on the concentration of the substrate. Except for acetophenone all P were higher for MTBE. Therefore, regarding the ketones the IL is better for the equilibrium of the reaction.

5 Biocatalysis in a biphasic ionic liquid/water system



Scheme 5.7: Partition coefficients of ketones at 20°C

Reduction of 2-butanone

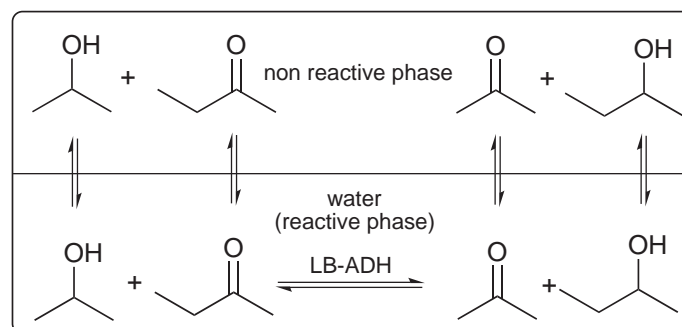


Figure 5.3: Reduction of 2-butanone catalysed by LB-ADH and NADPH

In this study 2-butanone was chosen as benchmark substrate for the comparison of the two biphasic systems (Scheme 5.3). The data is depicted in figures 5.4, 5.5 and 5.6 at the end of this section. 2-Butanone was selected as substrate due to the *P* of the ketone and the corresponding alcohol. Despite the fact that 2-pentanol showed the higher coefficient and therefore should have been more suitable for this reaction, 2-butanol was chosen. Here, the coefficient of the ketone tipped the balance. A low value for the ketone is crucial for a sufficient transfer of ketone into the reactive phase. In case of these two ketones, altogether the system butanone/butanole provides the best starting situation. Furthermore, this substrate has not yet been investigated under these conditions. Mainly ketones with longer chains or more complex structures have been tested in catalysis. Due to its resemblance to 2-propanol, it is also a more challenging substrate.^[20,23] Conversion and selectivity were monitored for different substrate and 2-propanol concentrations.

For the system MTBE/H₂O it is known that acetone and 2-propanol are equally soluble in both layers.^[20] Their *P*s are close to parity. Therefore no influence on the thermodynamics and kinetics can be expected. In the case of the IL, however, the situation differs. Acetone shows is completely miscible with the ILs whereas 2-propanol shows a poor solubility and forms a biphasic system with the IL. It will therefore predominately be found in the aqueous phase. This is beneficial to the regeneration of the cofactor NADPH, as it depends on a high concentration of the alcohol and continuous removal of acetone (fig. 5.3 on page 148). Table 5.3 on the next page shows the results

for the hydrogenation of 1-butanone with 0.2 M 2-propanol for the two biphasic systems.

Table 5.3: Biphasic reaction after 100 min with 2-propanol 0.2 mol L⁻¹:

entry	butanone / mmol L ⁻¹	conv. / ee MTBE /%	conv. / ee IL /%
1	20	38 / 75	13 / 99
2	50	30 / 95	7 / 72
3	100	29 / 75	3 / 99

$c(2\text{-butanone}) = x \text{ mmol L}^{-1}$, $c(2\text{-propanol}) = 0.2 \text{ mol L}^{-1}$, $c(\text{NADP}^+)$, $c(\text{LB-ADH}) = 1.0 \text{ mg mL}^{-1}$, $c(\text{buffer}) = 50 \text{ mmol L}^{-1}$, $V_{\text{reaction}} = 5.0 \text{ mL}$

Immediately it can be seen that for all substrate concentrations the yield is higher in the MTBE system compared to the IL. However, in both cases it is obvious that increasing the concentration of the substrate has a negative impact on the conversion. For the MTBE system only a decrease of 10% can be seen when the concentration is increased from 20 to 100 mM, whereas in case of the IL the reaction almost shows no conversion anymore. The effects can be attributed to the partition coefficient of the substrate. As mentioned above, with increasing amount of 2-butanone the value changes to disfavoured higher values. As the cofactor regeneration is the rate limiting step, this could explain the observation. A higher butanone concentration in the non-reactive phase increases the solubility of 2-propanol in this phase and hence frustrates catalyst regeneration. In case of MTBE this effect is not pronounced. The influence of the 2-butanone concentration on the regeneration did not carry that much weight. This could be explained by the P_s of 2-butanone in MTBE in the presence of 2-propanol. The figure 5.7 on page 157 shows that the influence of the concentration is almost negligible. Interestingly there seems to be a optimum butanone concentration concerning the ee . The experiment using 50 mM 2-butanone results in the best selectivity for MTBE in contrast to the IL. There, the opposite effect is observed.

Increasing the 2-propanol concentration from 0.2 to 2.0 M (Table 5.4 on the next page) supports the theory that the increasing 2-butanone concentration has a negative effect on the catalyst regeneration by reducing the 2-propanol concentration in the reactive layer.

The effect on the yield is far less pronounced under these circumstances. Only at 100

Table 5.4: Biphasic reaction with 2-propanol 2.0 mol L⁻¹ after 100 min

entry	butanone / mmol L ⁻¹	conv. / ee MTBE /%	conv./ee IL /%
1	20	35 / 97	13 / 99
2	50	60 / 95	13 / 97
3	100	38 / 95	6 / 99

$c(2\text{-butanone}) = x \text{ mmol L}^{-1}$, $c(2\text{-propanol}) = 2.0 \text{ mol L}^{-1}$, $c(\text{NADP}^+)$, $c(\text{LB-ADH}) = 1.0 \text{ mg mL}^{-1}$, $c(\text{buffer}) = 50 \text{ mmol L}^{-1}$, $V_{\text{reaction}} = 5.0 \text{ mL}$

mM 2-butanone for the IL system a decrease of the yield can be observed. Strikingly, for the MTBE system 50 mM 2-butanone seems to be the optimum reaction condition. Here the highest conversion of all is observed. Regarding the *ee* in almost all reactions the highest values are obtained in the IL system. This, however, holds true when looking at the *ee* at 100 min reaction time. Comparing the *ee* at the same conversion reveals that there is no significant difference for all reactions observed. The selectivity drops in almost all cases in the MTBE system in the course of the reaction, whereas it remains stable with the IL present. Obviously the MTBE slowly destabilises the active site in the enzyme. In some cases the degradation proceeded quickly in other cases the decrease of the *ee* is only a few percent in 100 min. The most dramatic decrease was observed in case of a low 2-propanol concentration. However, in many cases the reaction stops completely for both reaction systems. For the selectivity remaining stable this can most likely be attributed to a failed regeneration of the cofactor, either due to thermodynamical reasons, as a consequence of insufficient 2-propanol in the reactive phase, or to decomposition. A decrease in selectivity in combination with the reaction stopping indicated a denaturation of the enzyme.

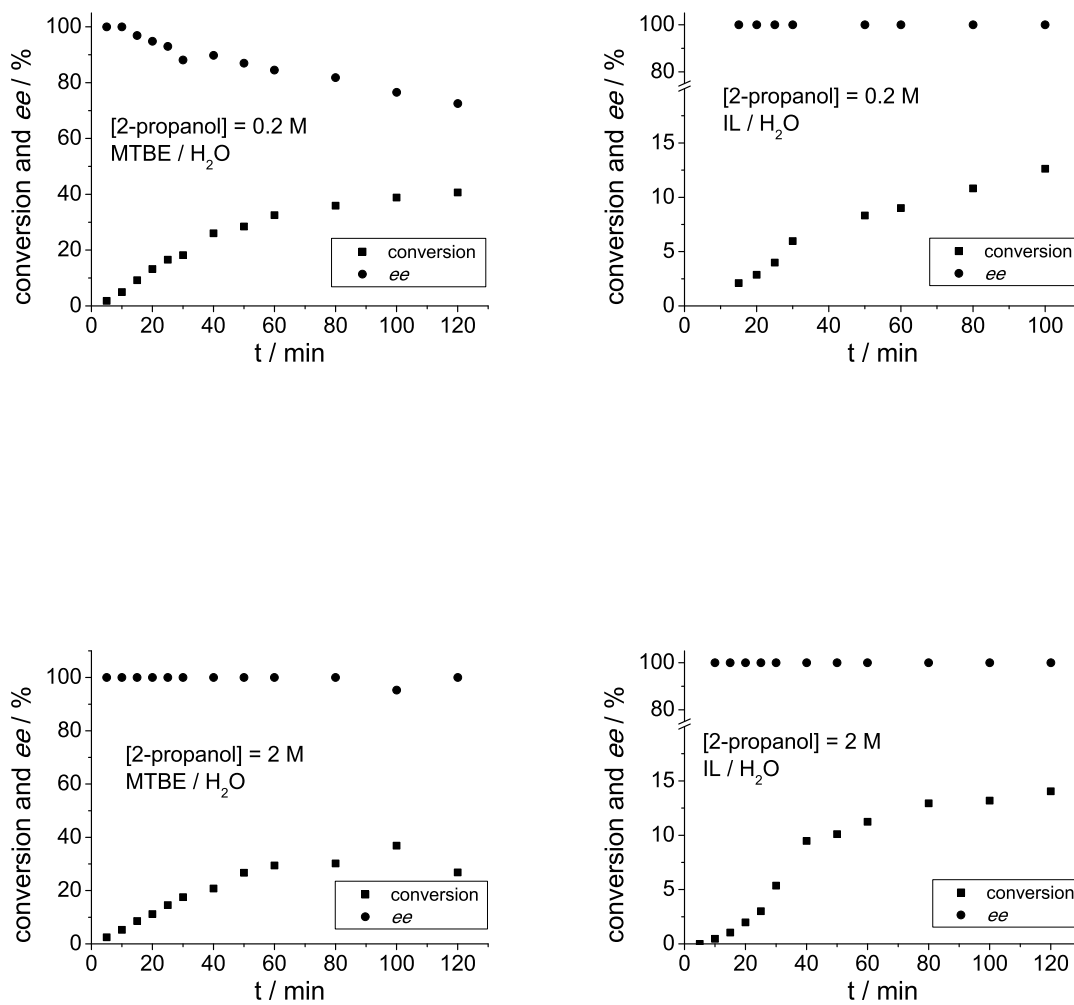


Figure 5.4: Biphasic reaction using 20 mmol L⁻¹ 2-butanol, left: MTBE, right: IL

$c(2\text{-butanone}) = 20 \text{ mM}$, $c(\text{NADP}^+)$, $c(\text{LB-ADH}) = 1.0 \text{ mg mL}^{-1}$, $c(\text{buffer}) = 50 \text{ mM}$,
 $V(\text{reaction}) = 5.0 \text{ mL}$

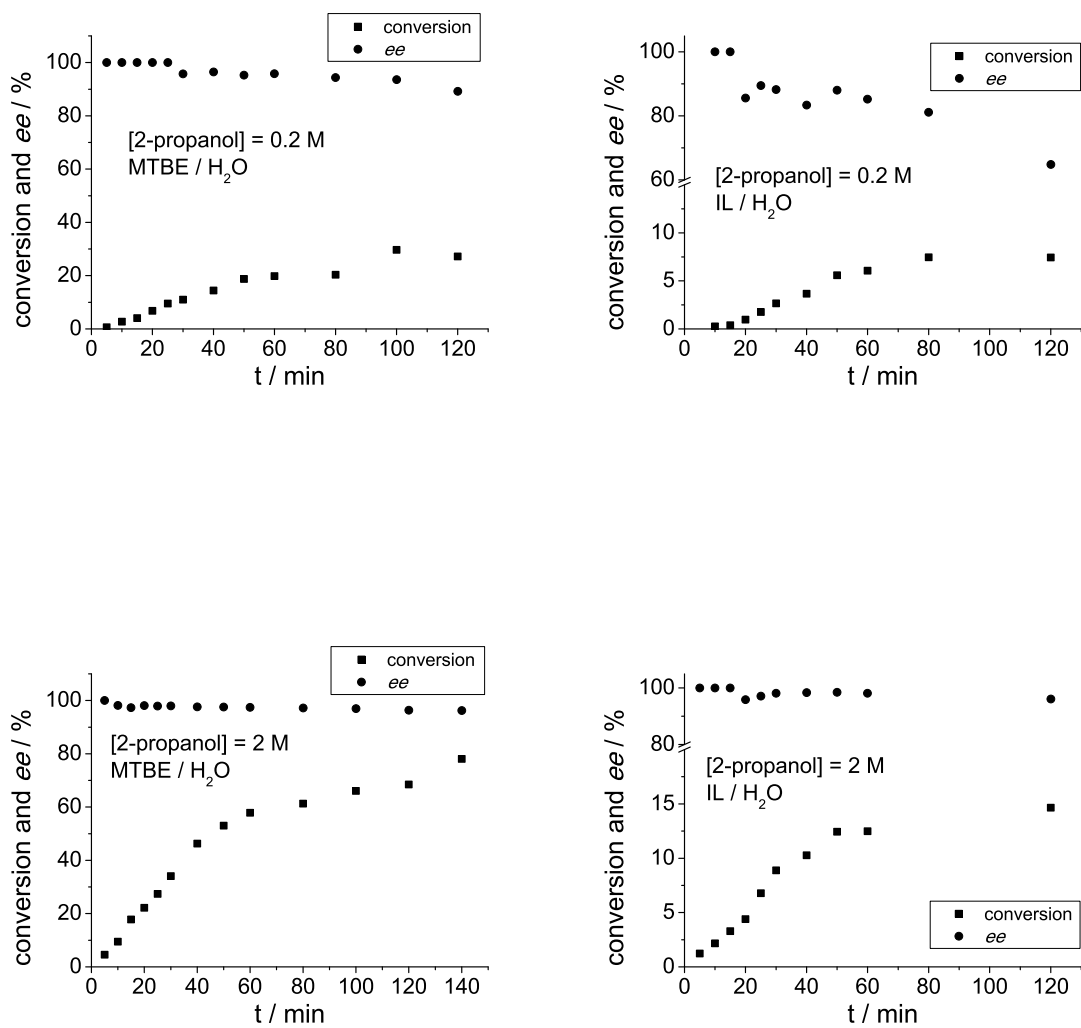


Figure 5.5: Biphasic reaction using 50 mM 2-butanone, left: MTBE, right: IL

$c(2\text{-butanone}) = 50 \text{ mM}$, $c(\text{NADP}^+) = 1.0 \text{ mg mL}^{-1}$, $c(\text{LB-ADH}) = 1.0 \text{ mg mL}^{-1}$, $c(\text{buffer}) = 50 \text{ mM}$, $V(\text{reaction}) = 5.0 \text{ mL}$

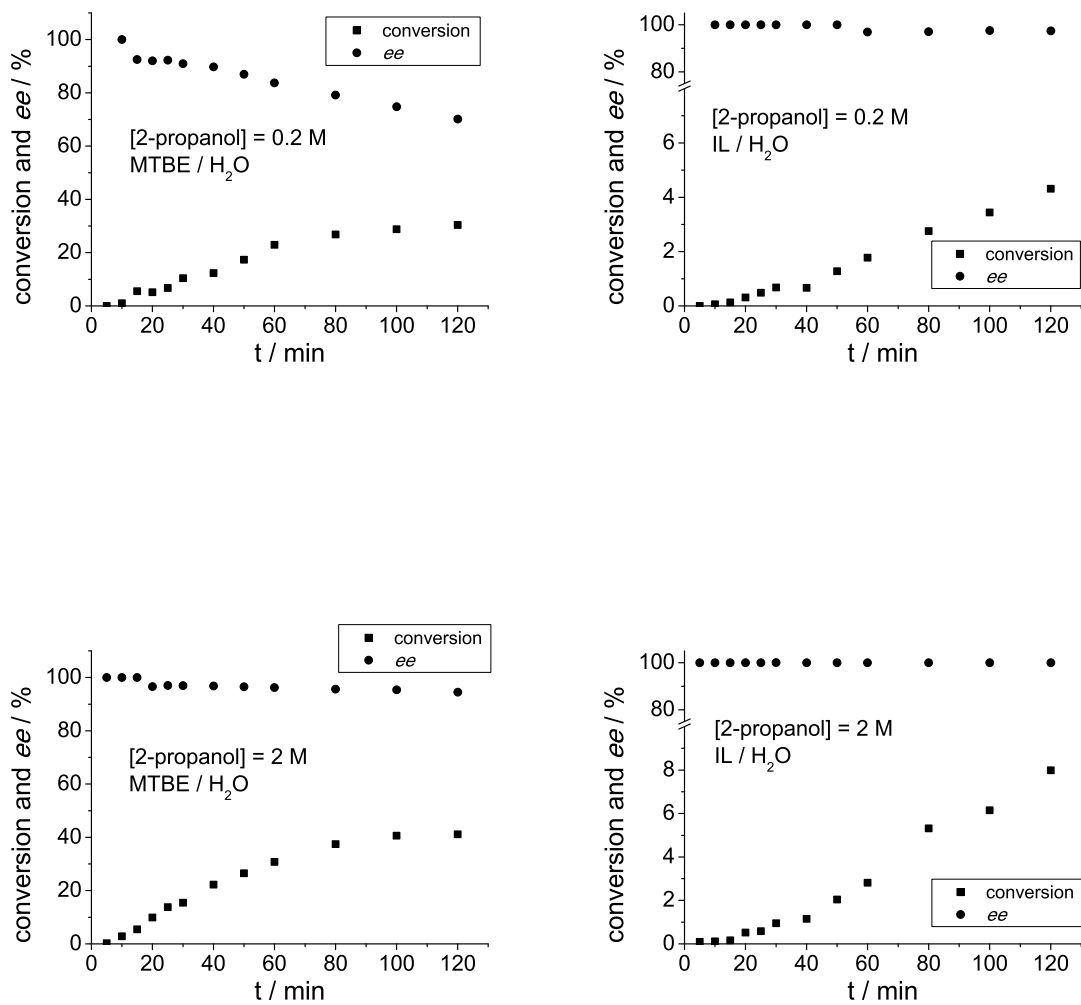


Figure 5.6: Biphasic reaction using 100 mM 2-butanol, left: MTBE, right: IL

$c(2\text{-butanone}) = 100 \text{ mM}$, $c(\text{NADP}^+)$, $c(\text{LB-ADH}) = 1.0 \text{ mg mL}^{-1}$, $c(\text{buffer}) = 50 \text{ mM L}^{-1}$,
 $V(\text{reaction}) = 5.0 \text{ mL}$

5.3 Conclusions

In this chapter it has been shown that ILs can be a replacement for classical solvents, such as MTBE in an alcohol dehydrogenase catalysed reduction of short chain ketones, although this particular IL showed a lower activity. The IL [PMIM][PF₆] forms a biphasic system with water. Phase separation occurs quickly and distinctly. Furthermore, no denaturation of the enzyme or the cofactor induced by the IL was observed. However, it has to be mentioned that in almost all cases the reaction gave a better result with MTBE for 2-butanone as the substrate with respect to conversion. Selectivity is, even though only marginal, better when the IL is applied. It seems that MTBE does denature the catalytically active site in the enzyme and hence reduces the *ee*. In a batch reaction this might not pose a problem. Considering the future employment of this enzyme in a continuous reactor, a denaturation of the enzyme is a serious issue. Therefore, despite the low conversion, ILs still can contribute substantially to this reaction. Further modification of the cation by introducing longer side chains or even functional groups, such as ether or ester, could help to increase the yield in this reaction and to cut the reaction time. One advantage of the IL used over MTBE does exist, though. It is possible in the end to collect and reuse it as it only contains substances used in the reaction. Also it will be possible to purify it by removing these substances under reduced pressure. Furthermore, this study showed that biphasic systems are not trivial. The concentrations and all compounds employed have an impact on the *P* and therefore, predictions about the behaviour of a system are difficult, if not impossible. Too many parameters depend on each other. The application of a genetic algorithm for multi-parameter optimisation can be helpful here.

5.4 Experimental

All chemicals were purchased from Aldrich, Carl Roth, Acros or Merck and used as received. NMR spectra were recorded on a Varian Unity Inova 500 (VT NMR) and Mercury 400-spectrometer. ^1H -NMR, ^{13}C -NMR referenced using residual solvent peaks. ^{19}F NMR were referenced externally. The pH meter model ph211, VWR Collection was used for pH-measurements. The enzyme LB-ADH was purchased as a powder (Lyophilisat) from X-Zyme.

Standard assay LB-ADH

The composition of the standard assay is based on the information provided by the enzyme supplier X-Zyme GmbH and on own investigations:

$c(\text{Acetophenon}) = 5 \text{ mM}$

$c(\text{NADP}^+) = 0.5 \text{ mM}$

$c(\text{Buffer}) = 50 \text{ mM}$

$K_m = 0.01 \text{ mM}$

Activity = 4.4 U/mg

GC-Analysis

GC:	Agilent Technologies HP 6890, JAS-Unis Inlet
Column:	CP-Chirasil-DEX CB, 25 m, inner diameter 0.25 mm, Varian film thickness 0.25 μm
Colum:	Lipodex G, 25 m, inner diameter 0.25 mm, Macherey-Nagel
Carrier gas:	H_2

Quantitative and chiral analysis were carried out using the same method. CP-Chirasil-DEX CB was used for C2-C6-alcohols and Lipodex G for alcohols > C6.

Buffer solutions

For 500 mL of a 500 mM potassium phosphate buffer 29.65 g (0.17 mol) KH_2PO_4 and 10.85 g (0.08 mol) K_2PO_4 are dissolved in 300 mL deionised water. The pH-value is adjusted to 6.5 by 85 % H_3PO_4 , and the volume is filled up to 500 mL with deionised water.

Partition coefficient

For the preparation of the stock solutions MTBE and $[\text{PMIM}][\text{PF}_6]$ are saturated with water. The water used is saturated with the respective non-aqueous phase. The reaction vessels are thoroughly closed with Parafilm, mixed for 30 seconds using a Vortex, and stored at 30 °C for four days. From each phase 50 μL samples are taken and 100 μL of the respective GC standard are added. The samples are measured three times each, and the concentrations of each phase are calculated from the GC measurements.

General procedure for the batch reactions

The stock solutions are prepared using the non-aqueous phases as solvents. The needed amounts of enzymes and cofactors are dissolved in 0.5 mL of the respective 50 or 100 mM buffer. The reactions are always started by addition of the enzyme solution and are stirred slowly. Samples of 50 μL are regularly taken from the non-reactive phase and mixed with 100 μL of the suitable standard solution. To ensure equal phase volumes in spite of sample taking 50 μL are taken out of the aqueous phase with each sample and discarded. The reactions are conducted at room temperature.

1-Methyl-3-pentyl-imidazolium hexafluorophosphate ($[\text{PMIM}][\text{PF}_6]$)

1-Methylimidazole (60 mL, 0.752 mol) was mixed with 1-bromopentane (93.20 mL, 0.752 mol). The mixture was stirred at 50°C for 24 h. The liquid received was dissolved in 150 mL water and potassium hexafluorophosphate (147.25 g, 0.8 mol) was added to this solution. The mixture was stirred for 2 h and a biphasic system was formed. The water layer was decanted and the ionic liquid was washed five times with 100 mL water.

The remaining water was removed under reduced pressure at 80°C.

¹H NMR (C₂D₆O) δ (ppm): 8.92 (s, 1H), 7.72 (s, 1H), 7.66 (s, 1H), 4.35 (t, 2H, $J=7.34$ Hz), 4.03 (s, 3H), 1.94 (m, 2H), 1.35 (m, 4H), 0.88 (t, 3H, $J=7.02$ Hz). **¹³C NMR**: 136.49, 123.85, 122.47, 49.54, 35.67, 29.51, 27.94, 21.77, 13.16. **¹⁹F NMR**: -137.82, 139.70.

Bibliography

- [1] A. Liese, K. Seelbach, C. Wandrey, *Industrial Biotransformations*, Wiley-VCH, Weinheim, **2000**.
- [2] A. Klivanov, *Chemtech*. **1986**, *16*, 354.
- [3] K. Faber, *Biotransformations in Organic Chemistry*, Springer-Verlag, Berlin, Heidelberg, New York, 5th ed., **2004**.
- [4] T. Welton, *Chem. Rev.* **1999**, *99*, 2071–2083.
- [5] P. Wasserscheid, *Chem. Unserer Zeit* **2003**, *1*, 52–63.
- [6] P. Wasserscheid, T. Welton, *Ionic Liquids in Synthesis, Vol. 2*, Wiley-VCH, Weinheim, 2nd ed., **2008**.
- [7] C. Roosen, P. Müller, L. Greiner, *Appl. Microbiol. Biotechnol.* **2008**, *81*, 607–614.
- [8] S. Cantone, U. Hanefeld, A. Basso **2007**, *9*, 954–971.
- [9] F. van Rantwijk, R. A. Sheldon, *Chem. Rev.* **2007**, *107*, 2757–2785.
- [10] S. Klemmt, S. Dreyer, M. Eckstein, U. Kragl in *Ionic Liquids in Synthesis, Vol. 2* (Eds.: P. Wasserscheid, T. Welton), Wiley-VCH, Weinheim, 2nd ed., **2008**, pp. 641–662.
- [11] P. Wasserscheid, W. Keim, *Angew. Chem.* **2000**, *112*, 3926–3945.
- [12] M. Picquet, I. Tkatchenko, I. Tommasi, P. Wasserscheid, J. Zimmermann, *Adv. Synth. Catal.* **2003**, *345*, 959–962.
- [13] N. S. Chowdari, D. B. Ramachary, C. F. Barbas III, *Synlett* **2003**, *12*, 1906–1909.
- [14] S. Park, R. Kazlauskas, *J. Org. Chem.* **2001**, *66*, 8395.
- [15] M.-J. Kim, M. Choi, J. Lee, Y. Ahn, *J. Mol. Catal. B: Enzym.* **2003**, *26*, 115.
- [16] S. Nara, S. Mohile, J. Harjani, P. Naik, M. Salunkhe, *J. Mol. Catal. B: Enzym.* **2004**, *28*, 39.
- [17] S. G. Cull, J. D. Holbrey, V. Vargas-Mora, K. R. Seddon, G. J. Lye, *Biotechnol. Bioeng.* **2000**, *69*, 227–233.

Bibliography

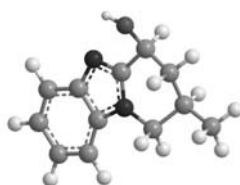
- [18] M. Peters, M. Eckstein, G. Hartjen, A. C. Spiess, L. Walter, L. Greiner, *Ind. Eng. Chem. Res.* **2007**, *46*, 7073–7078.
- [19] M. Erbedinger, A. J. Mesiano, A. J. Russell, *Biotechnol. Prog.* **2000**, *16*, 1129–1131.
- [20] M. Eckstein, M. V. Filho, A. Liese, U. Kragl, *Chem. Commun.* **2004**, 1084–1085.
- [21] A. J. Walker, N. C. Bruce, *Chem. Commun.* **2004**, 2570–2571.
- [22] K. Niefind, J. Müller, B. Riebel, W. Hummel, D. Schomburg, *J. Mol. Biol.* **2003**, *327*, 317–328.
- [23] J. Howarth, P. James, J. Dai, *Tetrahedron Lett.* **2001**, *42*, 7517–7519.

6

Chapter 6

Tandem reactions - An atom-efficient simple route to heterocyclic compounds

Ionic liquids stand out due to their exceptional properties and therefore often unique applicability. Their major drawback, however, remains their costs. When synthesising functionalised ionic liquids the expenses and labour often outweigh their benefit. Therefore finding straightforward routes to ionic liquids, starting from stock chemicals is the ideal path way. Amines and organic chlorides belong to this class. Therefore they constitute excellent raw materials for the synthesis of affordable functionalised ionic liquids. The general synthesis of these organic salts is described in chapter 1. Here the synthesis of new amine building blocks via a cascade reaction will be described and the subsequent transformation to organic salts. Furthermore, these amines can also serve as precursors for pharmaceutical products, chiral organocatalysts and ligands.



P.S. Bäuerlein, I.A. Gonzalez, J.J.M. Weemers, M. Lutz, A.L. Spek, D. Vogt, C. Müller, *Chem-Commun.* **2009**, 4944-4946.

6.1 Introduction

The synthesis of (bi)cyclic *N*-heterocycles receives a great deal of interest as they are the basis for many valuable compounds. *N*-heterocycles are often vital building blocks for various natural compounds and pharmaceuticals,^[1] such as Nagstatin^[2] or Cladoniamide G (Figure 6.1).^[3] These compounds have often to be synthesised in laborious multi-step syntheses. Therefore, new and simple routes to heterocycles are highly desired.

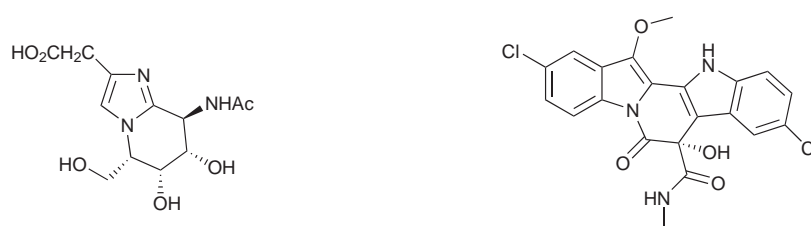


Figure 6.1: Biologically active natural products. From left to right: nagstatin^[2] and cladoniamide G,^[3]

Apart from being used in the total synthesis of natural products, *N*-heterocyclic compounds are attractive precursors for chiral ionic liquids,^[4–6] organocatalysts^[7] or ligands.^[8–12] There is a wide scope of applicability (Figure 6.2).

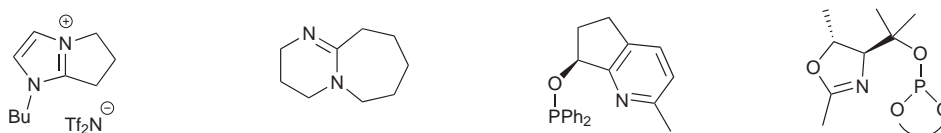
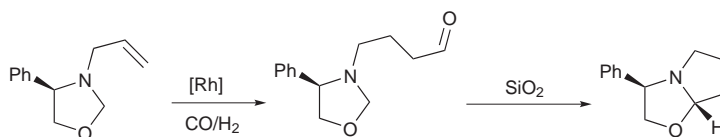


Figure 6.2: Applications of cyclic compounds in catalysis. From left to right: ionic liquids used in a Claisen rearrangement reaction,^[13] Baylis-Hillman organocatalyst,^[14] chiral P,N ligand used by Pfaltz *et al.*,^[9] chiral P,N ligands synthesised by Andersson *et al.*^[10]

In the field of organocatalysis tertiary (cyclic) amines are used in the Baylis-Hillmann reaction to catalyse the reaction between an aldehyde and an activated ketone.^[14] The resulting product is an alcohol. In case of ionic liquids nitrogen-containing compounds are the most prominent precursors to form organic salts. Quaternisation of the nitrogen

atom is very often the step to form the ionic liquid and as these compounds serve as solvent, they often have to be synthesised on large scale. Therefore, a straightforward and reasonably priced synthesis of new and functionalised precursors is beneficial. The application and synthesis of bicyclic ionic liquids has already been reported.^[13,15] The group of Chu synthesised various bicyclic ionic liquids. However, the synthesis is rather complex and not always straightforward. In the hydrogenation reaction chiral bicyclic amines are used as precursors for P,N-ligands. Pfaltz *et al.* have demonstrated in an elegant study that these ligands are excellent in the Ir-catalysed asymmetric hydrogenation of purely alkyl-substituted olefins.^[9]

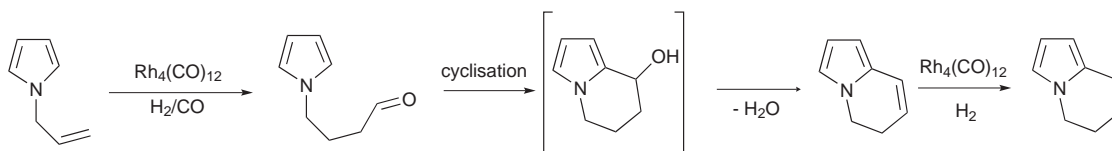
As synthesis of (functionalised) heterocyclic products is often laborious it is only reasonable to try to find ways to cut the often multistep syntheses. Bergman *et al.* used a rhodium-based catalytic system to promote an internal cyclisation reaction of alkenyl-substituted heterocycles via C-H activation.^[16,17] Furthermore, it has been come to attention that the metal-catalysed hydroformylation^[18,19] of vinyl and allyl heterocyclic compounds are a suitable route to functionlised compounds. It was discovered that the aldehyde groups could easily be attached to cyclic compounds, but also that these newly formed aldehydes can undergo intramolecular cyclisation. This led to bicyclic molecules in a one-pot reaction. Alper and co-workers recently reported on a rhodium-catalysed hydroformylation/silica deformylation sequence, leading to hexahydropyrrolo[2,1]oxazoles (Scheme 6.1).^[20]



Scheme 6.1: Rh-catalysed hydroformylation/silica-promoted deformylation sequence by Alper

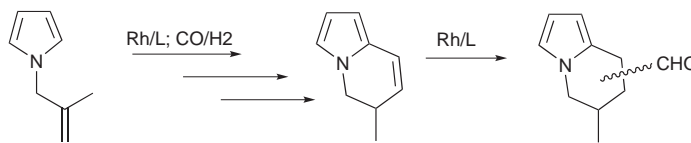
Lazzaroni and Settambolo discovered the formation of 5,6-dihydroindolizines and 5,6,7,8-tetrahydroindolizines in a tandem reaction.^[21-23] Under relatively harsh conditions (120 bar CO/H₂) the hydroformylation of *N*-((β)-methyl)pyrroles with Rh₄(CO)₁₂ clusters leads to the corresponding aldehydes. After intramolecular cyclisation the bicyclic alcohols spontaneously lose H₂O under formation of the corresponding alkenes.

These can, eventually, be hydrogenated (Scheme 6.2).



Scheme 6.2: Cascade reaction observed by Lazzaroni and Settambolo.

Müller *et al.* showed that this concept can be extended for the synthesis of formyl-functionalised indolizine derivatives. It was observed that even the unsaturated 5,6-dihydraindolizine derivative serves as an intermediate and can be hydroformylated with Rh-catalysts based on phosphabarrelenes in a one-pot four-step cascade reaction (Figure 6.3).^[24]

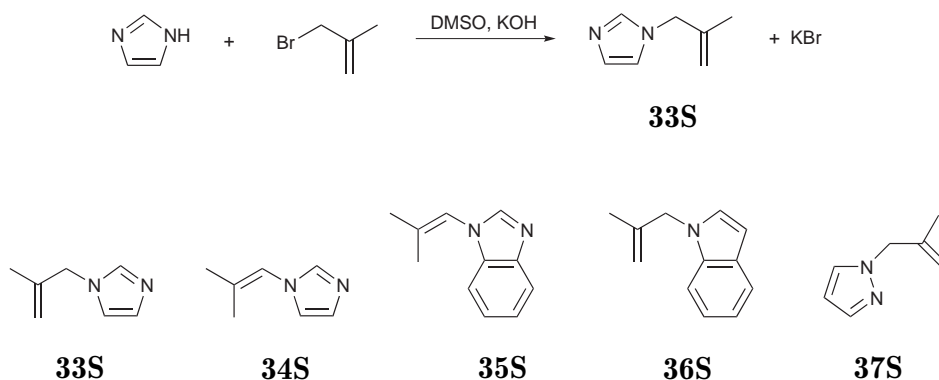


Scheme 6.3: One-pot four-step cascade reaction by Müller *et al.*^[24]

Interestingly, analogous tandem reactions starting from imidazole-based substrates have never been investigated. This is surprising as the products of such a reaction sequence could show antiulcer, anticancer, antidepressant or antimicrobial activity, as it is known for the structurally related Nagstatin. Furthermore, bicyclic imidazole derivatives could be suitable precursors for *e.g.* ionic liquids or P,N-ligands. The acidic proton in C2-position of the imidazole moiety should make it a suitable candidate for intramolecular cyclisation reaction by a nucleophilic attack of carbon atom on the carbonyl group of the aldehyde under formation of an alcohol. Therefore, in this chapter main focus will be laid on the Rh-catalysed hydroformylation of imidazole-based substrates and the subsequent reactions, such as intramolecular cyclisation. The imidazole substrates will be compared to various other *N*-heterocyclic compounds.

6.2 Synthesis of the substrates

Substrates **33S**, **35S**, **36S**, **37S** were all synthesised following a modified literature procedure. Various *N*-heterocyclic compounds were used. Whereas in the literature only expensive allyl bromides were used, the synthesis of the allyl substrates was achieved in DMSO by reaction of the *N*-heterocyclic compound with the generally cheaper chloroalkenes (Scheme 6.4). All substrates were obtained in good yields at room temperature, fully characterised by ^1H NMR and ^{13}C NMR spectroscopy as well as by mass spectrometry. To synthesise substrate **34S** containing an internal alkene moiety the reaction was conducted at 60°C to enhance isomerisation towards the thermodynamically more stable internal alkene. The compound was fully characterised by ^1H NMR and ^{13}C NMR spectroscopy as well as by mass spectrometry.

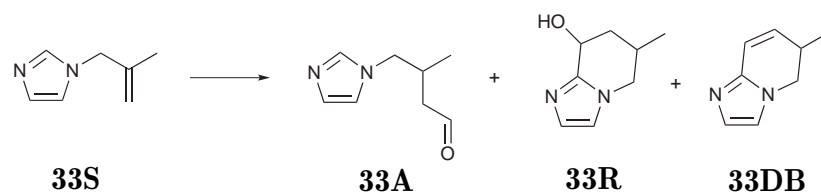


Scheme 6.4: General synthesis of the substrates using imidazole as an example

6.3 Imidazole substrate

Catalytic results

A rational approach for the investigation of the tandem reaction of the imidazole substrate **33S** (Scheme 6.5 on the following page) is to vary several parameters, such as temperature, preformation time, solvent, and ligand.

Scheme 6.5: Rh-catalysed hydroformylation of substrate **33S**

Firstly, a suitable ligand had to be identified. The reaction was first performed at a constant pressure of 20 bar and 80°C. The syngas uptake for the Rh-catalysed hydroformylation was monitored automatically during the course of the reaction. Four different ligands, the phosphine **L1**, the phosphite **L2**, the racemic mixture of phosphinine **L3** and the phosphabarrelene **L4**, were employed and assessed (Figure 6.3). The system Rh/**L1** and racemic Rh/**L4** showed a TOF of 40 h⁻¹ and 30 h⁻¹, respectively, measured at 20 % conversion. Almost all the substrate was consumed within 72 h, whereas the system Rh/**L4**, despite the lower TOF in the beginning, reaches a higher conversion in the end (Figure 6.4 on the following page). Interestingly, Rh/**L2** and Rh/**L3** are significantly less active. In case of Rh/**L2** a TOF could not be determined and for Rh/**L3** a value of merely 7 h⁻¹ was found. However, in all four reaction systems almost exclusively the terminal aldehyde **33A** was found. The internal aldehyde cannot be formed due to the methyl group in β position to the imidazole moiety.

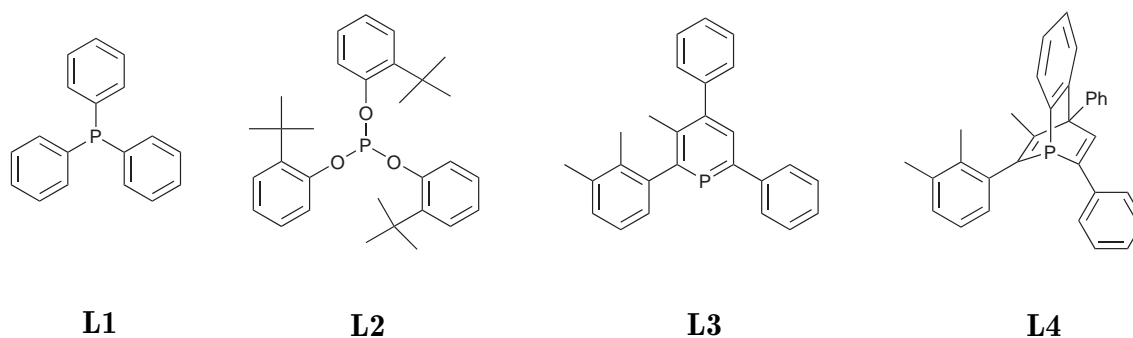


Figure 6.3: Ligands used for the Rh-catalysed hydroformylation reaction

A reasonable explanation for the difference in activity of the catalyst would be their nature. **L1** and **L4** have σ -donor properties,^[25] whereas **L2** and **L3** are π -acceptor ligands.

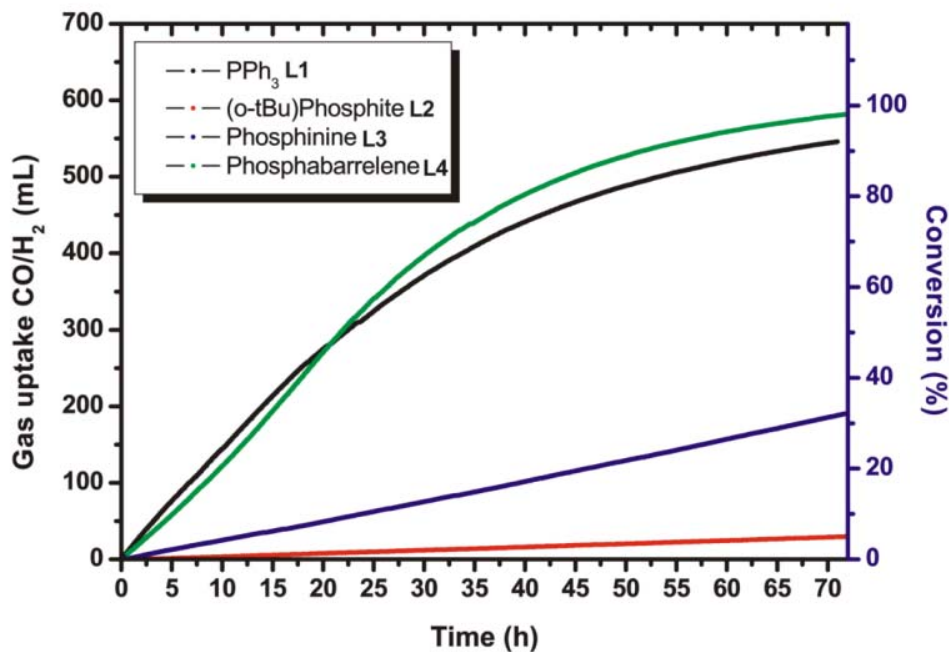
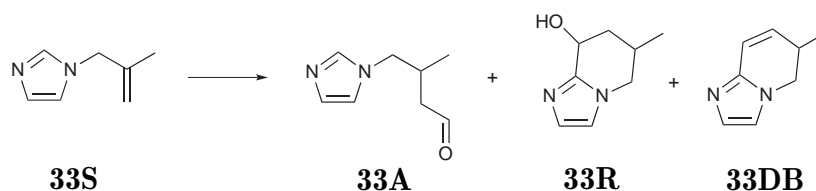


Figure 6.4: Rh-catalysed hydroformylation of **33S** in toluene with ligands **L1**, **L2**, **L3**, **L4**. S/Rh = 1500, L/Rh = 20, substrate **33S** = 12 mmol (1.5 mmol), toluene = 6.5 mL, T = 80°C, p = 20 bar (CO/H₂ = 1:1).

Obviously, the latter ones are not suitable for this kind of reaction. The reason might be that the imidazole substrate **33S** competes with the ligand for the vacant site of the Rh-centre. The excellent activity of the Rh-system based on ligand **L4** is of special interest as these ligands can be used enantiomerically pure, paving the way to synthesising exclusively desired stereoisomers. For further investigation of different parameters on the reaction, however, ligand **L1** was mainly applied, as it shows very good activity and the *ee* of the reaction is yet not the main concern. Unfortunately, it was observed that the terminal aldehyde did not react further to the corresponding bicyclic compounds **33R** under these conditions.

Therefore, the impact of the temperature was investigated. The temperature was elevated from 80°C to 120°C. Immediately, a change in the product composition became

obvious (entries 5 and 9 in tab 6.1). Under these conditions the cyclic compound **33R** becomes the major product (90%), whereas only 8% of the aldehyde **33A** is present. The temperature increase is noticeably crucial for the formation of the bicyclic alcohol **33R**. Interestingly, H₂O elimination from the alcohol cannot be observed, although it has been reported for similar compounds.^[21-23] Neither NMR spectroscopy nor mass spectrometry gave evidence for the presence of **33DB**.

Table 6.1: Hydroformylation of **33S**^a

Entry	Solvent	Time / h	Ligand	Temp / °C	Conv.	A	R	DB
1	THF	45	L1	120	99	5	94	n.d.
2	Me-THF	45	L1	120	78	5	73	n.d.
3	Me-THF ^b	45	L1	120	71	5	66	n.d.
4	THF ^c	72	L1	120	0	0	0	0
5	Toluene	72	L1	80	95	92	traces	n.d.
6	Toluene	72	L2	80	n.d.	n.d.	n.d.	n.d.
7	Toluene	72	L3	80	23	22	n.d.	n.d.
8	Toluene	72	L4	80	97	95	traces	n.d.
9	Toluene ^b	45	L1	120	98	8	90	n.d.
10	Toluene ^{b,d}	72	L5	80	8	8	n.d.	n.d.

(20 % *ee*)

a) All data concerning conversion and products are given in %. Conditions: S/Rh = 1500, Rh/L = 20, 12 mmol (1.5 mL) imidazole substrate **33S**, 6.5 mL solvent, preformation time = 2 h (60°C). b) no preformation, c) internal alkene **34S**, d) Rh/L = 4

Subsequently, at 120°C the influence of the solvent was evaluated. Solvents, such as DCM or chloroform, were excluded as they react with the substrate at elevated temperatures by forming organic chloride salts. Comparing toluene with THF revealed that there is only a minor difference in conversion and product composition (entries 1 and 9). Slightly less aldehyde **33A** is converted to the corresponding ring compound

33R. Comparing THF to Me-THF¹ showed a significant difference in yield (entries 1 and 2). The reaction is considerably slower in Me-THF. This effect might be attributed to the different polarity of the solvents. Performing the reaction with and without preformation time shows a small difference in conversion and product distribution. In case of the experiment with preformation time the conversion is about 7% higher after 45 h (entries 2 and 3). One other question needed to be answered: Is it possible to form the branched aldehyde? So far formation of internal aldehydes is not detected for the terminal alkene **33S**. For that reason the hydroformylation was performed with the internal alkene **34S** as substrate (entry 4). The outcome shows that the internal alkene is not reactive. At least no detectable amounts of any product are formed.

One catalytic experiment was performed to see whether it is possible to synthesise the enantiomerically pure aldehyde **33A**, by means of applying chiral bidentate ligands, such as (*R,R*)-Ph-BPE **L5** (Figure 6.5). However, the system Rh/**L5** shows hardly any activity. After 72 h reaction time merely 8% of the substrate is consumed and converted to the aldehyde with an *ee* of 20% (entry 10). The bulky bidentate ligand **L5** is obviously not suitable for this kind of substrate. The application of enantiomerically pure **L4** or ligands based on diphosphites are probably the better choice for future investigations.

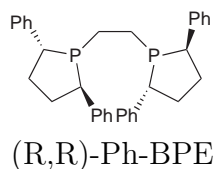


Figure 6.5: Bidentate phosphine ligand (*R,R*)-Ph-BPE **L5**

To get more insight into the course of the reaction, the product distribution in time was monitored. Samples were taken during the reaction and analysed by means of GC analysis. The corresponding distribution of species plot is depicted in figure 6.6 on the next page for the systems Rh/**L1** and Rh/**L4**.

In both cases the alkene substrate **33S** is consumed rapidly. The TOFs for Rh/**L1** and Rh/**L4** are found to be 460 h⁻¹ and 700 h⁻¹, respectively (measured at 20% conversion) and the hydroformylation rates with the phosphabarrelene ligand **L4** are thus

¹2-methyltetrahydrofurane

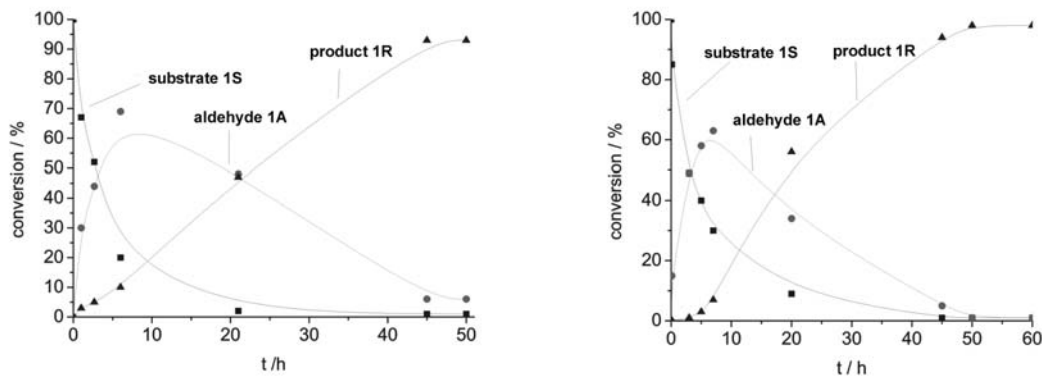


Figure 6.6: Distribution-of-species plot for the tandem hydroformylation/cyclisation sequence of substrate **33S** with ligands **L4** (left) and **L1** (right). S/Rh/L = 1500:1:20, 12mmol (1.5 mL), 6.5 mL THF, T = 120°C, p = 20 bar (CO/H₂ = 1:1).

almost comparable to the system using triphenylphosphine **L1**. The maximum aldehyde concentration **33A** is reached with Rh/**L1** at 6 hours and with Rh/**L4** at 7 hours. After 45 h the product composition is almost identical in both reaction mixtures.

To prove that the intramolecular cyclisation is not catalysed by the Rh-catalyst, the intermediate aldehyde **33A** was subject to a filtration over silica to remove the catalyst and subsequently, it was dissolved in toluene. The dissolved aldehyde **33A** was stirred for 170 h at 120°C to be converted to the bicyclic imidazole **33R** (Figure 6.7 on the following page). About 90% of the aldehyde **33A** were converted to the ring product **33R**. Interestingly, the two compounds are at equilibrium. Otherwise one would expect a reaction of zero order. This is clearly not the case. Also it is obvious that the cyclisation is slower than under hydroformylation conditions. The reason can be the different composition of the reaction mixture as more substances are present under hydroformylation conditions.

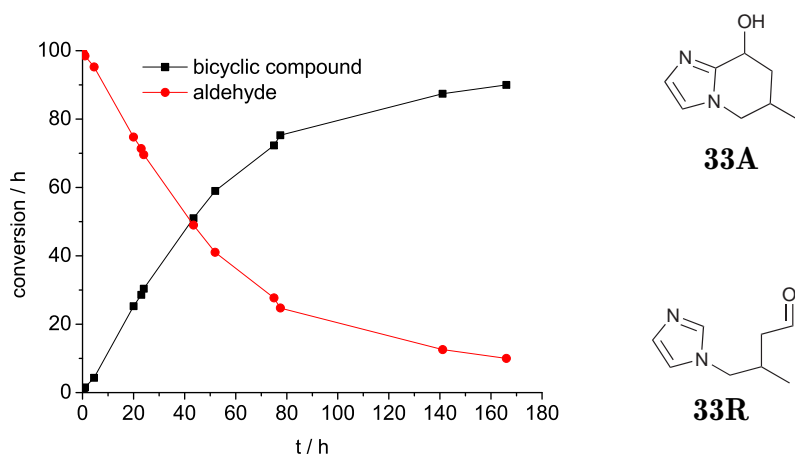


Figure 6.7: Conversion of aldehyde **33A** to **33R** in toluene.
Conditions: 12 mmol substrate **33A**, 120°C, 6.5 mL toluene

Structural analysis

The bicyclic imidazole **33R** was received as a colourless solid, after removal of all solvents and recrystallisation from hot THF or toluene. As this tandem reaction generates two stereogenic carbon atoms at C6 and C8, two pairs of enantiomers should be present in the products. The left graph in figure 6.8 shows the HPLC chromatogram for compound **33R**. A ratio of 1:2:2:1 of the signal intensity can be found, hence the ratio of the two diastereomers is 1:2. By means of chiral HPLC the four compounds were separated, collected and identified. In the right graph the four chromatograms of each of the four different stereoisomers are depicted. Suitable amounts for analysis were obtained for each of the four stereoisomers.

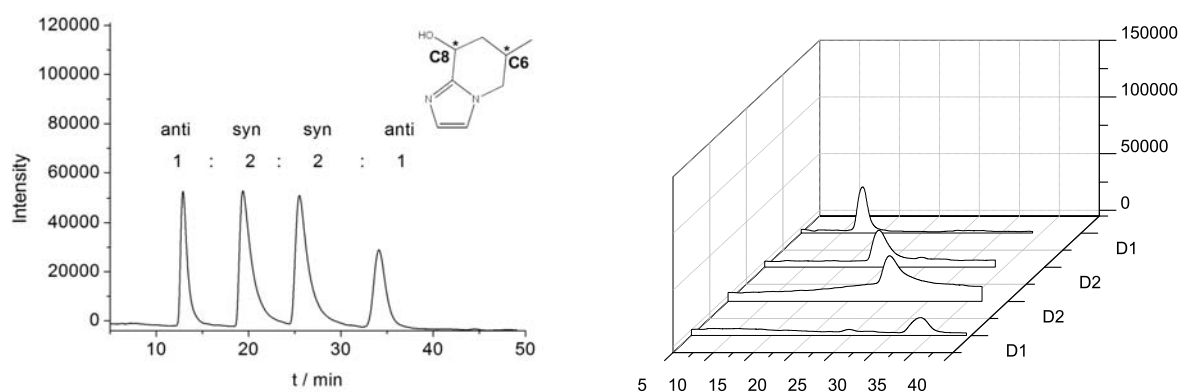


Figure 6.8: HPLC chromatograms of the imidazole alcohol **33R** on a chiral stationary phase (Chiralcel OD-H), using *n*-hexane/isopropanol (95:5) as eluent at room temperature. $\lambda = 200$ nm

The four compounds of **33R** were fully characterised by ^1H and ^{13}C NMR spectroscopy as well as by elemental analysis. Assuming that the methyl group is preferably located in the equatorial position, the four possible products are depicted in figure 6.9 on the following page along with the corresponding molecular models. The ^1H NMR spectra of the first and last fraction as well as the spectra of fraction two and three are identical. Consequently, these pairs are the two diastereomers. The ^1H NMR spectra show two sets of protons, which can be assigned to the proton at the C8 po-

sition.^[26] Characteristic resonances and coupling with the two adjacent protons at C7 are observed at $\delta = 4.90$ ppm (dd, $^3J_{\text{H-H}} = 6.6$ Hz) and $\delta = 5.02$ ppm (t, $^3J_{\text{H-H}} = 3.3$ Hz). These signals can be explained when looking at the Newman-projections along the C7-C8 axis of the compound (Scheme 6.9). In case compound **33R** adopts a *syn* configuration a doublet of doublets should be expected for the proton in C8 position. The *anti* configuration, hence, should result in a pseudo-triplet. In the ^1H NMR spectrum of the racemic mixture the integrals of the protons at C8 have a ratio of 1:2.

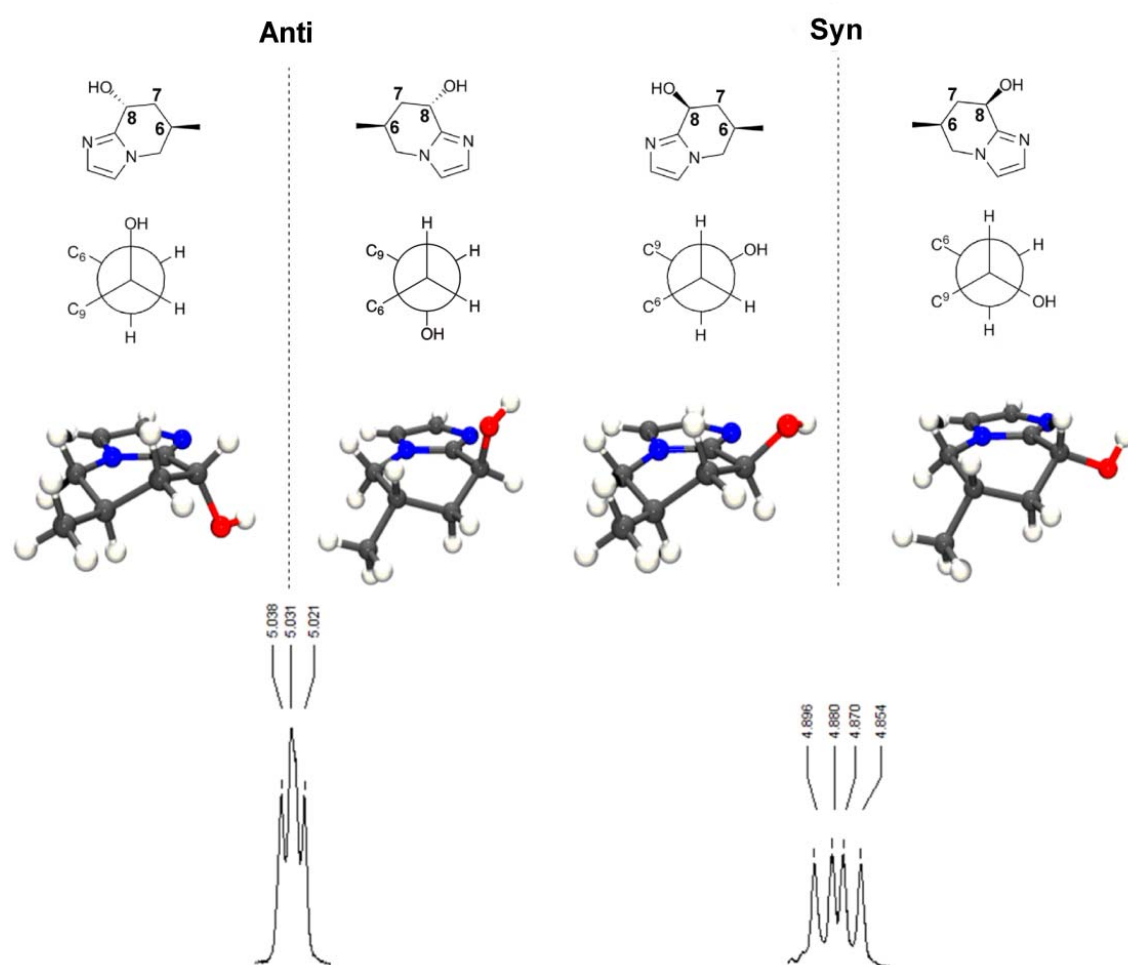


Figure 6.9: From top to bottom: Stereoisomers of **33R**, Newman-projections, 3D-models, ^1H NMR signal of the proton at C8 coupling with the two adjacent diastereotopic protons of methylene spacer at C7

This reflects the ratio found by means of HPLC analysis. Therefore, the fraction one and four can be assigned to the minor products with *anti* configuration and the fractions two and three belong to the major products with *syn* configuration. The 3D models in figure 6.9 on the preceding page for the four stereoisomers further offer an explanation for the ratio of 1:2. In case of the *anti*-diastereomers the OH-group is located in the unfavourable axial position. Therefore, adopting *syn* configuration, with the OH-group situated in the equatorial position is preferred. From the racemic mixture a crystal suitable for X-ray analysis was obtained by crystallisation from hot THF (Figure 6.10 on the next page). Due to the centrosymmetry of the space group the crystal structure is racemic, but on individual crystallographic sites a mixture of the *syn*-products is found $\mathbf{33R}(S,R):\mathbf{33R}(R,S) = 0.756(4):0.244(4)$ and consequently on an inverted site of $0.244(4):0.756(4)$. The molecular structure depicted in figure 6.10 on the following page is the major diastereomer $\mathbf{33R}(S,R)$. The figure shows hydrogen bonding between the oxygen and the nitrogen, which might explain the stability of the cyclic compound. One could expect H₂O elimination from the ring, as has been observed for related compounds.^[21-23] In this case, however, this does not occur. Of further interest is the arrangement of the molecules in the crystal. They are stacked in an alternating series.

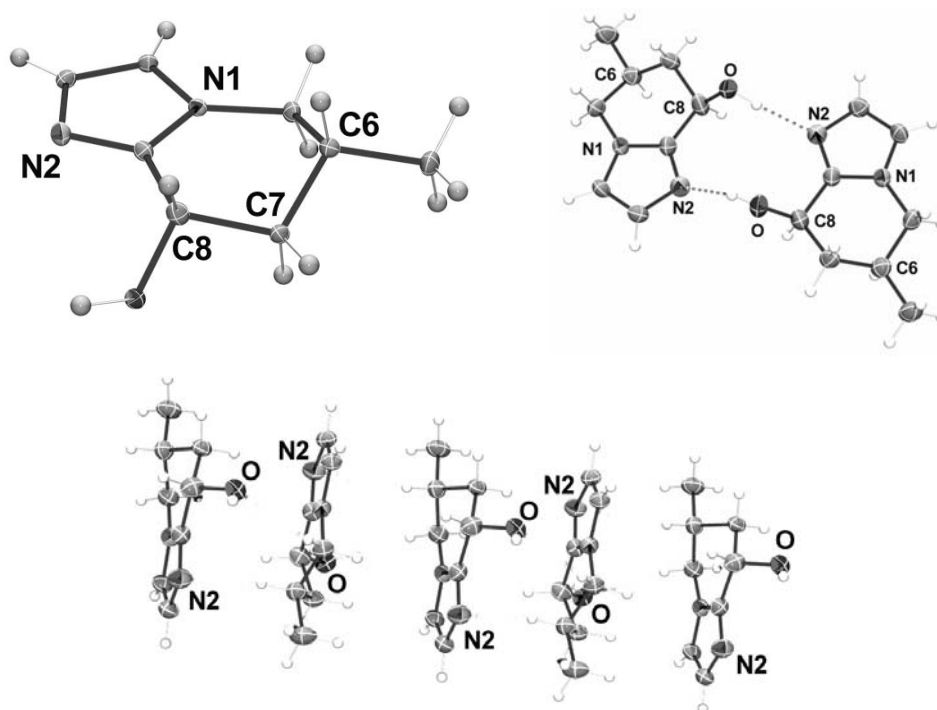
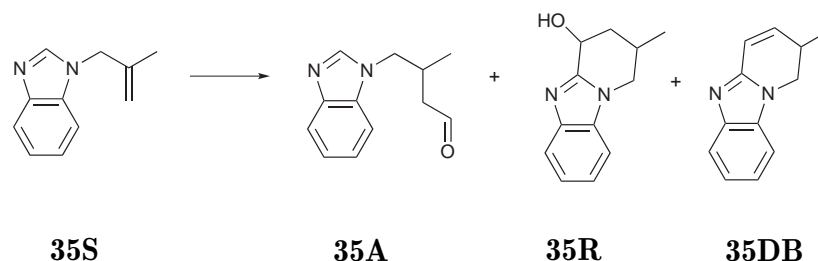


Figure 6.10: ORTEP representations. Above: Major stereoisomer **33R**(*R,S*) and the hydrogen bonding between two molecules of **33R**(*R,S*) in the same layer (along the X-axis). Below: Arrangement in the crystal including hydrogen bonding along the Y-axis. Displacement ellipsoids are drawn at 50% probability level.

6.4 Benzimidazole substrate

To investigate the influence of steric properties, the benzimidazole based substrate **35S** was applied in the Rh-catalysed hydroformylation reaction (Table 6.2 on the next page).

The two best performing systems from preceding experiments Rh/**L1** and Rh/**L4** were applied. The results show that both ligands are equally suitable to obtain the alcohol **35R**. Only small amounts of the aldehyde **35A** are still present after 45 h and no other products are formed. Of greater interest is the course of the reaction

Table 6.2: Tandem reaction of **35S**^a

Entry	Solvent	Time / h	Ligand	Temp / °C	Conv.	A	HF	DB
1	THF	45	L1	120	99	5	94	n.d.
2	THF	45	L4	120	99	4	95	n.d.

a) All data concerning conversion and products are in %. Conditions: S/Rh = 1500, Rh/L = 20, 12 mmol (1.5 mL) substrate **35S**, 6.5 mL solvent, $p = 20$ bar (CO/H₂ = 1:1)

with the benzimidazole substrate **35S** compared to the imidazole substrate **33S**. In figure 6.11 on the following page the product distribution of each of the two compounds is depicted. It is obvious that the hydroformylation reaction is somewhat slower for **35S**. The TOF at 20% conversion for this substrate is only 600 h⁻¹, whereas for substrate **33S** it is 700 h⁻¹ (a difference of 15%). The disparity becomes even more pronounced at a conversion of 60%. Here the TOFs of the two substrate differ significantly (225 h⁻¹ for **33S** and 150 h⁻¹ for **35S**). There is a variation of 34%. Furthermore, it can be seen that for **35S** the formation of the alcohol **35R** is slower and hence the consumption of the intermediate **35A**. After 45 h reaction time, though, both substrates are almost completely converted. The product **35R** was collected as a white solid after recrystallisation from hot THF or toluene. The crystals became subject to a HPLC-analysis (Scheme 6.12 on the next page). It was possible to separate the four stereoisomeres and from the integrals of the signals a diastereomeric ratio of 1:3 can be concluded. The higher diastereomeric ratio compared to **35R** is attributed to the bulkiness of the benzimidazole moiety.

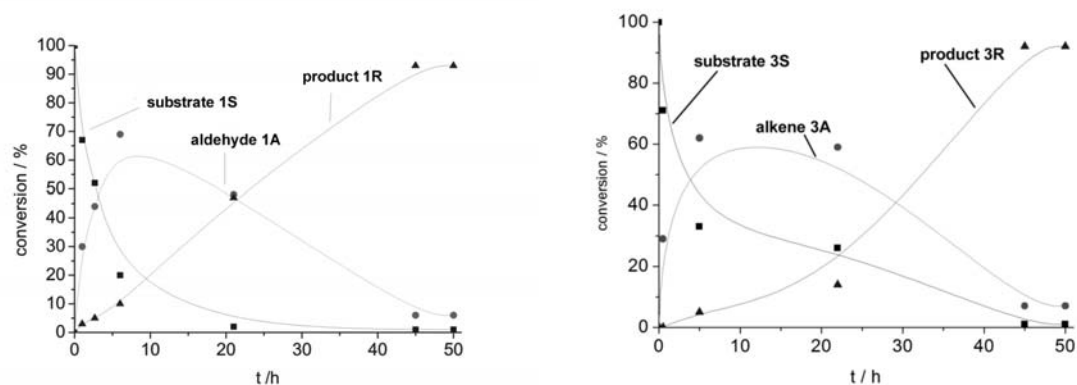


Figure 6.11: Distribution-of-species plot for the tandem hydroformylation/cyclization sequence of substrates **33S** and **35S** with ligand **L4**. S/Rh/L = 1500:1:20, 12mmol (1.5 mL), 6.5 mL THF, T = 120°C, p = 20 bar (CO/H₂ = 1:1).

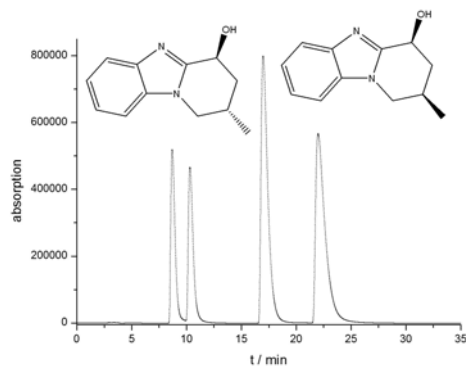


Figure 6.12: HPLC chromatogram of the benzimidazole alcohol **35R** on a chiral stationary phase (Chiralcel OJ-H), using *n*-hexane/isopropanol (95:5) as eluent, $\lambda = 254$

Also in this case the characteristic resonances of the proton adjacent to the OH-group can be detected in the ^1H NMR spectrum.^[26] From the NMR-spectra of the diastereomeric mixture the same ratio is received. Single crystals suitable for X-ray analysis were obtained by crystallisation from hot THF or toluene. The molecular structure of the *syn*-stereoisomer of **35R** in the crystal is depicted in figure 6.13.

As in the crystal of **33R** hydrogen bonding between the nitrogen N2 and the oxygen of two adjacent molecules can be noticed. Furthermore, the molecules align *via* stacking. In this case also an alternating order can be observed. This time, however, also π -stacking between the imidazole moieties is present.

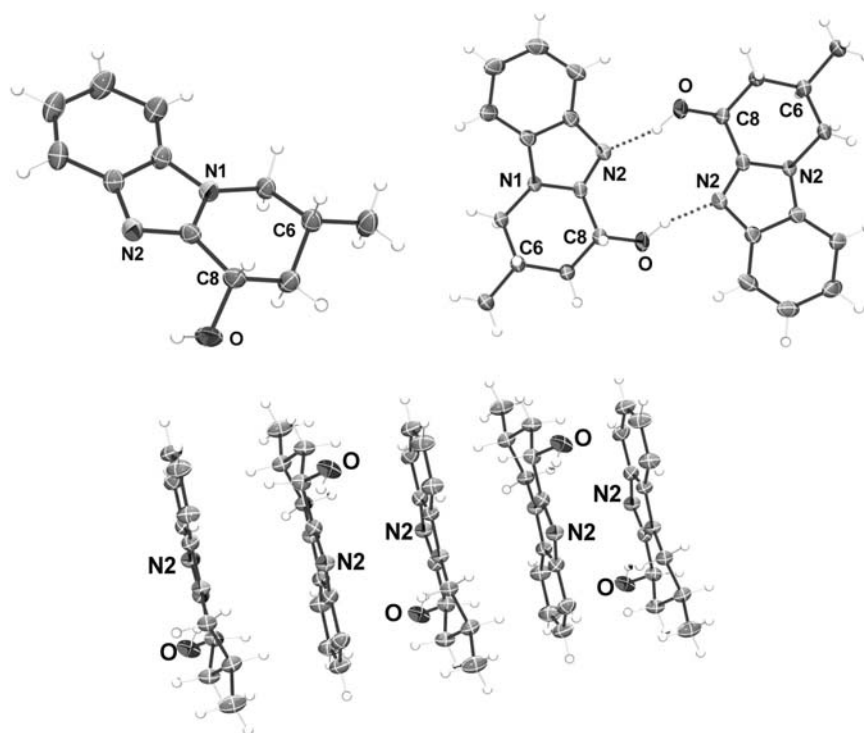
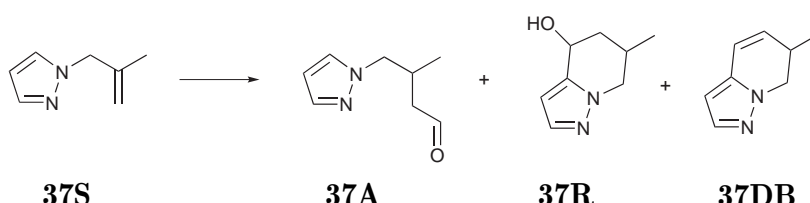


Figure 6.13: ORTEP representations. Above: Stereoisomer **35R**(*R,S*) and the hydrogen bonding between two molecules of **35R**(*R,S*). Below: Arrangement in the crystal. Displacement ellipsoids are drawn at 50% probability level. Distance between the nitrogen atoms of two adjacent molecules (N1,N1A or N2,N2A): 3.765 Å. The angle between N1,N2,N1A is 89.50° and the angle between N2,N1,N2A is 90.50 Å

Pyrazole substrate

The substrate **37S** became subject to the hydroformylation/cyclisation reaction using the catalyst systems Rh/**L1** and Rh/**L4** (Table 6.3). Strikely, in both systems the reaction stops at the aldehyde **37A**, even at the reaction temperature of 120°C. Obviously, the reactivity of the pyrazole moiety in the aldehyde **37A** is considerably less compared to the imidazole aldehyde **33S**. However, both catalyst systems are equally fast. Full conversion is reached with in 45 h. To enforce the cyclisation step the Lewis-acid LiTf₂N was added to the reaction mixture in a third catalytic experiment. But also here no evidence for the cyclisation reaction was found. However, the Li-ions apparently catalyse the aldole reaction of the aldehydes. Only 22% of aldehyde were found, despite a conversion of 85%. GC-MS analysis reveal that the new products formed have masses characteristic for aldol products. Obviously, the pyrazole aldehyde **37A** is less reactive than the corresponding imidazole compounds **33A** and **35A**. A reasonable explanation is the decreased nucleophilicity of the pyrazole moiety in comparison to the imidazole moiety. A comparable tendency applies for the basic strength of the heterocyclic compounds: pyridine > imidazole > pyrazole. The more electronegative atoms are present in the ring or linked to each other, the less reactive adjacent carbons become.

Table 6.3: Tandem reaction of **37S**^a



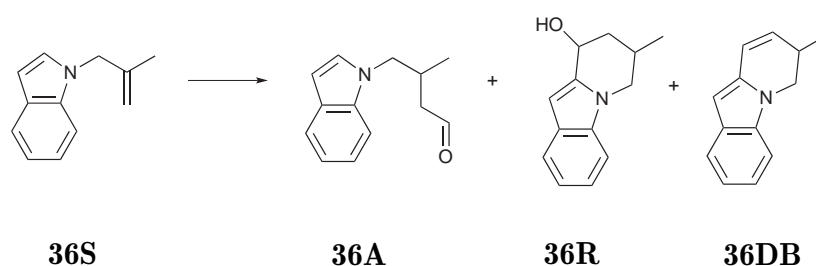
The reaction scheme shows the conversion of pyrazole substrate **37S** (1-(2-methylallyl)pyrazole) to aldehyde **37A** (1-(2-methyl-3-oxopropyl)pyrazole). From **37A**, two cyclized products are formed: **37R** (2-(1-methyl-1H-pyrazol-5-yl)ethanol) and **37DB** (2-(1-methyl-1H-pyrazol-5-yl)ethane).

Entry	Solvent	Time	Ligand	Temp	Conv.	A	R	DB
1	THF	45	L4	120	99	99	n.d.	n.d.
2	THF	45	L1	120	94	94	n.d.	n.d.
3	THF ^a	45	L1	120	85	22	n.d.	n.d.

Conditions: S/Rh = 1500, Rh/L = 20, 12 mmol (1.5 mL) pyrazole substrate, 6.5 mL solvent, preformation time = 2 h (60°C). a) addition of 1.2 mmol Lewis acid LiTf₂N

Indol substrate

The Rh-catalysed hydroformylation reaction with the indol substrate **36S** stops at the aldehyde **36A** (Table 6.4). The system Rh/**L1** converts **36S** to the corresponding aldehyde **36A** almost completely. However, no other products can be found in the reaction mixture by means of ¹H NMR spectroscopy and GC/MS analysis (Table 6.4).

Table 6.4: Tandem reaction of **36S**^a

Entry	Solvent	Time	Ligand	Temp	Conv.	A	R	DB
1	THF	45	PPh ₃	120	99	99	n.d.	n.d.

Conditions: S/Rh = 1500, L/Rh = 20, 12 mmol (1.5 mL) indol substrate **36S**, 6.5 mL solvent, preformation time = 2 h (60°C)

6.5 Conclusions

A new and simple route to cyclic imidazole compounds by a tandem hydroformylation/cyclisation sequence has been developed. In just two steps chiral imidazole derivatives can be synthesised. In case of the imidazole substrate it was possible to steer the reaction by choice of the temperature. At a lower temperature the reaction stops after the Rh-catalysed hydroformylation, whereas higher temperatures promote the cyclisation of the aldehyde to the corresponding ring. Interestingly, this cyclisation step does not occur, even at elevated temperatures, for the pyrazole or indole substrates tested. Furthermore, it became obvious that Rh/ π -acceptor ligand systems are not suitable for the hydroformylation of these substrates. Ligands with pronounced σ -donor properties, such as phosphabarrelenes or PPh_3 are required to get good yields. Especially the imidazole- and benzimidazole-based compounds are possible precursors for other compounds, suitable building blocks for ionic liquids, organocatalysts, ligands, and possibly biologically active substances. This scope is currently under investigation (Figure 6.14).

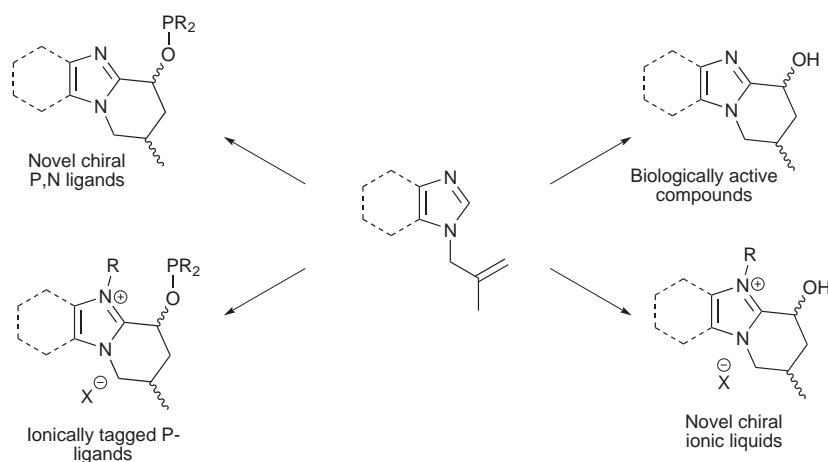


Figure 6.14: Possible application of the imidazole-base compounds

6.6 Experimental

Reactions in 75-mL home-made stainless steel autoclaves

In a typical experiment, the autoclave equipped with a sampling unit was charged with a solution of 2.1 mg (8 μmol) $[\text{Rh}(\text{acac})(\text{CO})_2]$ and 20 eq. ligand in 5 mL of toluene. A dropping funnel connected to the reaction chamber of the autoclave was charged with a solution of 12 mmol substrate in toluene (total volume 3 mL). The autoclave was pressurised with 20 bar CO/H_2 (1:2) and heated to preformation temperature and stirred for 2 h. Subsequently, the substrate was added to the catalyst solution and the reaction was started by elevating the temperature. After completion the reactor was cooled and the substrate collected.

Reactions in the Amtec SPR 16

Catalysis experiments under constant pressure were performed in the parallel autoclave system AMTEC SPR16, equipped with pressure sensors and a mass-flow controller suitable for monitoring and recording gas uptakes throughout the reactions. The stainless steel autoclaves (12 mL) of the AMTEC SPR16 were flushed automatically with argon 6 times to remove oxygen traces (3 times at $T = 90^\circ\text{C}$, 3 times at room temperature). In the meanwhile, 2.1 mg of $\text{Rh}(\text{acac})(\text{CO})_2$ (8.0 μmol) and 20 equivalents of the monodentate ligands were weighted and put in a Schlenk tube. Both were dissolved in 5 mL of dried and degassed toluene. The reactors were charged with a solution of this precatalyst (5 mL) under argon. The atmosphere was further exchanged with a 1:1 mixture of CO/H_2 (gas exchange cycle 1) and the reactors were heated to the desired preformation temperature and pressurized with CO/H_2 to the desired preformation pressure. The preformation of the catalyst under the applied conditions was performed for 2 hours. Subsequently, the substrate dissolved in toluene (total volume 3 mL) was injected and the desired temperature as well as the final pressure was adjusted and kept constant throughout the experiment. The gas uptake of CO/H_2 was monitored and recorded automatically. At the end of the catalysis experiments, the reactors were cooled to room temperature and the autoclave contents were analysed by means of GC, chiral GC and HPLC.

GC Analysis

GC:	Shimadzu GC 17A
Column:	Ultra 2 (crosslinked 5% Ph Me Siloxane), 25m, inner diameter 0.20 mm film thickness 0.33 μm
Carrier gas:	Helium 102 kPa (total flow 53 mL/min)
GC:	Shimadzu GC-2010
Column:	DB1(30m, inner diameter 0.32 mm)
Carrier gas:	Helium 58.2 kPa
GC:	Shimadzu GC-2010
Column:	Lipodex E (25m, inner diameter: 0.25 mm)
Carrier gas:	Hydrogen 118 kPa

HPLC Analysis

Substrate:	33R
Pump:	Shimadzu LC-20AD
Eluents:	n-hexane / 2-propanol mixture (95:5 v/v)
Column:	Chiracel OD-H
UV-VIS Detector	Shimadzu SPD-20A
Wavelength:	200 nm
Temperature:	20°C
Substrate:	35R
Pump:	Shimadzu LC-20AD
Eluents:	n-hexane / 2-propanol mixture (98:2 v/v)
Column:	Chiracel OJ-H
UV-VIS Detector	Shimadzu SPD-20A
Wavelength:	254 nm
Temperature:	20°C

General procedure for the substrates

To dimethyl sulfoxide (120 mL) was added 16.3 g (290 mmol) KOH. The mixture was stirred for 5 min and 72.50 mmol substrate was dissolved in it. This solution was stirred for another 45 min. Subsequently, it was cooled in an ice-bath and 4.7 mL (48.30 mmol) 3-chloro-2-methylpropene was added dropwise. After 5 hours of stirring, water (120 mL) was poured into the reaction mixture. The aqueous layer was extracted with ether (3 times 50 mL). The organic layers were combined, dried with Na₂SO₄ and concentrated.

1-(2-Methylallyl)-1H-imidazole (33S)

¹H NMR (CDCl₃) δ (ppm): 7.44 (s, 1H), 7.05 (s, 1H), 6.86 (s, 1H), 4.94 (s, 1H), 4.78 (s, 1H), 4.42 (s, 2H), 1.68 (s, 3H). ¹³C NMR: 140.56, 137.49, 129.47, 119.21, 113.87, 53.04, 19.62. MS:(m/z) 121.08 [M]⁺. Yield: 60% (4.41 g).

N-(β-Methylallyl)benzimidazole (35S)

¹H NMR (CDCl₃) δ (ppm): 7.84 (dd, 1H, *J*=8.8 Hz, *J*=2.4 Hz), 7.78 (dd, 1H, *J*=6.0 Hz, *J*=2.8 Hz), 7.33 (dd, 1H, *J*=5.6 Hz, *J*=2.4 Hz), 7.35 (m, 2H), 4.98 (d, 1H, *J*=6.8 Hz), 4.80 (d, 1H, *J*=6.8 Hz), 4.63 (s, 2H), 1.68 (s, 1H). ¹³C NMR: 143.2, 139.3, 122.6, 121.8, 119.9, 116.2, 113.3, 109.9, 50.5, 19.4. MS:(m/z) 171.10 [M]⁺. Yield 57 % (11.36 g)

N-(β-Methylallyl)pyrazole (37S)

¹H NMR (CDCl₃) δ (ppm): 7.50 (d, 1H, *J*=2.2 Hz), 7.38 (d, 1H, *J*=2.2 Hz), 6.26 (t, 1H, *J*=2.2 Hz), 4.93 (dd, 1H, *J*=1.6 Hz, *J*=0.8 Hz), 4.78 (dd, 1H, *J*=1.6 Hz, *J*=0.8 Hz), 4.66 (s, 2H), 1.65 (s, 3H), CNMR: 140.8, 138.6, 128.9, 112.9, 105.2, 57.4, 19. MS:(m/z) 121.08 [M]⁺. Yield 65 % (4.84 g).

N-(β-Methylallyl)indole (36S)

¹H NMR (CDCl₃) δ (ppm): 7.71 (d, 1H, *J*=7.6 Hz), 7.38 (d, 1H, *J*=7.6 Hz), 7.26 (t, 1H, *J*=7.6 Hz), 7.17 (t, 1H, *J*=7.6 Hz), 7.13 (d, 1H, *J*=3.2 Hz), 6.58 (d, 1H, *J*=3.2 Hz), 4.96 (d, 1H, *J*=1.2 Hz), 4.78 (d, 1H, *J*=1.2 Hz), 4.68 (s, 2H), 1.73 (s, 3H). ¹³C NMR:

141.6, 129.1, 121.3, 199.9, 119.8, 112.8, 110.2, 101.7, 52.6, 20.1. MS:(m/z) 170.23 [M]⁺. Yield: 59 % (9.75 g).

Procedure for 1-(2-methylprop-1-enyl)-1H-imidazole (34S)

To dimethyl sulfoxide (120 mL) was added 16.3 g (290 mmol) KOH. The mixture was stirred for 5 min and 72.50 mmol substrate was dissolved in it. This solution was stirred for another 45 min. Subsequently, it was heated to 60°C and 4.7 mL (48.30 mmol) 3-chloro-2-methylpropene was added dropwise. After 5 hours of stirring, water (120 mL) was poured into the reaction mixture. The aqueous layer was extracted with ether (3 times 50 mL). The organic layers were combined, dried with Na₂SO₄ and concentrated.

¹H NMR (CDCl₃) δ (ppm): 7.51 (s, 1H), 7.03 (s, 1H), 6.83 (s, 1H), 4.58 (s, 1H), 1.80 (s, 3H), 1.76 (s, 3H). ¹³C NMR: 136.98, 133.06, 128.56, 119.25, 118.44, 22.18, 17.42. MS:(m/z) 121.08 [M]⁺. Yield: 70% (5.15 g).

syn-6-Methyl-5,6,7,8-tetrahydroimidazo[1,2-a]pyridin-8-ol (33R)

¹H NMR (CDCl₃) δ (ppm): 7.04 (d, 1H, *J*=1.15 Hz), 6.76 (s, 1H, *J*=1.10 Hz), 4.89 - 4.85 (dd, 1H, *J*=10.50 Hz, *J*=6.45 Hz), 3.98 - 3.94 (ddd, 1H, *J*=11.98 Hz, *J*=5.11 Hz, *J*=1.34 Hz), 3.53 (t, 1H, *J*=11.56 Hz), 2.36 - 2.31 (m, 1H), 2.24 - 2.12 (m, 1H), 1.66 - 1.57 (dt, 1H, *J*=12.62 Hz, *J*=10.58 Hz), 1.15 - 1.14 (d, 3H, *J*=6.67 Hz). ¹³C NMR: 148.43, 128.30, 117.77, 63.63, 51.43, 38.70, 28.22, 18.67. Elemental Analysis: calculated for C₈H₁₂N₂O: %C 63.13, %H 7.95, %N 18.41, found: %C 62.99, %H 7.82, %N 18.44. MS: (m/z) 151.09 [M]⁺.

anti-6-Methyl-5,6,7,8-tetrahydroimidazo[1,2-a]pyridin-8-ol (33R)

¹H NMR (CDCl₃) δ (ppm): 6.99 (s, 1H), 6.76 (s, 1H), 5.05 - 5.04 (t, 1H, *J*=3.27 Hz), 4.07 - 4.03 (ddd, 1H, *J*=12.15 Hz, *J*=5.07 Hz, *J*=0.79 Hz), 3.46 - 3.40 (t, 1H, *J*=11.67 Hz), 2.72 - 2.59 (m, 1H), 2.20 - 2.16 (m, 1H), 1.77 - 1.69 (ddd, 1H, *J*=13.87 Hz, *J*=12.30 Hz, *J*=4.08 Hz), 1.13 - 1.11 (d, 3H, *J*=6.71 Hz). ¹³C NMR: 146.86, 128.07, 118.04,

61.04, 51.61, 37.94, 24.36, 18.44. Elemental Analysis: calculated for C₈H₁₂N₂O: %C 63.13, %H 7.95, %N 18.41, found: %C 62.99, %H 7.82, %N 18.44. **MS:** (m/z) 151.09 [M]⁺.

anti-(*S,S*)-2-Methyl-1,2,3,4-tetrahydrobenzo[4,5]imidazo[1,2- α]pyridin-4-ol (35R)

¹H NMR (CDCl₃) δ (ppm): 7.77 - 7.75 (m, 1H), 7.35 - 7.25 (m, 3H), 6.23 (b, 1H), 5.25 (t, 1H, *J*=3.46 Hz), 4.29 - 4.24 (ddd, 1H, *J*=11.85 Hz, *J*=5.23 Hz, *J*=0.77 Hz), 3.55 - 3.49 (t, 1H, *J*=11.30 Hz), 2.82 - 2.78 (b, 1H), 2.34 - 2.30 (m, 1H), 1.90 - 1.82 (ddd, 1H, *J*=13.99 Hz, *J*=12.02 Hz, *J*=4.09 Hz), 1.25 - 1.23 (d, 3H, *J*=6.74 Hz). ¹³C NMR: 153.52, 142.25, 133.77, 122.44, 122.37, 119.19, 109.38, 61.14, 49.20, 37.58, 23.94, 18.71. **MS:**(m/z) 201.11 [M]⁺.

syn-(*S,R*)-2-Methyl-1,2,3,4-tetrahydrobenzo[4,5]imidazo[1,2- α]pyridin-4-ol (35R)

¹H NMR (CDCl₃) δ (ppm): 7.77 - 7.75 (m, 1H), 7.35 - 7.25 (m, 3H), 5.98 (b, 1H), 5.08 (dd, 1H, *J*=10.95 Hz, *J*=6.26 Hz), 4.21 - 4.16 (ddd, 1H, *J*=11.43 Hz, *J*=5.17 Hz, *J*=1.07 Hz), 3.56 - 3.50 (t, 1H, *J*=11.44 Hz), 2.51 - 2.46 (m, 1H), 2.36 - 2.29 (m, 1H), 1.81 - 1.72 (dt, 1H, *J*=12.62 Hz, *J*=11.15 Hz), 1.27 - 1.25 (d, 3H, *J*=6.66 Hz). ¹³C NMR: 155.22, 142.64, 133.93, 122.44, 122.37, 119.19, 109.38, 63.98, 49.07, 38.65, 28.01, 18.89. **MS:**(m/z) 201.11 [M]⁺.

4-(1H-Imidazol-1-yl)-3-methylbutanal (33A)

¹H NMR (CDCl₃) δ (ppm): 9.64 (s, 1H), 7.37 (s, 1H), 6.98 (d, 1H, *J*=7.2 Hz), 6.83 (d, 1H, *J*=7.2 Hz), 3.84 (dd, 1H, *J*=13.8 Hz, *J*=6.8 Hz), 3.76 (dd, 1H, *J*=13.8 Hz, *J*=7.2 Hz), 2.43 (m, 1H), 2.33 (ddd, 1H, *J*=17.2 Hz, *J*=5.6 Hz, *J*=1.2 Hz), 2.26 (ddd, 1H, *J*=17.2 Hz, *J*=7.6 Hz, *J*=1.6 Hz), 0.91 (d, 3H, *J*=6.4 Hz). ¹³C NMR: 200.4, 137.4, 129.6, 119.2, 52.0, 47.5, 29.7, 17.6. **MS:**(m/z) 151.08 [M]⁺.

3-Methyl-4-(1H-pyrazol-1-yl)butanal (37A)

¹H NMR (CDCl₃) δ (ppm): 9.66 (s, 1H), 7.51 (d, 1H, *J*=17.2 Hz), 7.37 (d, 1H, *J*=8.0 Hz), 6.25 (dd, 1H, *J*=11.8 Hz, *J*=8.0 Hz), 4.06 (m, 2H), 2.68 (m, 1H), 2.44 (m, 1H), 2.27 (m, 1H), 0.99 (d, 3H, *J*=6.8 Hz). ¹³C NMR: 201.1, 139.5, 129.7, 105.5, 57.1, 47.9, 29.8, 17.8. MS:(*m/z*) 151.08 [M]⁺.

4-(1H-Indol-1-yl)-3-methylbutanal (36A)

¹H NMR (CDCl₃) δ (ppm): 9.63 (t, 1H, *J*=1.6 Hz), 7.68 (dd, 1H, *J*=7.8 Hz, *J*=0.8 Hz), 7.41 (dd, 1H, *J*=8.0 Hz, *J*=1.0 Hz), 7.27 (td, 1H, *J*=7.8 Hz, *J*=1.2 Hz), 7.16 (td, 1H, *J*=7.8 Hz, *J*=1.2 Hz), 7.07 (d, 1H, *J*=3.2 Hz), 6.54 (dd, 1H, *J*=3.2 Hz, *J*=1.0 Hz), 4.05 (m, 2H), 2.70 (m, 1H), 2.34 (m, 2H), 1.01 (d, 3H, *J*=6.8 Hz). ¹³C NMR: 201.2, 136.2, 128.6, 128.3, 121.7, 121.1, 119.5, 109.6, 101.5, 51.8, 48.2, 29.4, 18.1. MS:(*m/z*) 200.12 [M]⁺.

Selected crystallographic data

Table 6.5: Selected crystallographic data of the cyclic compounds **33R** and **35R**

	33R	35R
formula	C ₈ H ₁₂ N ₂ O	C ₁₂ H ₁₄ N ₂ O
Crystal system	monoclinic	triclinic
Space group	C2/c	P-1
A (Å)	13.4857(5)	6.39757(16)
B (Å)	8.0251(6)	8.2853(2)
C (Å)	19.0553(9)	10.3507(3)
α (⁰)	90	82.022(1)
β (⁰)	129.266(2)	77.139(1)
γ (⁰)	90	79.627(1)
V(Å ³)	1596.62(16)	523.35(2)
Z	8	2
T (K)	150	150
F(000)	656.0	216
Reflections collected	1497	2400
R indices (all data)	R1 = 0.0583 wR2 = 0.1497	0.0428 0.1177

X-ray crystal structure determinations X-ray intensities were measured on a Nonius KappaCCD diffractometer (graphite monochromator, $\lambda = 0.71073$ Å) at a temperature of 150(2) K. Intensity integration was performed with EvalCCD^[27] (**33R**) or Eval15^[28] (**35R**). The SADABS^[29] programme was used for absorption correction and scaling based on multiple measured reflections. The structures were solved with Direct Methods using the programme SHELXS-97^[30] and refined with SHELXL-97^[30] against F² of all reflections. Non hydrogen atoms were refined with anisotropic displacement parameters. Hydrogen atoms were introduced in calculated positions (**33R**) or located in difference Fourier maps (**35R**). The O-H hydrogen atom of **35R** was refined freely with isotropic displacement parameters; all other hydrogen atoms in **33R** and **35R** were refined with a riding model. Geometry calculations and checking for higher symmetry was performed with the PLATON programme.^[31]

Compound **33R**: C₈H₁₂N₂O, Fw = 152.20, colourless block, 0.33 x 0.18 x 0.12 mm³, monoclinic, C2/c (no. 15), a = 13.4857(5), b = 8.0251(6), c = 19.0553(8) Å, = 129.266(2)°, V = 1596.62(16) Å³, Z = 8, Dx = 1.266 g/cm³, = 0.09 mm⁻¹. 10235 Reflections were measured up to a resolution of (*sinθ/λ*)_{max} = 0.61 Å⁻¹. 0.88-0.99 Absorption correction range. 1487 Reflections were unique (R_{int} = 0.045), of which 1122 were observed [I > 2σ(I)]. The structure was refined as a mixture of two stereoisomers on the same crystallographic site with occupancies of 0.756(4):0.244(4). 139 Parameters were refined with 103 restraints (distance and angle restraints concerning the disorder and restraints to approximate isotropic behavior of the displacement parameters). R1/wR2 [I > 2σ(I)]: 0.0584 / 0.1379. R1/wR2 [all refl.]: 0.0812 / 0.1481. S = 1.158. Residual electron density between 0.23 and 0.24 e/Å³.

Compound **35R**: C₁₂H₁₄N₂O, Fw = 202.25, colourless plate, 0.42 x 0.24 x 0.12 mm³, triclinic, P1 (no. 2), a = 6.39757(16), b = 8.2853(2), c = 10.3507(3) Å, = 82.022(1), = 77.139(1), = 79.627(1)°, V = 523.35(2) Å³, Z = 2, Dx = 1.283 g/cm³, = 0.08 mm⁻¹. 9024 Reflections were measured up to a resolution of (*sinθ/λ*)_{max} = 0.65 Å⁻¹. 0.80-0.99 Absorption correction range. 2400 Reflections were unique (R_{int} = 0.029), of which 2022 were observed [I > 2σ(I)]. 141 Parameters were refined with no restraints. R1/wR2 [I > 2σ(I)]: 0.0428 / 0.1114. R1/wR2 [all refl.]: 0.0515 / 0.1177. S = 1.036. Residual electron density between 0.21 and 0.28 e/Å³.

Bibliography

- [1] K. Nicolaou, E. Sorensen, *Classics in Total Synthesis*, VCH, New York, **1996**.
- [2] K. Tatsuta, S. Miura, *Tetrahedron Lett.* **1995**, *36*, 6721–6724.
- [3] D. E. Williams, J. Davies, B. O. Patrick, H. Bottriell, T. Tarling, M. Roberge, R. J. Andersen, *Org. Lett.* **2008**, *10*, 3501–3504.
- [4] D. Chen, M. Schmitkamp, G. Francio, J. Klankermayer, W. Leitner, *Angew. Chem. Int. Ed.* **2008**, *47*, 7339–7341.
- [5] M. Schmitkamp, D. Chen, W. Leitner, J. Klankermayer, G. Francio, *Chem. Commun.* **2007**, 4012–4014.
- [6] P. Wasserscheid, W. Keim, *Angew. Chem.* **2000**, *112*, 3926–3945.
- [7] P. I. Dalko, L. Moisan, *Angew. Chem.* **2001**, *113*, 3840–3864.
- [8] Q. B. Liu, Y. G. Zhou, *Tetrahedron Lett.* **2007**, *48*, 2101–2104.
- [9] S. Kaiser, S. P. Smidt, A. Pfaltz, *Angew. Chem. Int. Ed.* **2006**, *45*, 5194 – 5197.
- [10] M. Dieguez, J. Mazuela, O. Pàmies, J. J. Verendel, P. G. Andersson, *J. Am. Chem. Soc.* **2008**, *130*, 7208.
- [11] P. Cheruku, J. S. Diesen, P. G. Andersson, *J. Am. Chem. Soc.* **2008**, *130*, 5595.
- [12] M. Engman, J. S. Diesen, A. Paptchikhine, P. G. Andersson, *J. Am. Chem. Soc.* **2007**, *129*, 4536.
- [13] Y.-L. Lin, J.-Y. Cheng, Y.-H. Chu, *Tetrahedron* **2007**, *63*, 10949–10957.
- [14] D. Basavaiah, P. D. Rao, R. S. Hyma, *Tetrahedron* **1996**, *52*, 8001–8062.
- [15] H.-C. Kan, M.-C. Tseng, Y.-H. Chu, *Tetrahedron* **2007**, *63*, 1644–1653.
- [16] A. S. Tsai, R. M. Wilson, H. Harada, R. G. Bergman, J. A. Ellman, *Chem. Commun.* **2009**, 3910–3912.
- [17] K. L. Tan, R. G. Bergman, J. A. Ellman, *J. Am. Chem. Soc.* **2001**, *123*, 2685–2686.

Bibliography

- [18] P. W. N. M. van Leeuwen, *Homogeneous Catalysis*, Kluwer Academic Publishers, Dordrecht, Boston, London, **2004**.
- [19] P. W. N. M. van Leeuwen, C. Carmen, *Rhodium Catalyzed Hydroformylation, Vol. 22*, Kluwer Academic Publishers, Dordrecht, Boston, London, **2000**.
- [20] M. Vasylyev, H. Alper, *Angew. Chem. Int. Ed.* **2009**, *48*, 1–5.
- [21] R. Lazzaroni, R. Settambolo, A. Caiazzo, L. Ponterno, *J. Organomet. Chem.* **2000**, *601*, 320–323.
- [22] R. Settambolo, A. Caiazzo, R. Lazzaroni, *Tetrahedron Lett.* **2001**, *42*, 4045.
- [23] S. Rocchiccioli, G. Guazzelli, R. Lazzaroni, R. Settambolo, *J. Heterocyclic Chem.* **2007**, *44*, 479.
- [24] C. Müller, *unpublished results*.
- [25] C. Müller, D. Vogt, *Dalton Trans.* **2007**, 5505–5523.
- [26] S. Mitsuni, A. Kasahara, K. Hanaya, *Bull. Chem. Soc. Jpn.* **1968**, *41*, 2526–2528.
- [27] A. J. M. Duisenberg, L. M. J. Kroon-Batenburg, A. M. M. Schreurs, *J. Appl. Cryst.* **2003**, *36*, 220–229.
- [28] X. Xian, A. M. M. Schreurs, L. M. J. Kroon-Batenburg, *Acta. Cryst.* **2006**, *A62*, 92.
- [29] G. M. Sheldrick, *SADABS: Area-Detector Absorption Correction*, **1999**.
- [30] G. M. Sheldrick, *Acta. Cryst.* **2008**, *A64*, 112–122.
- [31] A. L. Spek, *J. Appl. Cryst.* **2003**, *36*, 7–13.

Summary

Ionic Liquids - Are they worth their salts?

Ionic Liquids receive more and more attention as alternative reaction media due to their properties which clearly discriminate them from water or classical organic solvents. They are tuneable like no other solvent and therefore unique. A short introduction to these unique solvents and their properties is given in the **first chapter** of this thesis to outline their characteristics and applications.

Chapter II deals with the application of ionic liquids in the Pd(0)-catalysed Hiyama cross-coupling reaction. A problem often encountered with this kind of reaction is product and catalyst separation as they often share the same physical properties. Therefore, a laborious work-up of the reaction mixture is the logical consequence. By applying ionic liquids this problem could be circumvented. Newly developed ionic π -acidic-ligands along with the catalyst precursor and the substrates were dissolved in an ionic liquid. These novel ionic ligands differ significantly from the products and the substrates applied in the Hiyama-reaction. As a consequence, the purification of the products is significantly simplified. Various ligands and substrates were tested in the ionic liquid to get an insight into the reaction. The effect of the ligands on the Pd(0)-nanoparticles was investigated by means of TEM and it was found that the nature of the ligands can influence the size of the particles significantly and consequently the reaction rate. The size of the particles varied from 2 up to 10 nm depending on the ligand employed. Furthermore, it was found that the commonly employed imidazolium-based ionic liquids are not suitable for this kind of reaction, presumably due to the presence of acidic protons in the imidazolium moiety.

Chapter III deals with the synthesis of newly developed ionically tagged heterocyclic ligands. Tagging of these ligands was aimed for to facilitate catalyst recycling. All ligands were developed to enable the application of phosphinines and pyridines in biphasic systems using ionic liquids. These new ligands were fully characterised and tested in the Rh-catalysed hydroformylation reaction. They allow the recycling of the

reaction system by removing the apolar products from the reaction mixture.

One major attribute of ionic liquids is their modularity. By changing the cation or anion it is possible to alter the properties of these liquids entirely. One physical property, the coordination behaviour of the anion, was investigated in **chapter IV**. The reaction under scrutiny was the hydroaminomethylation. This reaction was chosen to investigate the influence of the anion on the reaction, as one of the catalytically active species is cationic. Therefore, a difference in employing an ionic liquid, bearing coordinating or non-coordinating anions, should be expected. The result of this research showed that indeed a pronounced disparity between these two kinds of anions can be observed. Application of a coordinating anion rendered the cationic catalyst ineffective under certain conditions, whilst a neutral catalytic species is less-influenced by the nature of the anion. The neutral hydroformylation species catalyses the reaction three times faster in the non-coordinating ionic liquid than in the coordinating one, whilst the effect on the cationic hydrogenation species is more pronounced. The hydrogenation rate in the non-coordinating ionic liquid is about 15 times faster.

Chapter V involves the application of an ionic liquid in the enzyme-catalysed transferhydrogenation. The main goal of this research was to evaluate the applicability of ionic liquids in the biocatalysis as well as to assess the influence of the ionic liquid on the reaction outcome. For several substrates and products the partition coefficients were measured and one selected substrate was tested in the transferhydrogenation. The results show that these reaction systems are non-trivial and that the nature of the substrates and the amount of substrates can influence the reaction rates dramatically.

Finding new routes to ionic liquids precursors is the main goal of **chapter VI**. Although there are already numerous possible ionic liquids precursors, the amount of functionalised or chiral ones is still rather limited. In this chapter the development of chiral ionic liquid precursors is reported. Via a tandem reaction, involving a hydroformylation and a cyclisation reaction, new multicyclic alcohols were synthesised, that do not only bear the potential to become ionic liquids, but also can serve as building blocks for ligands or pharmaceuticals. The substrates that were subject to this

tandem reaction could be synthesised in a straightforward and economic manner. Also the multicyclic alcohols were received in high yield (up to 95%). Furthermore, these newly synthesised compounds were fully characterised and crystals suitable for X-ray analysis were obtained.

Samenvatting

Ionische vloeistoffen krijgen steeds meer aandacht als alternatieve oplosmiddelen vanwege hun unieke eigenschappen, door welke ze zich duidelijk van water en organische oplosmiddelen onderscheiden. Ze zijn tuneable als geen andere oplosmiddel. Het **eerste hoofdstuk** is een inleiding op deze bijzondere oplosmiddelen.

In **hoofdstuk II** wordt de applicatie van ionische vloeistoffen in de Pd(0)-gekatalyseerde Hiyama reactie beschreven. Bij deze reactie kom men vaak het probleem tegen, dat producten en katalysatoren de zelfde eigenschappen hebben en dus is scheiden een uitdaging. Door de applicatie van ionische vloeistoffen was het mogelijk dit probleem op te lossen. π -Zure-alkeenliganden tezamen met de katalysatorvoorloper en de substraten werden opgelost in de ionische vloeistoffen. Omdat deze liganden duidelijk verschillend zijn van de producten is het makkelijk de producten aan het einde van de reactie op te werken. Verschillende liganden en substraten werden getest om inzicht in deze reactie te krijgen. De invloed van de liganden op de Pd(0)-nanodeeltjes was onderzocht met TEM en het was duidelijk dat de liganden de grote van deeltjes beïnvloeden en met als gevolg ook de reactiesnelheid. Deeltjes van 2 tot 10 nm werden gevonden. Bovendien is door dit onderzoek duidelijk geworden, dat de imidazolium-gebaseerde ionische vloeistoffen niet geschikt zijn voor de Hiyama reactie, wellicht vanwege de zure protonen in het imidazoliumkation.

Hoofdstuk III behandelt de synthese van nieuw ontwikkelde ionische heterocyclische liganden. Door de ionische functionele groep zou het terugwinnen van de liganden worden vergemakkelijkt, omdat op deze manier de gebruik van ionische vloeistoffen

als oplosmiddel mogelijk werd. Deze nieuwe liganden werden in de Rh-gekatalyseerde hydroformylering ingezet.

Een belangrijk kenmerk van ionische vloeistoffen is hun modulariteit. Door het veranderen van het anion of kation is het mogelijk de eigenschappen van de vloeistof volledig te veranderen. Een fysieke eigenschap, het coördinatiegedrag van het anion, werd onderzocht in de hydroaminomethylering in **hoofdstuk IV**. Deze reactie werd gekozen omdat tijdens de reactie een ionische en een neutrale katalysator bestaan. Het kon dus verwacht worden dat het anion invloed op de reactie kan hebben. Daarom werden coördinerende en niet-coördinerende anionen getest en het werd duidelijk dat het schelt welk anion gebruikt wordt. De ionische katalysator wordt door het coördinerende anion vrijwel inactief terwijl de neutrale katalysator minder beïnvloed wordt.

Hoofdstuk V betreft de toepassing van een ionische vloeistof in de enzymgekatalyseerde transferhydrogenering. Het belangrijkste doel van dit onderzoek was de toepassing van ionische vloeistoffen in de biokatalyse te evalueren. Voor verschillende substraten en producten werden de partiticoëfficiënten gemeten en substraat werd voor een reactie gebruikt. De resultaten tonen aan dat het reactiesysteem niet triviaal is en dat zowel de substraatsoort als ook de hoeveelheden een grote invloed op het systeem hebben.

Het vinden van nieuwe mogelijkheden om voorlopers voor ionische vloeistoffen te maken was het doel van **hoofdstuk VI**. Hoewel er al veel zijn, is de aantal gefunctionaliseerde voorlopers nog erg beperkt. In dit hoofdstuk wordt de ontwikkeling van chirale voorlopers beschreven. Via een tandemreactie, waarbij een hydroformylering en een cyclisatiereactie, nieuwe chirale multicyclische alcoholen konden worden gesynthetiseerd. Deze alcoholen kunnen belangrijk zijn voor ionische vloeistoffen, maar ook voor medicijnen. De substraten, welke gebruikt werden in de tandemreactie, konden makkelijk gesynthetiseerd worden. Ook het rendement in de tandemreactie was uitstekend (ca. 95%). Bovendien zijn de nieuwe alcoholen volledig gekarakteriseerd, inclusief via Röntgendiffractie.

Curriculum Vitae

Patrick S. Bäuerlein werd geboren op 28 maart te Lippstadt, Duitsland. Na studie aan de middelbare school 'Marienschule' te Lippstadt/Lipperbruch werd na een jaar militaire dienst in 1999 begonnen aan de studie Scheikunde aan de RWTH Aachen. Het afstudeerproject werd uitgevoerd in het 'Institute of Technical and Macromolecular Chemistry' onder begeleiding van prof.dr. W. Leitner en dr. L. Greiner. Het onderzoek betrof de applicatie en verbetering van een ATR-IR-probe in de homogene katalyse. Na het afstuderen besloot Patrick naar Nederland te verhuizen om in de Laboratorium voor Homogene Katalyse en Coördinatie Chemie onder begeleiding van prof.dr. D. Vogt een doctoraal studie te beginnen. Zijn onderzoek omvatte vooral de applicatie van ionische vloeistoffen in de homogene katalyse. De belangrijkste resultaten van zijn onderzoek staan beschreven in dit proefschrift.

Patrick S. Bäuerlein was born in Lippstadt, Germany on March 28th, 1979. He finished the secondary school at the 'Marienschule' in Lippstadt/Lipperbruch in 1998. After one year of military service, he started studying chemistry at the RWTH Aachen in 1999. He graduated in the department of Technical and Macromolecular Chemistry under supervision of Prof. Dr. W. Leitner and Dr. L. Greiner. His project dealt with the application and improvement of ATR-IR-probes in the homogeneous catalysis. Following this research project, Patrick moved to the Netherlands and started his doctoral research in the Laboratory of Homogeneous Catalysis and Coordination Chemistry of Prof. Dr. D. Vogt. His research was mainly focused on the application of ionic liquids in the homogeneous catalysis. The most important results of this research are described in this thesis.

List of publications

I.J.S. Fairlamb, P.S. Bäuerlein, L.R. Marrison, J.M. Dickinson, *ChemCommun.* **2003**, 5, 632.

C.B. Minnich, P. Buskens, H.C. Steffens, P.S. Bäuerlein, L.N. Butvina, L. Küpper, W. Leitner, L. Greiner, *Org. Process Res. Dev.* **2007**, 14, 94.

B. Hamers, P.S. Bäuerlein, C. Müller, D. Vogt, *Adv. Synth. Catal.* **2008**, 350(2), 332-342.

P.S. Bäuerlein, I.A. Gonzalez, J.J.M. Weemers, M. Lutz, A.L. Spek, D. Vogt, C. Müller, *ChemCommun.* **2009**, 4944-4946.

P.S. Bäuerlein, I.J.S. Fairlamb, A.G. Jarvis, A.F. Lee, C. Müller, J.M. Slattery, R. Thatcher, D. Vogt, A. Whitwood, *ChemCommun.* **2009**, accepted.

Dankwoord

Vier jaren zijn nu voorbij, fijne, gezellige en productieve jaren. Dus, wil ik nu een paar mensen bedanken, die ik tegen ben gekomen, die mij de afgelopen jaren hebben geholpen of de tijd gewoon gezellig hebben laten worden. En dat was een hoop mensen.

Ik wil beginnen met mijn promotor en co-promotor, Dieter en Christian. Dank aan jullie dat ik de mogelijkheid hebben gekregen in Eindhoven te promoveren in een prachtige groep met veel leuke mensen. Zonder jullie waren de laatste jaren nooit zo goed afgelopen. Bedankt Dieter, Christian.

Bijzondere nadruk wil ik op Bart leggen, met wie ik de hele vier jaren een kantoor en ook het lab mocht delen en dus mocht leren kennen. Het was een plezier met je te werken, Bart! Het was altijd mogelijk zelfs ook een minder goede dag op het lab met grapjes en de nieuwste mop van de dag op te frolijken. Daarom was het ook altijd buiten het lab heel gezellig met je, bij voorbeeld Engeland of Cochem. Dank daarvoor ook aan Nicole. Succes in de Kohlenpott, Bart! Ik ben overtuigd, dat je het uitstekend goed zal doen in Marl net zoals je het in Eindhoven hebt gedaan.

Dan zijn er ook mijn andere kantoorgenoten, Leandra en Jarno, die ik wil bedanken voor een prachtige sfeer en ook de goede wetenschappelijke discussies. Het was heel gezellig met jullie. Leandra, je wens ik veel succes in Venlo en met de NS. Jarno, al het goede voor je PhD.

Michèle, jou wil ik danken voor de hilarische momenten met de Duitse en Nederlandse taal, de wetenschappelijke praatjes en je gezelligheid. Het is leuk je kennen geleerd te hebben. Sterkte en succes tijdens je laatste maanden als AIO.

Maar eigenlijk kan ik gelukkig zeggen, dat de hele groep ontzettend gezellig is en ook buiten 't lab het een leuke tijd was, bijvoorbeeld in Göteborg om er maar een te noemen. Daarom ook mijn dank aan: Laura, Dennis, Andreas, Matthijs, Gilbere, Arjan, Tiina, Tiny, Freek, Jos, Ariadna, Erik, Marion, Etienne, Gijsbert, Daniel en Ismael. Ismael,

tambien quiero expresarte mi gratitud por tu trabajo en el laboratorio. Con tu trabajo aqui he sido muy contento. Gracias!

Ton wil ik graag apart bedanken omdat zonder hem zeker heel veel, misschien zelfs meer, niet gelukt was. Bedankt voor je hulp met alle apparaten, het oplossen van hun kuren en je geduld. Je was een grote hulp.

I also got the chance to work in York for half a year. Therefore, I'd like to thank John and Ian for allowing me to work in their labs and for the help on the project. John and Lucy, thank you for your hospitality. It was not just a successful time over there on the island, also it was a brilliant time. I enjoyed it a lot. This was mainly due to the Fairlamb, who were always helpful and gezellig (sorry, but the english language really lacks a proper word here, you have to look it up). Especially I want to thank Amanda for the help on the paper and Tom, Tony, Somia, Amanda, Mike, Jon, Petr for their help, the odd pint in the pub and the for the coffee breaks. But also outside the Fairlamb lab I met very nice people I would like to thank for their help and for the lovely time in York. Thanks Cécile, Bart, Daniel, Matthew, Jonny and Graeme. And there is another group I want to thank. The Norwegian outdoor society people (Hanne, Hanne, Ingrid, Harald). It was always hilarious with you and I enjoyed the walks and time spent. Tak!

Dann noch ein paar Worte des Dankes in Deutsch. Gerne möchte ich auch Pia und Lasse danken für die tolle Zusammenarbeit am 5. Kapitel. Es war schön wieder mit euch zu arbeiten, nachdem ich Aachen verlassen hatte.

Und zum Schluss danke ich noch meiner Familie. Meinen Eltern, meiner Schwester, meinem Schwager und den Zwillingen Tim und Niklas für die Unterstützung während der letzten vier Jahre. Ohne euch wäre sicher vieles anders gelaufen. Niklas, Tim, ich wünsche mir dass ihr eure Lebensfreude bewahrt. Zu sehen, wie ihr die Welt entdeckt, zeigt einem wie viel Spaß Erforschen machen kann und wie spannend es immer wieder ist.

BEDANKT ALLEMAL